

PARAMETRIC RESONANCES IN NONLINEAR
MECHANICAL SYSTEMS

PARAMETRIC RESONANCES IN NONLINEAR
MECHANICAL SYSTEMS

by

KURT G. J. ASMIS

A THESIS
SUBMITTED TO THE FACULTY OF GRADUATE STUDIES
IN PARTIAL FULFILMENT OF THE REQUIREMENTS
FOR THE DEGREE
DOCTOR OF PHILOSOPHY
McMASTER UNIVERSITY
August, 1971

DOCTOR OF PHILOSOPHY (1971)
(Civil Engineering and
Engineering Mechanics)

McMASTER UNIVERSITY
Hamilton, Ontario.

TITLE: PARAMETRIC RESONANCES IN NONLINEAR MECHANICAL SYSTEMS

AUTHOR: KURT G.J. ASMIS, B.A.Sc. (Univ. of Toronto)
M.A.Sc. (Univ. of Toronto)

SUPERVISOR: Professor W.K. Tso

NUMBER OF PAGES: xv, 252, A-10

SCOPE AND CONTENTS:

The resonant response of nonlinear dynamical systems of one and two degrees of freedom subjected to parametric external monofrequent periodic excitation is investigated. The nonlinearities involved in the system arise from the nonlinear restoring forces.

It is known that nonlinear systems subjected to external parametric excitation are susceptible to resonances. These are dependent upon the relationship of the natural frequencies of the system and the external exciting frequency. In addition to the study of resonant conditions, particular emphasis is laid in the present study on the amplitude of the oscillations once the system is excited into resonance. The nonlinear restoring forces are divided into two groups, those that can be represented by analytical expressions of the co-ordinates and those that are multi-valued, non-analytic, hysteretic functions of the co-ordinates.

Firstly, the phenomenon of internal resonance interacting with parametric resonance is studied. It is shown that a transfer of energy between modes is possible due to the nonlinear coupling between the modes and that the extent of the interaction depends on the frequency and damping relationships between the modes. The region of parametric resonance, the steady-state amplitudes of oscillations, and

the non-steady state time-history plots are presented.

A special feature of parametric resonance is that a monofrequent external excitation may induce either a one mode or two mode response. All previous studies in parametric resonance have assumed that the ratio of the natural frequencies of the system are such that a single mode resonance and combination mode resonance do not occur simultaneously. In Chapter III the interaction of these two forms of parametric resonance on a nonlinear system are investigated. The destabilizing effect of viscous damping and its effect on the growth behaviour of the oscillations is discussed.

The force-deformation relationships of physical systems under cyclic displacements often exhibit a hysteresis effect. Using three common hysteretic models known as the bilinear, double bilinear and the Ramberg-Osgood hysteretic models, the response of a single degree-of-freedom oscillation parametrically excited is examined. The steady-state response curves are given, the effect of the yield point, the effect of initial conditions and the possibility of unbounded response is discussed in Chapter IV.

The analysis is then extended to include the parametric resonance of a two degree-of-freedom hysteretic system. The destabilization effect as caused by the bilinear and the Ramberg-Osgood relationships is shown. The steady-state curves are verified by direct numerical integration. The transient solutions proceeding steady-state provide a qualitative behaviour of the meaning of destabilization in hysteretic systems.

ACKNOWLEDGEMENTS

The author expresses his sincere gratitude to his supervisor, Professor W.K. Tso, for his continuous encouragement and guidance not only for the preparation of this thesis but also throughout his graduate work at McMaster University.

The author also expresses his thanks to Professor A.C. Heidebrecht and Professor G. Fields for their interest in this work and the stimulus provided by their lecture courses.

The financial support provided by McMaster University and Post Graduate Scholarship provided by the National Research Council of Canada are gratefully acknowledged.

This thesis could not have been possible without the sacrifices and patience of my wife, Joan. My deepest appreciation and thanks for her support and understanding.

<u>TABLE OF CONTENTS</u>	<u>PAGE</u>
DESCRIPTIVE NOTE	ii
ACKNOWLEDGEMENTS	iv
TABLE OF CONTENTS	vi
LIST OF FIGURES	viii
NOMENCLATURE	xiii
CHAPTER I: INTRODUCTION	1
1.1 Preamble	1
1.2 Literature Survey	4
1.3 Review of Mathematical Methods	9
1.4 Scope of Investigation	20
CHAPTER II: COMBINATION RESONANCE AND INTERNAL RESONANCE OF A THIN-WALLED BEAM	21
2.1 Introduction	21
2.2 Derivation of the Equations of Motion	23
2.3 Statement of the Problem	30
2.4 Steady-State Solutions	43
2.5 Non-synchronized Quasi-Steady State Response	54
2.6 Observations and Discussions	64
CHAPTER III: THE INTERACTION OF TWO EXTERNAL PARAMETRIC RESONANCES IN A TWO DEGREE OF FREEDOM SYSTEM SUBJECTED TO NONCONSERVATIVE LOADING	67
3.1 Introduction	67
3.2 The Equations of Motion	69

<u>TABLE OF CONTENTS</u>	<u>PAGE</u>
3.3 The Averaged Equations	73
3.4 Stability of the Trivial Solution $Q_j = 0$	75
3.5 Uncoupled Parametric Type I and Type II Resonances	79
3.6 Steady-State Solutions	85
3.7 Transient Response	92
3.8 Example of a Double Pendulum with Circulatory Loading	98
3.9 Discussion and Observations	119
CHAPTER IV: PARAMETRIC RESONANCE OF A SINGLE DEGREE OF FREEDOM SYSTEM WITH HYSTERETIC DAMPING	123
4.1 Introduction	123
4.2 Statement of the Problem	125
4.3 Method of Solution	128
4.4 Steady State Response	131
4.5 Steady State Response Curves for the Bilinear, Double Bilinear and Ramberg-Osgood Hysteretic Models	133
4.6 Stability of Steady State Solution	144
4.7 Exact Analysis	147
4.8 Transient Response	150
4.9 Bounded Response Within the Linear Instability Zone	157
4.10 Characteristics of the Functions $C(\mu)/\mu$, $S(\mu)/\mu$	159
4-11 Observations and Discussion	175

<u>TABLE OF CONTENTS</u>	<u>PAGE</u>
CHAPTER V: PARAMETRIC RESONANCE OF A TWO DEGREE OF FREEDOM BILINEAR HYSTERETIC SYSTEM	179
5.1 Introduction	179
5.2 Statement of the Problem	180
5.3 Monofrequency Response	181
5.4 Combination Resonance	197
5.5 Observations and Discussion	216
CHAPTER VI: COMBINATION RESONANCE OF A TWO DEGREE OF FREEDOM SYSTEM WITH THE "RAMBERG-OSGOOD HYSTERETIC RESTORING FUNCTIONS	219
6.1 Introduction	219
6.2 The Equations of Motion	220
6.3 Approximate Method of Solution	222
6.4 Steady State Response	223
6.5 Transient Response	229
6.6 Presence of Higher Order Harmonics	238
6.7 Observations and Discussion	238
CHAPTER VII: CONCLUSIONS AND RECOMMENDATIONS FOR FUTURE RESEARCH	240
REFERENCES	247
APPENDIX A: EVALUATION OF THE HYSTERETIC FUNCTIONS $S(Q)$, $C(Q)$	A-1

LIST OF FIGURES

<u>FIGURE</u>	<u>TITLE</u>	<u>PAGE</u>
1.1	Nature of Response	18
2-1	Cross Section of Warp Free Thin-Walled Beam	26
2-2	Steady State Response Combination and Internal Resonance (Equal Damping)	48
2-3	Steady State Response Combination and Internal Resonance	49
2-4	Steady State Response for Q_2	50
2-5	Time History Plot for Steady State Response	51
2-6	Nonsynchronized Quasi Steady State	52
2-7	Effect of Internal Detuning on Threshold of Steady State Response	55
2-8a	Response Based on Averaged Equations with Internal Resonant Terms	57
2-8b	Response Based on Averaged Equations Neglecting Internal Resonant Terms	58
2-8c	Response Based on Exact Numerical Integration	59
2-9a	Response with Large Internal Detuning (Internal Resonant Terms Included)	60
2-9b	Response with Large Internal Detuning (Internal Resonant Terms Neglected)	61
2-9c	Response Based on Exact Numerical Integration	62
3-1	Uncoupled Type I Steady-State Response	89

<u>FIGURE</u>	<u>TITLE</u>	<u>PAGE</u>
3-2	Uncoupled Type II Response	90
3-3	Coupled Type I and Type II Steady-State Curves	91
3-4	Parametric Type I Time History Response	93
3-5	Combination Type II Time History Response	94
3-6	Coupled Type I and Type II Time History Response	96
3-7	Coupled Type I and Type II Time History Response	97
3-8	Double Pendulum with Circulatory Loading	100
3-9	Plot at Load F_0 vs Undamped Natural Frequencies	106
3-10	Uncoupled Type I and Type II Steady State Curves	108
3-11	Maximum Value $R(p)$ vs Frequency of Coupled System	109
3-12	Uncoupled Type I Response	111
3-13	Uncoupled Type II Response	112
3-14	Uncoupled Type II Response	113
3-15	Combined Type I and Type II Response	114
3-16	Combined Type I and Type II Response	115
3-17	Response of Physical Co-ordinates Obtained from Averaged Equations	117
3-18	Response of Physical Co-ordinates Obtained From Exact Equations	118
4-1	Simple Pendulum with Vibrating Support	127
4-2	Effect of Hysteresis Parameter u on Response Curve (First Approximation)	135
4-3	Effect of Hysteresis Parameter u on Response Curve (Second Approximation)	136

<u>FIGURE</u>	<u>TITLE</u>	<u>PAGE</u>
4-4	Effect of Yield Rotation ϕ_y on Response Curve (Second Approximation)	137
4-5	Response Curves (First Approximation)	139
4-6	Response Curves (Second Approximation) ($\phi_y = 0.2$)	140
4-7	Response Curves (Second Approximation) ($\phi_y = 1.0$)	141
4-8	Ramberg-Osgood Steady State Curve	143
4-9	Comparison of Approximate And Numerical Steady-State Response Curves	149
4-10	Effect of Initial Conditions	151
4-11	Effect of Initial Conditions	152
4-12	Effect of Initial Conditions (Small Disturbance)	154
4-13	Effect of Initial Conditions (Large Disturbance)	155
4-14	Trace of Ramberg-Osgood Hysteretic Curves	156
4-15	Detuning Characteristics - Bilinear Model	161
4-16	Damping Characteristics - Bilinear Hysteretic Model	162
4-17	Detuning Characteristic - Double Bilinear Model	163
4-18a	Detuning Characteristic Ramberg-Osgood Hysteretic Model	164
4-18b	Damping Characteristic Ramberg-Osgood Hysteretic Model	165
4-19	Comparison of Analytic and Hysteretic Restoring Functions ($S(\mu)/\mu$)	169
4-20	Comparison of Analytic and Hysteretic Restoring Functions ($C(\mu)/\mu$)	170

<u>FIGURE</u>	<u>TITLE</u>	<u>PAGE</u>
4-21	Plot of the Function Ψ of the Bilinear Hysteretic Model	172
4-22	Steady-State Response Curves at Large Amplitude Levels (Bilinear Hysteretic Model, $u = 0.2$)	173
4-23	Steady-State Response Curves at Large Amplitude Levels (Bilinear Hysteretic Model, $u = 0.4$)	174
5-1	Steady-State Response - One Mode Approximation	191
5-2	Time History Response of Averaged Equations ($\eta = 1.95$)	193
5-3	Time History Response of Exact Numerical Integrations	194
5-4	Time History Response of Averaged Equations ($\eta = 2.05$)	195
5-5	Time History Response of Exact Numerical Integration	196
5-6	No Figure	
5-7	No Figure	
5-8	Destabilizing Effect of the Bilinear Hysteretic Restoring Functions	208
5-9	Steady-State Response Curves (Ratio of Yield Points $r = 2$)	209
5-10	Steady-State Response Curves (Ratio of Yield Points $r = 1$)	210
5-11	Transient Response of the Avgd. Equations	211
5-12	Passage Through Resonance - Bilinear Hysteretic Function ($r = 2$)	214
5-13	Passage Through Resonance - Bilinear Hysteretic Function ($r = 1$)	215
6-1	Steady-State Curves of the Ramberg-Osgood Hysteretic Function	226

<u>FIGURE</u>	<u>TITLE</u>	<u>PAGE</u>
6-2	Steady State Curves of the Ramberg-Osgood Hysteretic Function	227
6-3	Steady State Curves of the Ramberg-Osgood Hysteretic Function	228
6-4	Effect of Small Initial Conditions Outside the Linear Resonance Zone	230
6-5	Effect of Large Initial Conditions Outside the Linear Resonance Zone	231
6-6	Response Within the Linear Resonance Zone	232
6-7	Passage Through Resonance - Ramberg-Osgood Function ($n_1 = 3$)	234
6-8	Passage Through Resonance - Ramberg-Osgood Function ($n_1 = 9$)	235
6-9	Analysis of Wave Form of First Mode	236
6-10	Response of Second Mode and Parametric Driving Force	237

APPENDIX

A-1	Bilinear Hysteretic Function	A-3
A-2	Double Bilinear Hysteretic Function	A-5
A-3	Ramberg-Osgood Hysteretic Function	A-8

NOMENCLATURE

a, \bar{a}	= nonlinear coefficients defined in Chapter III
a_j, a_{ij}, A_{ij}	= coefficients of nonlinear terms
b_j, b_{ij}, B_{ij}	= coefficients of parametric oscillation
c	= spring constant
$C(Q), C'(Q), C(\mu)$	= integrals defined in Chapter IV
d_j, d_{ij}, D_{ij}	= nonlinear coefficients of coupling terms
e, \bar{e}	= viscous damping coefficient defined in Chapter III
e_j, e_{ij}, E_{ij}	= viscous damping coefficients
$f(t)$	= base motion
F	= maximum amplitude of base motion
$f(x, \bar{x}, t)$	= general nonlinear function
$F(t)$	= normalized force
i	= $\sqrt{-1}$
I_y, I_p	= moment of inertia
K_j	= ratio of frequencies ω_j/Ω
L	= length of pendulum
m	= mass per unit length, mass of pendulum
M_o	= maximum amplitude of external moment
$M(\phi, u)$	= hysteretic restoring function
n	= parameter of Ramberg-Osgood Function
ΔN	= axial force, defined in Chapter II
P_o, P_t	= followers force, static and dynamic components
$Q(t), Q'(t)$	= response amplitude

R	= F/L excitation parameter defined in Chapter IV
r	= Ratio of yield points
$R(\phi, \dot{\phi})$	= analytic restoring function
S	= generalized force
$S(\mu), S(Q), S'(Q)$	= integral defined in Chapter IV
t	= time
T	= Kinetic Energy
u	= hysteresis loop parameter
$u(z, t)$	= lateral displacement
$x_j(t)$	= dependent variable
$y_j(t)$	= dependent variable
z	= independent variable, length of beam
α	= parameter of Ramberg-Osgood function
Δ, Δ_j	= detuning parameters
ϵ	= small parameter
$\theta(t), \theta'(t)$	= phase angle
θ^*, θ^*_j	= amplitude functions defined in Chapter IV
κ	= ratio K_1/K_2
λ	= detuning parameter
μ	= amplitude ratio Q/ϕ_y
τ, T	= dimensionless time
ϕ	= generalized co-ordinates
ϕ_y	= "yield" angle
ϕ_j	= combination of phase angles

ψ_j = total phase
 ω_j = natural frequencies
 Ω = external frequency

CHAPTER 1

INTRODUCTION

1.1 Preamble

The emphasis in modern structures in Civil, Mechanical and Aerospace engineering is on light-weight, complex assemblies fabricated of thin-walled shells, plates or beams, Many of these structures are exposed to complex dynamic environments. For example, buildings are subjected to wind and earthquake loading and machine vibrations, machine components are subjected to alternating reciprocating action and bridges and high speed track are subjected to moving loads. To ensure proper performance of these structures, a study of the response of structural systems to dynamic excitation is necessary.

Dynamic excitation can be classified into three main groups: (a) transient excitation such as occurs through wind gusts, ocean waves breaking on marine structures or earthquake ground motion, (b) complex periodic motion in which the excitation may consist of a multi-frequency input, and (c) monofrequency periodic motion. Structures exposed to periodic loading may be excited into large amplitude oscillations in the neighbourhood of certain critical frequencies of the external excitation. This phenomenon of resonance caused by periodic forces is one important area of the response study of structures to dynamic excitation. It is this phenomenon of resonance as caused by monofrequent periodic loading that will be investigated in this thesis.

(a) Ordinary Forced Resonance v.s. Parametric Resonance

Structures subjected to a complex dynamic environment

can exhibit a large number of possible resonances. The investigations in this thesis are concerned with parametric resonance. As such it is necessary to distinguish between parametric and ordinary forced resonance. The essential observable differences of these two resonances are: (a) the range of frequencies in which large amplitudes can occur, and (b) the growth history of the response from some small value to the steady-state amplitude.

As an example, consider a simple pendulum subjected to periodic excitation at its support. The horizontal component of the excitation leads to a forced resonance of the system while the vertical component of the excitation leads to parametric resonance of the system. Forced resonance occurs when the horizontal component excitation frequency is equal to the natural frequency of the system. Parametric resonance occurs when the vertical component excitation frequency is close to $2/n$, ($n = 1, 2, 3, \dots$) times the natural frequency of the system. Therefore the chance of a system being excited into parametric resonance is more numerous as compared to forced resonances. By comparing the transient response before the steady-state response is established, it is observed that the amplitude grows linearly in the case of ordinary forced resonance and exponentially for parametric resonance.

A practical example where a structure is parametrically excited is in a strut under axial load. The strut may buckle if the compressive load should exceed the buckling load. However, if the applied load is pulsating, parametric resonance may occur which leads to large amplitude flexural oscillations even if the load is less than the buckling load. A similar form of resonance can occur under the effect of periodically varying thrust perturbations in propulsion systems. Such thrust fluctuations have been encountered^[1, 10, 16]; other examples of mechanical systems that are susceptible to parametric resonance are given by Evan-Iwanowski^[12] and Bolotin^[4].

There is another essential difference between ordinary forced and parametric resonance. An analysis of a linear parametrically excited system predicts unbounded response. In contrast to ordinary forced resonance the inclusion of viscous damping terms in the analysis will not lead to bounded response. Consequently, the linearized analysis can give only, the bifurcation points where the equilibrium position becomes unstable. The resulting motion after the initial growth can only be obtained by taking into account the nonlinear behaviour. It is this fact that makes a nonlinear analysis mandatory for the complete response analysis of systems under parametric excitation.

(b) Multiple Degree of Freedom Systems

All engineering structures are continuous structures. However, their dynamic behaviour can often be studied satisfactorily by approximating that structural system into a multi-degree of freedom system, or even a single degree of freedom system. Whether a structural system should be approximated by a multi-degree of freedom system or a single degree of freedom system depends on the system and the external excitation. If the excitation is such that only one mode of the structure will be excited, then the structure can be treated as a single degree of freedom system.

But, a number of examples of dynamic resonance cannot be explained by the action of a one degree of freedom system. A parametric resonance may occur when the exciting frequency is near a combination of natural frequencies. With this type of combination resonance multi-modal response occurs and the physical system has to be analysed as a multiple degree of freedom system. The importance of this type of resonance is demonstrated by the fact that for some mechanical systems only combination resonance is possible and single mode response subjected to parametric excitation cannot occur^[31]. While

studies on the resonance of single degree of freedom nonlinear systems has been extensive^[3], resonance, particularly parametric resonance of multi-degree of freedom, nonlinear systems is less understood. The reason for this is that during resonance, it is possible that an interaction can occur between various degrees of freedom and between the degrees of freedom and the external excitation. Consequently, a wide variety of resonances can occur in a multi-degree, nonlinear, dynamical system.

(c) Area of Research

Traditionally each form of resonance is studied separately assuming other forms of resonance do not occur at the same time. There is however little research on the interaction of the different resonances in multiple degree of freedom systems. Not only is it very possible that several external resonances can occur simultaneously but the nonlinear response can also cause a strong coupling effect between modes of motion which causes an internal resonance condition to develop. This is particularly important in structures where two modes of motion have almost equal frequencies. One of the main objects of the present work is to study parametric resonance of nonlinear systems where more than one type of resonance occur simultaneously.

1.2 Literature Survey

An extensive literature exists on the subject of parametric resonance in a nonlinear single-degree of freedom system. For a complete response analysis there are three phases to be studied. First, it is necessary to determine the conditions under which a dynamic resonance can occur. This phase of study usually reduces to an examination of a set of linear differential equations with constant or periodic coefficients. The second phase of study involves the determination of the steady-state amplitude of vibration if it

exists. If it does not exist it is necessary to examine the time-history of the response to obtain quantitative and qualitative information as to the type of response that exists in lieu of the steady-state. The third phase of study is concerned with the transient growth of the oscillations from some small initial value to the final steady-state or quasi-steady response. Of particular interest in this phase of study is the amount of overshoot of the transient amplitude of oscillation to the steady-state amplitude. The literature survey will be presented under these three phases of investigation.

(a) Condition for Resonance

A dynamical system with multiple degrees of freedom and under parametric excitation is governed by a system of ordinary differential equations with periodic coefficients. The condition for parametric resonance is the condition under which the original equilibrium configuration becomes unstable. Extensive studies of parametric systems have been carried out by Bolotin^[4]. He however restricted his analysis to single mode response and did not consider combination resonance. Much of the earlier work done on combination parametric resonance is due to Mettler^[31]. However, he analysed only systems where the loading forces can be derived from potential functions. He also excluded the possibility of an inter-action of external resonance zones. Piszeczek^[38] extended Mettlers analysis to investigate the condition where the external loading followed the deformation of the system and first investigated the combination-minus resonance. Schmidt and Weidenhammer^[44] included the effect of viscous damping on the instability zone of combination resonance. In a series of papers Hsu^[19, 20], applied the method of averaging and completed to the first approximation the instability study of parametrically excited systems including the effect of viscous damping and the interaction of various

resonance zones.

(b) Nonlinear Analysis (Response Analysis)

To obtain the amplitudes of response of a parametrically excited system it is necessary to carry out a nonlinear analysis. The works on nonlinear vibration studies are divided into two sub-sections, (i) nonlinear analytic systems and (ii) nonlinear hysteretic systems.

(i) Nonlinear Analytic Systems

Studies of one degree nonlinear systems subjected to ordinary forced and parametric excitation have been extensively treated in the works of Bogoliobov and Mitropolsky^[3] and Minorsky^[36]. For multiple degree of freedom systems again an extensive literature exists for the case of monofrequency response. If the nonlinear terms cause a coupling effect between several modes an internal resonance condition may be possible. Where as an extensive literature also exists on the free vibration of nonlinear coupled systems, only a small number of papers have been written on the interaction effect as given by Miles^[35] and Sethna^[45,46].

Few studies exist on the nonlinear analysis, and steady-state behaviour of parametric systems. Mettler^[32] investigated the response of a thin-walled beam where the nonlinearity was introduced by the axial shortening affect, Piszeczek^[38] and Hagedorn^[15] analysed a similar problem and included the nonlinear affect due to torsion and nonlinear damping respectively. All authors avoided the case of an internal resonance condition and the coincidence of parametric resonance zones.

Experimental results for combination resonance involving a two mode response are also few in number. An experiment to determine the instability zones of combination resonance was carried out by Reckling^[41] for the case of an

I beam and plane section under pulsating end moments; for a mechanical two degree-of-freedom system Benz^[2] carried out a number of experiments on combination resonance. Close agreement was observed with the experimental and theoretical results. In the field of fluid mechanics, Hutton^[21] carried out an experimental investigation in the nonlinear coupling of modes. The experiment consisted of a liquid filled cylinder excited in a planar mode of motion. The results indicated that a nonlinear coupling can excite the non-planar or swirling mode of motion of the liquid surface.

(ii) Nonlinear Hysteretic Systems

Experimental results have shown, Hanson^[17], Popov^[39], Shiga^[47], Yamada^[56], that for many engineering structures, the force-displacement relationship shows a distinct, hysteretic behaviour. To describe the behaviour of hysteretic system under cyclic loading it is necessary to use non-analytic functions. These functions are characterized by the fact that the function and its derivatives may be discontinuous and multi-valued. In general, the load-displacement relation under cyclic loading beyond the elastic limit of the system is highly complex. In order that such characteristics may be incorporated into engineering analysis, there exists a variety of hysteretic models which approximates the true hysteretic load-displacement relation. Among the most common hysteretic models used are the bilinear hysteretic model (the elasto-plastic model is a special case of this), double bilinear hysteretic model and the Ramberg-Osgood hysteretic model.

There are two motives for the study of hysteretic systems: (a) As an accurate representation of the force deformation characteristics that exist in real structures as obtained in experiments. (b) As an alternate energy dissipation mechanism as compared to viscous damping. By far, the greatest effort has been expended on the first motive, in particular in the field of earthquake engineering. Research

in this area has focused on ordinary forced resonance of one degree of freedom structures subjected to transient and sinusoidal excitation. The response of a simple oscillator to sinusoidal excitation with bilinear hysteresis was carried out by Caughey^[7]. Sinusoidal excitation of a system with double bilinear hysteresis was studied by Iwan^[22] and that with the Ramberg-Osgood hysteretic function by Jennings^[27]. Steady-state response of a two degree of freedom system under sinusoidal excitation has been obtained by Iwan^[24] and by Dokainish & Sahay^[11]* for the bilinear and double bilinear hysteretic models respectively.

The second point concerns the use of the hysteretic functions as a replacement of viscous damping as a possible mechanism to account for the dissipation of energy. Viscous damping is a suitable model to use in free and forced oscillation studies because it provides the effect of damping out the motion of the system in free vibration and limiting the resonant response of the system to finite values in the case of forced resonance. However, the viscous damping model appears inadequate in many instances. A case in point is associated in the stability problems with non-conservative loads. It is known that there is a discontinuity of critical load values from the undamped system to a system with small viscous damping. Recently Jong^[28] has shown that if a bilinear hysteretic damping model is used instead of the viscous damping model, such a discontinuity in critical load values of the system vanishes.

Another area where the viscous damping model appears to be inadequate is in the area of parametric resonance. It is well known that the main effect of viscous damping is to modify the sizes of the unstable regions only, Bolotin^[4]. Once the system is excited into parametric resonance the response of the linearized system grows without bound. However, finite steady-state response is possible if the dissipation of energy is accredited to the hysteretic nature of the restoring

*Note: This is not a published paper.

forces^[55].

For combination parametric resonance it was shown by Schmidt and Weidenhammer^[44] that viscous damping may cause a widening of the instability zone as compared to the undamped case. Using a nonlinear but analytic representation of viscous damping, Hagedorn^[15] showed that the addition of nonlinear damping also causes widening of the resonance zone. No study has been made of the effect of hysteretic damping model on the instability zone of combination resonance.

(c) Transient Response

The transient growth of oscillations once a system is excited into resonance can be obtained by direct experimental observations or by numerical integration of the governing differential equations. An experimental investigation of the transient motion of parametrically excited systems was carried out by Benz^[2]. A numerical investigation of the effect of initial conditions and the effect of viscous damping was carried out by Ghobarah^[14] and Tso & Asmis^[55]. Additional experimental results are given in Bolotin^[4].

1.3 Review of the Mathematical Methods

Nonlinear mechanical systems subjected to periodic excitation can be described mathematically by a system of nonlinear ordinary differential equations with periodic coefficients. The techniques necessary to solve such a system requires a knowledge of the standard analysis of linear ordinary differential equations with constant coefficients, linear ordinary d.e. with periodic coefficients and nonlinear o.d.e. with constant and/or periodic coefficients. The method of analysis that is most widely used is the method of averaging as developed by Bogoliubov and Mitropolsky^[3] and Malkin^[30]. The popularity of this method is attested by the fact that it has been used on almost all present works on

nonlinear as well as some linear dynamic resonance problems [7, 15, 19, 24]. In addition, the smoothing effect of the averaging process makes the method an ideal analytical tool to study the behaviour of non-analytic hysteretic systems.

(a) The Method of Averaging

Consider a dynamical system with n degrees of freedom. Let x_j ($j = 1, 2 \dots n$) be the generalized coordinates of the system. The equations of motion can be written as

$$\ddot{x}_j + \omega_j^2 x_j + \epsilon f_j(x_1, \dots, x_n, \dot{x}_1, \dots, \dot{x}_n, t) = 0 \quad 1-1$$

$$(j = 1, \dots, n)$$

where $\epsilon \ll 1$, ω_j is the linear natural frequency and f_j represents a function of nonlinear terms. The system 1-1 is weakly nonlinear and weakly perturbed (in the sense of linear equations with periodic coefficients) whose perturbations can be considered small.

The method of averaging provides an approximate solution to the system of equations 1-1. In essence, the method transforms the equations 1-1 by a suitable change of variables to the system

$$\dot{z} = \epsilon F(z, t) \quad 1-2$$

where $z = \{z_1, \dots, z_{2n}\}$ is a vector of slowly varying variables and $F(z, t)$ is an almost periodic function of t . Once the differential equations have been brought into standard form the averaging principle is applied which consists of taking the mean value of equations 1-2. The averaged equations are:

$$\dot{\bar{z}} = \epsilon Y(\bar{z}) \quad 1-3a$$

where

$$Y(\bar{z}) = \lim_{T \rightarrow \infty} \frac{1}{T} \int_0^T F(z, t) dt \quad 1-3b$$

where the variables z are assumed constant during the integration process. The difference between the exact solutions of 1-2 and the approximate solutions represented by 1-3a have been studied^[37].

Several transformations exist which can reduce the system 1-1 to 1-2. A common method in dynamics is to use the polar transformation where

$$\begin{aligned} x_j &= Q_j(t) \cos(\omega_j t + \theta_j(t)) \\ &\equiv Q_j \cos \psi_j \end{aligned} \quad 1-4a$$

$$\begin{aligned} \text{and } \dot{x}_j &= -Q_j(t) \omega_j \sin(\omega_j t + \theta_j(t)) \\ &\equiv -Q_j \omega_j \sin(\psi_j) \end{aligned} \quad 1-4b$$

This leads to n system of equations

$$\begin{bmatrix} \cos \psi_j & -Q_j \sin \psi_j \\ -\omega_j \sin \psi_j & -Q_j \omega_j \cos \psi_j \end{bmatrix} \begin{Bmatrix} Q_j \\ \theta_j \end{Bmatrix} = \begin{Bmatrix} 0 \\ -\epsilon f_j \end{Bmatrix} \quad (j=1, \dots, n) \quad 1-5$$

Applying the averaging principle to 1.5 the averaged equations are

$$\dot{Q}_j = \lim_{T \rightarrow \infty} \frac{1}{T} \int_0^T \frac{\epsilon f_j}{\omega_j} \sin \psi_j dt \quad 1-6a$$

$$Q_j \dot{\theta}_j = \lim_{T \rightarrow \infty} \frac{1}{T} \int_0^T \frac{\epsilon f_j}{\omega_j} \cos \psi_j dt \quad 1-6b$$

(j = 1, ---, n)

Another transformation is the use of rectangular coordinates and is more suitable to study the stability of the trivial solution $Q_j = 0$. The transformation takes the form

$$x_j = A_j(t) \cos \omega_j t + B_j(t) \sin \omega_j t \quad 1-7a$$

$$\dot{x}_j = -A_j(t) \omega_j \sin \omega_j t + B_j(t) \omega_j \cos \omega_j t \quad 1-7b$$

Substituting 1-7 into 1-1 one obtains the n system of equations

$$\dot{A}_j = \frac{\epsilon f_j}{\omega_j} \sin \omega_j t \quad 1-8a$$

$$\dot{B}_j = \frac{-\epsilon f_j}{\omega_j} \cos \omega_j t \quad 1-8b$$

(j = 1, ---, n)

The rectangular and polar transformations are related by the equations

$$A_j = Q_j \cos \theta_j \quad 1-9a$$

$$B_j = -Q_j \sin \theta_j \quad 1-9b$$

Another transformation which was used by Hsu^[19] and Tondl^[53] is the complex transformation

$$\begin{Bmatrix} x_j \\ \dot{x}_j \end{Bmatrix} = \begin{bmatrix} e^{i\omega_j t} & e^{-i\omega_j t} \\ i\omega_j e^{i\omega_j t} & -i\omega_j e^{-i\omega_j t} \end{bmatrix} \begin{Bmatrix} A_j \\ B_j \end{Bmatrix} \quad 1-10$$

Since the x_j are by definition real, A_j and B_j must be complex conjugates and it can be seen that the transformations 1-10 and 1-7 are identical.

In practice, the polar transformation is used to obtain the steady-state curves. For stability analysis the use of the rectangular transformation is more convenient.

(b) Structure of the Averaged Equations

The method of averaging presents a unified mathematical approach to dynamic resonance problems. On the basis of the averaged equations the dynamic resonances can be classified and the nature of the response obtained. In many cases it is possible to obtain the regions of instability and steady-state curves by algebraic means and the transient motion can be obtained through step by step integration.

Resonance conditions can occur as a result of the interaction of the system's natural frequencies with the external excitation frequency or as a result of an interaction of natural frequencies only. The former will be called external resonance and the latter internal resonance. Internal and external resonances may occur simultaneously in a given dynamical system.

The number of first order equations of the type necessary for the analysis is governed by the number of modes that participate in the resonance conditions^[45]. If M is the number of modes $2M$ equations are necessary. However, if only one resonance condition occurs the phase angles can be combined and the number of equations reduced to $M + 1$. For

each additional resonance condition the equations are increased correspondingly up to $2M$. Each additional resonance condition complicates the equations and can completely alter the nature of the response.

If the forces ϵf_j of Equation 1-1 are analytic, single valued functions of the co-ordinates x_j and their time derivatives \dot{x}_j and f_j is periodic in Ωt then f_j can be expanded in the Taylor series.

$$\begin{aligned}
 f_j(\eta_1, \eta_2, \dots, \eta_{2n}, t) &= \sum_{m=-N}^N c_m e^{im\Omega t} f_m(\eta_1, \eta_2, \dots, \eta_{2n}) \\
 &= \sum_{m=-N}^N c_m e^{im\Omega t} \left[f_m^0(0, 0, \dots) \right. \\
 &\quad + \sum_{k=1}^{2n} \left(\frac{\partial f_m}{\partial \eta_k} \right)_0 \eta_k + \frac{1}{2!} \sum_{r,s} \left(\frac{\partial^2 f_m}{\partial \eta_r \partial \eta_s} \right)_0 \eta_r \eta_s \\
 &\quad \left. + \frac{1}{3!} \sum_{r,s,\ell} \left(\frac{\partial^3 f_m}{\partial \eta_r \partial \eta_s \partial \eta_\ell} \right)_0 \eta_r \eta_s \eta_\ell + \dots \right]
 \end{aligned} \tag{1-11}$$

where the η_j representing displacements and velocity. They are taken as small deviations from the equilibrium position. If the variables η_j are so small (throughout the motion of the system) that higher order terms can be ignored, the problem is linear. As the amplitudes increase the higher order terms begin to take effect. Breaking off the series after the third order term allows one to examine many of the important non-linear effects in the system.

Substituting 1-11 into 1-6 and carrying out the averaging process, the constant terms are the only non zero terms after the integration process. They have a long term effect on the behaviour of the variables Q_j and θ_j . As the coefficients of the trigonometric terms in f_j are stipulated to be polynomials the terms under the integral signs can be expanded and are of the form:

$$\frac{\sin}{\cos} \left\{ (m\Omega + n_1\omega_1 + n_2\omega_2 + \dots)t + n_1\theta_1 + n_2\theta_2 + \dots \right\} \quad 1-12a$$

or

$$\frac{\sin}{\cos} \left\{ (n_1\omega_1 + n_2\omega_2 + \dots)t + n_1\theta_1 + n_2\theta_2 + \dots \right\} \quad 1-12b$$

$$\left. \begin{array}{l} m > 0 \\ n_j > 0 \\ \quad < 0 \end{array} \right\} \text{integer}$$

If the frequencies of these terms are zero, i.e.

$$(m\Omega + n_1\omega_1 + n_2\omega_2 + \dots) = 0, \text{ the terms}$$

$$\frac{\sin}{\cos} \left\{ n_1\theta_1 + n_2\theta_2 + \dots \right\} \quad 1-13$$

will carry over into the averaged equations and cause an external or internal resonance condition depending on the presence of or absence of Ω the external excitation frequency. Thus the resonance condition according to the first approximation is

$$\Omega = \left| \frac{n_1\omega_1 + n_2\omega_2 + \dots}{m} \right| \quad 1-14a$$

If f_j is limited to a single frequency external excitation and $m = 1$, then

$$\Omega = | n_1 \omega_1 + n_2 \omega_2 + \dots | \quad 1-14b$$

For the general system excited by several periodic forms Malkin^[30] gives the resonance condition as

$$\sum_{k=1}^n m_k \Omega_k = \sum_{k=1}^l n_k \omega_k \quad 1-14c$$

$$m_k = 0, \pm 1, \pm 2, \dots; \quad n_k = 0, \pm 1, \pm 2, \dots$$

(c) Introduction of a Detuning

It is often desired to study the response in the neighbourhood of a critical resonance zone. To do this, a detuning is introduced either in the natural frequencies or in the external frequency or both. By introducing this detuning, the equations 1-1 can be written in the form

$$\ddot{x}_j + (\omega_j^\circ + \varepsilon \Delta_j)^2 x_j + \varepsilon f_j = 0 \quad 1-15a$$

where $\omega_j = \omega_j^\circ + \varepsilon \Delta_j$ and the ω_j° are chosen to satisfy exactly the resonance condition which is being investigated. The detuning now acts as an additional perturbation force proportional to ε

$$\ddot{x}_j + \omega_j^\circ{}^2 x_j + \varepsilon [2\omega_j^\circ \Delta_j x_j + f_j] = 0 \quad 1-15b$$

and has an important effect on the response.

(d) Nature of Response

Depending on the resonance conditions, detuning, damping, and nonlinear effects the response of the averaged equations in terms of amplitude and phase can be classified in the following four ways.

(a) Non-Resonant Response $Q_j = 0, \theta_j = \text{undetermined}$

The frequency of the external excitation is outside the possible resonance zone. The response of the system subjected to any initial disturbance will approach zero if damping is present in the system.

(b) Resonant Steady-State Response $Q'_j = 0, \theta'_j = 0$

The amplitudes Q_j and phase θ_j have constant values. This is a fully synchronized state and the frequencies of the response modes are entrained to their natural frequencies for a finite amount of detuning.

(c) Resonant, Partially Synchronized Response

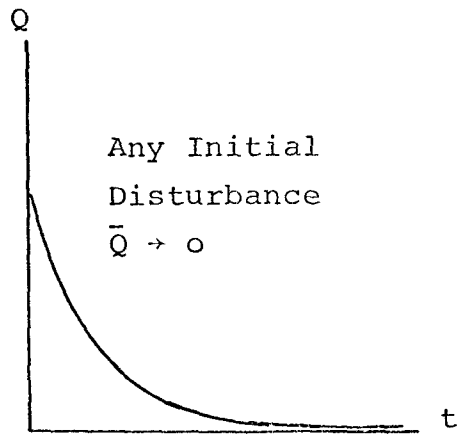
$$Q'_j = 0, (\theta_i + \theta_j)' = 0$$

This state may occur in systems of two degrees or higher where only one resonance condition occurs. Individual frequency corrections are possible but the combined effect of the frequency correction cancels so that the combined phase angles of all participating modes remain constant.

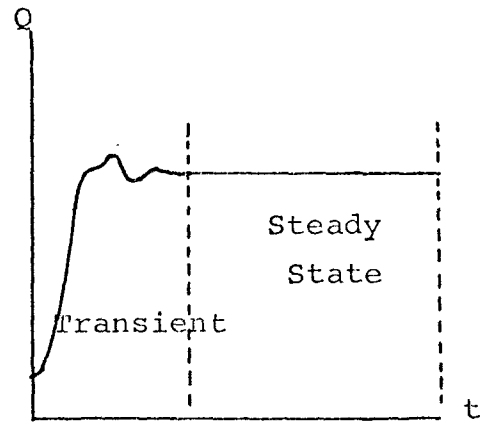
(d) Resonant-Quasi-Steady-State Response

$$Q'_j \neq 0, \theta'_j \neq 0$$

This system is in a resonant state with high modulated amplitude. This state can occur in a one degree of freedom system with large excitation parameters^[4]. In multiple degree of freedom systems this modulated response can also occur with damping present^[45].



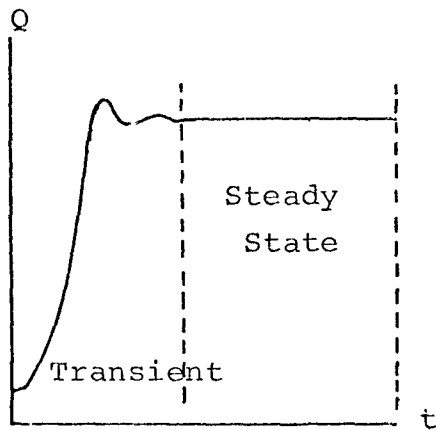
(a)



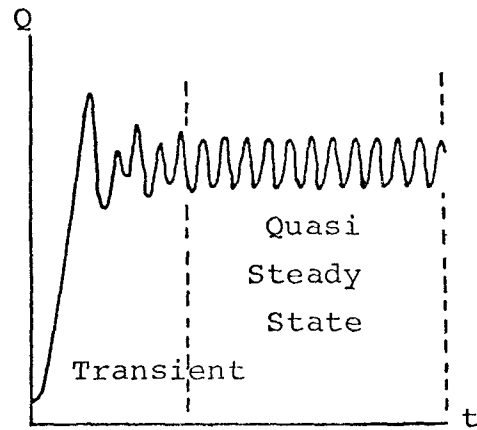
(b)

Non-Resonant Response

Resonant Steady-State Response



(c)



(d)

Resonant Partially Synchronized Response

Quasi-Steady-State Response

FIG. 1.1 NATURE OF RESPONSE

Cases (a) and (b) are the usual response conditions for the one degree of freedom system. For resonance to occur the phase angle relationship given by 1-13 must reach a constant state. This means that the detuning is restricted to a range of values dependent on damping and the strength of the excitation. Outside this allowable range of detuning, a resonance condition can not occur.

Systems having more than one degree of freedom can demonstrate a variety of phenomena that have no counterpart in single degree systems, as the response may depend on the interaction of modes. These systems may exhibit the type of response indicated by case (c) and (d) as well as (a) and (b).

(e) On the Classification of Resonances

Dynamic resonances in nonlinear systems can be divided into two categories. The first category concerns itself with systems in which a resonance condition can develop in the linear equations. The interest is then to see how the response is modified by the nonlinearities. The second category concerns itself with those resonance conditions that are only possible in nonlinear systems. Both categories have received extensive classification^[33,53,13] based according to the integers retained in 1-14a. By restricting the classification to only those resonances possible in linear systems subjected to monofrequency excitation as described by the averaged equations an external resonance can occur only in the following four cases: (a) $\Omega \approx \omega_j$ (b) $\Omega \approx 2\omega_j$ (c) $\Omega \approx \omega_j + \omega_k$ and (d) $\Omega \approx \omega_j - \omega_k$. The first case is called ordinary forced resonance, the second, parametric resonance (type I), the third, parametric combination plus resonance (type II), and the fourth parametric combination minus resonance (type II).

1.4 Scope of Investigation

The problems investigated in this thesis fall into two groups. The first group concerns the inter-action of dynamic resonances in nonlinear systems where the nonlinearities can be expressed as analytic, single valued functions of the generalized displacements. The second group concerns the response of nonlinear systems where the nonlinear functions are considered to be hysteretic and are non-analytic, multi-valued functions of the generalized displacements.

The interaction of resonance zones is divided into two chapters - Chapter 2 is devoted to the interaction of an external and internal resonance zone. A thin-walled beam excited by pulsating end-moments is considered. The parameters of the beam are chosen in such a way that both an external and internal resonance condition takes place simultaneously. The interaction of two external resonance zones is investigated in Chapter 3. The physical model used in the investigation is the double-pendulum of Ziegler^[58] subjected to a non-conservative thrust-type loading, where it is assumed that the thrust has a sinusoidal time-varying components. The interaction problem that is studied is the simultaneous occurrence of two parametric resonances. The effect of viscous damping is also included.

The response of a single degree of freedom hysteretic system subjected to parametric excitation is investigated in Chapter 4. A comparison is made on the parametric response of the bilinear, double bilinear and the Ramberg-Osgood hysteretic system. A detailed description of these hysteretic modals is given in Appendix A. Finally, the parametric response of two degree of freedom hysteretic systems is presented in Chapter 5 and Chapter 6.

The purpose of the present study is twofold: firstly, to examine new phenomena due to the interaction of resonances and secondly, to investigate the effect of hysteretic damping in parametrically excited dynamical systems.

CHAPTER II

COMBINATION RESONANCE AND INTERNAL RESONANCE OF THIN-WALLED STRUCTURES

2.1 Introduction

It is a modern feature of construction that more and more emphasis is placed on structures with long slender, lightweight members. In particular, thin-walled beams of open section are the common elements used in such structures. If these structures are exposed to periodic excitation the result is that a large number of possible resonance zones may be excited. Large amplitude vibrations will result if the excitation is in a resonant or near resonant zone.

Concerning the forced vibration of thin-walled structures, a distinction must be made between the forcing functions which are independent of the response of the system and those that are dependent upon the response. The former falls in the category of ordinary forced vibration. The latter is called parametric excitation and is the characteristic loading condition studied in the Theory of Dynamic Stability^[4]. The purpose of this chapter will be to investigate the latter loading condition. The majority of the work in dynamic stability concerns itself with the case when the frequency of the external excitation is approximately twice one of the natural frequencies of the structure. These regions are the principal unstable regions and the dynamic resonance is called parametric resonance Type I. In addition, principal regions of dynamic stability may occur if the external excitation frequency is equal to a combination of natural frequencies. Such resonance is called parametric resonance Type II. If the

analysis is limited to parametric resonance Type I the analysis can be based on a single nonlinear Mathieu-type equation. The analysis becomes more complicated for the Type II parametric resonances. If the frequencies of the problem are such that only one resonance condition is satisfied, it is still possible to obtain steady-state solutions in algebraic form. However, when more than one resonance condition is present in the system, the resulting analysis is not amenable to any simple format. In fact there is no guarantee that a steady-state solution is possible.

A special feature of nonlinear dynamical systems is the possibility of transferring energy from one mode to another mode within the system. Such transfer is possible due to the nonlinear coupling between the modes. This ability to transfer energy depends on the frequency relationship and the structure of the nonlinear coupling between the modes. Such a phenomenon is called internal resonance. Internal resonance in the absence of an external excitation has been studied^[49], the interaction of internal resonance and ordinary forced resonance has been investigated by Miles^[35] and Sethna^[46]. However, all studies of resonances in parametrically excited systems have assumed that the ratios of the natural frequencies in the system are such that an internal resonance will not occur. If an internal resonance condition does occur two things may happen.

(a) An otherwise dormant mode may begin large amplitude vibrations which was not directly excited by the external source.

(b) A non-linear interaction between two externally excited modes may take place.

Case (b) will be investigated in this chapter. Both modes are already externally excited and both amplitudes begin to grow under the action of the dynamic loading. The amplitudes will in general be different for the different modes. A number

of questions immediately come to mind. Will the amplitudes influence themselves in such a way that the overall maximum response will be more? Will there be a continual exchange of energy between the modes with the result that a steady-state motion can not exist? If such a modulated response occurs, is it possible that the amplitudes of the modulated response caused by the internal resonance condition may exceed that if internal resonance had not been considered?

These are important questions to be answered because the response behaviour of a large class of structural systems due to the existence of more than one dynamic resonance condition is completely unknown. For design purposes it is important to know the amplification factor caused by the occurrence of an internal resonance condition. Bolotin^[4] and Mettler^[32] have treated the nonlinear response of thin-walled beams when only one resonance condition was possible. Bolotin treated the parametric resonance case Type I and Mettler the parametric resonance Type II.

It is the purpose of the present Chapter to examine the nonlinear equations of a thin-walled beam subjected to parametric excitation. The equations of motion are reduced to a system of two nonlinear ordinary differential equations. The parameters of the system are chosen such that both parametric resonance and internal resonance occurs simultaneously. The effect of viscous damping is included in the analysis. Only the parametric resonance type II (combination resonance) is considered.

2.2 Derivation of the Equations of Motion

Consider a thin-walled beam of uniform cross-section area A and length L simply supported in flexural and rotational deformation but restrained from axial shortening. The section is symmetrical and warp free and loaded by a periodic end moment $M = M_0 \cos \Omega t$, acting in the plane of largest

rigidity^[32]. The equations that describe the lateral and torsional oscillations of the beam are:^[4]

$$EI_y \frac{\partial^4 u}{\partial z^4} + M_o \cos(\Omega t) \frac{\partial^2 \phi}{\partial z^2} - \Delta N \frac{\partial^2 u}{\partial z^2} + m \frac{\partial^2 u}{\partial t^2} = 0 \quad 2-1a$$

$$M_o \cos(\Omega t) \frac{\partial^2 u}{\partial z^2} - GI_d \frac{\partial^2 \phi}{\partial z^2} - \Delta N \rho^2 \frac{\partial^2 \phi}{\partial z^2} + m \rho^2 \frac{\partial^2 \phi}{\partial t^2} = 0 \quad 2-1b$$

with the boundary conditions

$$\frac{\partial^2 u}{\partial z^2} = \frac{\partial^2 \phi}{\partial z^2} = 0, u = 0, \phi = 0, z = 0, \text{ and } z = L \quad 2-2$$

EI_y is the bending stiffness in lbs in^2 , GI_d is the torsional stiffness in lbs in^2 , u is the lateral displacement of the centroid (in), ϕ is the angle of rotation in radius, m is the mass per unit lengths $\frac{\text{lbs sec}^2}{\text{in}^2}$, ρ^2 is the radius of gyration

(in^2), M_o is the amplitude of the external moment in in.lbs. and Ω is the frequency of the external excitation. The axial force ΔN is not an impressed axial force but is developed by the axial tension caused when the beam is deflected from its equilibrium position into lateral, torsional movement.

The periodic load can be expected to excite bending vibrations in the plane of action of the load (Y-z plane). This load also appears as a parametric load with respect to the lateral bending and torsional modes of motion. The beam is considered dynamically stable if small lateral and torsional perturbations are damped out with time. But if small initial

perturbations give rise to intensive bending-torsional vibrations, the beam is considered dynamically unstable and is parametrically excited by the end couples. The present analysis is focused on the lateral bending and torsional response of the system once it is parametrically excited into resonance. For convenience, it is assumed that the frequency of the load is far enough removed from one of the natural frequencies of bending in the strong direction so that little dynamical amplification of the inplane displacement exists.

(a) Nonlinear Forces

When the beam is excited into lateral, torsional movement a shortening effect takes place due to the twisting and bending of the cross section. The shortening effect due to lateral bending was examined by Mettler^[4], the shortening effect due to torsion was first explored by Cullimore^[9]. The nonlinear force terms due to the shortening effect of bending and torsion can be obtained as follow:

Shortening Effect Due To Bending: Let ds be a segment of the centre line of the deformed beam as shown in Fig. 2-1a.

Let e denote the strain. Then

$$e = \frac{ds - dz}{dz} \quad 2-3a$$

$$= \frac{\sqrt{dz^2 + \left(\frac{\partial u}{\partial z}\right)^2 dz^2}}{dz} - dz \quad 2-3b$$

$$\approx \frac{1}{2} \left(\frac{\partial u}{\partial z}\right)^2 \quad 2-3c$$

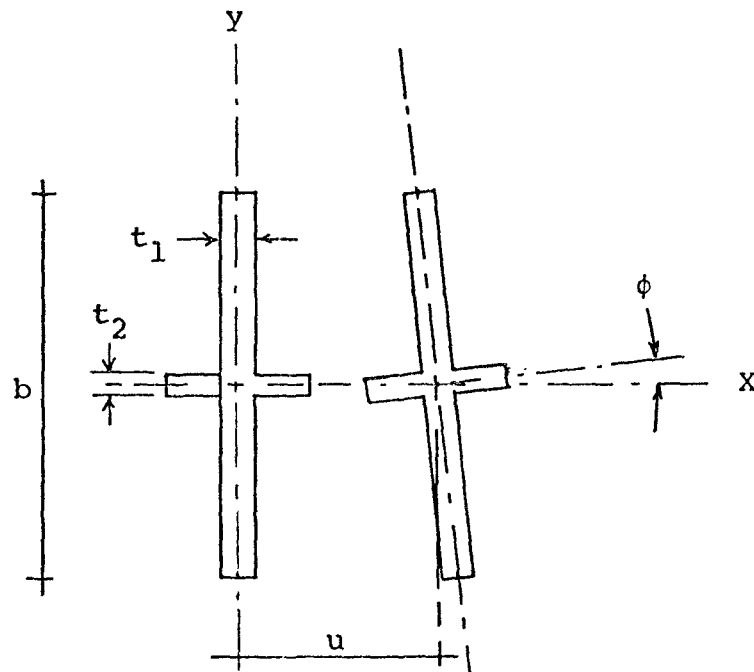


Fig. 1a Cross Section of Member

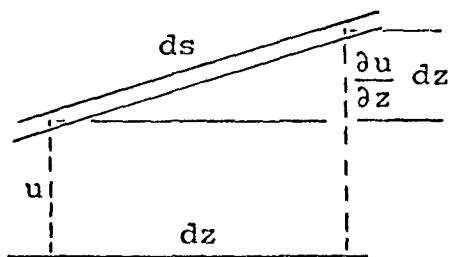


Fig. 1b Bending

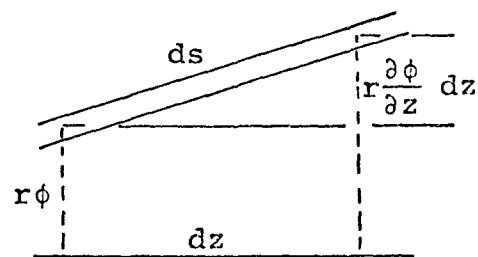


Fig. 1c Twisting

FIG. 2-1 CROSS-SECTION OF WARP-FREE
THIN-WALLED BEAM

The strain due to bending of the total length is

$$\Delta_{\text{Bending}} = + \frac{1}{2L} \int_0^L \left(\frac{\partial u}{\partial z} \right)^2 dz \quad 2-4$$

The axial force developed because the beam is restrained from movement in the axial direction is

$$\begin{aligned} \Delta N_{\text{Bending}} &= EA \Delta_B \\ &= + \frac{EA}{2L} \int_0^L \left(\frac{\partial u}{\partial z} \right)^2 dz \end{aligned} \quad 2-5$$

Shortening Effect Due to Torsion: Let ds be a segment of a longitudinal fibre a distance r from the centroid as shown in Fig. 1c. Then the strain due to twist is approximately

$$e \approx \frac{1}{2} r^2 \left(\frac{\partial \phi}{\partial z} \right)^2 \quad 2-6$$

The strain at the centre-line if it is assumed that plane sections remain plane can be obtained by equating forces over the cross section.

and

$$e_{\text{centre}} = \frac{1}{2} \left(\frac{\partial \phi}{\partial z} \right)^2 \frac{1}{A} \int_A y^2 dA \quad 2-7a$$

$$= \frac{1}{2} \frac{I_p}{A} \left(\frac{\partial \phi}{\partial z} \right)^2 \quad 2-7b$$

and the total shortening over the length of the beam is

$$\Delta_T = \frac{1}{2} \frac{I_\rho}{A} \int_0^L \left(\frac{\partial \phi}{\partial z} \right)^2 dz \quad 2-8$$

and the axial force developed is

$$\Delta N_T = \frac{\Delta_T EA}{L} \quad 2-9a$$

$$= + \frac{1}{2} \frac{E I_\rho}{L} \int_0^L \left(\frac{\partial \phi}{\partial z} \right)^2 dz \quad 2-9b$$

The combined axial force due to bending and twisting is

$$\Delta N = + \frac{1}{2} \frac{E}{L} \int_0^L \left\{ A \left(\frac{\partial u}{\partial z} \right)^2 + I_\rho \left(\frac{\partial \phi}{\partial z} \right)^2 \right\} dz \quad 2-10$$

Inserting the axial force ΔN into equations 2-1 there results:

$$\left. \begin{aligned} EI_Y \frac{\partial^4 u}{\partial z^4} + M_O \cos(\Omega t) \frac{\partial^2 \phi}{\partial z^2} - \frac{1}{2} \frac{E}{L} \left\{ \int_0^L \left\{ A \left(\frac{\partial u}{\partial z} \right)^2 \right. \right. \\ \left. \left. + I_\rho \left(\frac{\partial \phi}{\partial z} \right)^2 \right\} dz \right\} \end{aligned} \right\} \frac{\partial^2 u}{\partial z^2} + m \frac{\partial^2 u}{\partial t^2} = 0 \quad 2-11a$$

$$\left. \begin{aligned} M_O \cos(\Omega t) \frac{\partial^2 u}{\partial z^2} - GI_d \frac{\partial^2 \phi}{\partial z^2} - \frac{\rho^2}{2} \frac{E}{L} \left\{ \int_0^L \left\{ A \left(\frac{\partial u}{\partial z} \right)^2 \right. \right. \\ \left. \left. + I_\rho \left(\frac{\partial \phi}{\partial z} \right)^2 \right\} dz \right\} \end{aligned} \right\} \frac{\partial^2 \phi}{\partial z^2} + m \rho^2 \frac{\partial^2 \phi}{\partial t^2} = 0 \quad 2-11b$$

This is the system of partial differential equations which describes the lateral and torsional response of the structure due to the periodic moment. The axial forces cause nonlinear forces to develop when the motions become large.

(b) Reduction to Ordinary Differential Equations

An approximate solution of 2-11 can be obtained. Let

$$u(z,t) = x_1(t) \sin \frac{\pi z}{L} \quad 2-12$$

$$\phi(z,t) = x_2(t) \sin \frac{\pi z}{L} \quad 2-13$$

where we limit the expansion of u and ϕ to one mode in translation and one in rotation. Substituting 2-12,13 into 2-11a and applying the Galerkin averaging technique, there is obtained

$$\begin{aligned} \frac{d^2 x_1}{dt^2} + \frac{EI_y}{m} \left(\frac{\pi}{L}\right)^4 x_1 - \frac{M_o}{m} \left(\frac{\pi}{L}\right)^2 \cos(\Omega t) x_2 \\ + \frac{1}{4} \frac{EA}{m} \left(\frac{\pi}{L}\right)^4 x_1^3 + \frac{1}{4} \frac{EI_\rho}{m} \left(\frac{\pi}{L}\right)^4 x_2^2 x_1 = 0 \end{aligned} \quad 2-14$$

Similarly substituting 2-12,13 in 2-11b there results

$$\begin{aligned} \frac{d^2 x_2}{dt^2} + \frac{GI_d}{m\rho} \left(\frac{\pi}{L}\right)^2 x_2 - \frac{M_o \cos(\Omega t)}{m\rho} \left(\frac{\pi}{L}\right)^2 x_1 \\ + \frac{1}{4} \frac{EI_\rho}{m} \left(\frac{\pi}{L}\right)^4 x_2^3 + \frac{1}{4} \frac{EA}{m} \left(\frac{\pi}{L}\right)^4 x_2 x_1^2 = 0 \end{aligned} \quad 2-15$$

2.3 Statement of the Problem

Equations 2-14 and 2-15 are a quasi-linear system of ordinary differential equations with periodic coefficients which in matrix notation can be written as.

$$\begin{aligned}
 & \begin{bmatrix} 1 & 0 \\ 0 & 1 \end{bmatrix} \begin{Bmatrix} \ddot{x}_1 \\ \ddot{x}_2 \end{Bmatrix} + \varepsilon \begin{bmatrix} e_1 & 0 \\ 0 & e_2 \end{bmatrix} \begin{Bmatrix} \dot{x}_1 \\ \dot{x}_2 \end{Bmatrix} + \begin{bmatrix} \omega_1^2 & 0 \\ 0 & \omega_2^2 \end{bmatrix} \begin{Bmatrix} x_1 \\ x_2 \end{Bmatrix} \\
 & - \varepsilon \cos(\Omega t) \begin{bmatrix} 0 & b_1 \\ b_2 & 0 \end{bmatrix} \begin{Bmatrix} x_1 \\ x_2 \end{Bmatrix} + \varepsilon \begin{bmatrix} a_1 & 0 \\ 0 & a_2 \end{bmatrix} \begin{Bmatrix} x_1^3 \\ x_2^3 \end{Bmatrix} \\
 & + \varepsilon \begin{bmatrix} d_1 & 0 \\ 0 & d_2 \end{bmatrix} \begin{Bmatrix} x_1 x_2^2 \\ x_1^2 x_2 \end{Bmatrix} = \begin{Bmatrix} 0 \\ 0 \end{Bmatrix}
 \end{aligned}
 \tag{2-16}$$

where $\varepsilon \ll 1$, $x_1(t)$ and $x_2(t)$ represent the generalized co-ordinates of the system. x_1 represents the lateral deflection in the minor axis direction and x_2 the rotation of the section as specified by equations 2-12. The e_j , ω_j , ($j = 1, 2$) denote the damping coefficients and natural frequencies associated with mode j . The fourth term represents the pair of equal but opposite periodic moments applied to the end of the beam in the plane of the major axis and consists of a monofrequent parametric excitation. It should be noted that the matrix associated with this term is antisymmetric and consequently it can be shown that parametric resonance of the first kind cannot occur in this system. With the coefficients b_1 , b_2

taken to be positive only combination resonance of the sum type can occur. The nonlinear terms in the system consist of a cubic nonlinearly associated with each coordinate with coefficients a_1 and a_2 and the last term in the equation represents the nonlinear coupling between x_1 and x_2 with the coefficients d_1 and d_2 . Mathematically, the coefficients are defined as

$$\omega_1^2 = \frac{EI}{m} \left(\frac{\pi}{L} \right)^4 \quad 2-17a$$

$$\omega_2^2 = \frac{GI_d}{m\rho} \left(\frac{\pi}{L} \right)^2 \quad 2-17b$$

$$\epsilon b_1 = \frac{M_o}{m} \left(\frac{\pi}{L} \right)^2 \quad 2-17c$$

$$\epsilon b_2 = \frac{M_o}{m\rho} \left(\frac{\pi}{L} \right)^2 \quad 2-17d$$

$$\epsilon a_1 = \frac{1}{4} \frac{EA}{m} \left(\frac{\pi}{L} \right)^4 \quad 2-17e$$

$$\epsilon a_2 = \frac{1}{4} \frac{EI_\rho}{m} \left(\frac{\pi}{L} \right)^4 \quad 2-17f$$

$$\epsilon d_1 = \frac{1}{4} \frac{EI_\rho}{m} \left(\frac{\pi}{L} \right)^4 \quad 2-17g$$

$$\epsilon d_2 = \frac{1}{4} \frac{EA}{m} \left(\frac{\pi}{L} \right)^4 \quad 2-17h$$

Equation 2-16 is a homogeneous system and $x_1 \equiv x_2 \equiv 0$ is a solution. The central problem in the present analysis is to find the non trivial solutions.

Neglecting the nonlinear terms and the damping terms, the equation 2-16 has been studied by Mettler^[4] to determine the condition under which non-trivial solutions exist. It was found that a combination resonance condition exists provided the external frequency Ω and the natural frequencies ω_1 and ω_2 satisfy the condition

$$\Omega \approx \omega_1 + \omega_2 \quad 2-18$$

Including the uncoupled cubic nonlinearities in the system Mettler further determined the steady-state amplitude of $x_1(t)$ and $x_2(t)$ once combination resonance takes place^[4]. Schmidt and Weidenhammer^[44] neglected the nonlinear terms in equation 2-16 to study the effect of viscous damping on the conditions under which combination resonance is possible. It was found that unequal damping coefficients in the system have a destabilizing effect. In other words, a system with unequal damping coefficients is more susceptible to combination resonance than the one with equal damping coefficients. Hagedorn^[15] included nonlinear cubic velocity dependent damping terms in the equation to find that the destabilizing effect of damping is not only confined to linear viscous damping. In all the above investigations, the non-linear coupling terms $x_1^2 x_2$ and $x_1 x_2^2$ were neglected and the two co-ordinates were only coupled by the parametric excitation term. In this case, the problem of internal resonance does not arise. In this chapter, equation 2-16 will be studied under the conditions where both the combination resonance condition and the internal resonance condition are approximately satisfied.

It is convenient to express equations 2-16 in terms of nondimensional variables. Using the non-dimensional time variable τ defined by

$$\tau \equiv \Omega t$$

2-19

equation 2-16 can be written as

$$\begin{aligned} x_1'' + E_1 x_1' + K_1^2 x_1 + 2K_1^2 (\Delta_1 + \lambda) x_1 + A_1 x_1^3 - B_1 \cos(\tau) x_2 \\ + D_1 x_1 x_2^2 = 0 \end{aligned} \quad 2-20a$$

$$\begin{aligned} x_2'' + E_2 x_2' + K_2^2 x_2 + 2K_2^2 (\Delta_2 + \lambda) x_2 + A_2 x_2^3 - B_2 \cos(\tau) x_1 \\ + D_2 x_1^2 x_2 = 0 \end{aligned} \quad 2-20b$$

where

$$K_j = \omega_j^\circ / \Omega^\circ \quad 2-21a$$

$$A_j = \epsilon a_j / (\Omega^\circ)^2 \quad 2-21b$$

$$B_j = \epsilon b_j / (\Omega^\circ)^2 \quad 2-21c$$

$$D_j = \epsilon d_j / (\Omega^\circ)^2 \quad 2-21d$$

$$E_j = \epsilon e_j / \Omega^\circ \quad 2-21e$$

$$\omega_j = \omega_j^\circ (1 + \Delta_j) \quad (j = 1, 2) \quad 2-21f$$

$$\text{and} \quad \Omega = \Omega^\circ (1 - \lambda) \quad 2-21g$$

Ω° , ω°_1 and ω°_2 represent the nominal value of the parametric frequency and natural frequencies of the system. λ , Δ_1 , and Δ_2 are small quantities representing small detuning of the actual frequencies from the nominal values. Primes denote differentiation with respect to the nondimensional time τ .

2.4 Derivations of the Averaged Equations

An approximate solution of equations 2-20 can be obtained by the method of averaging. Realizing that the periodic excitation and the non-linear terms act as small perturbations to the free vibration of the system, the solutions can be approximated by

$$x_j(\tau) = Q_j(\tau) \cos(K_j\tau + \theta_j(\tau)) \quad 2-22a$$

$$\equiv Q_j \cos \psi_j \quad (j = 1, 2) \quad 2-22b$$

where $Q_j(\tau)$ and $\theta_j(\tau)$ can be considered as slowly varying functions of time. Stipulating that

$$x'_j = -Q_j(\tau) K_j \sin \psi_j \quad 2-22c$$

the system of equations 2-20 can be replaced by the system of first order equations.

$$\begin{bmatrix} \cos \psi_j & -Q_j \sin \psi_j \\ -K_j \sin \psi_j & -Q_j K_j \cos \psi_j \end{bmatrix} \begin{Bmatrix} Q_j' \\ \theta_j' \end{Bmatrix} = \begin{Bmatrix} 0 \\ -\epsilon f_j \end{Bmatrix} \quad 2-22d$$

(j = 1, 2)

where

$$\begin{aligned}
 \epsilon f_j = & - E_j Q_j K_j \sin \psi_j + 2K_j^2 (\Delta_j + \lambda) Q_j \cos \psi_j \\
 & + A_j Q_j^3 \cos^3 \psi_j - B_j \cos(\tau) Q_m \cos \psi_m \quad 2-23 \\
 & + D_j Q_j \cos \psi_j Q_m^2 \cos^2 \psi_m \quad (j = 1, 2, m = 1, 2) \\
 & \quad \quad \quad j \neq m
 \end{aligned}$$

Equations 2-22d are an exact representation of the system 2-20. To obtain an approximate asymptotic solution of equations 2-22d the method of averaging is applied. This consists of taking the mean values of the terms occurring in 2-22d. These equations can be expanded into the format

$$Q'_j = \frac{\epsilon f_j}{K_j} \sin \psi_j \quad 2-24a$$

$$(j = 1, 2)$$

$$Q_j^{\theta'} = \frac{\epsilon f_j}{K_j} \cos \psi_j \quad 2-24b$$

The mean value is defined by the integration process.

$$Q'_j = \lim_{T \rightarrow \infty} \frac{1}{T} \int_0^T \frac{\epsilon f_j}{K_j} \sin \psi_j dt \quad 2-25a$$

$$Q_j^{\theta'} = \lim_{T \rightarrow \infty} \frac{1}{T} \int_0^T \frac{\epsilon f_j}{K_j} \cos \psi_j dt \quad 2-25b$$

where the variables Q_j , θ_j are considered as constants during the averaging process. Only the terms that are constant can be expected to have a long-term effect on the slowly varying variables and it is these terms that will enter over into the averaged equations. If the integrands of 2-25 are periodic the integration can be carried over a specific period. In general, however, the integrands are almost periodic functions and the averaging process consist of taking the mean values of each term after the integrand has been expanded. Expanding 2-24 there is obtained

$$\begin{aligned}
 Q'_j &= 2K_j[\Delta_j + \lambda] Q_j \cos \psi_j \sin \psi_j - \frac{B_k Q_k}{K_j} \cos \psi_k \sin \psi_j \cos \tau \\
 &- E_j Q_j \sin^2 \psi_j + \frac{A_j}{K_j} Q_j^3 \cos^3 \psi_j \sin \psi_j \\
 &+ \frac{D_j}{K_j} Q_j Q_k^2 \cos \psi_j \cos^2 \psi_k \sin \psi_j
 \end{aligned} \tag{2-26a}$$

$$\begin{aligned}
 Q_j \theta'_j &= 2K_j Q_j [\Delta_j + \lambda] \cos^2 \psi_j - \frac{B_k Q_k}{K_j} \cos \psi_k \cos \psi_j \cos \tau \\
 &- E_j Q_j \cos \psi_j \sin \psi_j + \frac{A_j}{K_j} Q_j^3 \cos^4 \psi_j \\
 &+ \frac{D_j}{K_j} Q_k^2 Q_j \cos^2 \psi_j \cos^2 \psi_k
 \end{aligned} \tag{2-26b}$$

(j \neq k)

(j = 1, 2)

(k = 1, 2)

(a) External Resonance: The external resonance terms are those terms multiplied by the parametric coefficient B_j . Expanding $\sin \psi_j \cos \psi_k \cos \tau$ leads to terms.

$$\sin \{(K_j \pm K_k \pm 1)\tau + \theta_j \pm \theta_k\} \quad 2-27a$$

it is seen that a resonance term will only occur if

$$K_j \pm K_k - 1 = 0 \quad 2-27b$$

similarly $\cos \psi_j \cos \psi_k \cos \tau$ will lead to terms.

$$\cos \{(K_j \pm K_k \pm 1)\tau + \theta_j \pm \theta_k\} \quad 2-28$$

and the same resonance condition [2-27b] applies.

(b) Internal Resonance: Internal resonance can be caused by those terms multiplied by the nonlinear coupling coefficient D_j . Expanding

$$\begin{aligned} \sin \psi_j \cos \psi_j \cos^2 \psi_k &= \frac{1}{4} \sin 2\psi_j + \frac{1}{8} [\sin(2\psi_j - 2\psi_k) \\ &+ \sin(2\psi_j + 2\psi_k)] \end{aligned} \quad 2-29$$

it can be seen that only the term

$$\sin[2\psi_j - 2\psi_k] = \sin[(2K_j - 2K_k)\tau + 2\theta_j - 2\theta_k] \quad 2-30$$

can lead to an internal resonance condition, if

$$2K_j - 2K_k = 0 \quad 2-31$$

or $\omega_j^0 = \omega_k^0$. Consequently an internal resonance condition can only occur if $\omega_j \approx \omega_k$. A similar conclusion can be drawn by considering the term

$$\cos^2 \psi_j \cos^2 \psi_k \quad 2-32$$

The prime purpose of this chapter is to investigate the situation where both combination resonance and internal resonance occurs simultaneously. Hence it will be assumed in the derivation of the averaged equations that the nominal values of the natural frequencies and the parametric frequency satisfy the following relation.

$$K_1 + K_2 = 1 \quad (\text{combination resonance condition}) \quad 2-35$$

$$K_1 = K_2 = K \quad (\text{internal resonant condition}) \quad 2-36$$

Equation 2-35 specifies that the parametric frequency is approximately equal to the sum of the natural frequencies while equation 2-36 states that the two natural frequencies are approximately the same. It can be seen from equation 2-20 f and g that λ , and $\Delta = \Delta_1 - \Delta_2$ are measures of how close the actual frequencies of the system satisfy the combination resonant and internal resonant condition. They shall be referred to as external detuning and internal detuning respectively in the subsequent analysis.

For thin-walled beams it is very possible that a torsional frequency is approximately the same as a bending frequency. Consequently the study of internal resonance in

addition to external resonance should be of practical interest.

The averaging technique is now applied to the equations 2-26. During the averaging procedure the conditions imposed by the combination resonance 2-35 and internal resonance 2-36 are borne in mind to obtain the non-zero terms in the averaged equations.

$$Q'_1 = \frac{-B_1}{4K} Q_2 \sin(\theta_1 + \theta_2) - \frac{E_1}{2} Q_1 + \frac{1}{8} \frac{D_1}{K} Q_1 Q_2^2 \sin(2\theta_1 - 2\theta_2)$$

2-37a

$$Q'_2 = \frac{-B_2}{4K} Q_1 \sin(\theta_1 + \theta_2) - \frac{E_2}{2} Q_2 - \frac{1}{8} \frac{D_2}{K} Q_2 Q_1^2 \sin(2\theta_1 - 2\theta_2)$$

2-37b

$$\begin{aligned} \theta'_1 = & (\Delta_1 + \lambda)K - \frac{B_1}{4K} \frac{Q_2}{Q_1} \cos(\theta_1 + \theta_2) + \frac{3}{8} \frac{A_1}{K} Q_1^2 \\ & + \frac{1}{4} \frac{D_1}{K} Q_2^2 + \frac{1}{8} \frac{D_1}{K} Q_2^2 \cos(2\theta_1 - 2\theta_2) \end{aligned}$$

2-37c

$$\begin{aligned} \theta'_2 = & (\Delta_2 + \lambda)K - \frac{B_2}{4K} \frac{Q_1}{Q_2} \cos(\theta_1 + \theta_2) + \frac{3}{8} \frac{A_2}{K} Q_2^2 \\ & + \frac{1}{4} \frac{D_2}{K} Q_1^2 + \frac{1}{8} \frac{D_2}{K} Q_1^2 \cos(2\theta_1 - 2\theta_2) \end{aligned}$$

2-37d

where Q_j and θ_j ($j = 1, 2$) are now denoting the average value

of the amplitudes and phase angles over one cycle of oscillation.

Since it is the combination of phase angles that determine the behaviour of equations 2-37 the equations 2-37c and 2-37d are rewritten as:

$$\begin{aligned}
 \frac{d\phi_1}{dt} = & \lambda + (\Delta_1 + \Delta_2)K - \frac{1}{4} \frac{1}{K} \left(B_1 \frac{Q_2}{Q_1} + B_2 \frac{Q_1}{Q_2} \right) \cos \phi_1 \\
 & + \frac{3}{8} \frac{1}{K} \left(A_1 + A_2 \frac{Q_2^2}{Q_1^2} \right) Q_1^2 + \frac{1}{4} \frac{1}{K} \left(D_1 \frac{Q_2^2}{Q_1^2} + D_2 \right) Q_1^2 \\
 & + \frac{1}{8} \frac{1}{K} \left(D_1 \frac{Q_2^2}{Q_1^2} + D_2 \right) Q_1^2 \cos \phi_2
 \end{aligned} \tag{2-37e}$$

$$\begin{aligned}
 \frac{d\phi_2}{dt} = & 2(\Delta_1 - \Delta_2)K - \frac{1}{2K} \left(B_1 \frac{Q_2}{Q_1} - B_2 \frac{Q_1}{Q_2} \right) \cos \phi_1 \\
 & + \frac{3}{4} \frac{1}{K} \left(A_1 - A_2 \frac{Q_2^2}{Q_1^2} \right) Q_1^2 + \frac{1}{2} \frac{1}{K} \left(D_1 \frac{Q_2^2}{Q_1^2} - D_2 \right) Q_1^2 \\
 & + \frac{1}{4} \frac{1}{K} \left(D_1 \frac{Q_2^2}{Q_1^2} - D_2 \right) Q_1^2 \cos \phi_2
 \end{aligned} \tag{2-37f}$$

where $\phi_1 = \theta_1 + \theta_2$

$$\phi_2 = 2\theta_1 - 2\theta_2$$

It is observed that the external detuning λ does not appear in equation 2-37f and that if $\Delta_1 = -\Delta_2$ the internal detuning will not appear in equation 2-37e. In the response plots it will be assumed that $\Delta_1 = -\Delta_2$ and the internal detuning will be defined by the new detuning parameter

$$\begin{aligned}\Delta &= \Delta_1 - \Delta_2 \\ &\equiv 2\Delta_1\end{aligned}\tag{2-37g}$$

In equations 2-37a and 2-37b the first term on the right hand side arises as a result of the fact that the combination resonance condition 2-35 is satisfied, the second term represents the viscous damping contribution, and the third term arises due to the fact that the internal resonance condition 2-36 is satisfied. Similarly, the first term on the right hand side of equations 2-37c and 2-37d is due to detuning, the second term is due to combination resonance, the third and fourth terms represent the contributions due to the nonlinear restoring forces and the last term arises due to internal resonance.

If the natural frequencies of the system are such that internal resonance does not occur, (i.e. $K_1 \neq K_2$), then the last terms in equations 2-37 do not arise as a result of the averaging process. In this case it is convenient to combine equations 2-37c and 2-37d to form a single equation relating the amplitudes Q_1 , Q_2 and the sum of the phase angles $(\theta_1 + \theta_2)$. The averaged equations for the system where the internal resonance condition 2-36 is not satisfied can be written as

$$Q'_1 = -\frac{B_1}{4K_1} Q_2 \sin \phi - \frac{E_1}{2} Q_1\tag{2-38a}$$

$$Q'_2 = -\frac{B_2}{4K_2} Q_1 \sin \Phi - \frac{E_2}{2} Q_2 \quad 2-38b$$

$$\begin{aligned} \Phi' = & [\lambda(K_1 + K_2) + \Delta_1 K_2 + \Delta_2 K_2] - \frac{1}{4} \left(\frac{B_1}{K_1} \frac{Q_2}{Q_1} + \frac{B_2}{K_2} \frac{Q_1}{Q_2} \right) \cos \Phi \\ & + \frac{3}{8} \left(\frac{A_1}{K_1} Q_1^2 + \frac{A_2}{K_2} Q_2^2 \right) + \frac{1}{4} \left(\frac{D_1}{K_1} Q_2^2 + \frac{D_2}{K_2} Q_1^2 \right) \quad 2-38c \end{aligned}$$

$$\text{where } \Phi(\tau) \equiv \theta_1(\tau) + \theta_2(\tau) \quad 2-38d$$

Therefore, the analysis of the system subjected to combination resonance only is simplified, involving the solution of three equations 2-38a, b, c only, while the analysis of the system with combination and internal resonances interacting involves the solution of four equations 2-37a, b, c, d.

The analysis of equations 2-38 is considerably simpler than equations 2-37. It is to be expected that even if $\omega_1 \approx \omega_2$ equations 2-38 can provide certain important details of the response of 2-37. It is evident from the nonlinear terms of 2-37 that the response of 2-38 and 2-37 are similar for sufficiently small amplitudes. Consequently, the boundaries of instability and behaviour at small amplitude levels can be obtained from 2-38. For large amplitude motion however it must be expected that the nonlinear resonance terms will have a marked effect on the amplitude-frequency relationship. It is also to be expected that the response of 2-37 passes over to the response of 2-38 as the detuning of the natural frequencies Δ_1, Δ_2 becomes large.

The study of 2-38 thus forms the background against

which the more complicated analysis of 2-37 will be compared to illustrate the effect of internal resonance on a combination resonant system.

2-4 Steady-State Solutions

(a) Analysis Neglecting Internal Resonance

The steady-state amplitudes Q°_1 and Q°_2 can be found by setting the first derivative terms on the left hand side of equations 2-38 to zero and solving the resulting set of nonlinear algebraic equations. From equations 2-38a and 2-38b, the ratio of the steady state amplitude is found to be

$$\pi \equiv \frac{Q^{\circ}_1}{Q^{\circ}_2} = \sqrt{\frac{\beta}{\gamma\kappa}} \quad 2-39$$

$$\text{and} \quad \sin \phi^{\circ} = \frac{2E_1}{B_1} K_1 \pi \quad 2-40a$$

Therefore,

$$\cos \phi^{\circ} = \pm \left[1 - 4 \left(\frac{E_1 K_1 \pi}{B_1} \right)^2 \right]^{1/2} \quad 2-40b$$

Substituting 2-39 and 2-40b into 2-38c and applying the notation for the ratio of the amplitudes and coefficients.

$$\pi = Q^{\circ}_1/Q^{\circ}_2, \quad \beta = B_1/B_2, \quad \gamma = E_1/E_2, \quad \kappa = K_1/K_2, \quad \alpha = A_1/A_2,$$

$$v = D_1/D_2$$

the steady state response curves for Q°_1 is obtained, namely

$$s(Q^{\circ}_1)^2 = -\delta \pm \frac{1}{4} \left[\frac{B_1 B_2}{K_1 K_2} - 4 E_1 E_2 \right]^{1/2} \left((\gamma)^{1/2} + \left(\frac{1}{\gamma}\right)^{1/2} \right) \quad 2-41a$$

$$\text{and} \quad \delta = \lambda + \Delta_1 K_1 + \Delta_2 K_2 \quad 2-41b$$

$$s = \frac{3}{8} \frac{A_1}{K_1} \left(1 + \frac{\kappa^2 \delta}{\alpha \beta}\right) + \frac{1}{4} \frac{D_1}{K_2} \left(\frac{1}{\nu} + \frac{\gamma}{\beta}\right) \quad 2-41c$$

A plot of equation 2-41 is given in Fig. 2-2 and Fig. 2-3 for equal damping ratios and unequal damping ratios respectively. The equation yields two branches, one stable and one unstable branch. The unstable branch is shown in dashed lines in the graphs.

(b) Analysis Including Internal Resonance

The steady-state amplitudes in this case can be obtained by setting the first derivative terms on the left hand side of equations 2-37 to zero. Due to the existence of the additional internal resonance terms in equations 2-37a and 2-37b, the ratio of the steady-state solutions cannot be obtained as readily. From equations 2-37a and 2-37b one obtains

$$\sin \phi_1 = -\frac{E_1}{B_1} \pi \frac{[1 + \frac{\nu}{2}]}{\gamma \pi^2} \frac{1}{[1 + \frac{\nu}{\beta}]} \quad 2-42$$

$$\sin \phi_2 = 2 \frac{E_1}{D_1} \frac{1}{(Q^{\circ}_2)^2} \frac{[1 - \frac{\beta}{2}]}{\gamma \pi^2} \frac{1}{[1 + \frac{\beta}{\nu}]} \quad 2-43$$

where $\phi_1 = \theta_1 + \theta_2$

$$\phi_2 = 2\theta_1 - 2\theta_2$$

From equations 2-37c, d one obtains

$$\cos \phi_1 = \frac{\pi(\Delta_1 + \lambda)}{B_1} \frac{(-1 + \frac{\nu}{\pi^2})}{(-1 + \frac{\nu}{\beta})} + \frac{3}{2} \frac{A_1}{B_1} (Q^{\circ}_1)^2 \pi \frac{[-1 + \frac{\nu}{\alpha} (\frac{1}{\pi})^4]}{[-1 + \frac{\nu}{\beta}]} \quad 2-44$$

$$= \frac{\pi}{B_1 (-1 + \frac{\nu}{\beta})} [(\Delta_1 + \lambda) (-1 + \frac{\nu}{\pi^2})$$

$$+ \frac{3}{2} (Q^{\circ}_1)^2 A_1 (-1 + \frac{\nu}{\alpha} (\frac{1}{\pi})^4)]$$

$$\cos \phi_2 = \frac{2(\Delta_2 + \lambda)}{D_1} \frac{1}{Q^{\circ}_2 Q^{\circ}_1} \frac{1}{\pi} \frac{[1 - \frac{\pi^2}{\beta}]}{[-\frac{1}{\nu} + \frac{1}{\beta}]} \quad 2-45a$$

$$+ 3 \frac{A_1}{D_1} \frac{[1/(\alpha\pi)^2 - \pi^2/\beta]}{[-1/\nu + 1/\beta]}$$

$$= \frac{\nu\beta}{D_1(\nu - \beta)} \left[\frac{2(\Delta_2 + \lambda)}{(Q^{\circ}_1)^2} \left(\frac{\beta - \pi^2}{\beta} \right) \right.$$

$$\left. + 3A_1 \left(\frac{\beta/(\alpha\pi^2)}{\beta} - \pi^2 \right) \right]$$

$$= \frac{\nu}{D_1(\nu - \beta)} \left[\frac{2(\Delta_2 + \lambda)}{(Q_1^\circ)^2} (\beta - \pi^2) + 3A_1(\beta/(\alpha\pi^2) - \pi^2) \right]$$

For a given set of system parameters and excitation condition equations 2-42, 43, 44 and 45 are the equations to determine the four unknowns Q_1° , π , ϕ_1 and ϕ_2 .

The algebraic equations must satisfy the condition

$$|\sin \phi_j| \leq 1 \quad ; \quad |\cos \phi_j| \leq 1 \quad (j = 1, 2) \quad 2-46$$

With these requirements the equations 2-43 to 2-46 can be examined to determine the approximate limits of the steady-state solutions. Firstly, considering 2-42, it is seen that the parametric excitation represented by B_1 must have a certain threshold value to overcome the effects of viscous friction represented by E_1 . As the coefficients are positive $\sin \phi_1$ will always be negative. Equation 2-43 indicates that the inequalities 2-46 can not be met for $Q_2^\circ \ll 1$ unless the numerator is zero and this suggests that a steady-state may not be possible at low amplitude levels.

Equation 2-44 suggests that steady-state may not be possible for large values of Q_1° because of the free form $Q_1^\circ{}^2$ and equation 2-46 again suggests that a steady state value may not be possible for small values of Q_2° and Q_1° .

The external detuning λ can be eliminated between 2-37c and 2-37d to obtain

$$\Delta_1 - \Delta_2 + B_1(-1/\pi + \pi/\beta) \cos \phi_1^\circ + \frac{3}{2} A_1(Q_1^\circ)^2 (1 - 1/(\alpha\pi)^2) + \frac{D_1}{2} (Q_1^\circ)^2 (1/\pi^2 - 1/\nu) (2 + \cos \phi_2^\circ) = 0 \quad 2-47$$

The procedure for an algebraic trial and error solution is now as follows. A value of \bar{Q}°_1 is chosen and the value of \bar{Q}°_2 is found which when substituted into 2-42 and 2-43 obeys the inequalities 2-46 and simultaneously satisfies the equation 2-47. The corresponding frequency is then found from equation 2-37c and 2-37d and is:

$$(1 - \lambda) = 1 + \Delta_1 - \frac{B_1}{4\pi} \cos \phi^{\circ}_1 + \frac{3}{8} A_1 Q^{\circ}_1{}^2 + \frac{1}{8} D_1 (Q^{\circ}_2)^2 (2 + \cos \phi^{\circ}_2) \quad 2-48$$

Plots of the steady state curves are shown in Figs. 2-2, 3, and 4). All calculations are based on the following data $A_1 = 0.05$, $A_2 = 0.08$, $B_1 = B_2 = 0.05$, $D_1 = 0.06$, $D_2 = 0.09$.

In Fig. 2-2 is shown the steady state curves of Q°_1 as a function of the external detuning parameter λ . It is assumed that the damping coefficients of the system are the same, namely, $E_1 = E_2 = 0.01$. Also the internal detuning $\Delta = \Delta_1 - \Delta_2$ is taken to be zero. It can be seen that by neglecting the effect of internal resonance, (solution of equations 2-38), the steady-state amplitude is underestimated by 30% or more. The unstable branch of the curve is shown in dashed lines.

By changing the damping of the system $E_1 = 0.01$, $E_2 = 0.03$, so that the damping coefficients are no longer equal, the corresponding steady-state curves for Q°_1 and Q°_2 are shown in Figs. 2-3 and 2-4 respectively. A number of interesting features can be observed by comparing Figs. 2 and 3. First, the range of detuning frequencies over which combination resonance becomes possible is increased for the

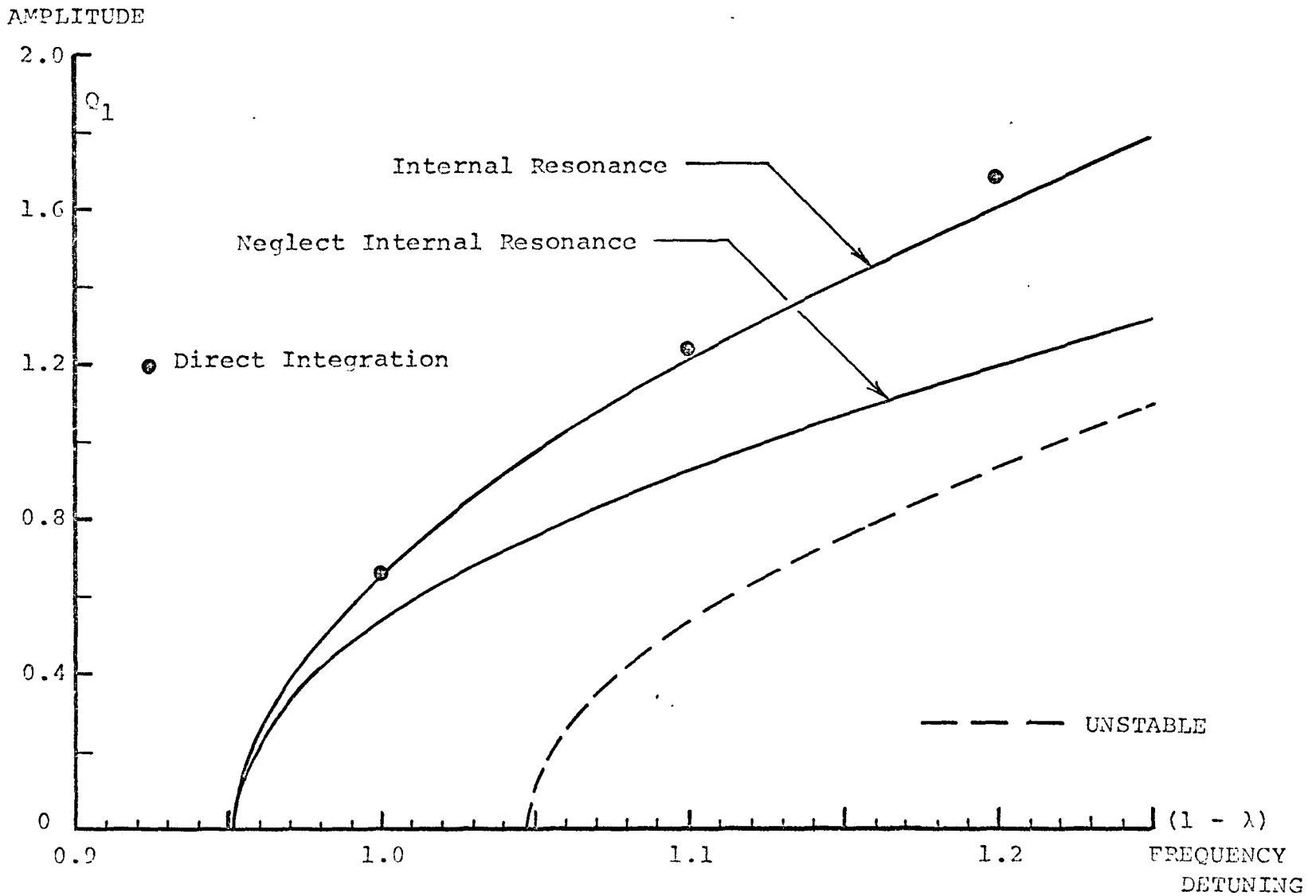


FIG. 2-2 STEADY STATE RESPONSE COMBINATION AND INTERNAL RESONANCE

$(A_1 = 0.05, \Lambda_2 = 0.08, B_1 = B_2 = 0.05, \Gamma_1 = 0.06, D_2 = 0.09, E_1 = E_2 = 0.01, \Delta = 0)$

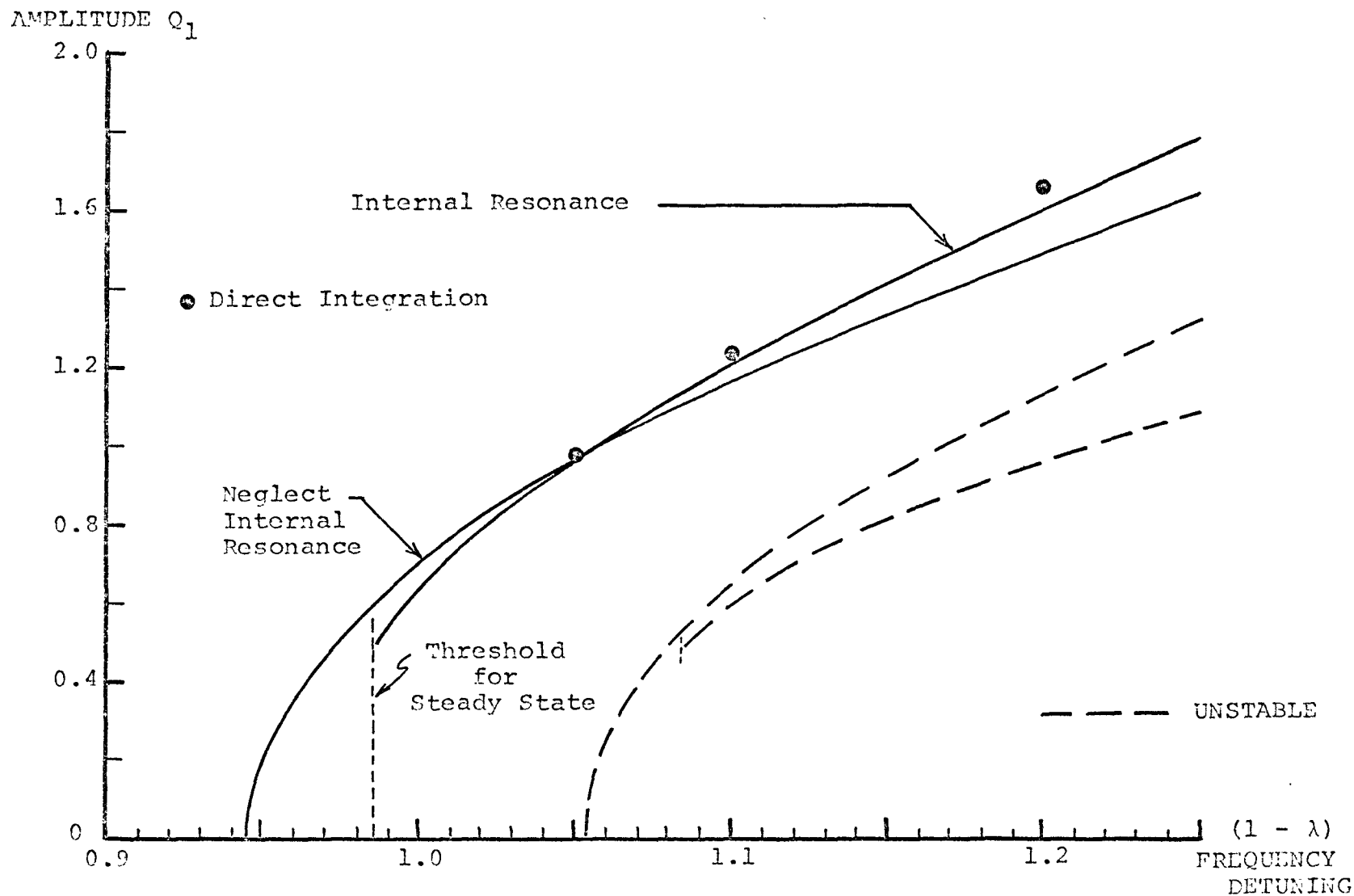


FIG. 2-3 STEADY STATE RESPONSE COMBINATION AND INTERNAL RESONANCE

$(A_1 = 0.05, A_2 = 0.08, B_1 = B_2 = 0.05, D_1 = 0.06, D_2 = 0.09, E_1 = 0.01, E_2 = 0.03, \Delta = 0)$

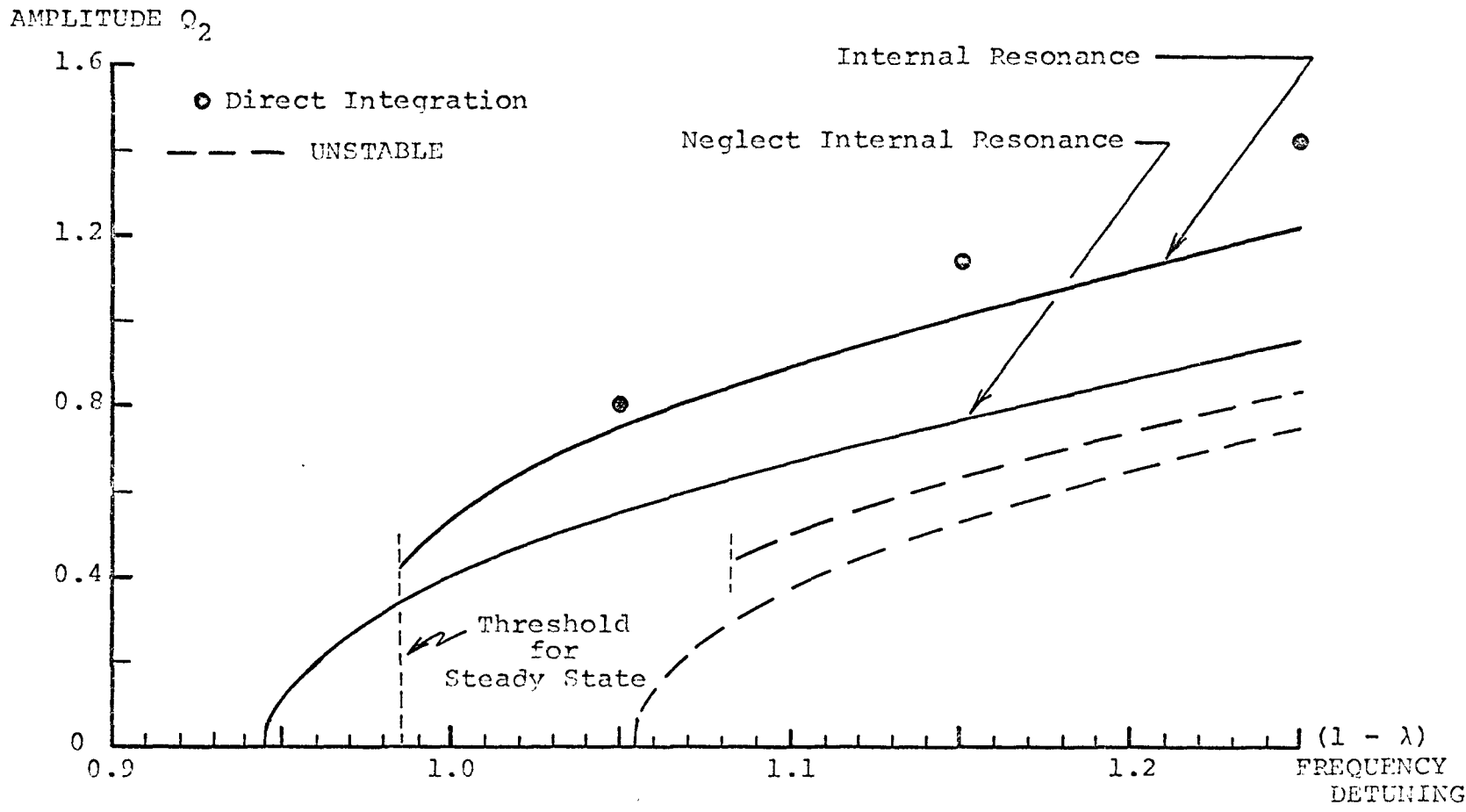


FIG. 2-4 STEADY STATE RESPONSE FOR Q_2

($A_1 = 0.05, A_2 = 0.08, B_1 = B_2 = 0.05, D_1 = 0.06, D_2 = 0.09, E_1 = 0.01, E_2 = 0.03, \Delta = 0$)

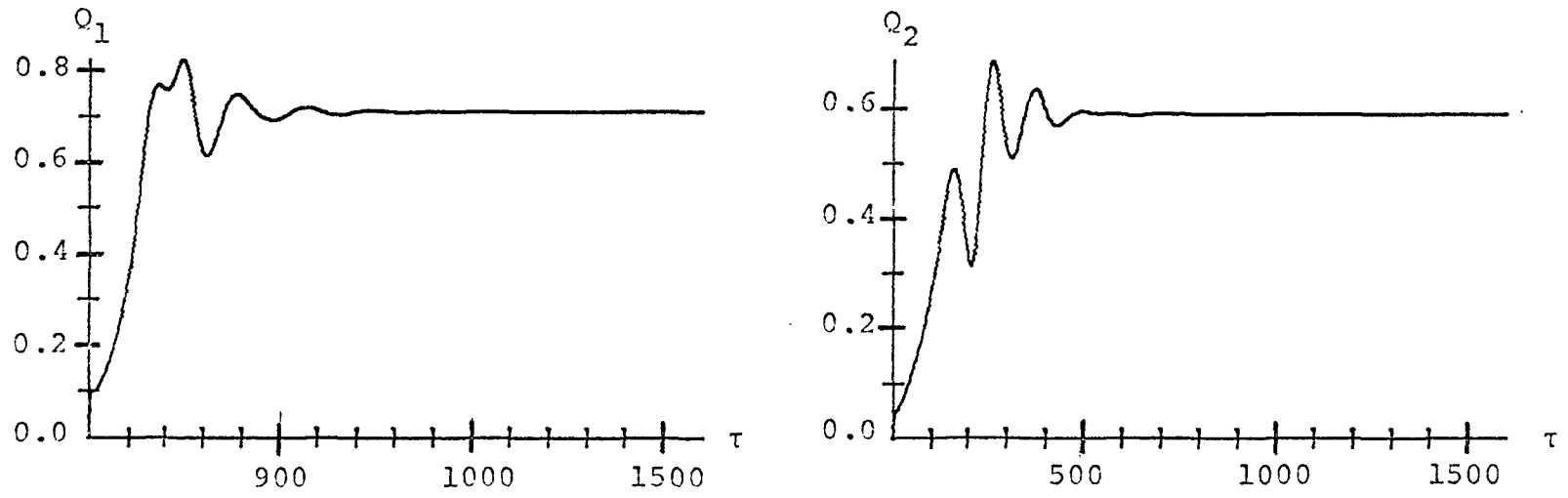


FIG. 2-5 TIME HISTORY PLOT FOR STEADY STATE RESPONSE

$$(\Delta = 0, \lambda = -0.01, E_1 = 0.01, E_2 = 0.03)$$

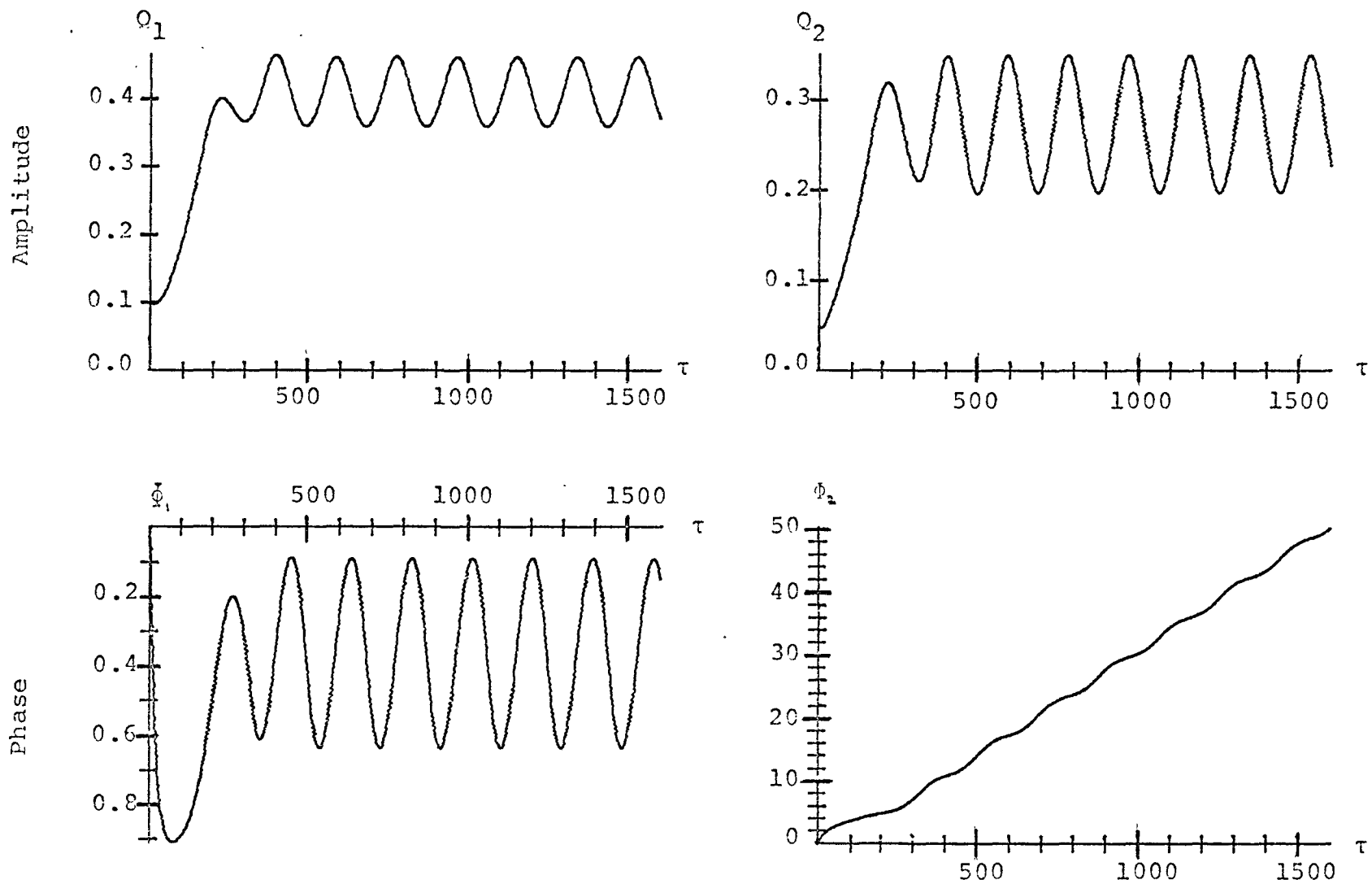


FIG. 2-6 NONSYNCHRONIZED QUASI STEADY STATE

$$(\Delta = 0, \lambda = 0.03, E_1 = 0.01, E_2 = 0.03)$$

case of unequal damping coefficients. In the case of equal damping coefficients, the unstable range is $|1 - \lambda| < 4.8\%$ while the system with unequal damping coefficients has an unstable detuning range of $|1 - \lambda| < 5.5\%$. This increase in the combination resonant range, due to unequal damping coefficients is evident from equation 2-41 and was first pointed out by Schmidt and Weidenhammer^[44]. Secondly, while there is a substantial shift in the steady state curves with the internal resonance effect neglected, (equation 2-38), the steady state curves with internal resonance are essentially the same in both figures.

The third point is that the steady-state curve with internal resonance in Fig. 2-3 does not exist for small values of Q_1° . The same feature is observed in Fig. 2-4 where the steady-state response of Q_2° is shown. In other words, within the unstable range of frequency detuning, a true steady-state where the amplitudes of the generalized co-ordinates remain constant does not always exist. In the present case, a steady-state exists only when the detuning parameter $(1 - \lambda)$ is larger than 0.985, or the external detuning $\lambda < 0.015$. If the influence of internal resonance is neglected, a steady-state is always possible within the unstable detuning range. Also shown in Figs. 2-3, 4 are the results obtained from the direct numerical integration of the equations 2-16. It can be seen that the solutions neglecting the internal resonance terms always under estimate the steady state response of the system. Also, by comparing the numerical integration results with the steady-state response curve with internal resonance, it can be seen that the solutions based on the method of slowly varying parameters becomes increasingly inaccurate as the external detuning $(1 - \lambda)$ increases.

Shown in Fig. 2-5 are time history plots to indicate how the amplitudes Q_1 and Q_2 grow from a small initial value to the final steady-state value. These results were obtained by integrating the set of equations 2-37. The initial values have no effect on the final steady-state. Only the time at

which steady state is reached is affected by the initial conditions.

2.5 Non-Synchronized Quasi-Steady Response

(a) Internal Detuning $\Delta_1 = \Delta_2 = 0$

As indicated in the example with unequal damping coefficients, a steady state cannot be reached for an external detuning $(1 - \lambda) < 0.985$. Since the unstable range of detuning lies in the range $0.945 < (1 - \lambda) < 1.055$ it is now necessary to investigate the type of response of the system when the external detuning lies in the range $0.945 < (1 - \lambda) < 1.985$. Shown in Fig. 2-5 is the time history response of Q_1 and Q_2 where the system is in a combination and an internal resonance state with $(1 - \lambda) = 0.97$. The plots were obtained by numerically integrating the set of equations 2-37. It can be seen that the amplitudes Q_1 and Q_2 initially have a rapid rate of rise and then oscillate about some value which may be termed the "quasi steady-state value".

(b) Effect of Internal Detuning

To study the effect of internal detuning the frequencies of free vibration $\omega_j = \omega^0 (1 + \Delta_j)$ are separated by letting $\Delta_2 = -\Delta_1$ and Δ now represents $2\Delta_1$. In terms of the averaged equations this internal detuning has no direct effect on 2-37e but has a very important effect on 2-37f. The steady-state synchronized state becomes increasingly difficult to obtain as the detuning is increased. If the detuning is large enough no synchronized state can be reached.

Although the reasons for a synchronized state not obtainable may be difficult to explain in physical terms, an explanation can be based on the averaged equations. By including the internal resonance, an extra equation 2-37f describing the phase angle variable $\phi_2 = 2\theta_1 - 2\theta_2$ must be considered. For a steady state condition to exist $\phi'_2 = 0$ is a necessary condition. From 2-37f it is difficult to say

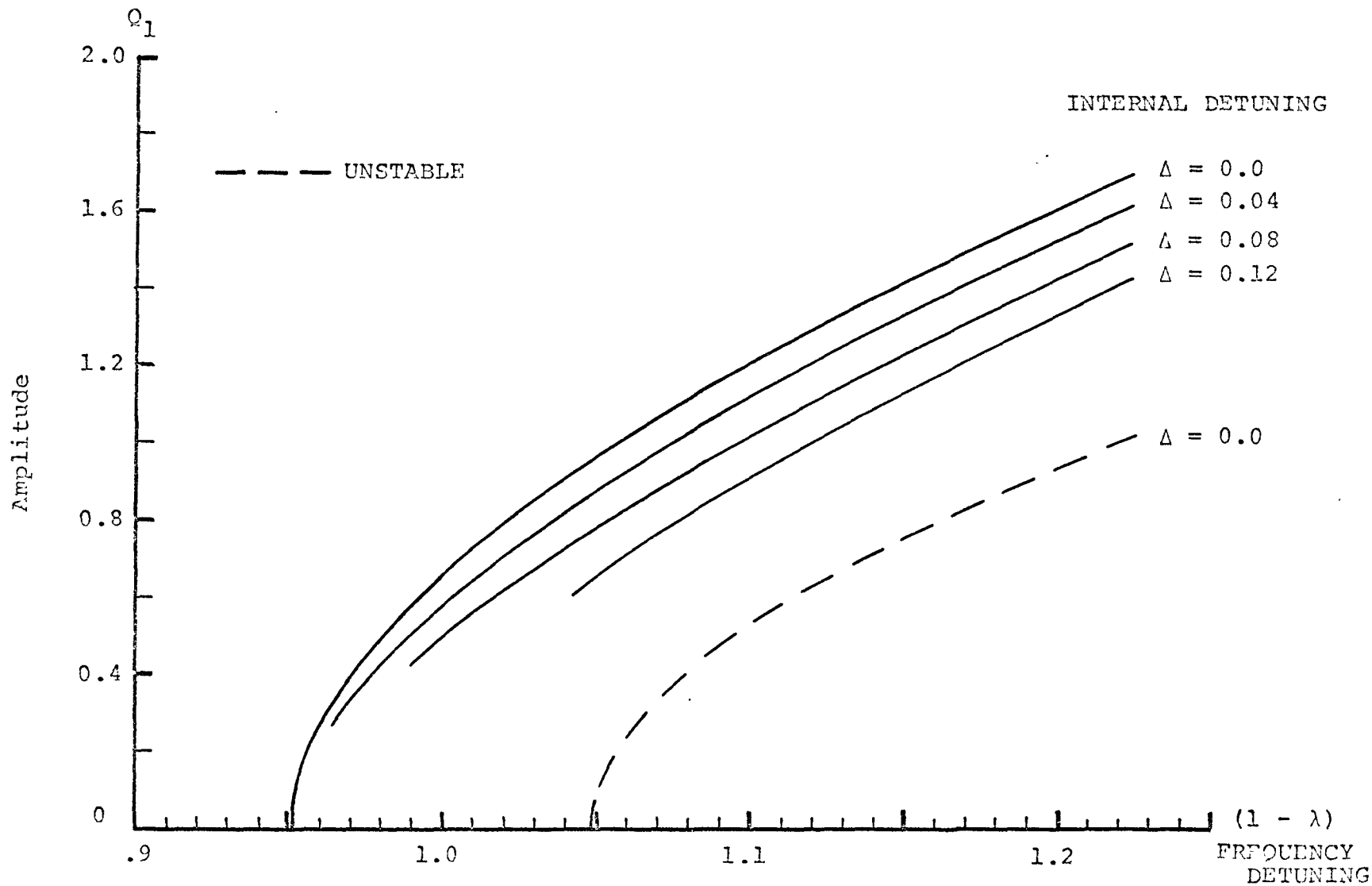


FIG. 2-7 EFFECT OF INTERNAL DETUNING ON THRESHOLD OF STEADY STATE RESPONSE

($E_1 = 0.01, E_2 = 0.01$)

exactly when this state is possible but it is evident that this condition is dependent at least in part on the detuning parameter Δ . In Fig. 2-7 the effect of the internal detuning on the threshold of steady-state response is plotted. Here the viscous damping coefficients E_1, E_2 are set equal to 0.01 and from Fig. 2-2 it is seen that steady-state response is possible for $\Delta = 0.0$. As Δ is increased the range in which a steady-state is possible changes. For $\Delta = 0.04$, a steady state is only possible for $(1 - \lambda) > .985$. At $\Delta = 0.12$ no steady state is possible over almost the entire instability zone. The synchronized state is dependent on the value of the internal detuning. As Δ increases the condition $\Phi'_2 = 0$ is no longer possible. When this happens the trigonometric terms $\sin \Phi_2, \cos \Phi_2$ in equations 2-37 will begin oscillatory motion. The resulting cross-modulations between the amplitudes and phases will be extremely complicated. But it can be seen that as Δ increases, Φ_2 increase more rapidly and the influence of the trigonometric functions of Φ_2 will take on the nature of a high frequency superposition on the system of equations 2-37 similar to the terms whose mean value were calculated to be zero in the averaging process of the equations 2-26. Consequently, the equations with internal resonance 2-37 will pass over to the equations 2-38 where the internal resonance effect is not included. However $K_1 = K_2 = K$ must then be substituted into 2-38.

Fig.2-8a shows the time history response of Q_1 and Q_2 for $\Delta = 0.12$, and $(1 - \lambda) = 1$. From Fig. 2-7 it is seen that these parameters are such that no steady-state is possible. Following an initial disturbance the amplitudes grow rapidly and reach a maximum at time $\tau = 100$. After this initial overshoot the oscillations appear to become periodic for $\tau > 800$ and a quasi-steady state motion exists. As the detuning increases the frequency of the modulated motions increase, and the amplitude of the modulations decrease.

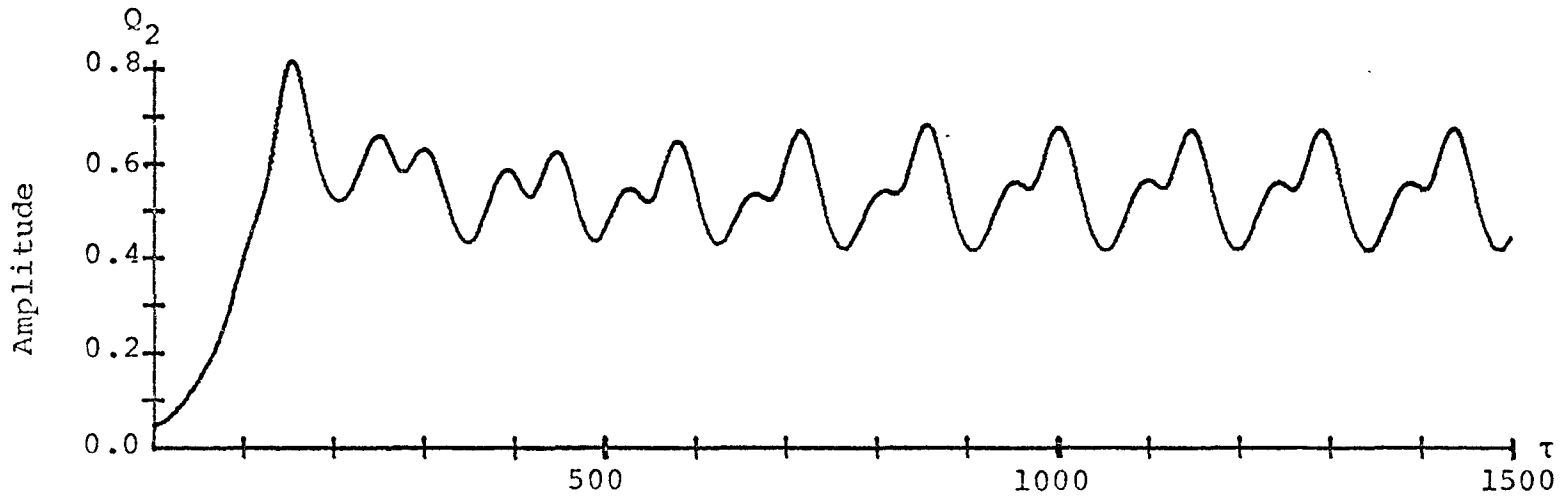
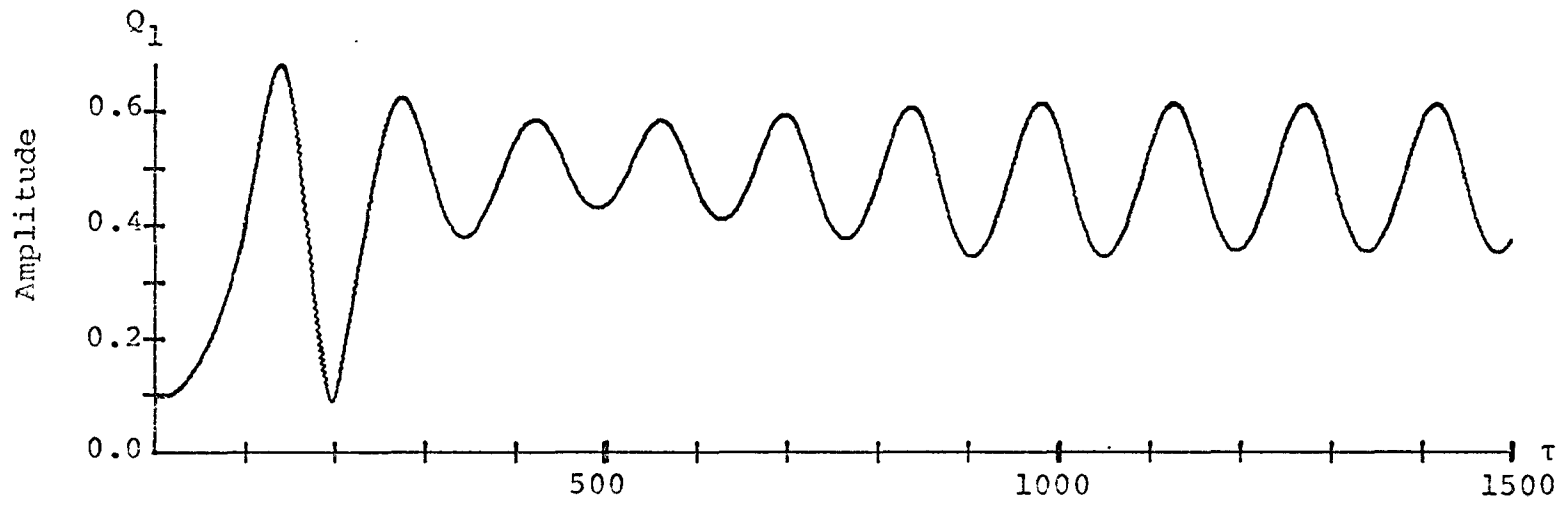


FIG. 2-8A RESPONSE BASED ON AVERAGED EQUATIONS WITH INTERNAL RESONANT TERMS
 $(\Delta = 0.12, \lambda = 0, E_1 = E_2 = 0.01)$

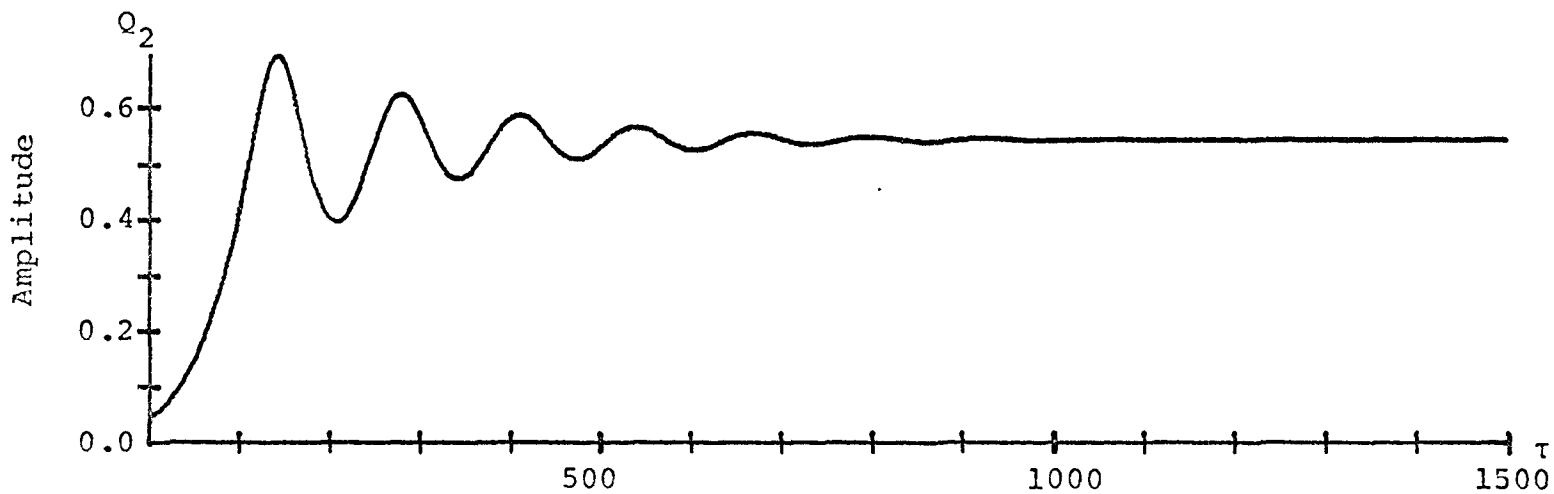
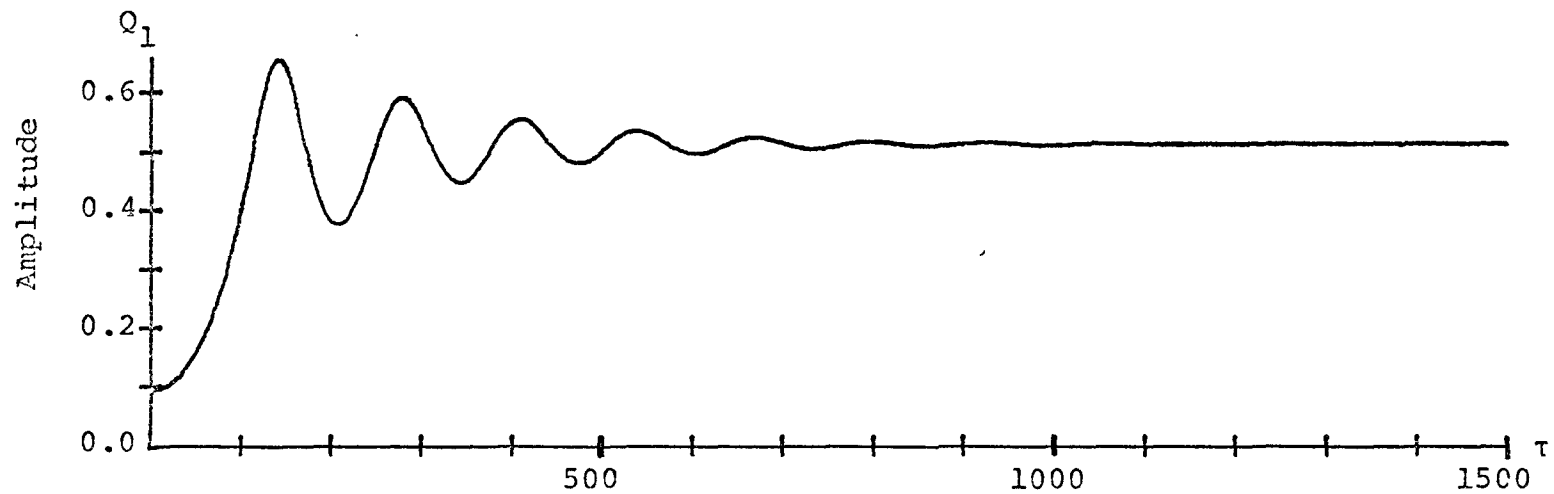


FIG. 2-83 RESPONSE BASED ON AVERAGE EQUATION NEGLECTING INTERNAL RESONANT TERMS
 ($\Delta = 0.12, \lambda = 0, E_1 = E_2 = 0.01$)

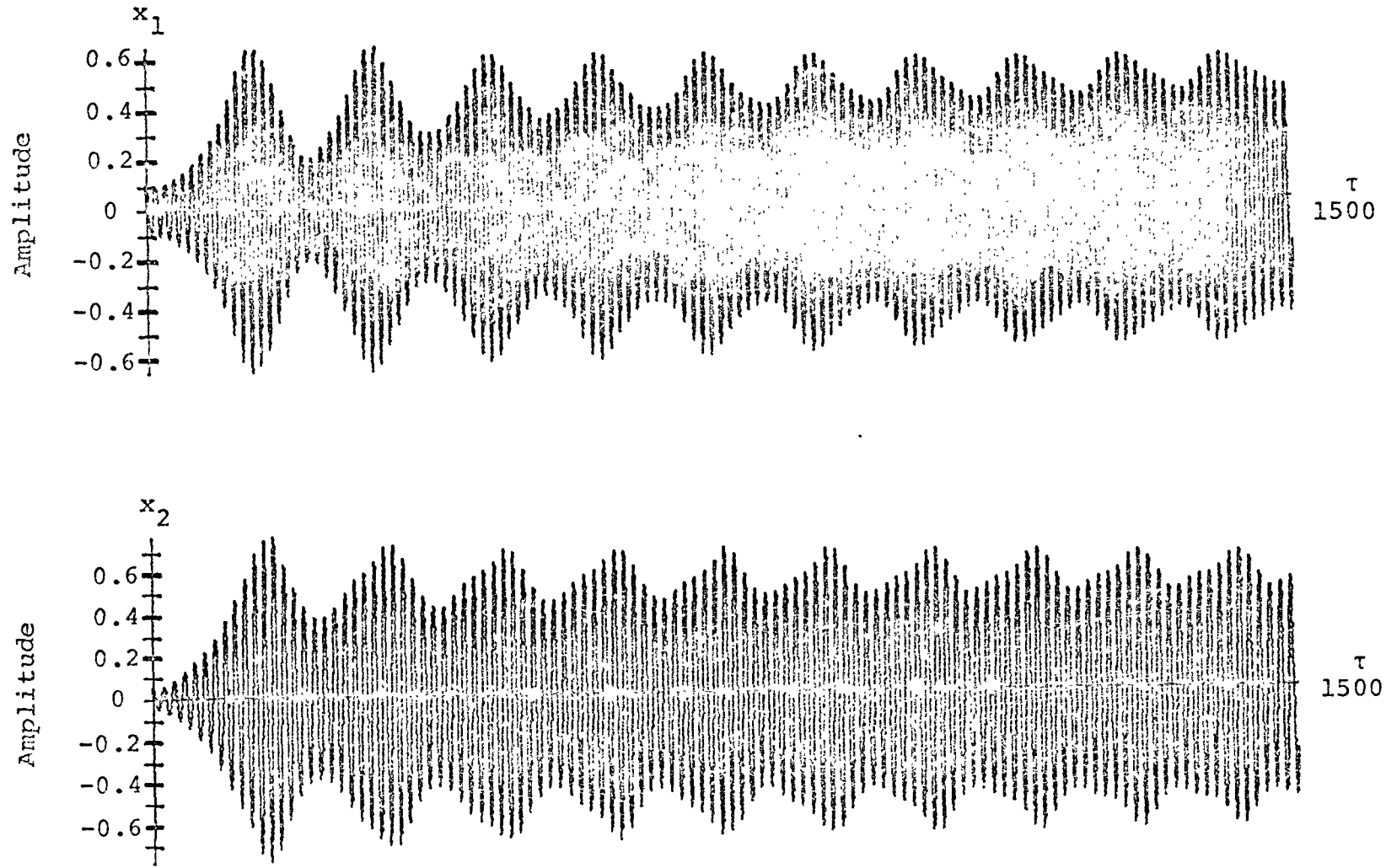


FIG. 2-8C RESPONSE BASED ON NUMERICAL INTEGRATION
($\Delta = 0.12, \lambda = 0, E_1 = E_2 = 0.01$)

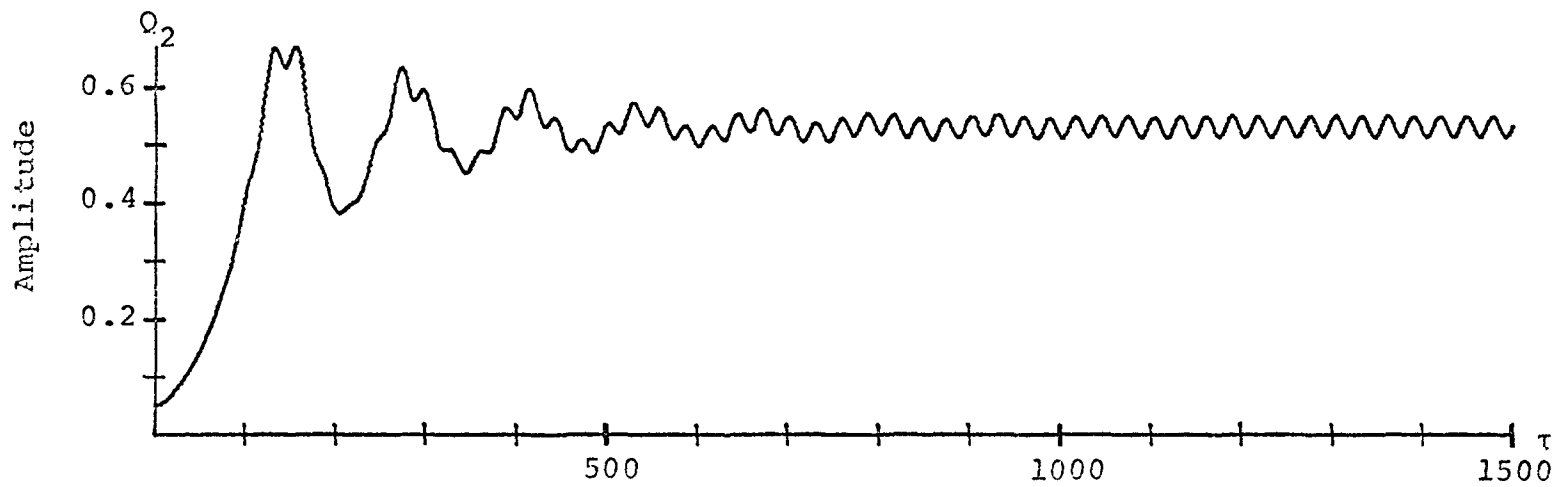
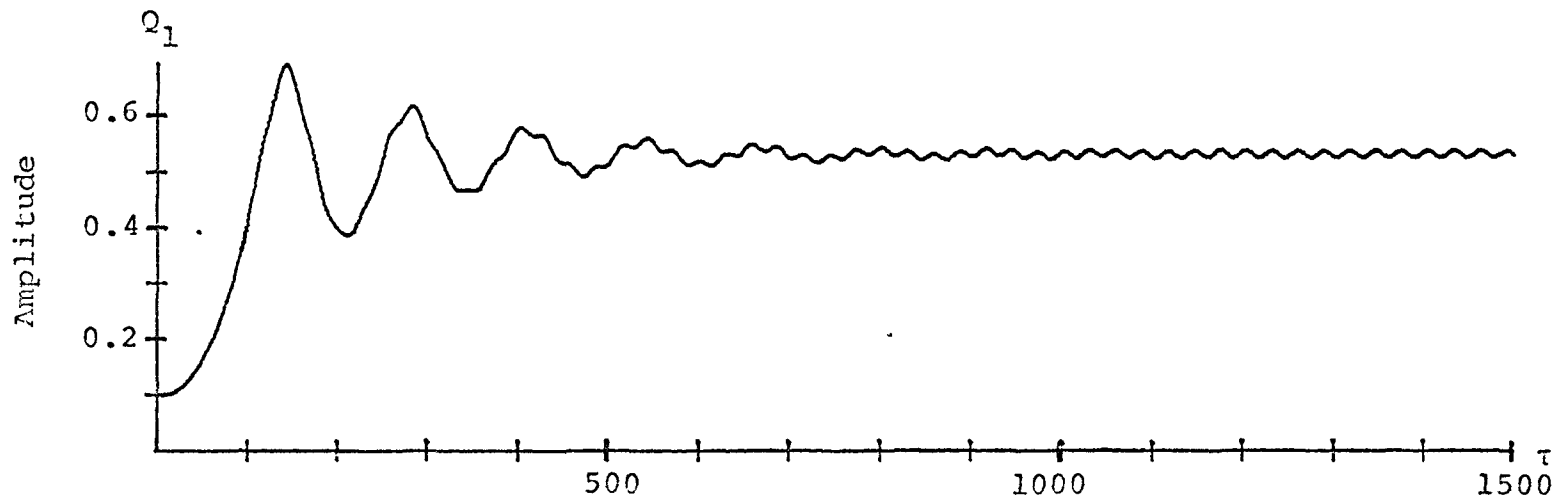


FIG. 2-9A RESPONSE WITH LARGE INTERNAL DETUNING (INTERNAL RESONANT TERM INCLUDED)
 $(\Delta = 0.24, \lambda = 0, E_1 = E_2 = 0.01)$

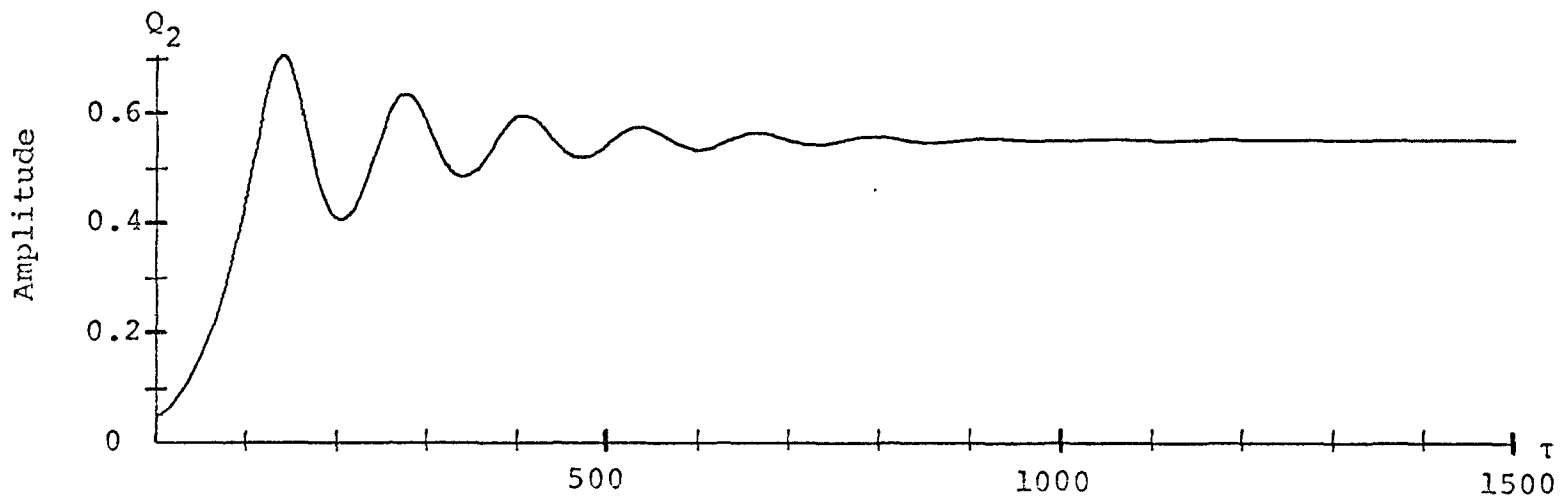
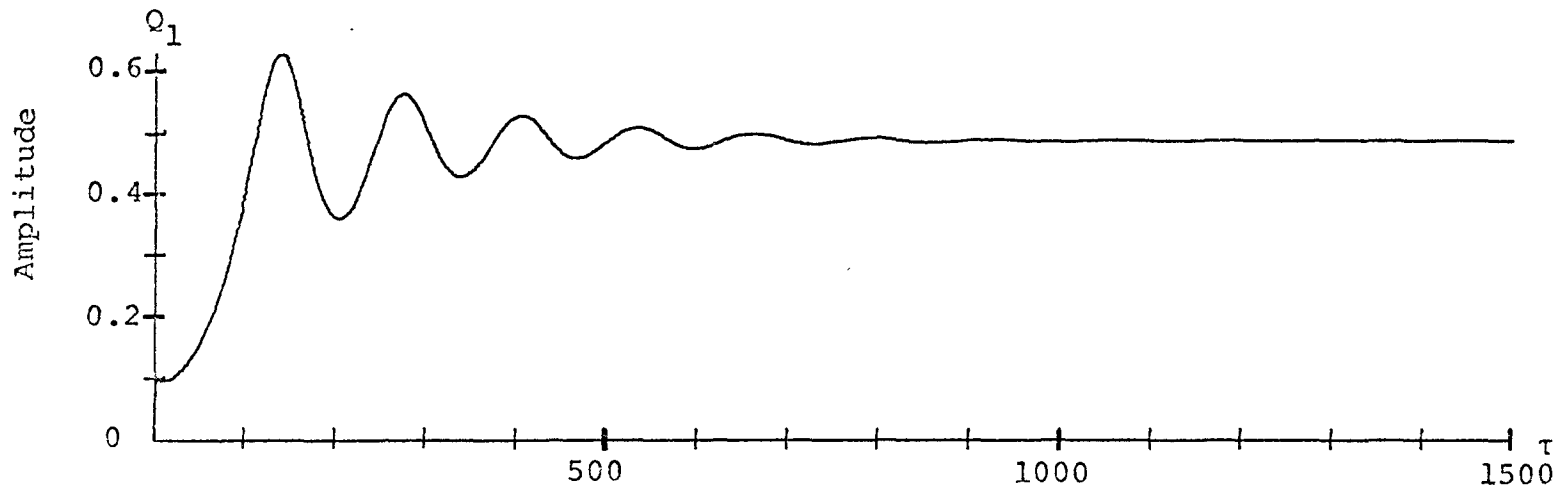


FIG. 2-9B RESPONSE WITH LARGE DETUNING (INTERNAL RESONANT TERMS NEGLECTED)
 $(\Delta = 0.24, \lambda = 0, E_1 = E_2 = 0.01)$

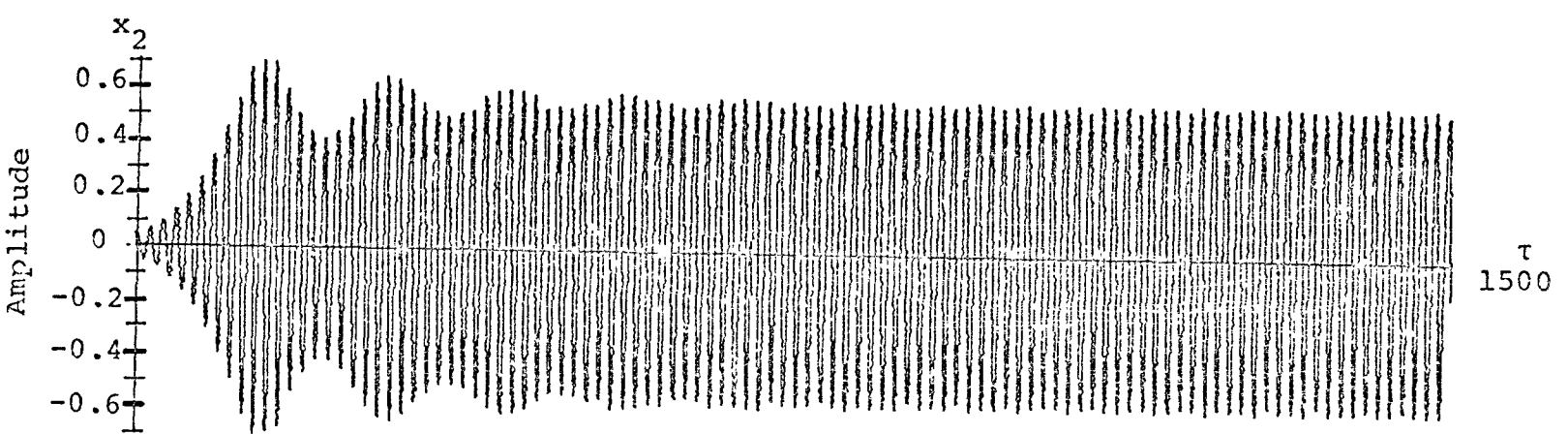
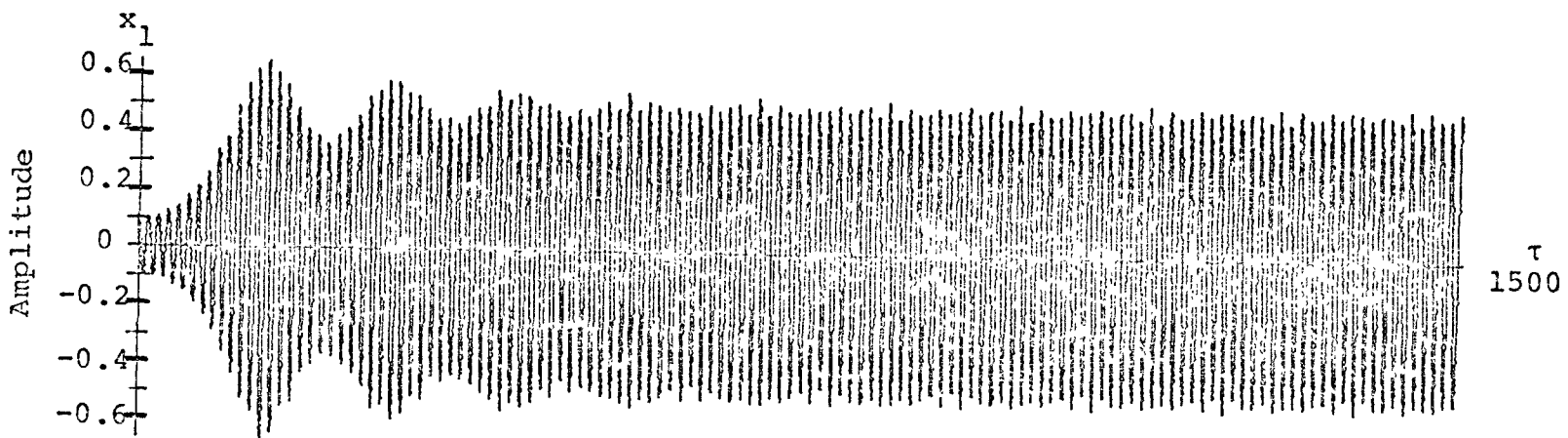


FIG. 2-9C RESPONSE BASED ON NUMERICAL INTEGRATION
 ($\Delta = 0.24, \lambda = 0, E_1 = E_2 = 0.01$)

Fig. 2-9a shows the effect of a large internal detuning on the quasi steady state response of $\Delta = 0.24$. By comparing Fig. 2-9a with Fig. 2-2 it is seen that the mean value of Q_1 of the quasi-steady state mean coincides with the value of Q_1° of Fig. 2-2 for the steady-state curve where the internal resonance effect had been neglected.

For $\Delta = .24$, $K_1 = 0.56$ and $K_2 = 0.44$ and the internal resonance condition 2-36 is no longer satisfied. This means that equations 2-37 which have assumed the internal resonance condition to be at least approximately satisfied are not valid if Δ is extrapolated to large values. Then, the equations 2-38 will provide a more accurate description of the solutions of 2-16, the original equations. The problem of deciding which set of equations to use can be approached from two points of view. Qualitatively, an analysis of the system of equations 2-38 will not reveal the high amplitude, modulated motion as shown in Fig. 2-8a. Quantatively, the analysis of equations 2-38 will provide the correct mean values of Q_1 and Q_2 for large internal detuning only. To decide the relative accuracy of the two sets of averaged equations the solutions of the exact equation 2-16 were compared against the solutions of 2-37 and 2-38 for increasing Δ_1 . Shown in Fig. 2-8b and 2-8c are the solutions of 2-38 and 2-16 respectively for $\Delta = 0.12$. In Fig. 2-9 b, c are the respective solutions for $\Delta = 0.24$.

In Fig. 2-9a, the mean values of the quasi-steady state response for both Q_1 and Q_2 is equal to 0.54. This value coincides to the value of the steady state response neglecting internal resonance obtained in Fig. 2-2. This was to be expected as $K_1 = K_2 = 0.5$. But with $\Delta = 0.24$, $K_1 = 0.56$, $K_2 = 0.44$ and the response of equations 2-38 is as shown in Fig. 2-9b. Here $Q_1^{\circ} = 0.49$ and $Q_2^{\circ} = 0.55$. Fig. 2-9c shows the response of the exact equations 2-16. Examining the response it is seen that while a steady-state has not been exactly obtained the mean value of the quasi-

steady state amplitudes $\bar{x}_1 = 0.50$ and $\bar{x}_2 = 0.56$. Therefore for $\Delta = 0.24$ the equations 2-38 provide a more accurate evaluation of the response than the equations 2-37. As Δ is increased further the accuracy of equation 2-38 is increased.

2.6 Observation and Discussion

On the basis of this investigation on the parametric response of thin-walled beams the following observations are made.

1. The method of averaging provides an accurate, approximate mathematical analysis to nonlinear dynamic stability problems. The solutions obtained by the averaged equations were checked by direct integration of the exact equations and were found to be in close agreement. In general, while the exact integration would provide a small quantitative correction the solutions were identical in a qualitative behaviour. This would indicate that extending the averaging method to higher order approximations would not introduce any qualitative change in the behaviour of the solutions in the neighbourhood of the external combination resonance zone which was studied in this chapter.
2. A resonant solution leading to large amplitude oscillations upon a small disturbance from the equilibrium position, can only occur if the external excitation is within the boundaries of instability. The width of the instability zone in which the trivial solution is unstable is governed by the size of the parametric coefficients, the absolute value of damping, the ratio of the damping terms and the distribution of natural frequencies. The characteristics of the response following the transient solution is primarily dependent upon the damping ratio and the extent of the internal detuning. Outside the instability zone in the region of the "overhang" large amplitude resonant solutions may be excited by large

initial values.

3. The system under investigation satisfies an internal resonant condition when $\omega_1 \approx \omega_2$. This resonance has a very important effect on the resonant response of the system. First, the system with internal resonance leads to larger steady-state responses than one without. The increase can be up to 30%. Secondly, an internal resonance condition can cause steady-state response in which the frequency of motion of both co-ordinates is entrained to exactly 1/2 the external excitation. Thirdly, the system with internal resonance may have a resonant nonsynchronized solution where the maximum amplitude of the modulated response exceeds the steady-state. This modulated motion appears to be periodic and persists even under large values of damping.

4. It was the purpose of this analysis to compare the special condition when the natural frequencies of lateral bending and torsion coincide. It was shown that this condition leads to an internal resonance and that the resonant response of the system has marked differences over the response of the system when the natural frequencies are not approximately equal. The modulated response which may occur under these conditions takes the form of a continual energy exchange between the lateral and torsional modes of motion. The peak amplitudes of these surges may exceed by 50% the value of the steady-state amplitudes. Detuning of the natural frequencies by an order of $\Delta > 0.16$ will eliminate the internal resonance effect. Consequently it is proposed that the structural system be designed with this separation of frequencies in mind.

5. This theoretical investigation of the simultaneous occurrence of an internal and external resonance condition has shown that the resulting motion is sufficiently different from the case when only an external resonance is considered.

While the investigation was applied to a two mode approximation of a simple thin-walled beam it may have far reaching consequences in the dynamic stability study of other elastic bodies where the natural frequencies of various modes of motion may coincide.

CHAPTER III

THE INTERACTION OF TWO EXTERNAL PARAMETRIC RESONANCES IN A TWO DEGREE-OF-FREEDOM SYSTEM SUBJECTED TO NON-CONSERVATIVE LOADING

3.1 Introduction

When a two-degree of freedom dynamical system is subjected to an external parametric excitation, it may be excited into resonance. A special feature of parametric resonance is that a monofrequent external excitation may induce in a linear system either a one mode or two mode response depending on the relation between the external and natural frequencies. A large number of possible resonance zones exist for both the one mode and two mode response. The most important resonance zones occur when the external frequency is in the neighbourhood of twice the value of either of the natural frequencies $\Omega \approx 2 \omega_{1,2}$ and if the external frequency is close to the sum or difference of the two natural frequencies $\Omega \approx \omega_1 \pm \omega_2$. The former is called parametric resonance Type I while the latter is called combination resonance or parametric resonance Type II^[31]. The study of parametric resonance Type I in nonlinear system has been carried out in the context of the theory of nonlinear oscillations by Bogoliobov & Mitropolsky^[3] and in the context of dynamic stability of structures by Bolotin^[4] and Mettler^[33]. The study of combination resonance in nonlinear system has been more recent.^[38, 34, 15, 16]

All studies of parametric resonance in nonlinear dynamical systems have assumed that the ratios of the natural frequencies of the system are such that a single mode resonance and a combination resonance do not occur simultaneously. However, it is possible to have both types of parametric resonance occur simultaneously. It can be expected

that if this happens the two resonances will reinforce each other to cause a greater response than each resonance treated individually. Also it is to be expected that the instability region of such a system will differ from the individual zones of the uncoupled system.

By examining the resonance conditions it is clear that an interaction of a parametric and combination resonance is possible say if $\omega_1 = 1$, $\omega_2 \approx 3$ and an external frequency $\Omega \approx 2$. In this case, both the parametric resonance $\Omega \approx 2\omega_1$ and the combinational resonance condition $\Omega \approx \omega_2 - \omega_1$ are satisfied. It has been shown by Mettler^[31] that a combination minus resonance is not possible in systems where the forces are derivable from potential functions. However Piszeczek^[38] has proven that systems subjected to non-conservative forces such as followers forces that change their direction of application with the deformation of the system are susceptible to the combination minus resonance. In the present study a physical system consisting of a double pendulum, subjected to a follower's force P is considered. This model was first presented by Ziegler^[58] and formed the basis of the early studies in the theory of non-conservative stability.

For a constant thrust P this model is an example of a self-excited system. At a certain critical load P_c , flutter oscillations with increasing amplitude will result following a small disturbance from its equilibrium position. Below the critical load flutter oscillations can also occur if the thrust force P has a periodic component

$$P = P_o + P_t \cos (\Omega t)$$

for then a parametric instability will result when $\Omega \approx 2\omega_{1,2}$ or $\omega_2 - \omega_1$. The natural frequencies of the loaded system are a function of the constant load component P_o . Thus even if the physical system is designed in such a way that the natural

frequencies of the unloaded system are well separated from the ratio $\omega_2/\omega_1 \approx 3$, the action of the external loading P_0 can cause this ratio to occur and cause the superposition of the two external resonance zones.

It is the purpose of this chapter to investigate the nonlinear response of a non-conservative two degree of freedom system subjected to parametric excitation. The parameters of the system are chosen such that both a type I and type II resonance occurs simultaneously. The effect of the interaction on the linear instability zone is obtained and the response of the coupled system is compared against the response of each resonance treated on an individual basis. First the general two degree of freedom systems will be examined and the important features discussed. Then a specific numerical example of the double pendulum will be investigated. It is shown that the interaction effect has a strong qualitative difference when compared to the uncoupled response.

3.2 The Equations of Motion

The equations of motion of a general two-degree of freedom system, with cubic nonlinearities, can be written in the form

$$\ddot{x}_j + \omega_j^2 x_j + \varepsilon \left\{ \sum_{m=1}^2 e_{jm} \dot{x}_m + \cos(\Omega t) \sum_{m=1}^2 b_{jm} x_m + g_j \right\} = 0 \quad 3-1a$$

$$\text{where } g_j = a_{j1} x_j^3 + a_{j2} x_j^2 x_n + a_{j3} x_j x_n^2 + a_{j4} x_n^3 \quad 3-1b$$

$$(j = 1, 2 \quad n = 1, 2) \\ (j \neq n)$$

where the x_j represent the normal co-ordinates, ω_j the undamped

natural frequencies, e_{jm} the viscous damping coefficients, b_{jm} the parametric excitation parameter, a_{jK} the coefficients of the nonlinear terms and Ω the frequency of the external excitation. It is assumed that self-excited oscillations of the system 3-1 can not occur, that is the circulatory loading is assumed to be below it's damped critical value^[18]. This means that flutter oscillations can only occur due to the action of a parametric resonance zone.

Equation 3-1 can be transformed by the change of variables

$$\tau = \Omega t \quad 3-2a$$

$$K_1 = \frac{\omega_1}{\Omega_0} \quad 3-2b$$

$$K_2 = \frac{\omega_2}{\Omega_0} \quad 3-2c$$

$$\Omega = \Omega_0 (1 - \lambda) \quad 3-2d$$

to

$$\begin{aligned} \ddot{x}_j + K_j^2 x_j + \epsilon \{ \epsilon^{-1} (2K_j^2 \lambda x_j) + \sum_{m=1}^2 \frac{e_{jm}}{\Omega_0} x'_m \\ + \cos(\tau) \left[\sum_{m=1}^2 \frac{b_{jm}}{\Omega_0} x_m + \frac{g_m}{\Omega_0} \right] \} = 0 \end{aligned} \quad 3-3$$

where λ represents a small detuning in the external frequency which allows the response of the system 3-1 to be studied in the neighbourhood of the critical resonance zone.

The equation 3-3 is now cast into a suitable form to apply the method of averaging. By introducing the polar trans-

formation

$$x_j = Q_j(\tau) \cos (K_j \tau + \theta_j(\tau)) \quad 3-4a$$

$$\equiv Q_j \cos \psi_j$$

$$\dot{x}_j = - Q_j(\tau) K_j \sin (K_j \tau + \theta_j(\tau)) \quad 3-4b$$

$$\equiv - Q_j K_j \sin \psi_j$$

Substituting 3-4a, b into 3-3 the system of 4 first order equations in the variables $Q_{1,2}, \theta_{1,2}$ is obtained

$$\begin{bmatrix} \cos \psi_j & - Q_j \sin \psi_j \\ - K_j \sin \psi_j & - Q_j K_j \cos \psi_j \end{bmatrix} \begin{bmatrix} \dot{Q}_j \\ \dot{\theta}_j \end{bmatrix} = \begin{bmatrix} 0 \\ -\epsilon f_j \end{bmatrix} \quad 3-5a$$

$$(j = 1, 2)$$

where

$$f_j = \epsilon^{-1} (2K_j \lambda x_j) + \sum_{m=1}^2 \frac{e_{jm}}{\Omega_0} x'_m + \cos(\tau) \sum_{m=1}^2 \frac{b_{jm}}{\Omega_0} x_m + \frac{g_m}{\Omega_0} \quad 3-5b$$

Expanding the equations 3-5 there results the following system

of first order equations.

$$\begin{aligned}
 K_j Q_j' &= 2\lambda K_j^2 Q_j \cos \psi_j \sin \psi_j + B_{jj} Q_j \cos \psi_j \sin \psi_j \cos \tau \\
 &+ B_{jm} Q_m \cos \psi_m \sin \psi_j \cos \tau - K_j E_{jj} Q_j \sin^2 \psi_j \\
 &- E_{jm} Q_m K_m \sin \psi_m \sin \psi_j + A_{j1} Q_j^3 \cos \psi_j \sin \psi_j \\
 &+ A_{j2} Q_j^2 Q_m \cos^2 \psi_j \cos \psi_m \sin \psi_j \\
 &+ A_{j3} Q_j Q_m^2 \cos \psi_j \cos^2 \psi_m \sin \psi_j \\
 &+ A_{j4} Q_m^3 \cos^3 \psi_m \sin \psi_j
 \end{aligned} \tag{3-6a}$$

$$\begin{aligned}
 K_j Q_j \theta_j' &= 2\lambda K_j^2 Q_j \cos^2 \psi_j + B_{jj} Q_j \cos^2 \psi_j \cos \tau \\
 &+ B_{jm} Q_m \cos \psi_m \cos \psi_j \cos \tau - Q_j E_{jj} K_j \sin \psi_j \cos \psi_j \\
 &- E_{jm} Q_m K_m \sin \psi_m \cos \psi_j + A_{j1} Q_j^3 \cos^4 \psi_j \\
 &+ A_{j2} Q_j^2 Q_m \cos^3 \psi_j \cos \psi_m + A_{j3} Q_m^2 Q_j \cos^2 \psi_j \cos^2 \psi_m
 \end{aligned}$$

$$+ A_{j4} Q_m^3 \cos^3 \psi_m \cos \psi_j \quad 3-6b$$

$$(j = 1, 2 \quad m = 1, 2)$$

$$(j \neq m)$$

$$\text{where } E_{jm} = \frac{\epsilon e_{jm}}{\Omega_0}, \quad B_{jm} = \frac{\epsilon b_{jm}}{\Omega_0^2}, \quad A_{jm} = \frac{\epsilon a_{jm}}{\Omega_0^2}$$

3.3 The Averaged Equations

A combination resonance type II and a parametric resonance type I can occur simultaneously when the values of the natural frequencies and the parametric frequency satisfy the following relationships.

$$K_2 - K_1 = 1 \quad (\text{combination minus resonance condition}) \quad 3-7a$$

$$2K_1 = 1 \quad (\text{parametric type 1 resonance condition}) \quad 3-7b$$

Equation 3-7a specifies that the parametric frequency is approximately equal to the difference of the natural frequencies while equation 3-7b states that it is also approximately equal to twice the first natural frequency. From equation 3-2d it is seen that the quantity λ is a measure of how close the external frequency of the system satisfies the parametric resonance conditions. This external detuning is reflected in the expression $\epsilon^{-1}(2K_j^2 \lambda x_j)$ in equation 3-3.

The method of averaging is now applied to equations 3-6a and 3-6b. During the averaging procedure, the conditions

imposed by the parametric resonance conditions 3-7a and 3-7b are born in mind to obtain the averaged equations.

$$\begin{aligned} K_1 \frac{dQ_1}{d\tau} = & \frac{B_{11}}{4} Q_1 \sin 2\theta_1 + \frac{B_{12}}{4} Q_2 \sin(\theta_1 - \theta_2) - \frac{E_{11}}{2} Q_1 K_1 \\ & + \frac{A_{12}}{8} Q_1^2 Q_2 \sin(3\theta_1 - \theta_2) \end{aligned} \quad 3-8a$$

$$\begin{aligned} K_2 \frac{dQ_2}{d\tau} = & -\frac{B_{21}}{4} Q_1 \sin(\theta_1 - \theta_2) - \frac{E_{22}}{2} Q_2 K_2 \\ & - \frac{A_{24}}{8} Q_1^3 \sin(3\theta_1 - \theta_2) \end{aligned} \quad 3-8b$$

$$\begin{aligned} K_1 Q_1 \frac{d\theta_1}{d\tau} = & \lambda K_1^2 Q_1 + Q_1 \frac{B_{11}}{4} \cos 2\theta_1 + \frac{B_{12}}{4} Q_2 \cos(\theta_1 - \theta_2) \\ & + \frac{3}{8} A_{11} Q_1^3 + \frac{A_{13}}{4} Q_2^2 Q_1 + \frac{A_{12}}{8} Q_1^2 Q_2 \cos(3\theta_1 - \theta_2) \end{aligned} \quad 3-8c$$

$$\begin{aligned} K_2 Q_2 \frac{d\theta_2}{d\tau} = & \lambda K_2^2 Q_2 + \frac{B_{21}}{4} Q_1 \cos(\theta_1 - \theta_2) + \frac{3}{8} A_{21} Q_2^3 \\ & + \frac{A_{23}}{4} Q_1^2 Q_2 + \frac{A_{24}}{8} Q_1^3 \cos(3\theta_1 - \theta_2) \end{aligned} \quad 3-8d$$

The variables $Q_j(\tau)$ and $\theta_j(\tau)$ in equations 3-8 now represent the mean values of Q_j and θ_j over one period of oscillation. In equation 3-8a the first term on the right

hand side is caused by the fact that the parametric type 1 resonance condition of equation 3-7b is satisfied. The second term arises due to the combination resonance condition 3-7a. The third term is due to viscous damping and the fourth term is due to the internal resonance condition caused by the fact that the parametric resonance conditions stipulate that $3K_1 = K_2$. In the second equation 3-8b the type 1 resonance condition was not satisfied for coordinate x_2 and consequently no term representing this resonance was carried over into the averaged equations. The terms in equation 3-8c, d are similar except that here the first terms on the right hand side are due to detuning, the terms with the coefficients A_{11} , A_{13} , A_{21} and A_{23} represent the contributions due to the nonlinear restoring forces and the terms with coefficients A_{12} , A_{24} arise due to internal resonance.

As was shown in Chapter 11 an internal resonance condition can affect the nature of the response with respect to a variation in the steady-state values and with respect to obtaining a steady-state. In this chapter, it is intended to concentrate on the interaction of the external resonance zones only. Consequently, it will be assumed that the internal resonance coefficients A_{12} , A_{24} , as a first approximation can be neglected in the analysis that follows.

3.4 Stability of the Trivial Solution $Q_j = 0$

The stability of the trivial solution, $Q_j = 0$, can be obtained from the linearized equations. Using the rectangular transformation,

$$y_j = Q_j \cos \theta_j \quad 3-9a$$

$$z_j = Q_j \sin \theta_j \quad (j = 1, 2) \quad 3-9b$$

the stability condition can be studied conveniently by considering the conditions $y_j \rightarrow 0$, $z_j \rightarrow 0$. Taking the derivatives of 3-9

$$y'_j = Q'_j \cos \theta_j - Q_j \sin \theta_j \theta'_j \quad 3-10a$$

$$z'_j = Q'_j \sin \theta_j + Q_j \cos \theta_j \theta'_j \quad 3-10b$$

Each pair of equations 3-8

$$K_1 Q'_1 = \frac{B_{11}}{4} Q_1 \sin 2\theta_1 + \frac{B_{12}}{4} Q_2 \sin(\theta_1 - \theta_2) - \frac{E_{11}}{2} Q_1 K_1 \quad 3-11a$$

$$K_1 Q \theta'_1 = \lambda K_1^2 Q_1 + \frac{B_{11}}{4} Q_1 \cos 2\theta_1 + \frac{B_{12}}{4} Q_2 \cos(\theta_1 - \theta_2) \quad 3-11b$$

can be transformed by multiplying 3-11a by $\cos \theta_1$ and 3-11b by $\sin \theta_1$ and subtracting and rearranging to obtain

$$\begin{aligned} K_1 y'_1 &= -\frac{E_{11} K_1}{2} y_1 - \lambda K_1^2 z_1 + \frac{B_{11}}{4} Q_1 [\sin 2\theta_1 \cos \theta_1 \\ &\quad - \cos 2\theta_1 \sin \theta_1] + \frac{B_{12}}{4} Q_2 [\sin(\theta_1 - \theta_2) \cos \theta_1 \\ &\quad - \cos(\theta_1 - \theta_2) \sin \theta_1] \end{aligned} \quad 3-12a$$

which can be rewritten as:

$$K_1 y'_1 = -\frac{E_{11}K_1}{2} y_1 - \lambda K_1^2 z_1 + \frac{B_{11}}{4} z_1 - \frac{B_{12}}{4} z_2 \quad 3-12b$$

Similarly the other three equations for y'_2 , z'_1 and z'_2 can be obtained. Together they form the homogeneous system of first order equations:

$$\begin{Bmatrix} K_1 y'_1 \\ K_1 z'_1 \\ K_2 y'_2 \\ K_2 z'_2 \end{Bmatrix} = \begin{bmatrix} -\frac{E_{11}K_1}{2} & -\lambda K_1^2 + \frac{B_{11}}{4} & 0 & -\frac{B_{12}}{4} \\ \frac{B_{11}}{4} + \lambda K_1^2 & -\frac{E_{11}K_1}{2} & \frac{B_{12}}{4} & 0 \\ 0 & -\frac{B_{21}}{4} & -\frac{E_{22}K_2}{4} & -\lambda K_2^2 \\ \frac{B_{21}}{4} & 0 & \lambda K_2^2 & -\frac{E_{22}K_2}{2} \end{bmatrix} \begin{Bmatrix} y_1 \\ z_1 \\ y_2 \\ z_2 \end{Bmatrix} \quad 3-13a$$

which can be written compactly as

$$\{\zeta'\} = [A]\{\zeta\} \quad 3-13b$$

where $\{\zeta\}$ represents the vector of the variables y_1 , z_1 , y_2 , z_2 and $[A]$ a matrix of constant coefficients. The stability of the variables y_j , z_j and in turn the stability of the Q_j is based on the eigenvalues of the matrix A . Let

$$\{\zeta\} = \{\beta\}e^{p\tau} \quad 3-14$$

Substitute 3-14 into 3-13b and solve the resulting eigenvalue problem

$$|[A] - pI| = 0 \quad 3-15$$

If any of the eigenvalues of 3-15 have a real part greater than zero the solutions of 3-14 are unstable and hence the trivial solution is unstable.

In general, an explicit solution of 3-15 may be extremely difficult and it is most convenient to solve 3-15 by standard computer techniques. For only a single resonance condition and zero damping coefficients the instability zones can be determined explicitly as was done in a similar manner by Hsu.^[19] For $B_{11} = E_{11} = E_{22} = 0$, the equation 3-15 can be written as:

$$\begin{vmatrix} -p & 0 & -\lambda K_1 & -\frac{B_{12}}{K_1^4} \\ 0 & -p & -\frac{B_{21}}{K_2^4} & -\lambda K_2 \\ \lambda K_1 & \frac{B_{12}}{K_1^4} & -p & 0 \\ \frac{B_{21}}{K_2^4} & \lambda K_2 & 0 & -p \end{vmatrix} = 0 \quad 3-16$$

Expanding 3-16 the characteristic equation is

$$p^4 + p^2 \left((\lambda K_2)^2 + (\lambda K_1)^2 + \frac{1}{8} \frac{B_{12}}{K_1} \frac{B_{21}}{K_2} \right) + (\lambda K_1 \lambda K_2 - \frac{1}{16} \frac{B_{12}}{K_1} \frac{B_{21}}{K_2})^2 = 0 \quad 3-17a$$

$$p^2 = -\frac{1}{2}((\lambda K_2)^2 + (\lambda K_1)^2 + \frac{1}{8} \frac{B_{12}}{K_1} \frac{B_{21}}{K_2}) \pm \frac{1}{2} \sqrt{[(\lambda K_2)^2 + (\lambda K_1)^2 + \frac{1}{8} \frac{B_{12}}{K_1} \frac{B_{21}}{K_2}]^2 - 4(\lambda K_1 \lambda K_2 - \frac{1}{16} \frac{B_{12}}{K_1} \frac{B_{21}}{K_2})^2}$$

3-17b

Roots with positive real parts can only exist if

$$[(\lambda K_2)^2 + (\lambda K_1)^2 + \frac{1}{8} \frac{B_{12}}{K_1} \frac{B_{21}}{K_2}]^2 - 4(\lambda K_1 \lambda K_2 - \frac{1}{16} \frac{B_{12}}{K_1} \frac{B_{21}}{K_2})^2 < 0$$

3-18a

$$(\lambda K_1 - \lambda K_2)^2 < -\frac{1}{4} \frac{B_{12} B_{21}}{K_1 K_2} \quad 3-18b$$

$$\lambda^2 (K_1 - K_2)^2 < -\frac{1}{4} \frac{B_{12} B_{21}}{K_1 K_2} \quad 3-18c$$

$$|\lambda| < \frac{1}{2} \sqrt{-\frac{B_{12}}{K_1} \frac{B_{21}}{K_2}} \quad 3-18d$$

Equation 3-18d shows that the external detuning must be within the limits $\pm \frac{1}{2} \sqrt{-\frac{B_{12} B_{21}}{K_1 K_2}}$ for an instability to occur.

3.5 Uncoupled Parametric Type 1 and Type 11 Resonances

If the natural frequencies are such that the two parametric resonances can not occur simultaneously (i.e. $K_2 \neq 3K_1$)

then each resonance can be treated on an individual basis. The type 1 resonance can be obtained from equations 3-8 by setting $B_{12} = B_{21} = A_{12} = A_{24} = 0$ and the type 11 resonance can be obtained by setting $B_{11} = A_{12} = A_{24} = 0$. In these uncoupled resonance cases the analysis is considerably simplified involving either the solution of 2 or 3 averaged equations as compared to the analysis of the system with both resonances interacting which involves the solution of four equations (3-8). To evaluate properly the effect of the interaction of the two parametric resonances, a comparison will be made between the solutions of equation 3-8 and the equations which neglect the coupling effect. In this way, the qualitative and quantitative differences of the interaction effect will become apparent, including the error estimate of basing an analysis on the approximation that the interaction can be neglected.

(a) Uncoupled Parametric Type I Resonance

If the frequencies are not near an integer ratio, a parametric type I resonance will develop if $\Omega \approx 2\omega_1$. Applying the averaging operator to the equations 3-6a, b, the averaged equations are

$$K_1 Q'_1 = \frac{B_{11}}{4} Q_1 \sin 2\theta_1 - \frac{E_{11}}{2} K_1 Q_1 \quad 3-19a$$

$$K_2 Q'_2 = -\frac{E_{22}}{2} Q_2 K_2 \quad 3-19b$$

$$K_1 \theta'_1 = \lambda K_1^2 + \frac{B_{11}}{4} \cos 2\theta_1 + \frac{3}{8} A_{11} Q_1^2 + \frac{1}{4} A_{13} Q_2^2 \quad 3-19c$$

$$K_2 \theta'_2 = \lambda K_2^2 + \frac{3}{8} A_{21} Q_2^2 + \frac{1}{4} A_{23} Q_1^2 \quad 3-19d$$

It can be seen from equation 3-19b that Q_2 is not excited and any initial disturbance of Q_2 will die down due to the damping term $-\frac{E_{22}}{2} Q_2 K_2$. With $Q_2 \rightarrow 0$ the equations 3-19a and 3-19c are uncoupled from the system and can be written as:

$$K_1 Q'_1 = \frac{B_{11}}{4} Q_1 \sin 2\theta_1 - \frac{E_{11} Q_1}{2} K_1 \quad 3-20a$$

$$K_1 \theta'_1 = \frac{\lambda_1}{2} K_1 + \frac{B_{11}}{4} \cos 2\theta_1 + \frac{3}{8} A_{11} Q_1^2 \quad 3-20b$$

Equations 3-20 are the averaged equations of a non-linear Mathieu type equation and represent a single mode response of the system 3-1 to an external monofrequency excitation. The steady-state boundaries can be obtained by setting $Q_1 = Q_1^\circ$, $\theta_1 = \theta_1^\circ$, $Q'_1 = \theta'_1 = 0$. Then

$$\sin 2\theta_1^\circ = \frac{2 E_{11} K_1}{B_{11}} \quad 3-21$$

substituting into 3-20 and using the definition

$$\lambda = 1 - \frac{\Omega}{\Omega_0} \quad 3-22$$

the steady-state amplitude frequency relationship is obtained.

$$\frac{\Omega}{\Omega_0} = 1 \pm \frac{1}{2} \frac{B_{11}}{K_1} \sqrt{1 - \frac{4E_{11}^2 K_1^2}{B_{11}^2}} + \frac{3}{4} \frac{A_{11}}{K_1} Q_1^2 \quad 3-23$$

From equation 3-23 it is seen that viscous damping represented by the coefficient E_{11} diminishes the instability region for which a parametric resonance is possible. If

$$E_{11} > \frac{B_{11}}{2}$$

the instability zone vanishes and no parametric resonance is possible. This means that the parametric excitation coefficient B_{11} must exceed a certain threshold value for resonance to take place.

(b) Uncoupled Parametric Type 11 Resonance

If it is assumed that the frequencies are not near an integer ratio, the averaged equations for the combination minus resonance, $\Omega = \omega^{\circ}_2 - \omega^{\circ}_1$ can be obtained from equations 3-6 and are:

$$Q'_1 = \frac{B_{12}}{4K_1} Q_2 \sin(\theta_1 - \theta_2) - \frac{E_{11}}{2} Q_1 \quad 3-24a$$

$$Q'_2 = -\frac{B_{21}}{4K_2} Q_1 \sin(\theta_1 - \theta_2) - \frac{E_{12}}{2} Q_2 \quad 3-24b$$

$$\begin{aligned} \theta'_1 = & \lambda K_1 + \frac{B_{12}}{4K_1} \frac{Q_2}{Q_1} \cos(\theta_1 - \theta_2) + \frac{3}{8} \frac{A_{11}}{K_1} Q_1^2 \\ & + \frac{1}{4} \frac{A_{13}}{K_1} Q_2^2 \end{aligned} \quad 3-24c$$

$$\begin{aligned} \theta'_2 = & \lambda K_2 + \frac{B_{21}}{4K_2} \frac{Q_1}{Q_2} \cos(\theta_1 - \theta_2) + \frac{3}{8} \frac{A_{21}}{K_2} Q_2^2 \\ & + \frac{1}{4} \frac{A_{23}}{K_2} Q_1^2 \end{aligned} \quad 3-24d$$

The phase angles can be combined to

$$\begin{aligned} \phi' = \lambda(K_1 - K_2) + \frac{1}{4} \left(\frac{B_{12}}{K_1} \frac{Q_2}{Q_1} - \frac{B_{21}}{K_2} \frac{Q_1}{Q_2} \right) \cos \phi \\ + \frac{3}{8} \left(\frac{A_{11}}{K_1} Q_1^2 - \frac{A_{21}}{K_2} Q_2^2 \right) + \frac{1}{4} \left(\frac{A_{13}}{K_1} Q_2^2 - \frac{A_{23}}{K_2} Q_1^2 \right) \end{aligned} \quad 3-25a$$

$$\text{where} \quad \phi = \theta_1 - \theta_2 \quad 3-25b$$

Equation 3-25a can be rewritten in the form

$$\begin{aligned} \phi' = -\lambda + \frac{1}{4} \left(\frac{B_{12}}{K_1} \frac{Q_2}{Q_1} - \frac{B_{21}}{K_2} \frac{Q_1}{Q_2} \right) \cos \phi + \frac{Q_1^2}{4} \left(\frac{3}{2} \frac{A_{11}}{K_1} - \frac{A_{23}}{K_2} \right) \\ + \frac{Q_2^2}{4} \left(\frac{A_{13}}{K_1} - \frac{3}{2} \frac{A_{21}}{K_2} \right) \end{aligned} \quad 3-26$$

where the relationship $K_1 - K_2 = -1$ has been substituted.

The steady state equations can be obtained from 3-24 and 3-25 by setting $Q_1 = Q_1^\circ$, $Q_2 = Q_2^\circ$, $\phi = \phi^\circ$, $Q_1' = Q_2' = \phi' = 0$. The ratio of the steady state amplitudes can be obtained from 3-24a and 3-24b and is:

$$\frac{Q_2^\circ}{Q_1^\circ} = \sqrt{-\frac{E_{11}}{E_{22}} \frac{B_{21}}{B_{12}} \frac{K_1}{K_2}} \quad 3-27$$

It is to be noted that for this study of a combination minus resonance, $B_{12} B_{21} < 0$. The expression 3-27 is therefore a real quantity. Using the expression 3-27 the steady-state

amplitude response can be obtained as follows:

$$\frac{\Omega}{\Omega_0} = 1 \pm \frac{1}{4} \sqrt{-\frac{B_{12}B_{21}}{K_1K_2}} \left[\sqrt{\frac{E_{11}}{E_{22}}} + \sqrt{\frac{E_{22}}{E_{11}}} \right] \sqrt{1 + \frac{4E_{11}E_{22}K_1K_2}{B_{12}B_{21}}} - \frac{Q_1^2}{4} \left(\frac{3}{2} \frac{A_{11}}{K_1} - \frac{A_{23}}{K_2} \right) - \frac{Q_2^2}{4} \left(\frac{A_{13}}{K_1} - \frac{3}{2} \frac{A_{21}}{K_2} \right) \quad 3-28$$

where the substitutions

$$\sin \phi^\circ = 2 \frac{E_{11}}{B_{12}} \frac{Q_1^\circ}{Q_2^\circ} \frac{1}{K_1} \quad 3-29a$$

$$\cos \phi^\circ = \pm \sqrt{1 - \sin^2 \phi^\circ} \quad 3-29b$$

$$\frac{\Omega}{\Omega_0} = (1 - \lambda) \quad 3-29c$$

have been carried out.

Three important differences can be observed between the monofrequency response of the type I resonance and the two mode response of the combination minus type II resonance, namely

- (a) the destabilizing effect of viscous damping
- (b) the frequencies of the responding modes and
- (c) the effect of the nonlinear terms.

From equation 3-28 it can be seen that if $E_{11} \neq E_{22}$ but E_{11}, E_{22} are small, the width of the resonance zone can be made arbitrarily large. This is in distinct contrast to

equation 3-23 of the type 1 resonance where the addition of viscous damping can only decrease the width of the resonance zone.

For the steady-state response, the phase angle variable $\phi = \theta_1 - \theta_2$ must remain constant. This means that individual frequency corrections can occur in each mode but in such a way that the external resonance condition $K_2 - K_1 = 1$ is maintained. Consequently, both modes must have equal frequency corrections.

The nonlinear terms are expected to limit the maximum amplitude growth. By inspecting equation 3-26 it is seen that the coefficients of the nonlinear terms are made up of the difference of the constants A_{jm} . This will tend to reduce the effect of the nonlinearities. In fact, a special system could be conceived where the nonlinear effects could cancel out completely. Also, from the nature of the coefficients it is possible that the steady-state response curve can exhibit a hardening or softening type of nonlinearity even if the system is composed of hardening type nonlinear terms.

3.6 Steady-State Solutions

The steady-state response curves for the type 1 and type 11 resonances can be plotted directly from the equations 3-23 and 3-28 respectively. The steady-state curves for the coupled system can not be written out explicitly. The solutions in this case must be obtained by trial and error.

(a) Uncoupled Type 1 Resonance

In Fig. 3-1 the steady-state amplitude Q°_1 is plotted against the non-dimensional frequency ratio Ω/Ω_0 . The condition $\Omega/\Omega_0 = 1.0$ means that the external resonance condition is exactly satisfied and the external detuning λ is equal to zero. The value of the coefficients for which these curves are plotted are as indicated in the figure. It is to be noted

that the response curve has two branches and the unstable response curve is marked by dashed lines. The steady-state amplitude Q°_2 is zero in this resonance. The response curves exhibit a hardening type nonlinearity and lean towards the high frequency side. As predicted by equation 3-23, a steady-state response is always possible for $\lambda < 0$ or $\Omega/\Omega_0 > 1$. The width of the instability zone is given by equation 3-23 by setting $Q^{\circ}_1 = 0$. Within this zone any small initial disturbance will grow and finally reach the steady state value. Over the width of the instability zone it is seen that the steady-state amplitude Q°_1 is zero at the low frequency side of the instability zone and increases continuously as the external frequency increases. Outside the instability zone large initial disturbances may shock excite the system into resonance in the area of the "overhang" $(1 - \lambda) > 1.1$.

(b) Uncoupled Type 11 Resonance

The steady-state amplitudes Q°_1 and Q°_2 for the combination resonance are plotted in Figure 3-2 with the values of the coefficients shown in the figure. In contrast to the type 1 resonance curve, the response curves exhibit a lean towards the low frequency side as is characteristic of systems with softening type nonlinearities. The width in the instability zone is given by equation 3-28 by setting $Q^{\circ}_1 = Q^{\circ}_2 = 0$. Within this zone any small initial disturbance will again cause large amplitude oscillations.

(c) Coupled Type 1 and Type 11 Resonance

For the coupled system where both type 1 and type 11 resonance occur simultaneously the steady state must be sought by trial and error methods. Replacing the amplitudes $Q_{1,2}$ and phase angles $\theta_{1,2}$ of equation 3-8 by their steady-state values $Q^{\circ}_{1,2}$ and $\theta^{\circ}_{1,2}$ and neglecting the internal resonance condition by setting $A_{12} = A_{24} = 0$, the equations

from which the steady-state values are sought can be written as

$$0 = \frac{B_{11}}{4K_1} Q_1^\circ \sin (2\theta_1^\circ) + \frac{B_{12}}{4K_1} Q_2^\circ \sin (\theta_1^\circ - \theta_2^\circ) - \frac{E_{11}}{2} Q_1^\circ \quad 3-30a$$

$$0 = - \frac{B_{21}}{4K_2} Q_1^\circ \sin (\theta_1^\circ - \theta_2^\circ) - \frac{E_{22}}{2} Q_2^\circ \quad 3-30b$$

$$0 = + \lambda K_1 + \frac{B_{11}}{4K_1} \cos (2\theta_1^\circ) + \frac{B_{12}}{4K_1} \frac{Q_2^\circ}{Q_1^\circ} \cos (\theta_1^\circ - \theta_2^\circ) + \frac{3}{8} \frac{A_{11}}{K_1} Q_1^{\circ 2} + \frac{1}{4} \frac{A_{13}}{K_1} Q_2^{\circ 2} \quad 3-30c$$

$$0 = + \lambda K_2 + \frac{B_{21}}{4K_2} \frac{Q_1^\circ}{Q_2^\circ} \cos (\theta_1^\circ - \theta_2^\circ) + \frac{3}{8} \frac{A_{21}}{K_2} Q_2^{\circ 2} + \frac{1}{4} \frac{A_{23}}{K_2} Q_1^{\circ 2} \quad 3-30d$$

From equation 3-30b

$$\sin (\theta_1^\circ - \theta_2^\circ) = - 2 \frac{E_{22} K_2}{B_{21}} \frac{Q_2^\circ}{Q_1^\circ} \quad 3-31a$$

and

$$\cos (\theta_1^\circ - \theta_2^\circ) = \pm \sqrt{1 - 4 \left(\frac{E_{22} K_2}{B_{21}} \right)^2 \left(\frac{Q_2^\circ}{Q_1^\circ} \right)^2} \quad 3-31b$$

From (a)

$$\sin 2\theta_1^\circ = 2 \frac{B_{12}}{B_{11}} \left(\frac{Q_2^\circ}{Q_1^\circ} \right)^2 \frac{E_{22}}{B_{21}} + 2 \frac{E_{11}K_1}{B_{11}} \quad 3-32a$$

Because of the condition $|\sin (\theta_1^\circ - \theta_2^\circ)| \leq 1$, 3-32b equations 3-31 and 3-32 already impose restrictions on the values of the coefficients for which a steady-state is possible. By eliminating the external detuning between 3-30c and 3-30d a relationship between the amplitudes Q_1° and Q_2° can be obtained.

$$\begin{aligned} \frac{1}{K_1} \frac{B_{11}}{2} \left[-\frac{B_{11}}{4} \cos (2\theta_1^\circ) + \frac{B_{12}}{4} \frac{Q_2^\circ}{Q_1^\circ} \cos (\theta_1^\circ - \theta_2^\circ) + \frac{3}{8} A_{11} Q_1^{\circ 2} \right. \\ \left. + \frac{1}{4} A_{13} Q_2^{\circ 2} \right] + \frac{1}{K_2} \frac{B_{21}}{2} \left[\frac{B_{21}}{4} \frac{Q_1^\circ}{Q_2^\circ} \cos (\theta_1^\circ - \theta_2^\circ) \right. \\ \left. + \frac{3}{8} A_{21} Q_2^{\circ 2} + \frac{1}{4} A_{23} Q_1^{\circ 2} \right] = 0 \quad 3-33 \end{aligned}$$

By trial and error, using equations 3-31a, b, 3-33, and the condition 3-32b, steady-state amplitudes may be obtained. The amplitude-frequency relationship is then given by

$$\begin{aligned} \frac{\Omega}{\Omega_0} = 1 - \frac{1}{K_1} \frac{B_{11}}{2} \left[-\frac{B_{11}}{4} \cos (2\theta_1^\circ) + \frac{B_{12}}{4} \frac{Q_2^\circ}{Q_1^\circ} \cos (\theta_1^\circ - \theta_2^\circ) \right. \\ \left. + \frac{3}{8} A_{11} Q_1^{\circ 2} + \frac{1}{4} A_{13} Q_2^{\circ 2} \right] \quad 3-34 \end{aligned}$$

The results of the numerical solutions of equation 3-30

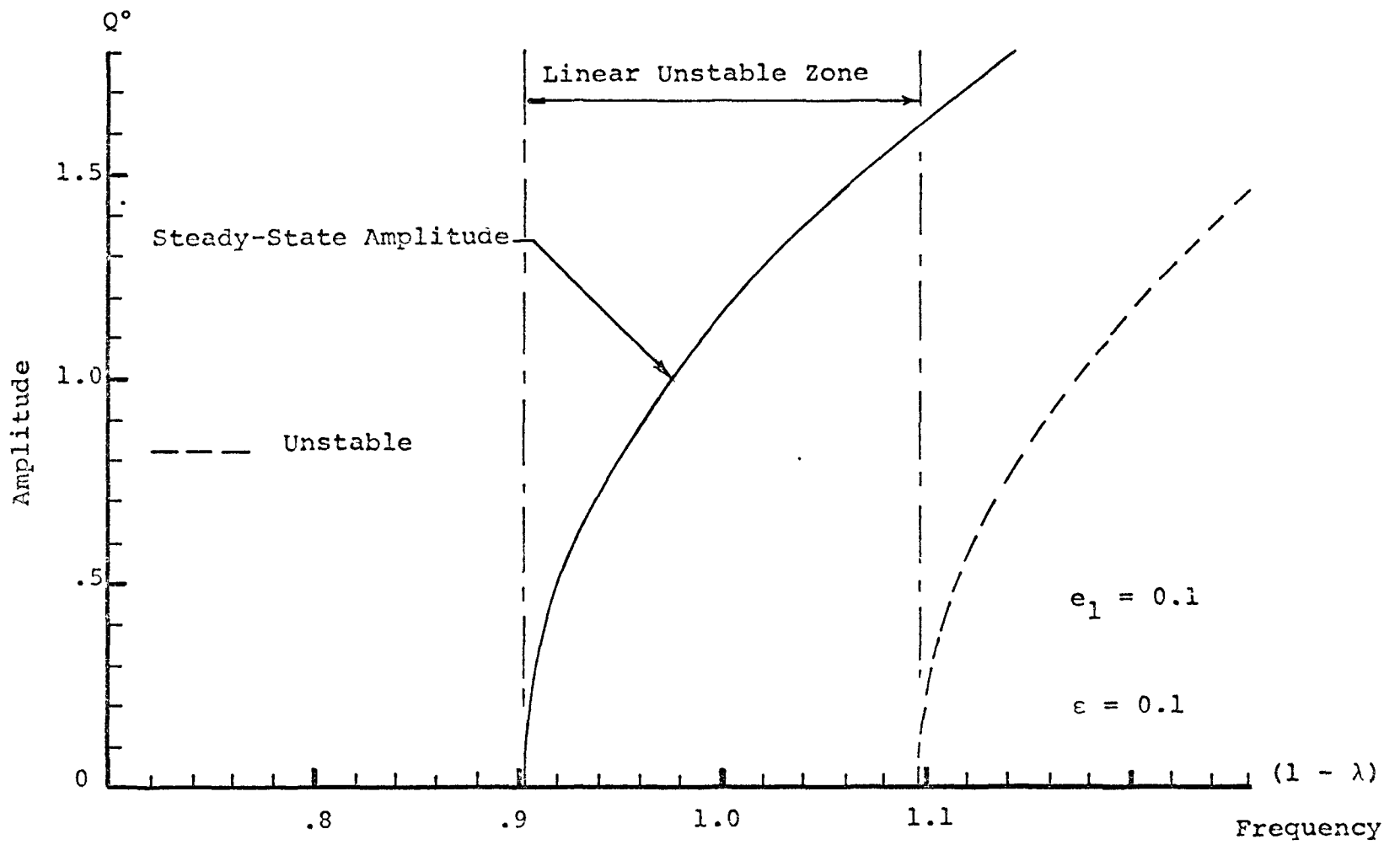


FIG. 3-1 UNCOUPLED TYPE I STEADY-STATE RESPONSE
 $(\omega_1 = 0.45, b_{11} = 0.8, a_{11} = 0.4)$

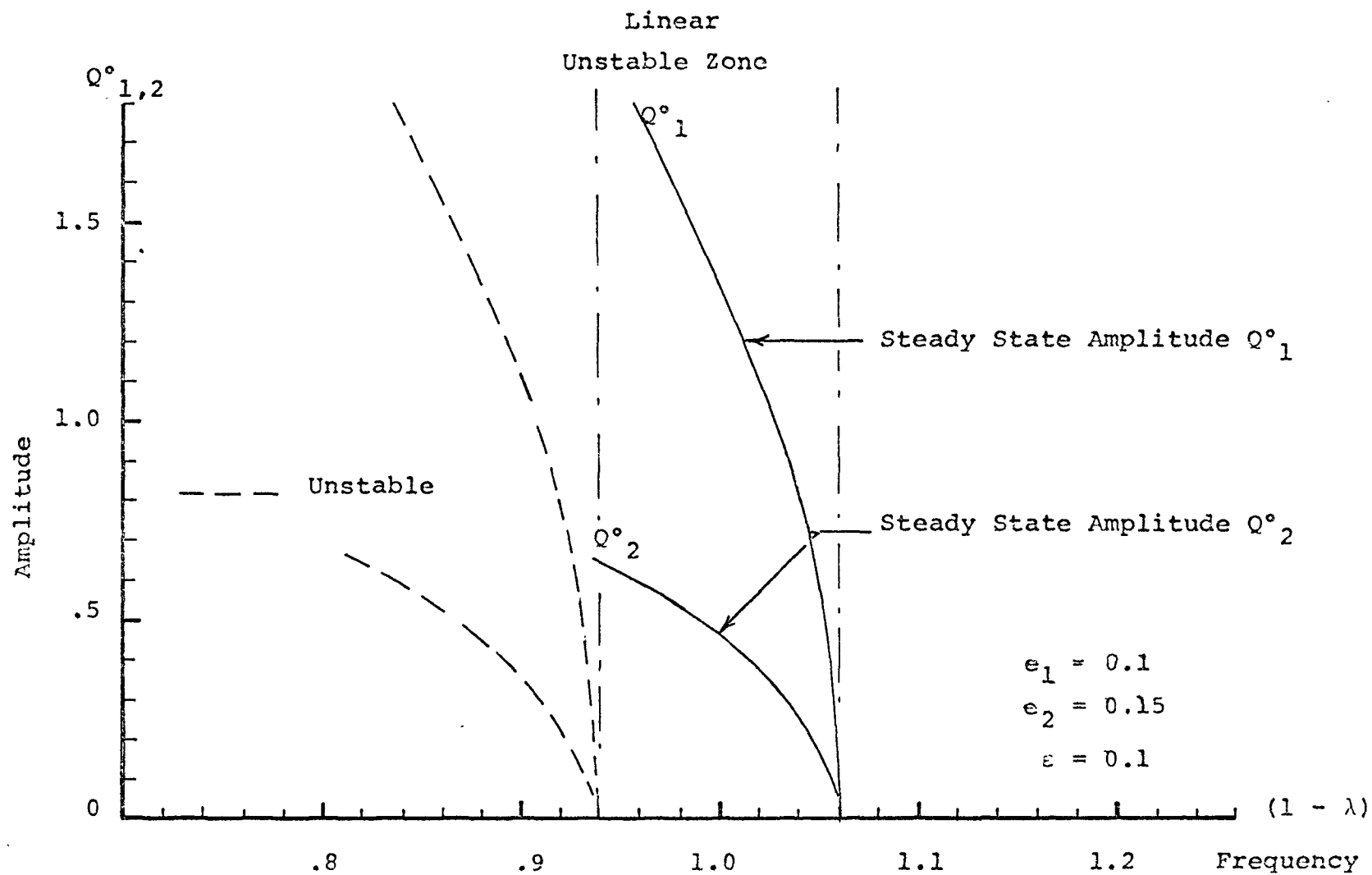


FIG. 3-2 UNCOUPLED TYPE II RESPONSE ($\omega_1 = 0.45$, $\omega_2 = 3 \times \omega_1$)

($b_{11} = 0.8$, $b_{12} = -1.2$, $b_{21} = 0.6$, $a_{11} = 0.4$, $a_{13} = 0.3$, $a_{21} = 0.5$, $a_{23} = 0.27$)

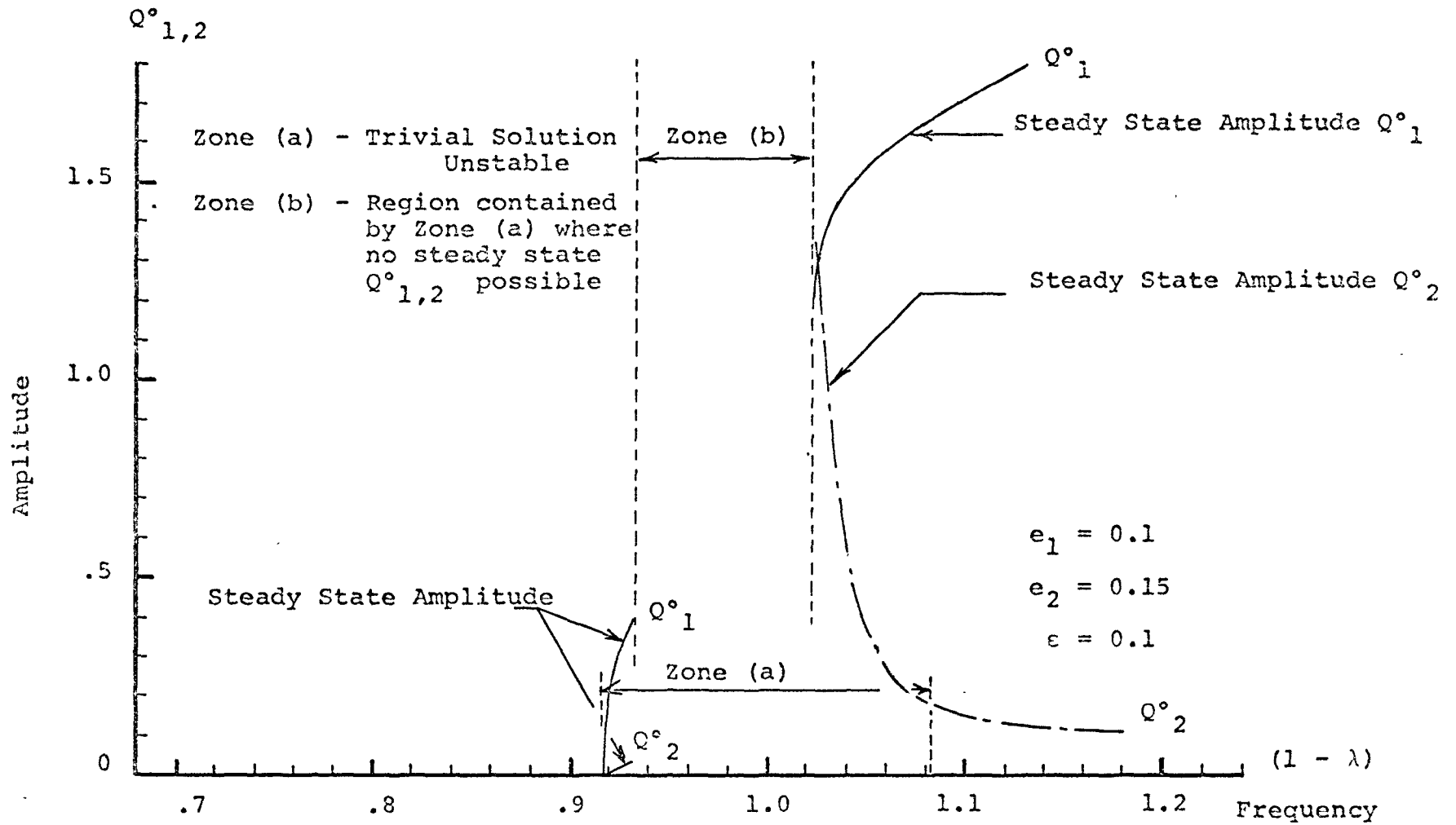


FIG. 3-3 COUPLED TYPE I AND TYPE II STEADY STATE CURVES ($\omega_1 = 0.45, \omega_2 = 3\omega_1$)

($b_{11} = 0.8, b_{12} = -1.2, b_{21} = 0.6, a_{11} = 0.4, a_{13} = 0.3, a_{21} = 0.5, a_{23} = 0.27$)

to 3-34 are as shown in Fig. 3-3. In addition to obtaining the steady-state values of the amplitudes it is also necessary to check the stability of the trivial solution $Q^{\circ}_{1,2} = 0$. This was done by numerically solving the eigenvalue problem given by equation 3-15. It was found that $R(p) > 0$ occurred in the range $\lambda = \pm .082$. Compared to Fig. 3-1, the coupled instability zone is less by 16% than the type 1 uncoupled zone. Only over a small portion of the instability zone, is a steady-state solution possible. The steady-state curves on the low frequency side coincide for $Q^{\circ}_j = 0$ with the boundary of the instability zone as determined by the instability analysis of the trivial solution. On the high frequency side a steady-state condition appears possible for $\Omega/\Omega_0 > 1.022$. In this case the amplitude Q°_1 has a much larger value than the amplitude Q°_2 . As Ω/Ω_0 increases the response is predominantly in the first mode as shown by the large value of Q°_1 . This may be expected by comparing Fig. 3-3 to Fig. 3-1 where it is seen that the uncoupled type 1 response curve slopes to the high frequency side.

3.7 Transient Response

In order to find out the nature of the response where the algebraic analysis has indicated that no steady-state is possible, a study of the transient response is necessary. For completeness, the transient response of the uncoupled cases will also be studied.

(a) Uncoupled Type 1 Transient Response

The time history response for $\lambda = .02$ is given in Fig. 3-4. The amplitude Q_1 grows exponentially following a small disturbance. As the amplitude builds up the nonlinear terms begin to take effect and the amplitude Q_1 after several oscillations takes on a steady-state value. Similarly the phase angle also takes on a steady-state value. At this point

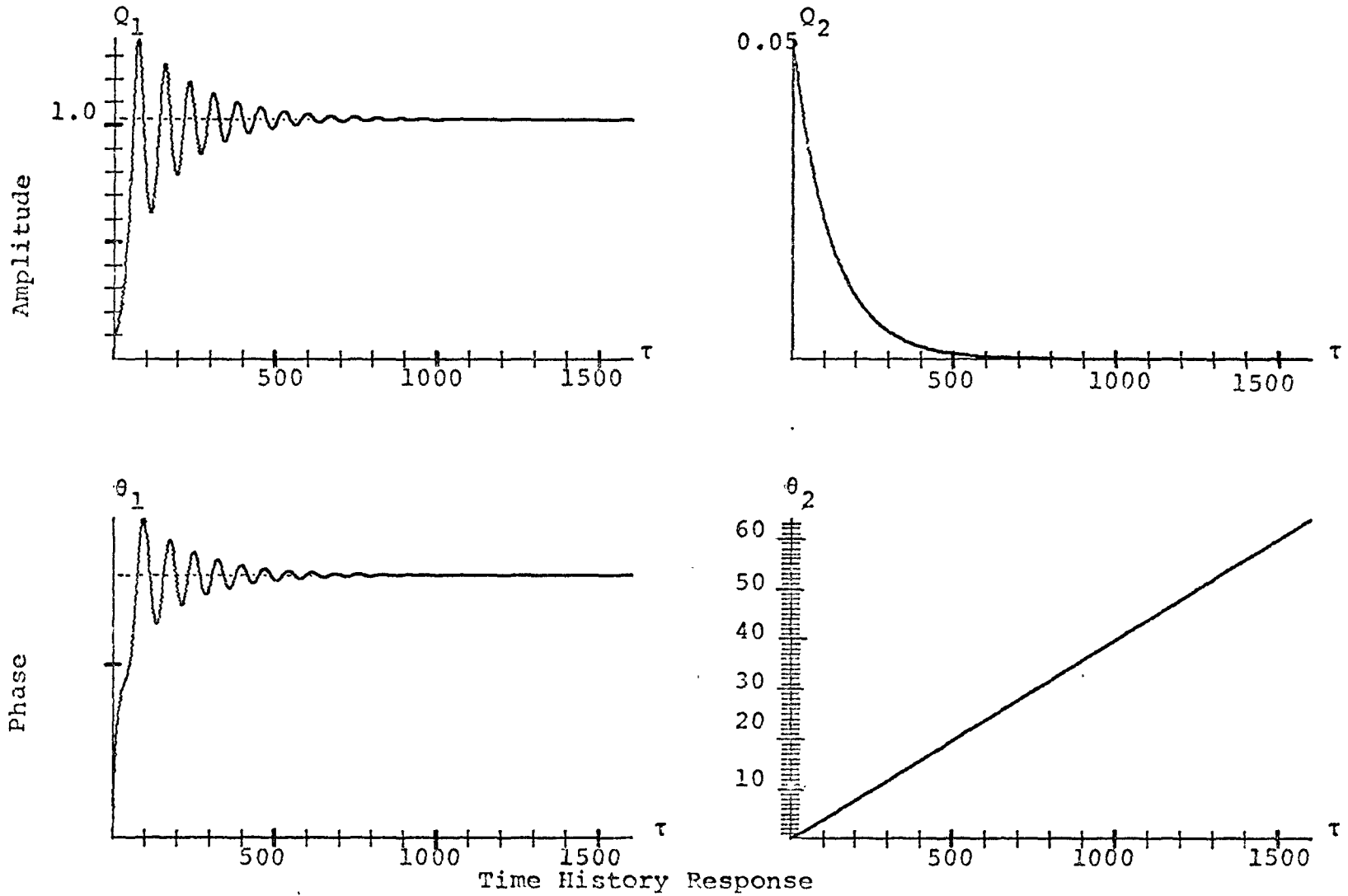


FIG. 3-4 PARAMETRIC TYPE I: $(1 - \lambda) = 0.98$, $\omega_1 = .45$, $\omega_2 = 1.35$,
 $(e_1 = 0.1, e_2 = 0.15, b_{11} = 0.8, a_{11} = 0.4, a_{13} = 0.3, a_{21} = 0.5, a_{23} = 0.27, \epsilon = 0.1)$

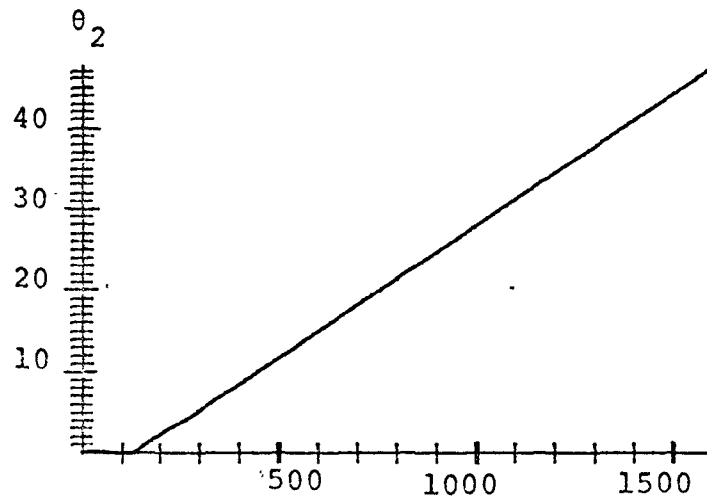
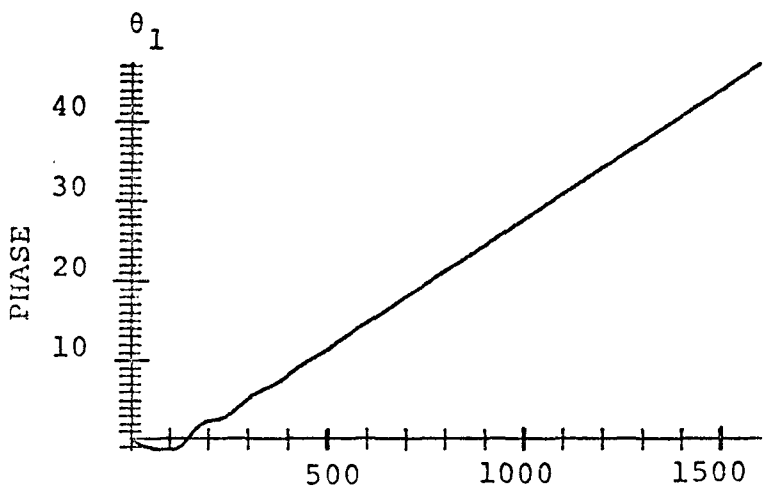
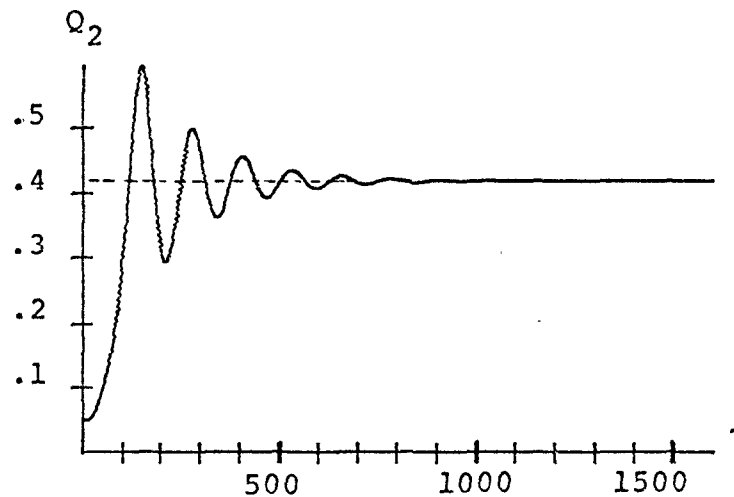
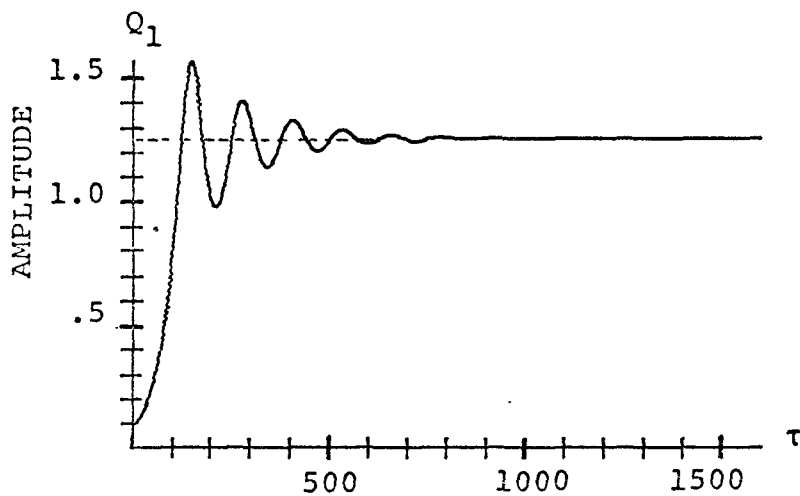


FIG. 3-5 COMBINATION TYPE II TIME HISTORY RESPONSE: $(1 - \lambda) = 1.01$; $\omega_1 = .45$, $\omega_2 = 1.35$,
 $(e_1 = 0.1, e_2 = 0.15, b_{12} = -1.2, b_{21} = 0.6, a_{11} = 0.4, a_{13} = 0.3, a_{21} = 0.5, a_{23} = 0.27, \epsilon = 0.1)$

the system is in a synchronized state and the frequency of the response is exactly one half the frequency of the external excitation. The amplitude Q_2 is not excited and approaches zero. The phase angle θ_2 is coupled to the amplitude Q_1 as shown by equation 3-19d and increases with time. The rate of change of θ_2 , however, reaches a steady state value. The overshoot, or maximum amplitude reached before steady-state takes place is in the order of 40% greater than the final steady-state value.

(b) Uncoupled Type 11 Transient Response

In Fig. 3-5 are shown the response curves by numerically integrating the system of equations 3-24. Again it is noticed that the transient solution has a pronounced overshoot after which the amplitudes settle in on a steady-state value. The overshoot for this case is in excess of 20% of the steady-state values. The phase angles θ_1 and θ_2 increase continuously with time but the difference $\theta_1 - \theta_2$ reaches a constant value. This means that each mode has an increased frequency correction which can be calculated from equations 3-24c and d.

(c) Coupled Type 1 and Type 11 Transient Response

The nature of the transient solutions preceding the steady-state and the nature of the solutions where no steady-state is possible is obtained by integrating the averaged equation system (3-8). The numerical integration is also used to verify the stability of the steady-state curves shown in Fig. 3-3. Fig. 3-6 shows the response at $(1 - \lambda) = 1.01$ in the region where no steady-state is possible. The two time-history curves plot the amplitudes Q_1, Q_2 against the non-dimensional time τ . The integration was continued until a quasi-steady-state condition was obtained. After $\tau > 600$ the response curves appear to become periodic although the nature of this

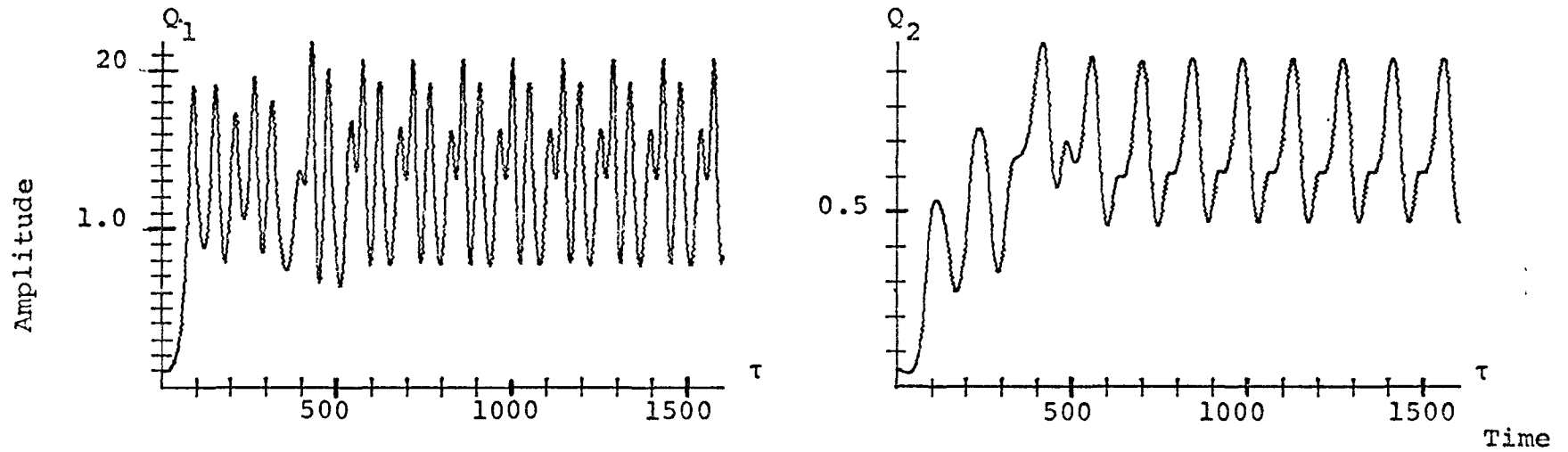


FIG. 3-6 COUPLED TYPE I AND TYPE II TIME HISTORY RESPONSE, $(1 - \lambda) = 1.01$, $\omega_1 = .45$, $\omega_2 = 1.35$
 $(e_1 = 0.1, e_2 = 0.15, b_{11} = 0.8, b_{12} = -1.2, b_{21} = 0.6, a_{11} = 0.4, a_{13} = 0.3, a_{21} = 0.5,$
 $a_{23} = 0.27, \epsilon = 0.1)$

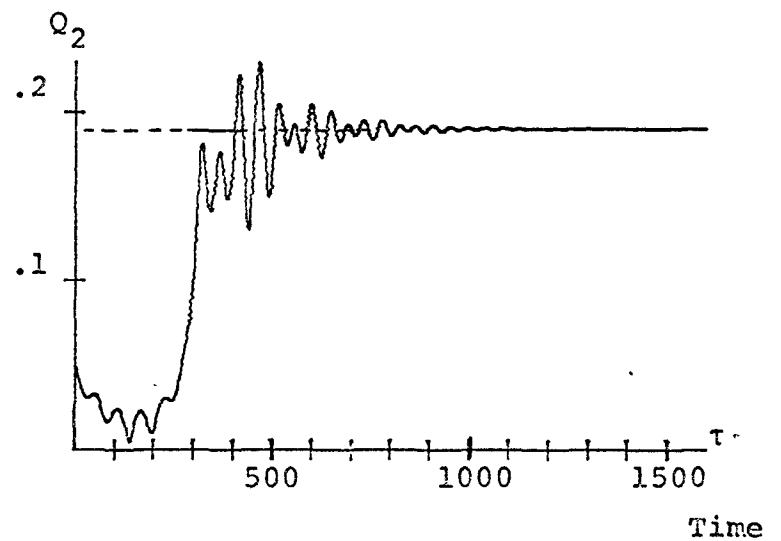
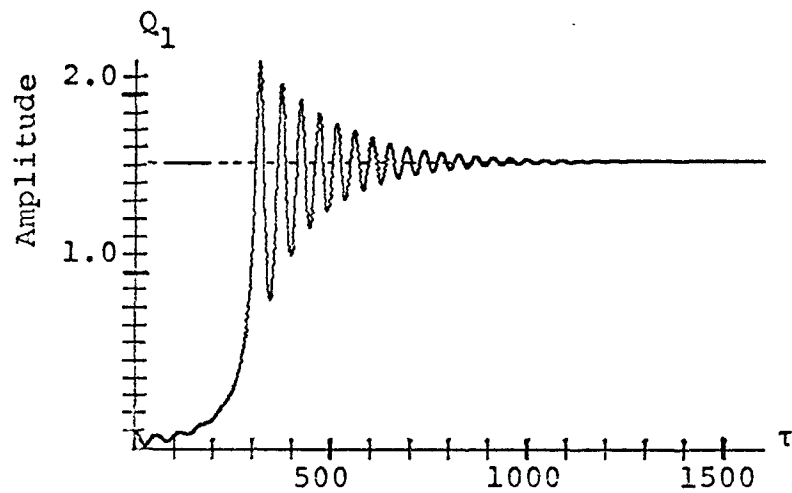


FIG. 3-7 COUPLED TYPE I AND TYPE II TIME HISTORY RESPONSE $(1 - \lambda) = 1.08$, $\omega_1 = .45$, $\omega_2 = 1.35$
 $(e_1 = 0.1, e_2 = 0.15, b_{11} = 0.8, b_{12} = -1.2, b_{21} = 0.6, a_{11} = 0.4, a_{13} = 0.3, a_{21} = 0.5,$
 $a_{23} = 0.27, \epsilon = 0.1)$

periodic response appears complex. The mean value of the amplitude Q_1 can be scaled from the plot and is approximately 1.4. This can be compared to Fig. 3-1 where the maximum amplitude Q_1 at $\Omega/\Omega_0 = 1.01$ is 1.22. The mean value of Q_2 is 0.7 and is in excess of 50% of the value of Q_2 given by the uncoupled parametric type 11 curve.

Fig. 3-7 shows the response curves for the frequency $(1 - \lambda) = 1.08$. This is just within the instability zone and the rate of growth of the amplitudes is at first very slow. However the amplitudes continue to grow and finally at $\tau > 1100$ reach a steady state. The steady-state values agree with the algebraic steady-state values as shown in Fig. 3-1. The overshoot in this case is approximately 30% in excess of the steady-state value.

3.8 Example of a Double Pendulum With Circulatory Loading

Statement of the Problem

The response curves obtained in section 3-6 and 3-7 were based on the mathematical model of the equations 3-1 without direct application to a specific physical model. This was done to demonstrate the key points of the interaction problem. To obtain a better physical insight and also to provide a basis for experimental investigation the physical modal of the double pendulum first proposed by Ziegler^[58] will be examined.

The model is shown in Fig. 3-8 and consists of a double pendulum which is allowed to rotate in a smooth horizontal plane. It has two rigid bars of negligible weights and equal length ℓ and two masses m_1 and m_2 . A force $P(t)$ is assumed to act tangentially at the free end of the bars. At the hinges act the restoring moments $cR_j(\phi_j, \dot{\phi}_j)$ which may be linear or nonlinear functions of the generalized co-ordinates ϕ_j and their time derivatives. It is assumed that the displacement of the angles ϕ_j is small so that the small

angle assumptions $\sin\phi = \phi$, $\cos\phi = 1$ hold. The Kinetic Energy T is:

$$T = \frac{1}{2} m_1 [\dot{\phi}_1^2 \ell^2] + \frac{1}{2} m_2 [\ell^2 \dot{\phi}_1^2 + 2\ell^2 \dot{\phi}_1 (\dot{\phi}_1 + \dot{\phi}_2) + \ell^2 (\dot{\phi}_1 + \dot{\phi}_2)^2] \quad 3-34a$$

For the case $m_1 = 2m_2 = 2m$, the kinetic energy can be written as

$$T = \frac{1}{2} m [6\dot{\phi}_1^2 \ell^2 + 4\ell^2 \dot{\phi}_1 \dot{\phi}_2 + \ell^2 \dot{\phi}_2^2] \quad 3-34b$$

The generalized forces S_j corresponding to the generalized co-ordinate ϕ_j can be obtained from the expression

$$\delta W_j = S_j \delta \phi_j \quad 3-35$$

where δW_j is the work done by all applied forces when ϕ_j alone is increased by $\delta \phi_j$. The generalized forces due to the applied load $P(t)$ can be obtained from the expression

$$\delta \bar{W}_1 = \{-P\ell \phi_2\} \delta \phi_1 \quad 3-36a$$

$$\delta \bar{W}_2 = 0 \quad 3-36b$$

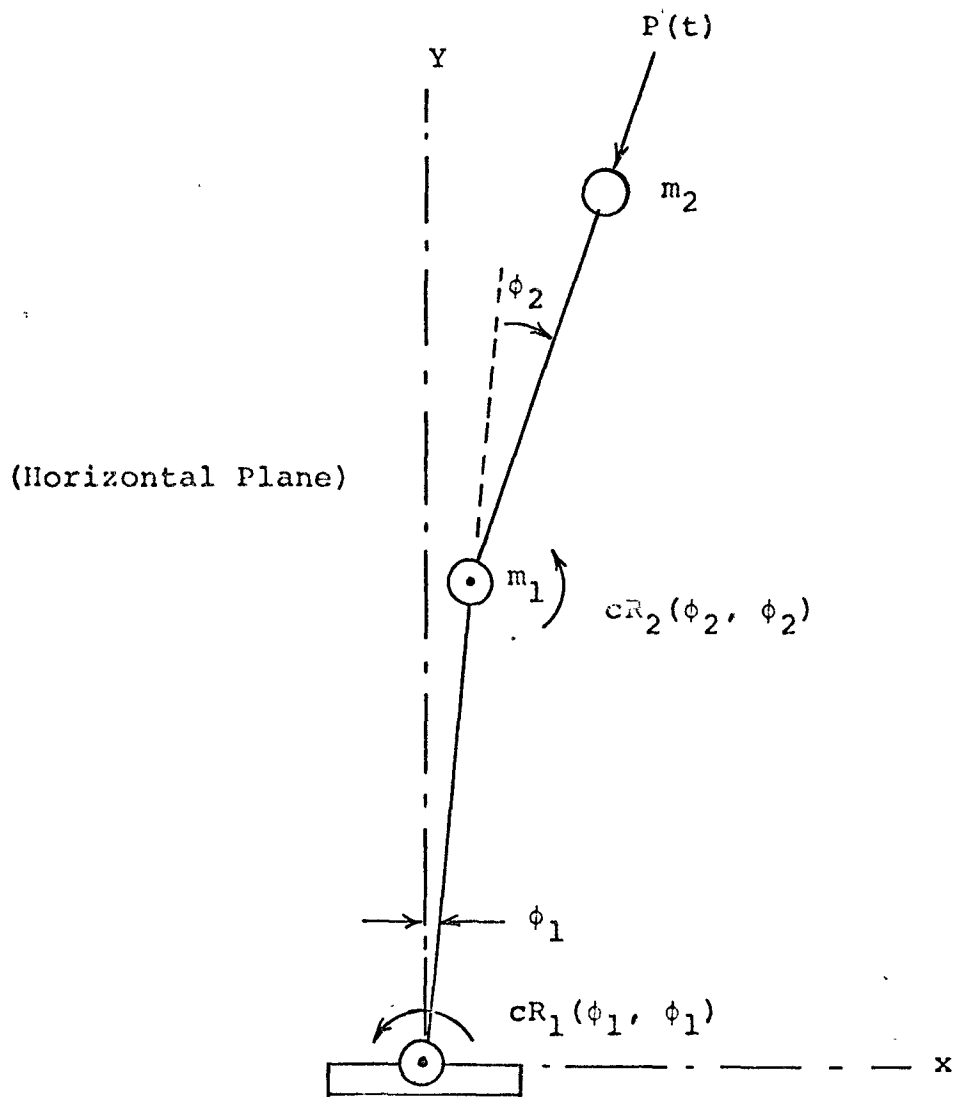


FIG. 3-8 DOUBLE PENDULUM WITH CIRCULATORY
LOADING

The generalized forces due to the external force and the restoring forces is then:

$$S_1 = - P\ell\phi_2 - cR_1 \quad 3-37a$$

$$S_2 = - cR_2 \quad 3-37b$$

By means of Lagrange's equations:

$$\frac{d}{dt} \left(\frac{\partial T}{\partial \dot{\phi}_j} \right) - \frac{\partial T}{\partial \phi_j} = S_j \quad (j = 1, 2) \quad 3-38$$

the equations of motion are:

$$6m\ell^2\ddot{\phi}_1 + 2m\ell^2\ddot{\phi}_2 + cR_1 + P\ell\phi_2 = 0 \quad 3-39$$

$$2m\ell^2\ddot{\phi}_1 + m\ell^2\ddot{\phi}_2 + cR_2 = 0$$

which can be re-ordered in the more convenient form

$$\ddot{\phi}_1 + 0.5 R_1 - R_2 + 0.5 F \phi_2 = 0 \quad 3-40a$$

$$\ddot{\phi}_2 - R_1 + 3R_2 - F \phi_2 = 0 \quad 3-40b$$

where primes now mean differentiation with respect to the normalized time T where

$$T = \frac{1}{\ell} \left(\frac{c}{m} \right)^{1/2} t \quad 3-41a$$

$$F(t) = \frac{P(t) \ell}{c} \quad 3-41b$$

(a) Description of the Restoring Functions $cR_j(\phi_j, \dot{\phi}_j)$

The restoring moments $cR_j(\phi_j, \dot{\phi}_j)$ are taken to be of the form

$$cR_j(\phi_j, \dot{\phi}_j) = [c + \bar{a}\phi_j^2]\phi_j + \bar{e}\dot{\phi}_j \quad 3-42$$

where \bar{a} represents the strength of the nonlinear cubic part of the restoring spring. The plus sign designates a hardening spring. The coefficient \bar{e} is a measure of the value of the viscous damping. The three coefficients c , \bar{a} and \bar{e} are taken to be equal for both restoring functions.

Instead of continuing the analysis in the variables ϕ_j which represent the actual physical co-ordinates at the double pendulum model, new variables x_j are introduced defined by

$$x_j = \frac{\phi_j}{\phi_y} \quad 3-43$$

For restoring functions which have a pronounced yielding effect ϕ_y would correspond with the yield point. For cubic restoring functions a pronounced yield point does not exist

and ϕ_y may be taken as the proportional limit. The variables $(x_j - 1)$ now measure the extent to which the angles have entered the nonlinear range.

(b) The Equations of Motion

By specifying a harmonic time varying component in the thrust force

$$F = F_o + F_t \cos (\Omega T) \quad 3-44a$$

and substituting

$$e = \frac{\bar{e}}{l (mc)^{1/2}} \quad 3-44b$$

$$a = \frac{\bar{a} \phi_y^2}{c} \quad 3-44c$$

the equations 3-40 can be rewritten in matrix notation.

$$\begin{bmatrix} 1 & 0 \\ 0 & 1 \end{bmatrix} \begin{Bmatrix} \ddot{x}_1 \\ \ddot{x}_2 \end{Bmatrix} + \begin{bmatrix} 0.5 & 0.5F_o^{-1} \\ -1 & 3-F_o \end{bmatrix} \begin{Bmatrix} x_1 \\ x_2 \end{Bmatrix} + e \begin{bmatrix} 0.5 & -1 \\ -1 & +3 \end{bmatrix} \begin{Bmatrix} x_1 \\ x_2 \end{Bmatrix} \\ + \cos (\Omega T) \begin{bmatrix} 0 & 0.5F_t \\ 0 & -F_t \end{bmatrix} \begin{Bmatrix} x_1 \\ x_2 \end{Bmatrix} + a \begin{bmatrix} 0.5 & -1 \\ -1 & 3 \end{bmatrix} \begin{Bmatrix} x_1^3 \\ x_2^3 \end{Bmatrix} = 0 \quad 3-45$$

The dots over the variables x_j now represent differentiation with respect to the normalized time T . In the numerical analysis to follow the values of ϵ , a and F_t will be taken as 0.01, 0.05 and 0.10 respectively.

(c) Transformation to Normal Co-ordinates

The equations 3-45 are now in the form

$$\ddot{x}_j + \sum_{m=1}^2 C_{jm} x_m + \epsilon f_j(x_j, \dot{x}_j, \Omega T) = 0 \quad 3-46$$

To obtain equations 3-46 in terms of normal co-ordinates the linear transformation

$$\{x\} \equiv [D]\{y\} \quad 3-47a$$

where

$$\{x\} = \begin{Bmatrix} x_1 \\ x_2 \end{Bmatrix}, \{y\} = \begin{Bmatrix} y_1 \\ y_2 \end{Bmatrix} \text{ and } [D] \equiv \begin{bmatrix} \frac{1}{\sqrt{1+\gamma_1^2}} & \frac{1}{\sqrt{1+\gamma_2^2}} \\ \frac{\gamma_1}{\sqrt{1+\gamma_1^2}} & \frac{\gamma_2}{\sqrt{1+\gamma_2^2}} \end{bmatrix}$$

$$\gamma_j = \frac{-C_{21}}{C_{22} - \omega_j^2} \quad (j = 1, 2) \quad 3-47b$$

is applied to equations 3-45. In equations 3-47b the ω_j

designates the natural frequencies of the abbreviated system $e = a = F_t = 0$. Pre-multiplying equations 3-45 by the inverse $[D]^{-1}$ the equations are brought into normal form

$$\begin{bmatrix} 1 & 0 \\ 0 & 1 \end{bmatrix} \begin{Bmatrix} \ddot{y}_1 \\ \ddot{y}_2 \end{Bmatrix} + \begin{bmatrix} \omega_1^2 & 0 \\ 0 & \omega_2^2 \end{bmatrix} \begin{Bmatrix} y_1 \\ y_2 \end{Bmatrix} + \begin{bmatrix} e_{11} & e_{12} \\ e_{21} & e_{22} \end{bmatrix} \begin{Bmatrix} \dot{y}_1 \\ \dot{y}_2 \end{Bmatrix} \quad 3-48$$

$$+ F_t \cos(\Omega T) \begin{bmatrix} b_{11} & b_{12} \\ b_{21} & b_{22} \end{bmatrix} \begin{Bmatrix} y_1 \\ y_2 \end{Bmatrix} + a \begin{Bmatrix} a_{11}y_1^3 + a_{12}y_1^2y_2 + a_{13}y_1y_2^2 + a_{14}y_2^3 \\ a_{21}y_2^3 + a_{22}y_2^2y_1 + a_{23}y_2y_1^2 + a_{24}y_1^3 \end{Bmatrix} = 0$$

The equations 3-48 are now in the form of the equations 3-1 and the approximate method of analysis of 3-48 can proceed as detailed in Section 3.2 to 3.7..

(d) Numerical Example

This model, described mathematically by Equation 3-45 has been analysed for the onset of instability. For zero damping coefficients the critical load F_c has been calculated to be $F_c = 2.086$. For the case of small damping $e = 0.01$ the critical load was calculated to be $F_d = 1.464$. It is a characteristic of this type of system that in the case of vanishing damping the critical load can be lower than the critical load for zero damping.

In Fig. 3-9 the natural frequencies of the undamped linear system are plotted as functions of the loading F_o . It can be seen that for $F_o \approx 1.15$ the ratio $\omega_2/\omega_1 \approx 3$. At this point of the external loading it is to be expected that the

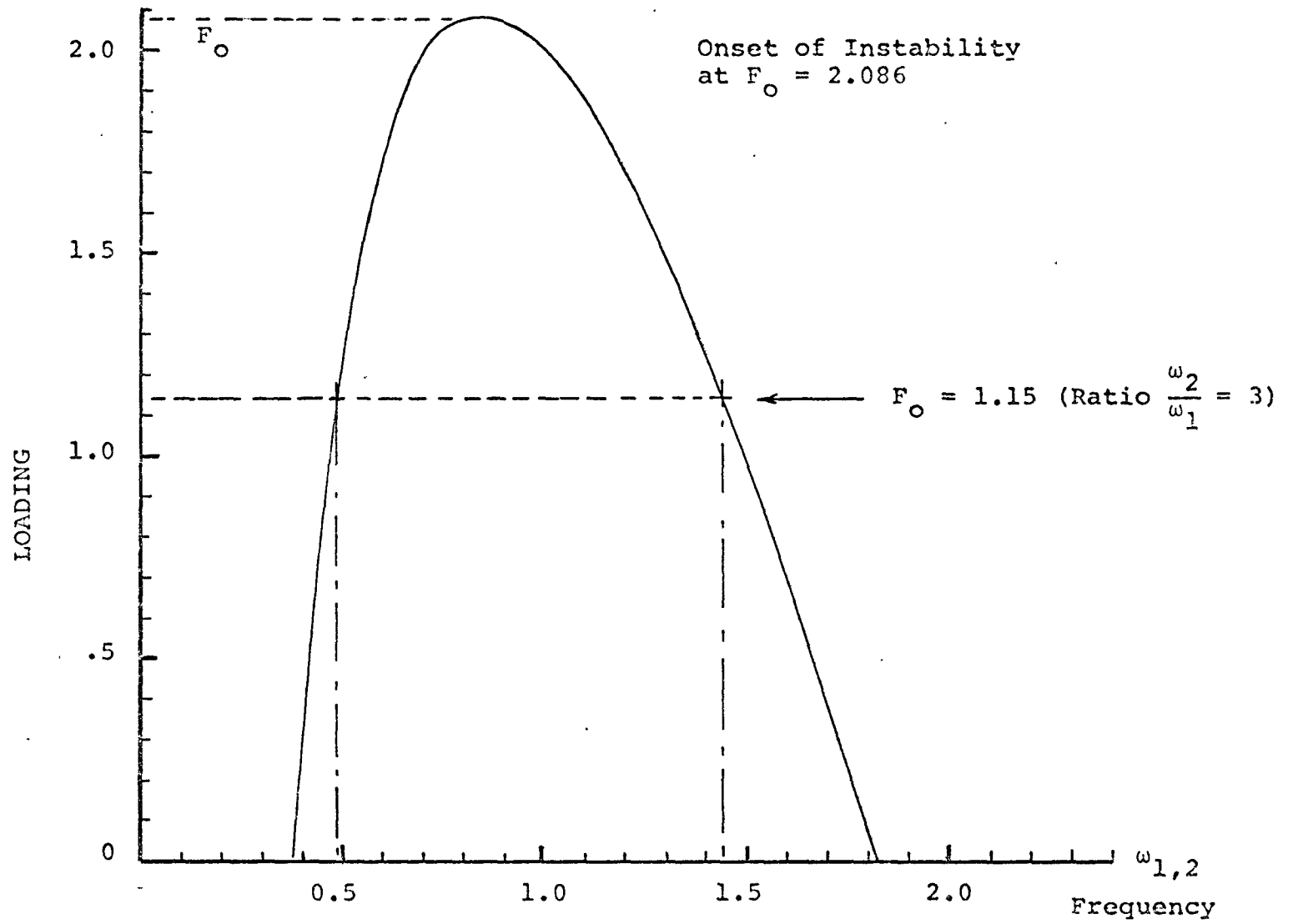


FIG. 3-9 PLOT OF LOAD F_o vs UNDAMPED NATURAL FREQUENCIES

two parametric zones type I and type II will coincide. The averaged equations will then be similar to the system of equations 3-8. For $F_0 = 1.15$ the coefficients of the equations 3-48 were calculated and are:

$$\omega_1 = .486; \quad e_{11} = .000916; \quad e_{12} = .0027$$

$$\omega_2 = 1.45; \quad e_{21} = - .0071; \quad e_{22} = .0341$$

$$b_{11} = .126; \quad b_{12} = - .2314; \quad a_{11} = .116; \quad a_{12} = .303$$

$$b_{21} = .6135; \quad b_{22} = - 1.126; \quad a_{13} = -.274; \quad a_{14} = .196$$

$$a_{21} = 2.93; \quad a_{22} = - 4.56 \quad ; \quad F_t = 0.1$$

$$a_{23} = 3.23; \quad a_{24} = .245 \quad ; \quad a = 0.05$$

Using these figures the uncoupled type I and type II steady state curves are obtained and plotted in Fig. 3-10. It is seen that the type I curve has a narrow instability zone of $|\lambda| < .017$. The type II resonance has a wider instability zone $|\lambda| < .081$ which is 4.8 x the size of the type I resonance. An indication of the instability zones can be seen by comparing the damping coefficients d_{ij} and the parametric coefficients b_{ij} . The damping ratio of the two modes d_{11}/d_{22} is in the order of 1/38 and by Equation 3-28 a large combination resonance zone can be expected. This shows the destabilization effect of viscous damping on the width of the instability zone. For zero damping the width is given by Equation 3-18d and is $|\lambda| < .0188$. Consequently the viscous damping effect has

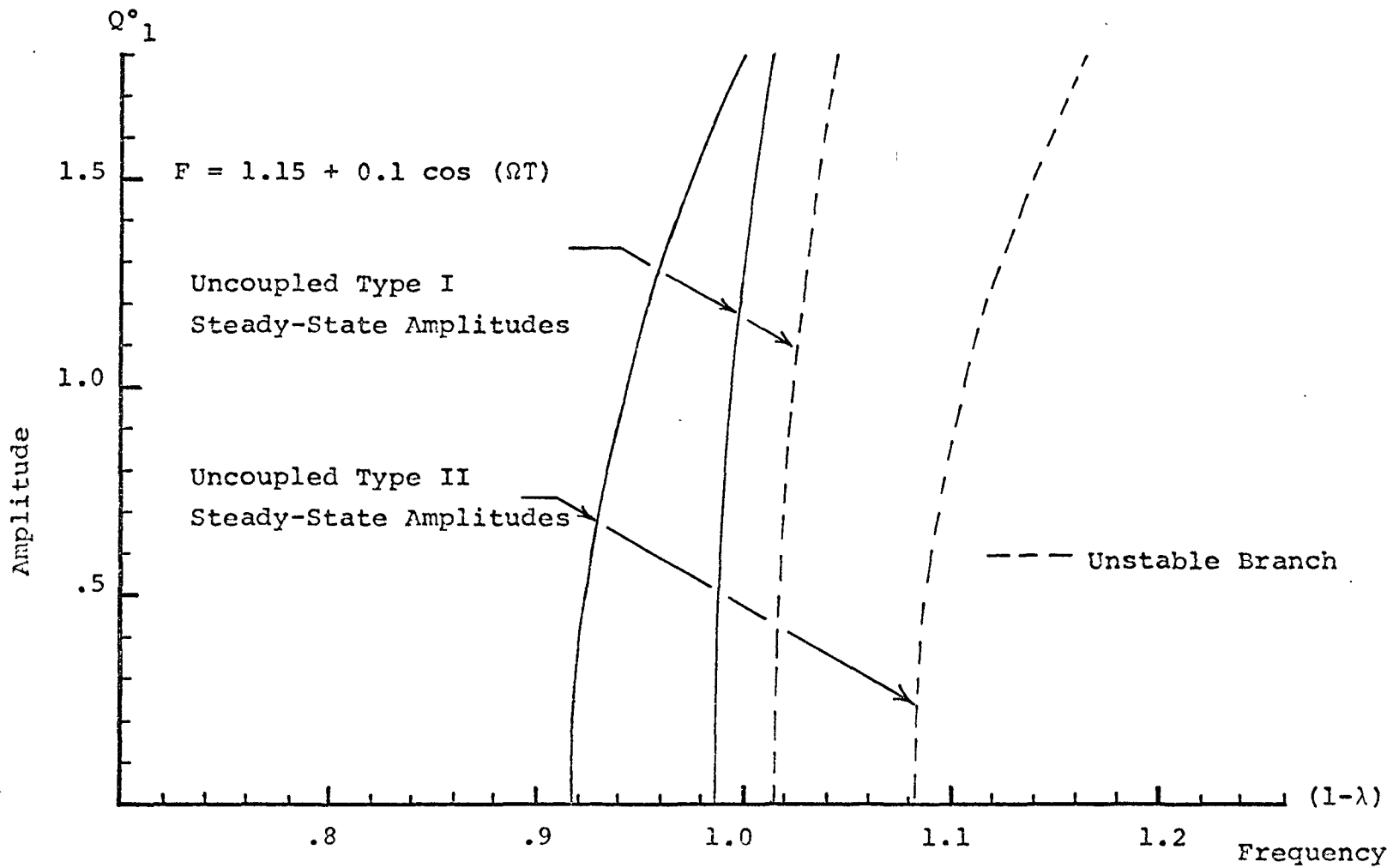


FIG. 3-10 UNCOUPLED TYPE I AND TYPE II STEADY-STATE CURVES

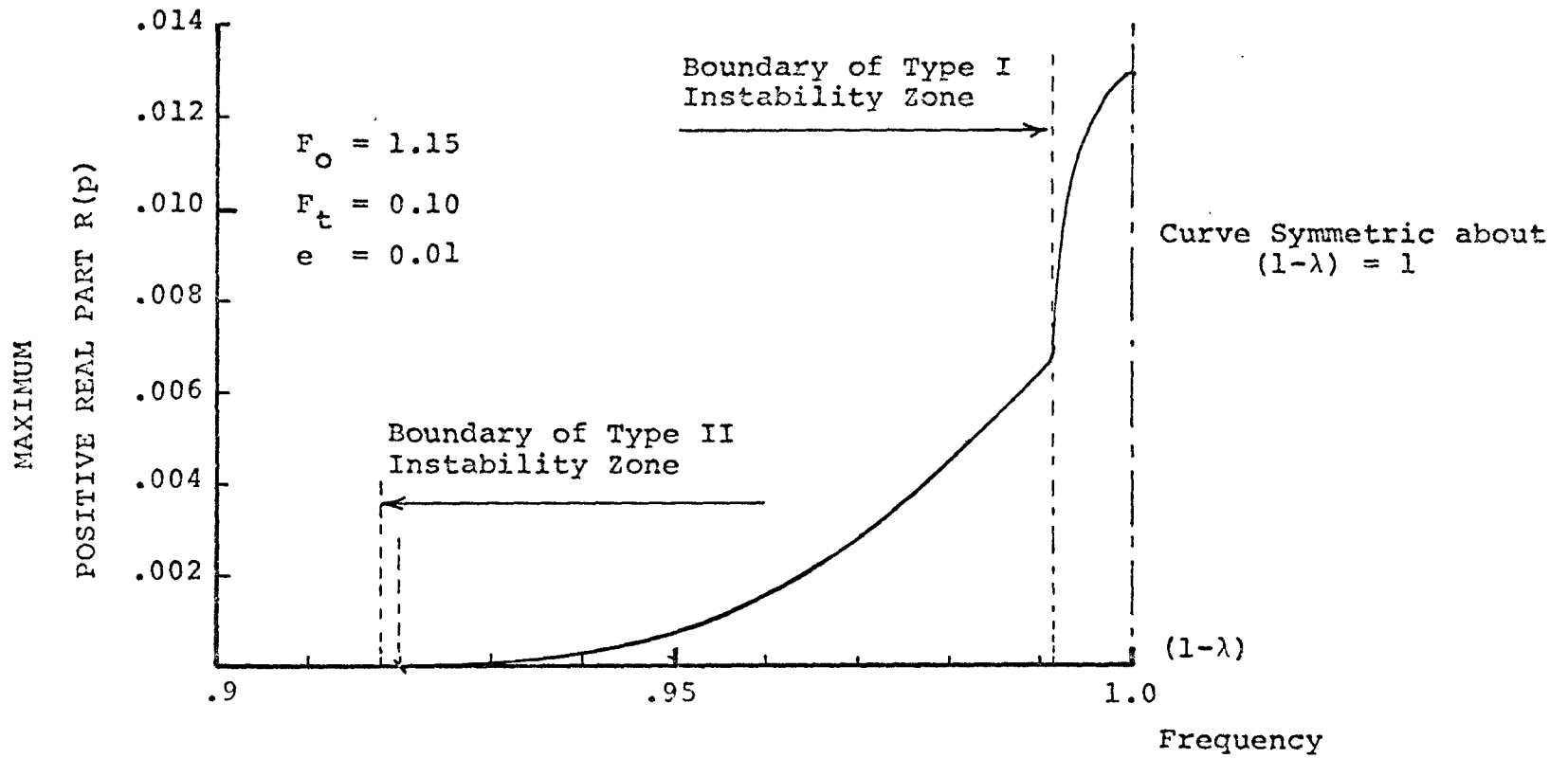


FIG. 3-11 MAXIMUM VALUE $R(p)$ vs FREQUENCY OF COUPLED SYSTEM

caused an increase of the width of the combination resonance zone by a factor of 4.3. This is quite a surprising fact particularly as the damping coefficients of the physical modal were chosen to be identical. It appears that the effect of the non-conservative loading is to reduce the effect of damping on the first mode and increase it on the second mode. In other words, the action of a non-conservative loading appears to favour excitation of the first mode.

The danger of destabilization must be viewed in a proper perspective and the rate of rise of amplitude following an initial disturbance must also be considered. If the positive real part of the roots of Equation 3-15 are very small the build-up of oscillations will take a long time. From a practical point of view, an instability becomes more dangerous if the increase in amplitude is fast once instability starts. A measure of the "degree of instability" can be obtained by plotting the maximum value of $R(p)$ of Equation 3-15. This was done in Fig. 3-11 where $R(p)$ is plotted against $(1 - \lambda)$. The intersect of $R(p) = 0$ is almost indiscernible as the value of $R(p)$ becomes nearly zero in the range $.9 < (1 - \lambda) < .93$. The actual intercept is at $(1 - \lambda) = .92$ or $\lambda = \pm .08$. The positive value $R(p)$ increases as the external detuning $|\lambda|$ decreases. At $(1 - \lambda) = 0.992$ there is a sudden increase in the value of $R(p)$ up to a maximum of $R(p) = .0129$. From this figure it is seen that not all points within the unstable zone have the same degree of instability. The most dangerous region is the one bounded by the parametric type 1 zone.

Fig. 3-12 to 3-14 show the time history plot of the uncoupled parametric type 1 and type 11 response. Fig. 3-11 represents a single mode response of the first mode at $(1 - \lambda) = 1.0$. There is a quick exponential rise of the amplitude Q_1 and an exponential decay for the amplitude Q_2 . Q_1 shows very large oscillations about a mean steady-state

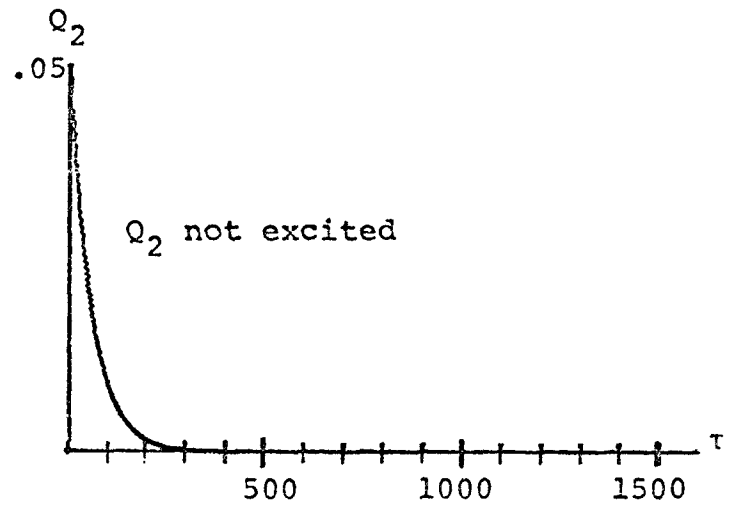
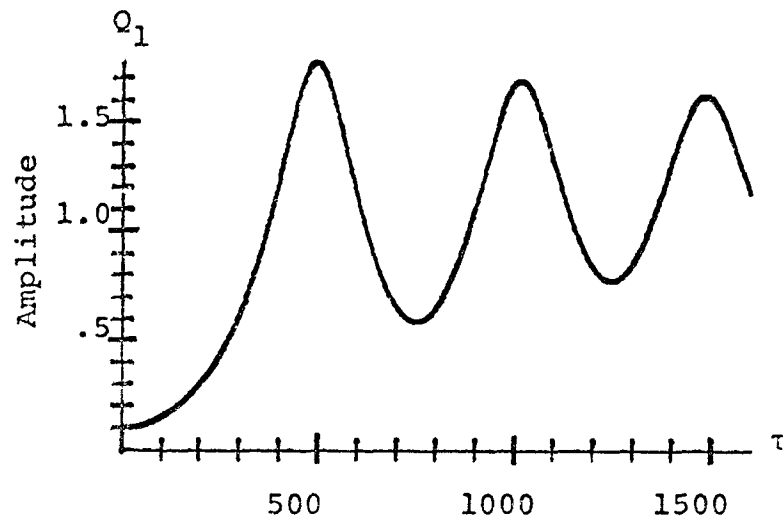


FIG. 3-12 UNCOUPLED TYPE I RESPONSE $(1-\lambda) = 1, b_{12} = b_{21} = 0$

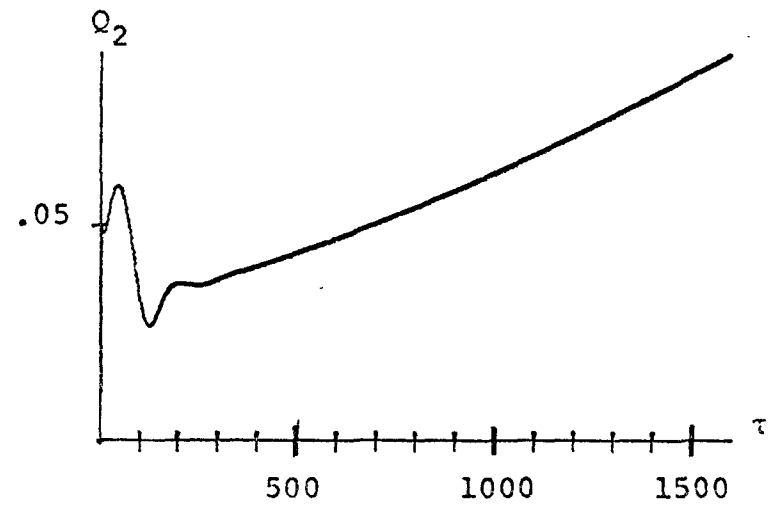
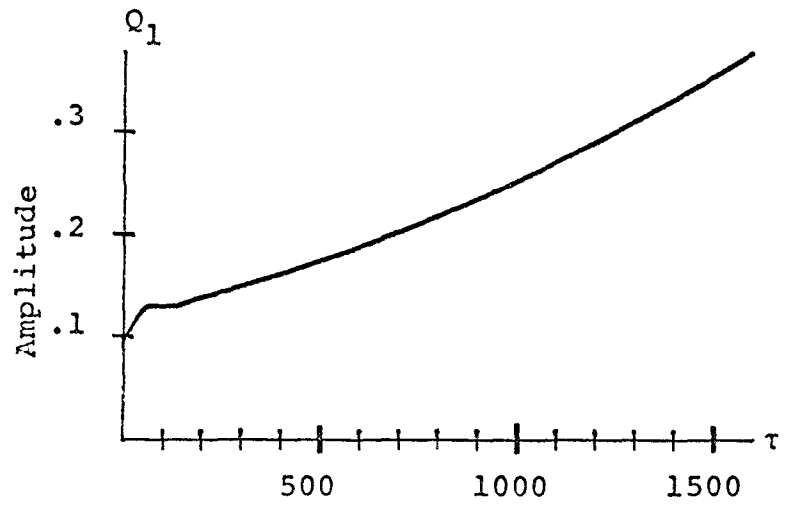


FIG. 3-13 UNCOUPLED TYPE II RESPONSE, $(1-\lambda) = 0.95$, $b_{11} = 0$

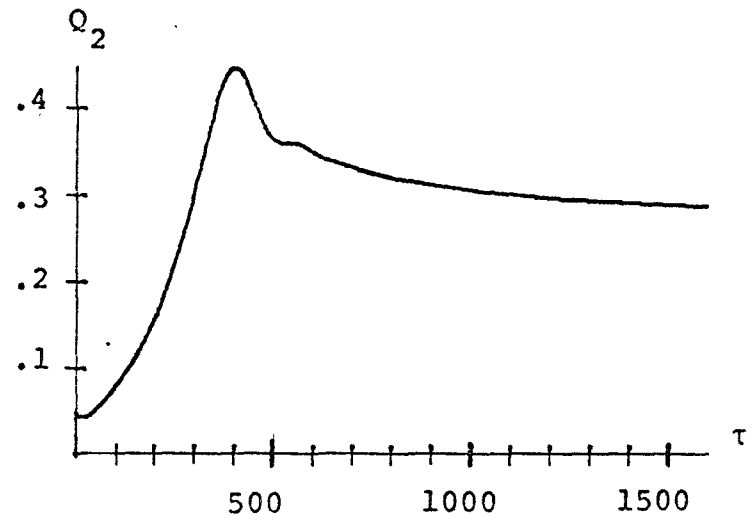
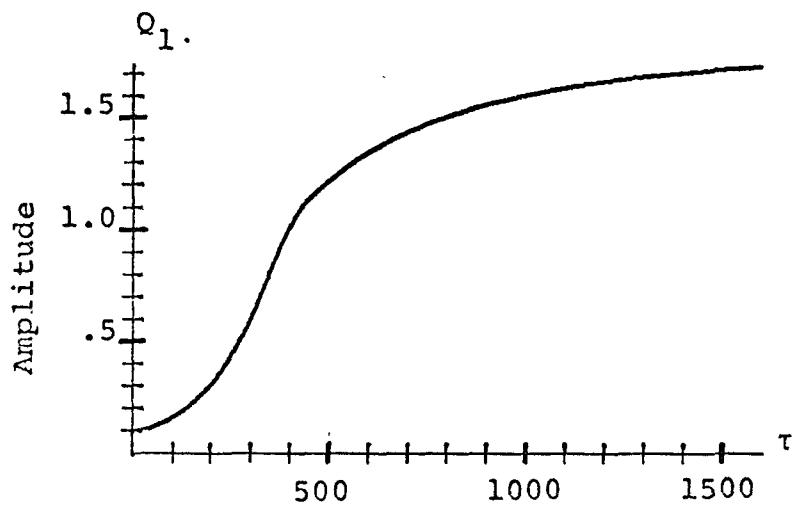


FIG. 3-14 UNCOUPLED TYPE II RESPONSE, $(1-\lambda) = 1$, $b_{11} = 0$

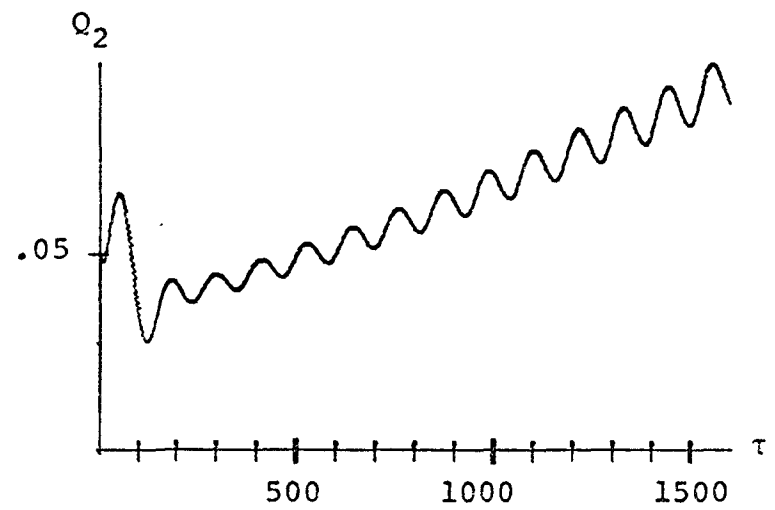
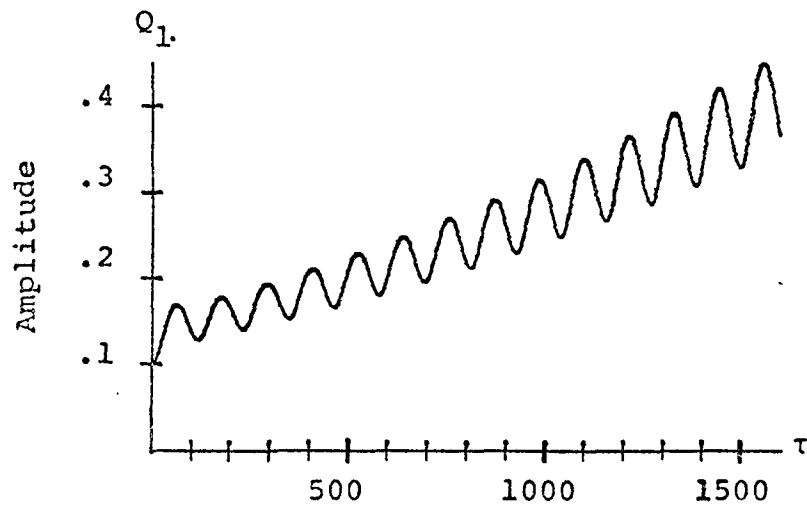


FIG. 3-15 COUPLED TYPE I AND TYPE II RESPONSE: $(1-\lambda) = 0.95$

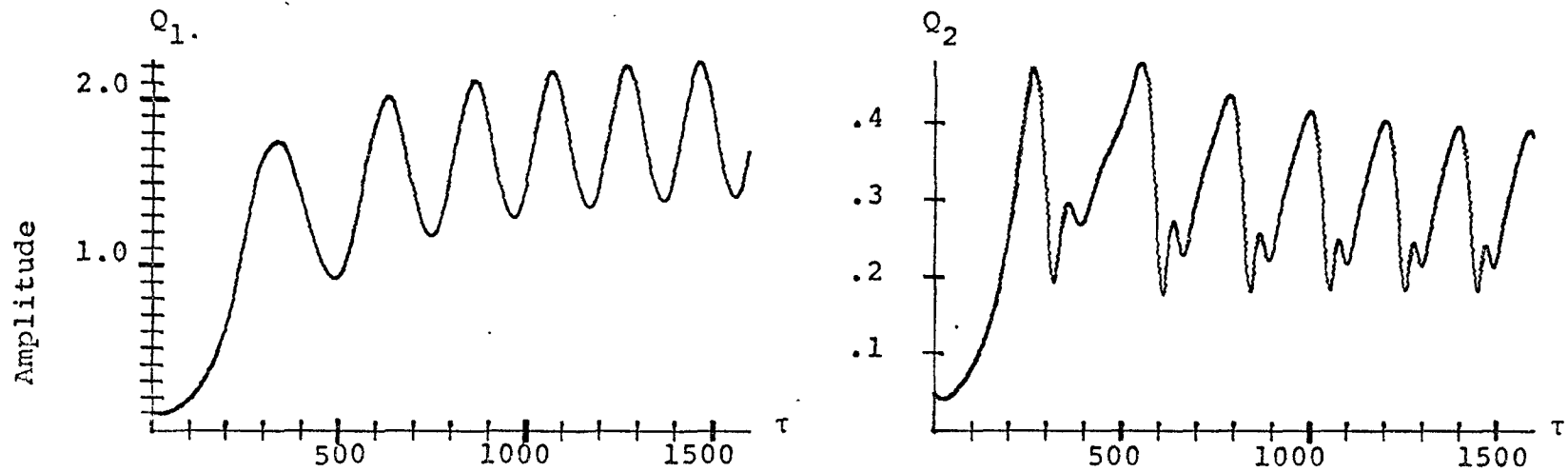


FIG. 3-16 COMBINED TYPE I AND TYPE II RESPONSE, $(1-\lambda) = 1.0$

value which was not obtained within the integration period $\tau = 1600$. This is because the damping coefficient in the first mode is extremely small. Fig. 3-13 shows the response of the uncoupled type 11 resonance at $\Omega/\Omega_0 = 0.95$. From Fig. 3-11, $R_{(p)} = .0007$ and it is to be expected that the build-up of amplitudes is extremely slow. This is indeed the case as the amplitude Q_1 has only tripled the value of the initial disturbance at $\tau = 1200$. At $\Omega/\Omega_0 = 1.0$ the build-up takes place at an increased rate, but the curve of Q_1 does not exhibit the large overshoot as was evident in Fig. 3-5.

For the coupled type 1 and type 11 response Fig. 3-15 is quite similar to Fig. 3-13 except that a modulated motion is superimposed on the response curves; the amplitudes of this modulated motion appears to be increasing in time. Fig. 3-16 is also similar to Fig. 3-14 with a modulated motion superimposed on the response curve of Fig. 3-14. The modulations are quite large reaching approximately 50% the values of amplitudes of the uncoupled type 11 resonance. The maximum value of Q_1 within the integration limit $\tau < 1600$ is 2.22 which is 1.3 times larger than the maximum amplitude reached in Fig. 3-14. The wave form for Q_1 and Q_2 appear to reach a quasi-steady-state although the form of wave motion for Q_2 is complex.

(e) Comparison of the Response of the Averaged Equations and the Exact Equations

The response of the averaged equations shown in Fig. 3-16 can be plotted in terms of the co-ordinates x_j by applying the transformation 3-47, i.e.

$$x_1 = d_{11} Q_1 \cos (K_1 \tau + \theta_1) + d_{12} Q_2 \cos (K_2 \tau + \theta_2)$$

$$x_2 = d_{21} Q_1 \cos (K_1 \tau + \theta_1) + d_{22} Q_2 \cos (K_2 \tau + \theta_2) \quad 3-49$$

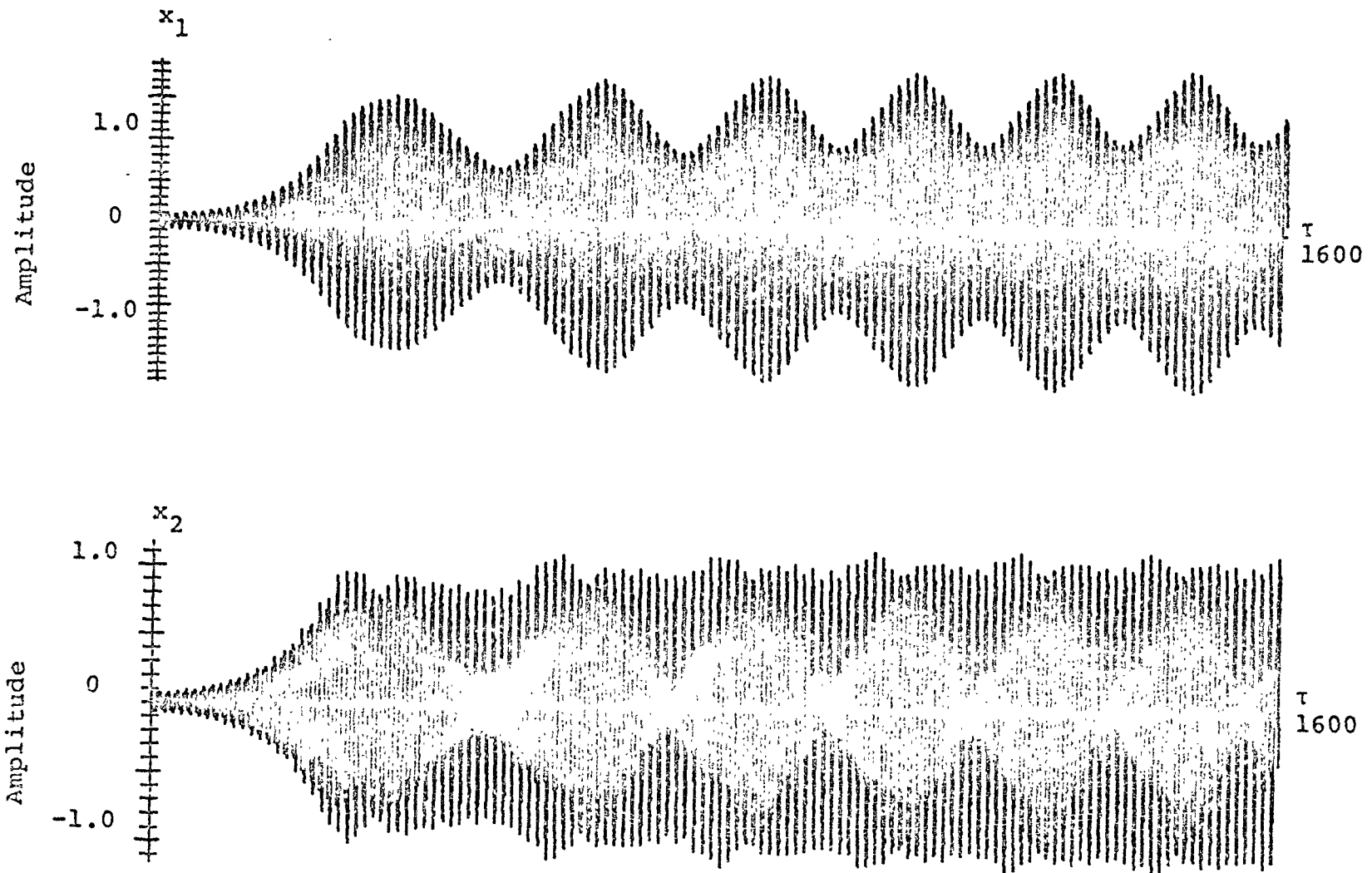


FIG. 3-17 RESPONSE OF PHYSICAL CO-ORDINATES OBTAINED FROM AVERAGED EQUATIONS
 $((1-\lambda) = 1.0)$

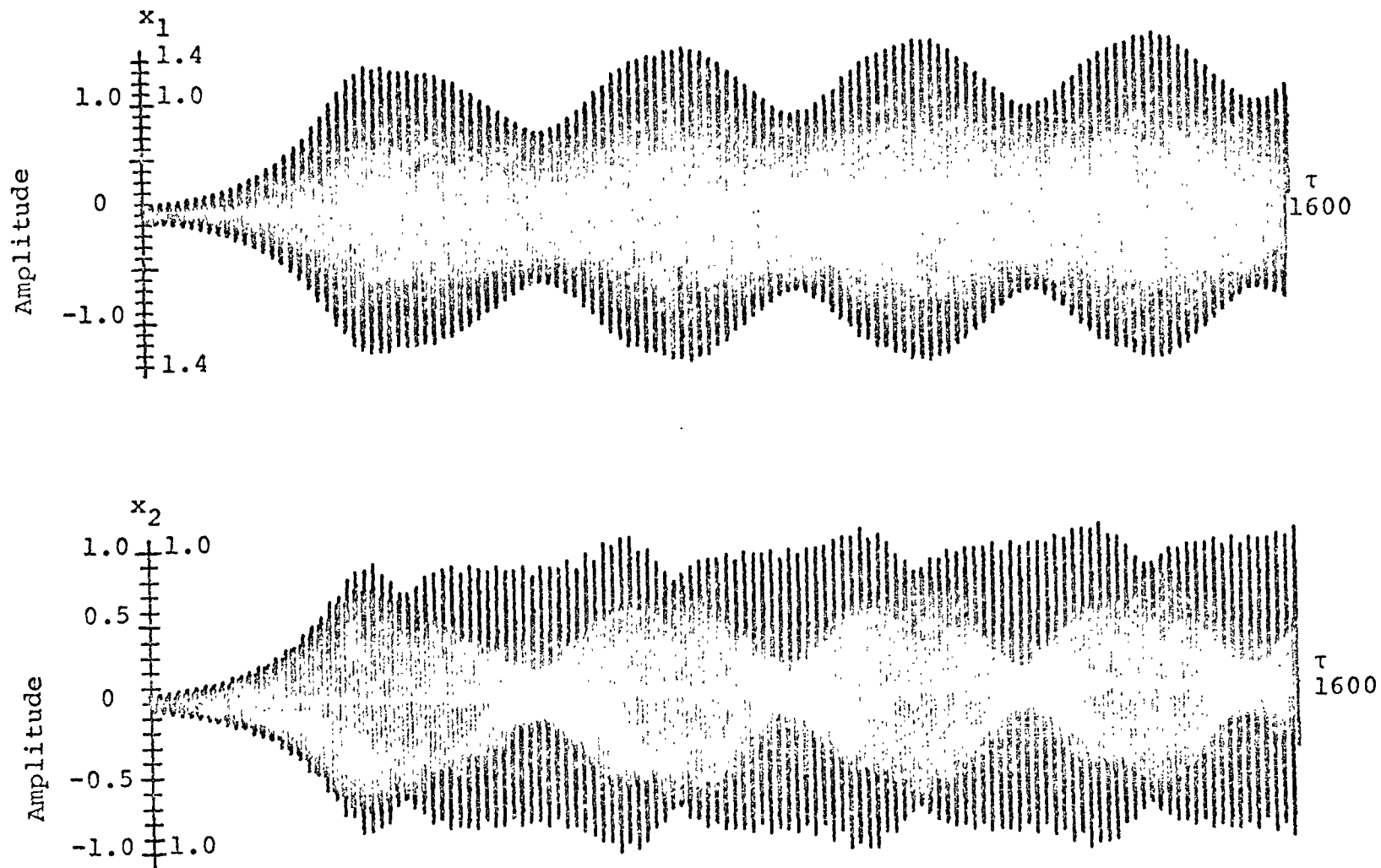


FIG. 3-18 RESPONSE OF PHYSICAL CO-ORDINATES OBTAINED FROM EXACT EQUATIONS
 ($\omega_1 = 0.4864$, $\Omega = 2\omega_1$, $e = 0.01$, $F_t = 0.1$, $F_o = 1.15$, $a = 0.05$)

The responses in terms of the original coordinates x_1 and x_2 are shown in Fig. 3.17. The numerical values used in the transformations are:

$$F_0 = 1.15, d_{11} = 0.85, d_{12} = 0.255, d_{21} = .527 \text{ and}$$

$$d_{22} = - 0.967$$

Fig. 3-18 shows the integration of the exact equations 3-45. The time scale has been normalized to τ and the frequency of the external excitation is taken to be $\Omega = 2\omega_1$. Comparing the two response curves it is seen that the qualitative behaviour is similar although the number of beats in the averaged equations are more frequent over the same time interval. The amplitude x_1 from the averaged equation is 1.3 times the amplitude of x_1 of the exact equations. The amplitude x_2 of the averaged equations is 1.05 times the amplitude x_2 of the exact equations. The averaged equations overestimate the response both in the sense of an increased modulation effect and increased maximum amplitude. From a design point of view, the averaged equations thus provide a conservative approximation of the actual response.

3.9 Discussion and Observations

Based on the analysis of a two degree of freedom system with viscous damping and cubic nonlinearities, the following observations are drawn concerning the interaction of two external parametric resonant zones.

1. A two degrees of freedom system in general has three main parametric resonance regions. A parametric resonance type 1 can occur when the frequency of the external periodic form is approximately equal to twice one of the natural frequencies and a parametric resonance type 11 can occur when the frequency

is approximately equal to the difference of the two natural frequencies. An interaction effect between the external parametric resonances occurs if the natural frequencies of the system are near the integer relation say $\omega_2/\omega_1 = 3$, ($\omega_1 < \omega_2$). When this latter ratio is satisfied a coupling of the parametric type 1 and type 11 resonance occurs. This coupling influences the size of the instability zones, the steady-state amplitude relationships and the transient response.

2. Viscous damping has a strong influence on the width of the instability zone. For the uncoupled type 1 parametric resonance viscous damping causes a narrowing of the instability zone. For the uncoupled type 11 resonance it is primarily the ratio of the viscous damping terms of the normalized system that dictates the width of the resonance zone. In general, the further the ratio of the damping terms is from unity, the greater is the width of the instability zone. For the coupled system both the stabilizing and destabilizing effect of viscous damping act simultaneously. Based on a numerical evaluation of the eigenvalues of the stability matrix, it was found that the width of the instability zone of the coupled system maintained a position between the two instability zones of the uncoupled system. With respect to design criterion the largest instability zone of the two uncoupled resonances can be taken as a conservative measure of the width of the coupled instability zone.

3. The interaction effect of the two external resonances causes both a qualitative and quantitative difference on the response amplitude. The resonant amplitude frequency relationship can be divided into two parts. In the one part, a steady-state response is possible and in the other part a steady-state condition is not possible. When a steady-state is possible the envelope of response amplitude remains at a constant value. The maximum steady-state amplitude in this case is about 10%

over the maximum steady state amplitude assuming there is no interaction between the two types of parametric resonance.

When a steady-state condition is not possible the envelope of maximum response undergoes large amplitude modulations. These modulations appear to be periodic although the wave form of the periodic motion becomes complex. The maximum amplitude of this quasi-steady-state motion exceeds the uncoupled steady-state amplitudes. From the present investigation it was observed that the maximum amplitude of the quasi-steady motion may be larger by 70% than the uncoupled steady-state amplitude.

4. Before either a quasi-steady state or a steady-state motion is reached, the system undergoes a transient phase. For the uncoupled system the transient growth follows a well-behaved pattern. From a small initial value, the amplitudes grow exponentially, overshoot the steady-state response to reach a maximum and then after several smaller oscillations finally reach a steady-state. For the coupled system, it was observed that the transient motion consists of the exponential build-up followed by a number of oscillations about the mean value of the quasi-steady state response. The maximum response however does not necessarily occur at the first overshoot but was also observed to occur near the end of the transient phase of the motion.

5. The rate of growth of amplitude varies considerably over the width of the parametric resonance zone. The fastest rate of rise occurs when the frequency of the external excitation is within that region enclosed by both the uncoupled resonance zones.

6. The solutions obtained by the method of averaging were checked by direct numerical integration. The method of

averaging does provide the correct qualitative nature of the response. In addition the method of averaging slightly over estimates both the maximum amplitude response and the modulation effect and can be considered as providing a conservative estimate for design purposes.

CHAPTER IV

PARAMETRIC RESONANCE OF A SINGLE DEGREE OF FREEDOM SYSTEM WITH HYSTERETIC DAMPING

4.1 Introduction

Restoring forces with a hysteretic force - deflection or moment-rotation characteristic have been found to be reasonable approximations to describe the behaviour of many engineering materials and structural assemblies under cyclic loading. Much attention has been given to the study of dynamical systems containing elements with hysteretic constitutive relationships. Due to the nonlinear and loading history dependent nature of such elements, such problems are in general not amenable to analytical treatment. However, successful analytical analysis has been carried out to systems with piecewise linear hysteretic elements. The two most common of these are the bilinear and the double bilinear models. The study of ordinary forced resonance of one degree of freedom problems have been made by Caughey^[7] and Iwan^[22] for the bilinear and double bilinear hysteretic models respectively. The bilinear model was used to describe the behaviour of composite structures, due to the action of slip and boundary shear effects at mating surfaces, interfaces or joints. It is also used to model the elasto-plastic behaviour of the materials in the system. Physical elements containing elements with double bilinear hysteretic characteristics are fewer in number; however, they have been used to model the behaviour of structures with degrading joints^[26] and cross-braced towers^[43]. Originally, the double bilinear hysteretic model was proposed as an alternative modelling of the structural damping mechanism^[22] as it was found that the hysteresis loss specified by the bilinear model was

higher than that which actually existed. For this reason the behaviour of hysteretic models having a lower hysteretic loss than the bilinear model were investigated. The double bilinear hysteretic loop has exactly one half the hysteretic loss of the bilinear modal for the same amplitude of response.

The third hysteretic model which is to be investigated is the general hysteretic force-deformation relationship described by the Ramberg-Osgood functions. Structures with this hysteretic characteristic have been investigated for the case of forced resonance and earthquake excitation by Jennings^[27]. The Ramberg-Osgood function is a smooth, continuous function and includes the linear and elasto-plastic relations as limiting cases. It presents a more accurate description of the real behaviour of materials under cyclic loading as shown by the experimental work of Hansen^[17]. The use of the Ramberg-Osgood functions necessitates a numerical analysis; however, because of it's accurate representation of the true behaviour of certain yielding structures the analysis can be used to verify the validity of the piecewise linear hysteretic models.

Most of the attention in the study of dynamical systems containing elements that exhibit hysteretic damping has been in the direction of forced excitation and particularly in the field of earthquake engineering^[51]. But another interest in the study of systems with hysteresis is to use it as an alternative possible mechanism to account for the dissipation of energy. Viscous damping is a suitable model to use in forced oscillation studies because it limits the resonant response of the system to a finite value. However, the viscous damping model is inadequate in the area of parametric excitation. The analysis of a one degree of freedom system under parametric excitation results in a Mathieu equation. It is well known that the main effect of viscous damping is to modify the sizes of the unstable regions only. Once the system is excited

into parametric resonance, the response of the linearized system grows without bound. A system with damping modelled by the bilinear, double-bilinear or Ramberg-Osgood hysteretic model gives in general, bounded response under parametric resonance. Only when the hysteretic loop is very narrow or the parametric excitation amplitude becomes large is unbounded response obtained.

It is the purpose of this chapter to study the parametric behaviour of a one degree of freedom system having restoring forces with the three above mentioned hysteretic characteristics. The model to be investigated is an inverted pendulum under sinusoidal base excitation.

4.2 Statement of the Problem

(a) The Mathematical Model

The system under study consists of a weight-less rod of length L with a mass m attached to one end. The rod is connected to the base by a hinge which provides a restoring moment cM when the system is disturbed from its equilibrium position. The system is subjected to periodic base motion $f(t)$ in the y -direction as shown in Fig. 4-1. The hinge is assumed to have one of the three forms of moment-rotation characteristics (a) bilinear, (b) double-bilinear and (c) the Ramberg-Osgood functions as shown in Figures A-1 A-2 and A-3 of the appendix. For the piecewise linear models it can be seen that

$$\lim_{u \rightarrow 0} M(\phi, u) = \phi \quad 4-1a$$

and for the smoothly curved hysteretic function

$$\lim_{\alpha \rightarrow 0} M(\phi, \alpha, n) = \phi \quad 4-1b$$

Therefore, the problem is similar to that studied by Skalak and Yarymovych^[48] when $u = \alpha = 0$. The kinetic energy T , and the generalized force S of the system can be written as

$$T = \frac{m}{2} \left[\left(L \cos \phi \frac{d\phi}{dt} \right)^2 + \left(\frac{df}{dt} - L \sin \phi \frac{d\phi}{dt} \right)^2 \right] \quad 4-2$$

$$S = - cM \quad 4-3$$

Taking the base motion in the form

$$f(t) = F \cos(\omega t) \quad 4-4$$

and by means of Lagrange's equation, the equation of motion can be put in dimensionless form as

$$\ddot{\phi} + M(\phi) + (R\Omega^2 \cos(\Omega\tau)) \sin \phi = 0 \quad 4-5$$

where

$$\Omega = \omega/\omega_0 \quad 4-6a$$

$$\omega_0 = \frac{1}{L} \left(\frac{c}{m} \right)^{1/2} \quad 4-6b$$

$$\tau = \omega_0 t \quad 4-6c$$

$$R = F/L \quad 4-6d$$

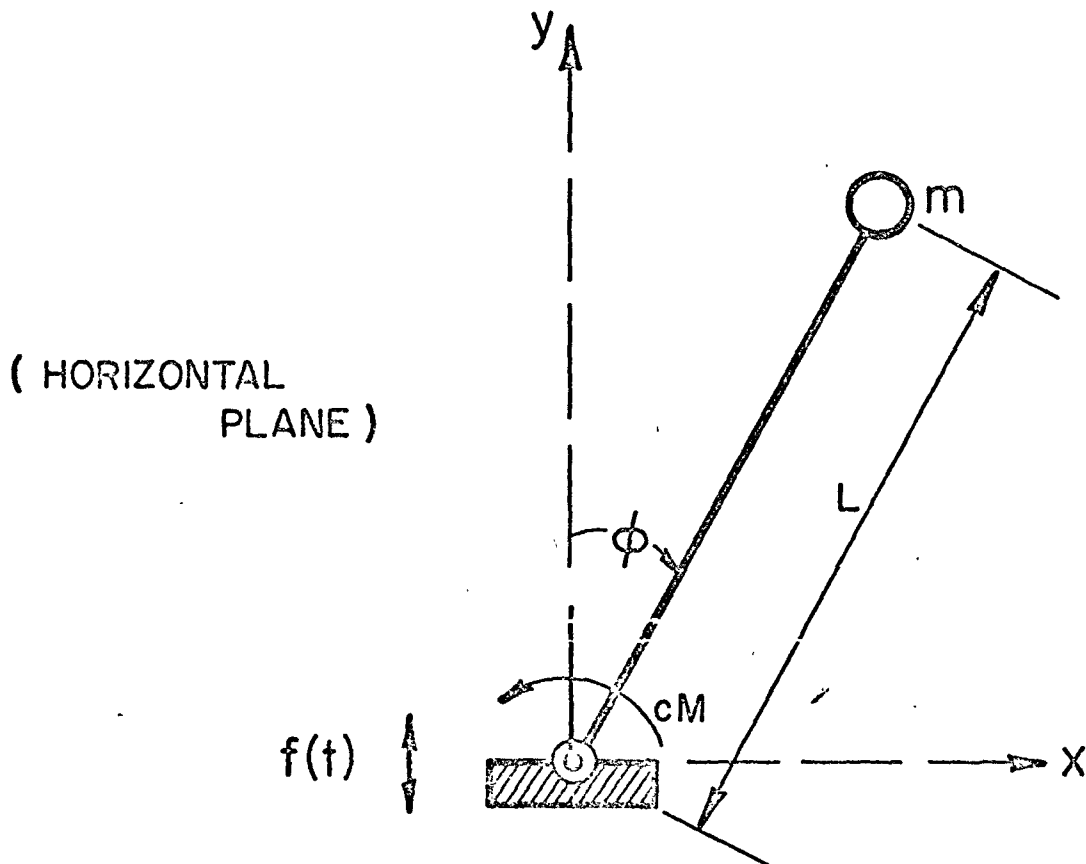


FIG. 4-1 SIMPLE PENDULUM WITH VIBRATING SUPPORT

and dots indicate differentiation with respect to the dimensionless time parameter τ .

Equation 4-5 is a nonlinear ordinary differential equation with periodic coefficients. There are two sources of nonlinearity in equation 5. The hysteretic form of $M(\phi)$ can be called nonlinear in material property while the $\sin\phi$ term is a geometric nonlinearity. Provided the maximum parametric response of the system ϕ_{\max} is small, $\sin\phi$ may be replaced by ϕ as an adequate first approximation. If the maximum response is large, higher order approximations of the expression $\sin\phi$ become necessary.

4.3 Method of Solution

(a) First Approximation ($\sin\phi = \phi$)

Assuming that ϕ_{\max} is sufficiently small such that the approximation $\sin\phi = \phi$ is valid equation 4-5 becomes.

$$\ddot{\phi} + M + (R\Omega^2 \cos(\Omega\tau))\phi = 0 \quad 4-7$$

Equation 4-7 is a homogeneous equation in ϕ and admits the trivial solution $\phi = 0$. For $|\phi| < \phi_y$, for the piecewise linear models, and $\alpha = 0$ for the Ramberg-Osgood hysteretic models $M(\phi) = \phi$ and equation 4-7 becomes

$$\ddot{\phi} + \phi + (R\Omega^2 \cos(\Omega\tau))\phi = 0 \quad 4-7a$$

which is a Mathieu equation with parametric exciting amplitude $R\Omega^2$ and parametric exciting frequency Ω . Hence, there are various ranges of frequency Ω within which the system can be parametrically excited into resonance. Here only the principal region of parametric resonance will be considered. To

study the response of the hysteretic system, a response with a frequency in the neighbourhood of $1/2 \Omega$, is sought. Assume a solution of the form

$$\begin{aligned} \phi(\tau) &= Q(\tau) \cos \left(\frac{1}{2} \Omega \tau + \theta(\tau) \right) \\ &\equiv Q(\tau) \cos \psi(\tau) \end{aligned} \quad 4-8$$

Substituting 4-8 into 4-7 and imposing the condition

$$\dot{Q} \cos \psi - Q \dot{\theta} \sin \psi = 0 \quad 4-9$$

to be satisfied, equation 4-7 becomes

$$-\frac{1}{2} \Omega \dot{Q} \sin \psi - \left(\frac{\Omega^2}{4} + \frac{\Omega}{2} \dot{\theta} - R \Omega^2 \cos \Omega \tau \right) Q \cos \psi + M = 0 \quad 4-10$$

Equations 4-9 and 4-10 can further be simplified so that one equation contains only the derivatives of Q and the other equation contains only the derivatives of θ . This can be done first by multiplying equation 4-9 by $\Omega \cos \psi$ and equation 4-10 by $\sin \psi$. Subtracting the resulting equation becomes

$$\frac{\Omega}{2} \dot{Q} + \frac{\Omega^2}{4} Q \cos \psi \sin \psi - M \sin \psi = R \Omega^2 Q \cos(\Omega \tau) \sin \psi \cos \psi \quad 4-11$$

Second, multiplying equation 4-9 by $\Omega \sin \psi$ and equation 4-10

by $\cos\psi$, and adding the two resulting equations lead to

$$\begin{aligned} \frac{1}{2} \Omega Q \dot{\theta} + \frac{1}{4} \Omega^2 Q \cos^2 \psi - M \cos \psi \\ = R \Omega^2 Q \cos(\Omega \tau) \cos^2 \psi \end{aligned} \quad 4-12$$

As the parameters $Q(\tau)$ and $\theta(\tau)$ are slowly varying functions of τ , the method of averaging is used to obtain approximate solutions to equations 4-11 and 4-12. The variables $Q(\tau)$ and $\theta(\tau)$ together with their derivatives may be treated as constant over one cycle of ψ . Thus integrating equations 4-11 and 4-12 with respect to ψ from zero to 2π and dividing the results by 2π there is obtained.

$$\Omega \dot{Q} - S(Q) = \frac{1}{2} R \Omega^2 Q \sin 2\theta \quad 4-13$$

$$\Omega Q \dot{\theta} + \frac{1}{4} \Omega^2 Q - C(Q) = \frac{1}{2} R \Omega^2 Q \cos 2\theta \quad 4-14$$

where

$$S(Q) \equiv \frac{1}{\pi} \int_0^{2\pi} M \sin \psi \, d\psi \quad 4-15$$

$$C(Q) \equiv \frac{1}{\pi} \int_0^{2\pi} M \cos \psi \, d\psi \quad 4-16$$

(b) Second Approximation ($\sin \phi = \phi - \phi^3/6$)

An examination of the hysteretic moment rotation characteristics will indicate that if "yielding" does not occur

until the rotation is large, the first approximation $\sin\phi = \phi$ would obviously be a poor approximation to the actual problem. In this section, the averaged equations will be derived by approximating the $\sin\phi$ term by the first two terms in its power series expansion. The equation of motion becomes

$$\ddot{\phi} + (R\Omega^2 \cos \Omega\tau) (\phi - \phi^3/6) + M = 0 \quad 4-17$$

Seeking the solution in the form given by equation 4-8 and carrying out the method of slowly varying parameter procedure the equations describing the average values of Q and θ can be written as

$$\dot{Q} - S(Q) - \frac{1}{2} R\Omega^2 Q (1 - Q^2/12) \sin 2\theta = 0 \quad 4-18a$$

$$\Omega Q \dot{\theta} + \frac{1}{4} \Omega^2 Q - C(Q) - \frac{1}{2} R\Omega^2 Q (1 - Q^2/12) \cos 2\theta = 0 \quad 4-18b$$

4.4 Steady-State Response

(a) First Approximation ($\sin\phi = \phi$)

The steady-state response of the system of averaged equations 4-13 and 4-14 can be obtained by setting \dot{Q} and $\dot{\theta}$ to zero, namely,

$$S(Q_0) = -\frac{1}{2} R\Omega^2 Q_0 \sin 2\theta_0 \quad 4-19a$$

$$\frac{1}{4} \Omega^2 Q_0 - C(Q_0) = \frac{1}{2} R\Omega^2 Q_0 \cos 2\theta_0 \quad 4-19b$$

where Q_o and θ_o denote the steady-state values of Q and θ . Eliminating θ_o from equations 4-19a and 4-19b, the equation describing the steady-state response curve is obtained and is:

$$\Omega^2 = \frac{4 \left(\frac{C(Q_o)}{Q_o} \right) \pm 4 \sqrt{4R^2 \left[\left(\frac{C(Q_o)}{Q_o} \right)^2 + \left(\frac{S(Q_o)}{Q_o} \right)^2 \right] - \left(\frac{S(Q_o)}{Q_o} \right)^2}}{(1 - 4R^2)} \quad 4-20$$

Instead of expressing the steady-state amplitude Q_o as a function of frequency Ω , the ratio $\mu = Q_o/\phi_y$ is plotted in the response plots. Written in terms of μ , the response curve Equation 4-19 can be written as

$$\Omega^2 = \frac{4C(\mu) \pm 4 \sqrt{4R^2 [C(\mu)^2 + S(\mu)^2] - S(\mu)^2}}{\mu (1 - 4R^2)} \quad 4-21a$$

where in comparison to equation 4-20 $C(\mu)$ and $S(\mu)$ are defined as:

$$C(\mu) \equiv \frac{C(Q_o)}{\phi_y} \quad 4-21b$$

$$S(\mu) \equiv \frac{S(Q_o)}{\phi_y} \quad 4-21c$$

It should be noted that in the first approximation, the steady state response of the system as given by equation 4-21a is independent at the yield rotation ϕ_y .

(b) Second Approximation ($s: n\phi = \phi - \phi^3/6$)

The steady-state response of the system of averaged equations 4-18a and 4-18b is given by

$$\Omega^2 = \frac{C(Q_0) \pm [4R^2\{C(Q_0)^2 + S(Q_0)^2\}\{1 - Q_0^2/12\}^2 - S(Q_0)^2]^{1/2}}{Q_0[\frac{1}{4} - R^2(1 - Q_0^2/12)^2]}$$

4-23

In terms of μ equation 4-23 can be written as

$$\Omega^2 = \frac{C(\mu) \pm [4R^2\{C(\mu)^2 + S(\mu)^2\}\{1 - (\mu\phi_Y)^2/12\}^2 - S(\mu)^2]^{1/2}}{\mu[\frac{1}{4} - R^2\{1 - (\mu\phi_Y)^2/12\}^2]}$$

4-24

The steady state equations 4-21a and 4-24 are applicable to systems with any of the three types of hysteretic characteristics. The different hysteretic characteristics of the system is accounted for by the evaluation of the expressions $S(Q)$ and $C(Q)$ as defined in 4-15 and 4-16.

4.5 Steady-State Response Curves For the Bilinear, Double Bilinear and Ramberg-Osgood Hysteretic Models

Up to now, the analysis has been on a general basis. In this section, the response calculations of each of the three hysteretic models will be presented separately.

(a) Bilinear Hysteretic Model

For the bilinear hysteretic model the values of $C(\mu)$

and $S(\mu)$ are^[7]

$$C(\mu) = \mu - \frac{u\mu}{\pi} (\pi - \theta^* + \sin\theta^* \cos\theta^*) \quad \text{for } \mu > 1 \quad 4-25a$$

$$S(\mu) = - \frac{u\mu}{\pi} \sin^2\theta^* \quad \text{for } \mu > 1 \quad 4-25b$$

$$\text{and } \theta^* = \cos^{-1} \left(1 - \frac{2}{\mu} \right) \quad 4-25c$$

A detailed derivation is given in the appendix. A plot of equation 4-21a is shown in Fig. 4-2 for different values of u ($0 \leq u \leq 1$). As indicated in Fig. A.1, $u = 0$ corresponds to a linear elastic hinge and $u = 1.0$ corresponds to a hinge with elastic, perfectly plastic moment-rotation characteristics. The steady-state response is unbounded over a range of frequency in the case $u = 0.1$. A bilinear hysteretic hinge with $u = 0.1$ is very close to a linear elastic hinge with a small hysteresis loop. Therefore, the dissipation power of the mechanism is limited. However, for hinges with larger values of u , the response is bounded for the whole range of parametric frequencies. The higher the values of u , the lower is the maximum steady-state response. For an elastic, perfectly plastic hinge characteristic, the maximum response is no more than 9 per cent over the yield rotation ϕ_y .

Response curves using equations 4-24 of the second approximation are shown in Fig. 4-3. The yield rotation is taken to be $\phi_y = 0.2$ rad. Comparison between Fig. 4-2 and Fig. 4-3 shows that the response curves for $u = 0.3, 0.5$ and 1.0 are essentially the same. Recalling that the magnitude of angular displacement in these cases are of the order of

FIG. 4-2 EFFECT OF HYSTERESIS PARAMETER U ON RESPONSE CURVE

FIRST APPROXIMATION ($\sin \phi = \phi$)

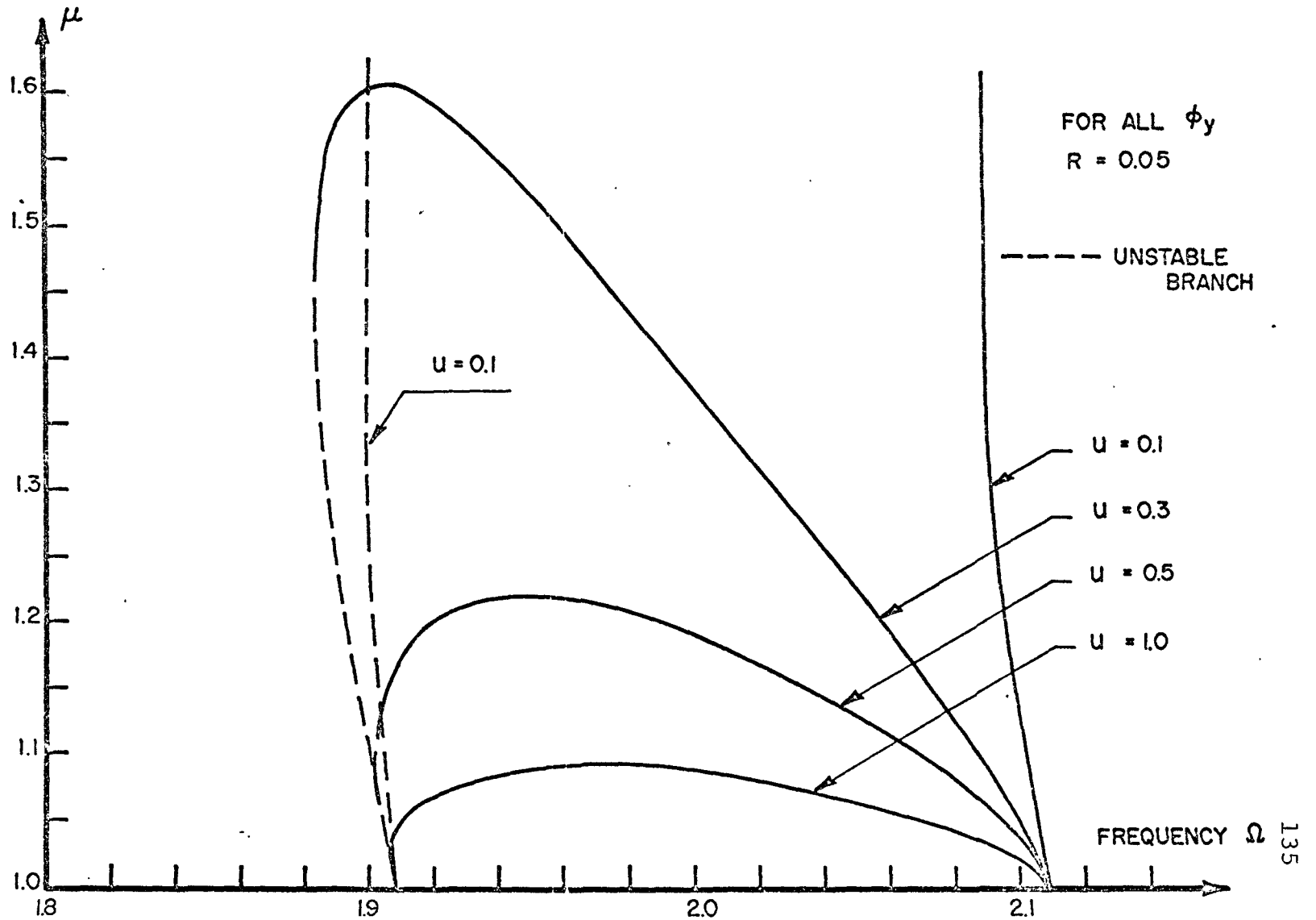


FIG. 4-3 EFFECT OF HYSTERESIS PARAMETER U ON RESPONSE CURVE (SECOND APPROXIMATION)

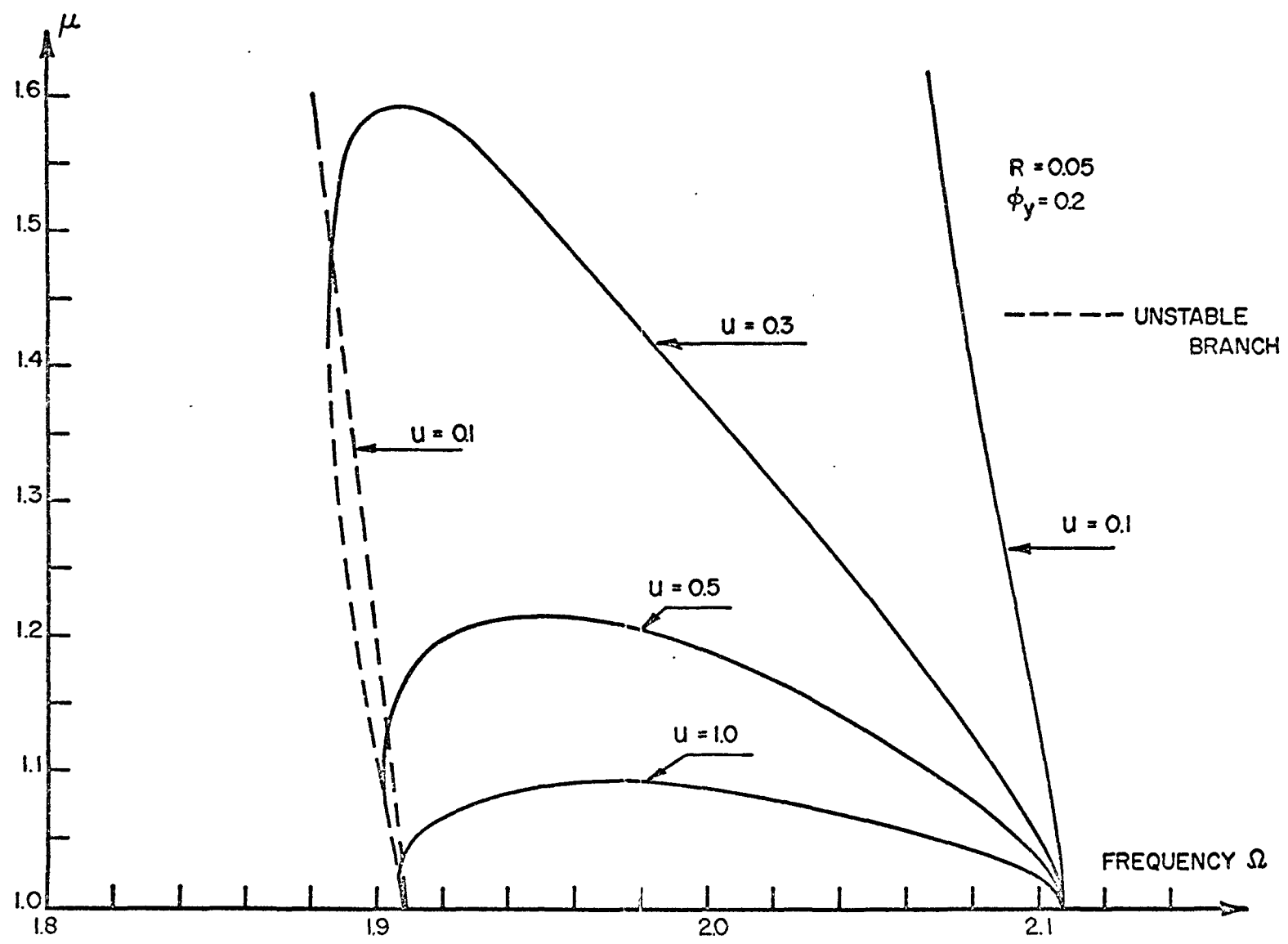
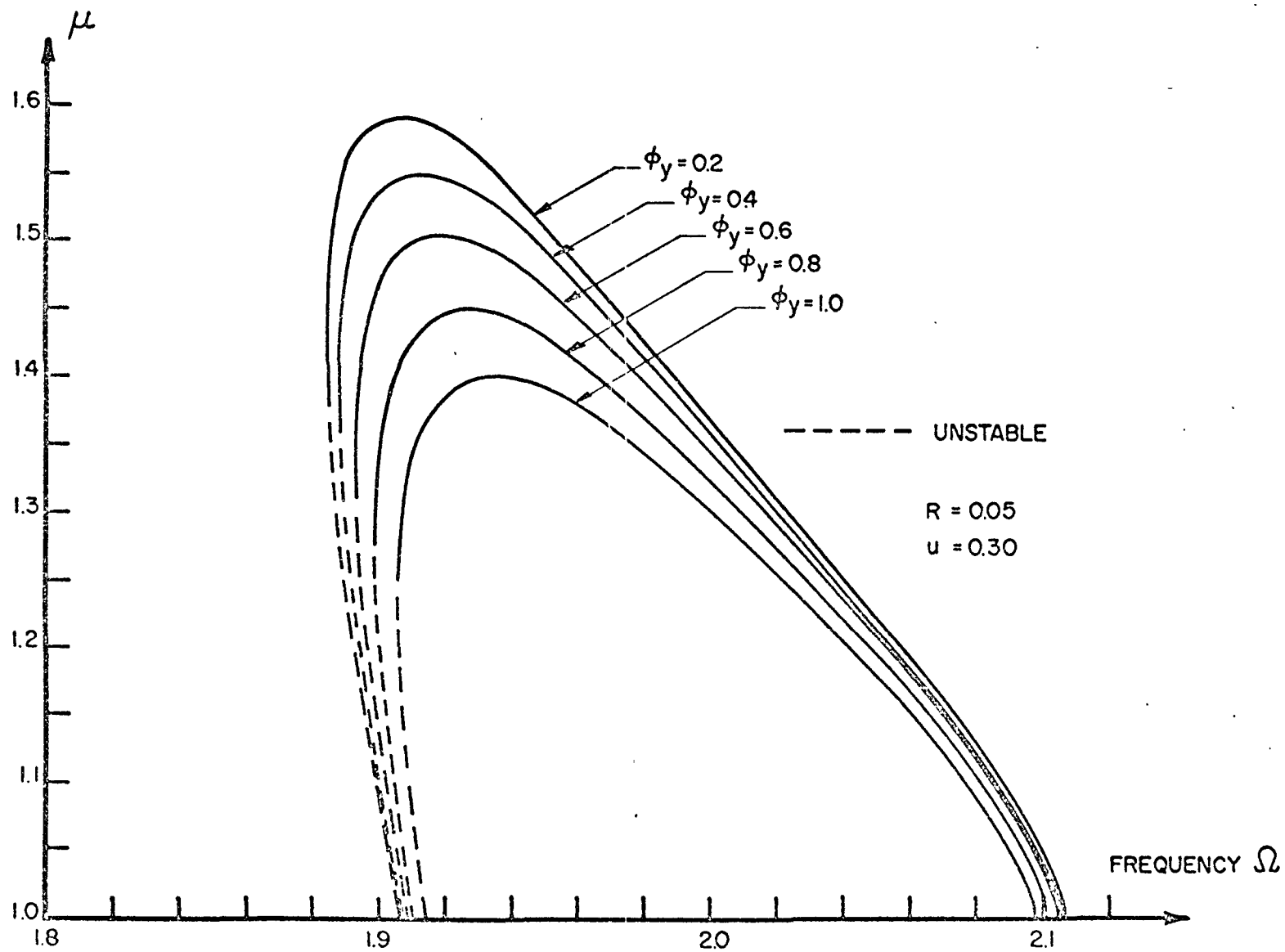


FIG. 4-4 EFFECT OF YIELD ROTATION ϕ_y ON RESPONSE CURVE (SECOND APPROXIMATION)



0.3 rad, it is not surprising that the first approximation of $\sin\phi = \phi$ gives results that are close to results obtained by the higher approximation.

The effect of the yield rotation magnitude on the steady amplitude is given in Fig. 4-4. It can be seen that if the yield rotation ϕ_y is large, the results based on the first approximation overestimates the response.

(b) Double Bilinear Hysteretic Model

For the double-bilinear hysteretic moment rotation characteristic the values of $C(\mu)$ and $S(\mu)$ were obtained by Iwan^[22] and are:

$$C(\mu) = \frac{\mu}{\pi} \left\{ u[\theta^*_1 + \theta^*_2 - \frac{\sin 2\theta^*_1}{2} - \frac{\sin 2\theta^*_2}{2} - \frac{\pi}{2}] + (1-u)\pi \right\} \quad 4-26a$$

$$S(\mu) = -\frac{2}{\pi} u \left(1 - \frac{1}{\mu} \right) \quad 4-26b$$

$$\theta^*_1 = \cos^{-1} \left(1 - \frac{1}{\mu} \right) \quad 4-26c$$

$$\theta^*_2 = \cos^{-1} \left(-\frac{1}{\mu} \right) \quad 4-26d$$

A plot of equation 4-21a is shown in Fig. 4-5 for the base motion amplitude $R = 0.05$ and the four values of u equal to 0.1, 0.3, 0.5, and 1.0. For small initial disturbances, Fig. 4-5 shows that finite amplitude steady-state vibrations are possible within the parametric resonant frequency range for $u = 0.3, 0.5$ and 1.0. However, unbounded resonance becomes possible in the case $u = 0.1$. The response curve has a greater "overhang" towards the direction of

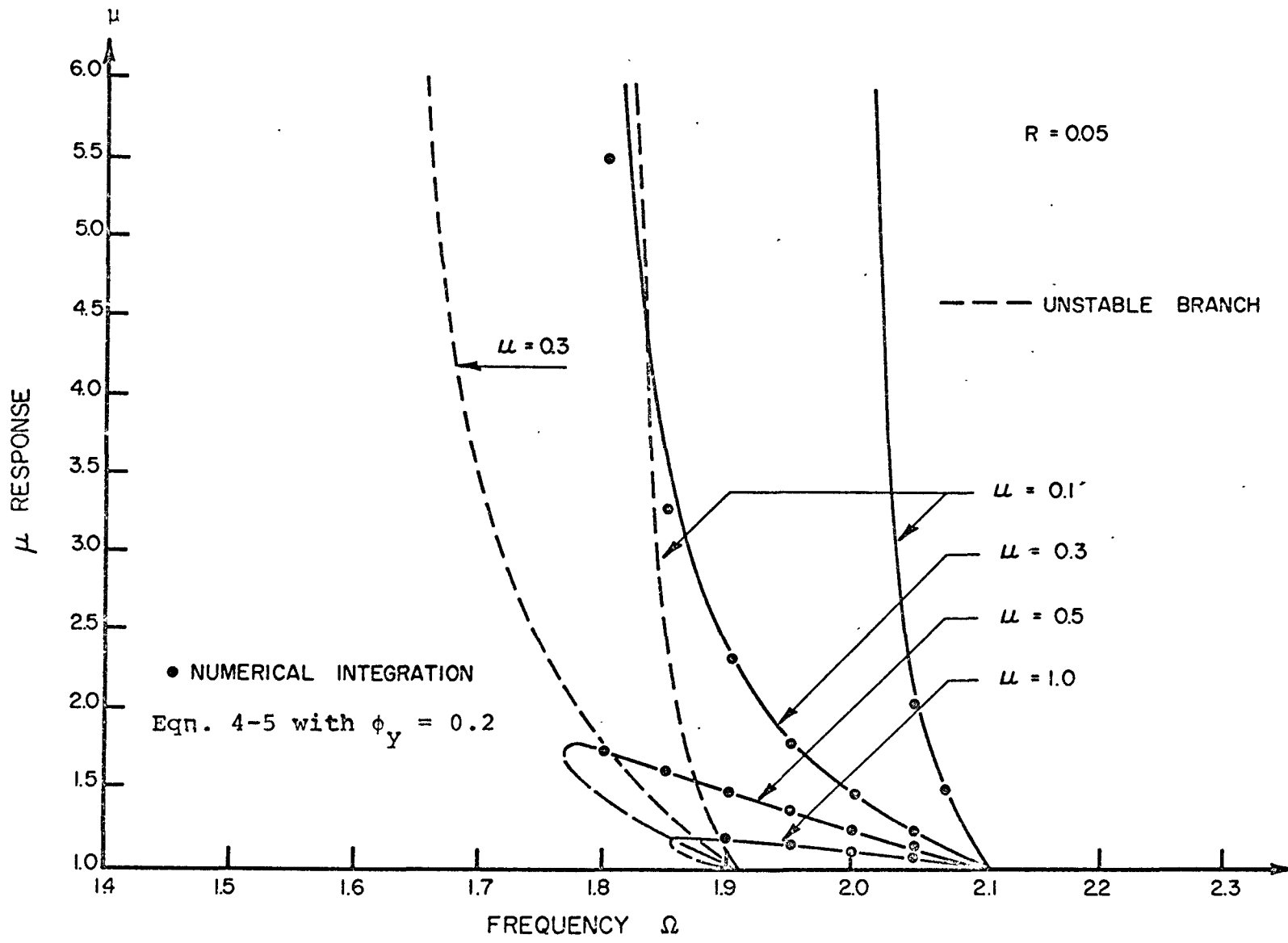


FIG. 4-5 RESPONSE CURVES (FIRST APPROXIMATION ($\sin \phi = \phi$))

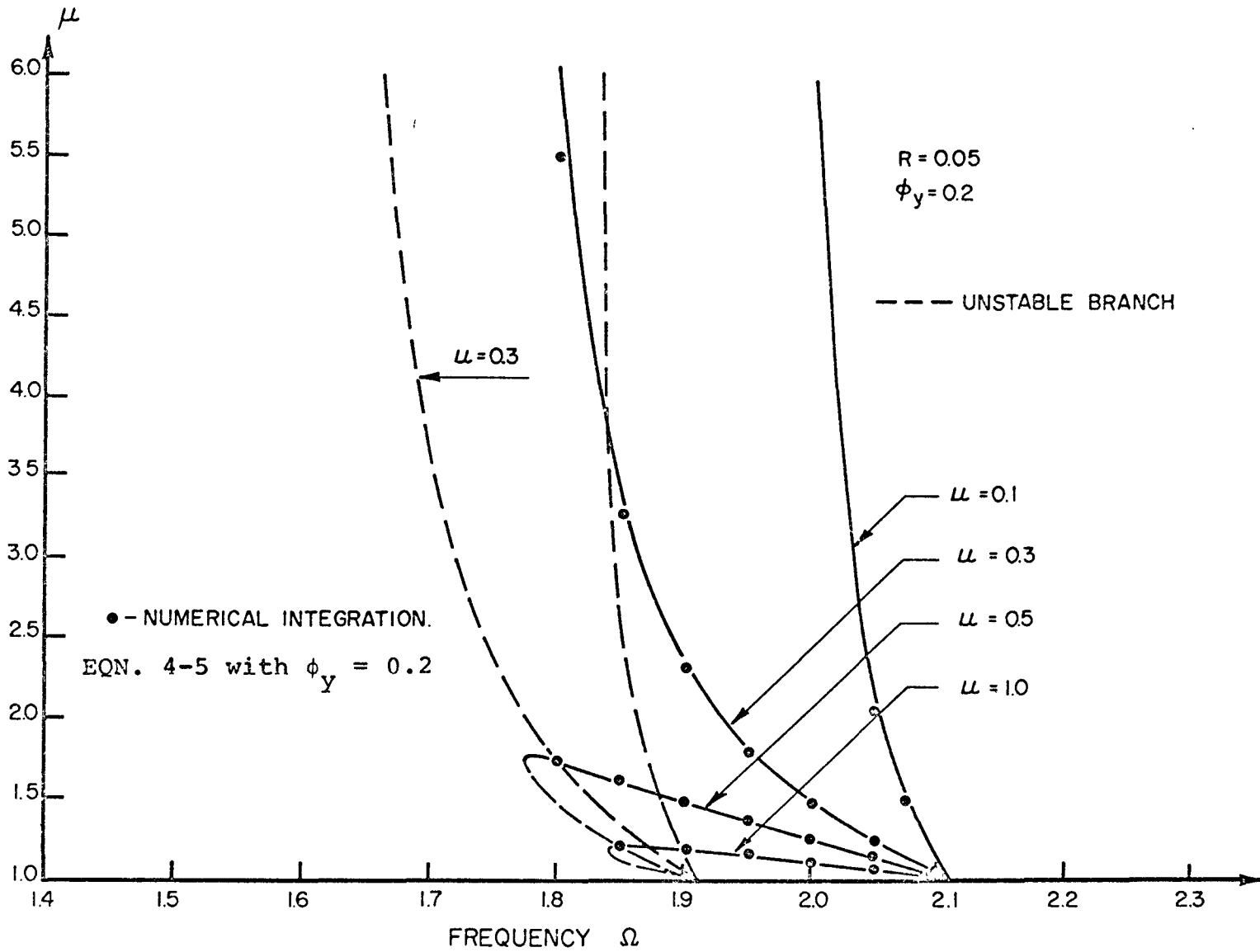


FIG. 4-6 RESPONSE CURVES (SECOND APPROXIMATION $\sin \phi = \phi - \frac{\phi^3}{6}$)

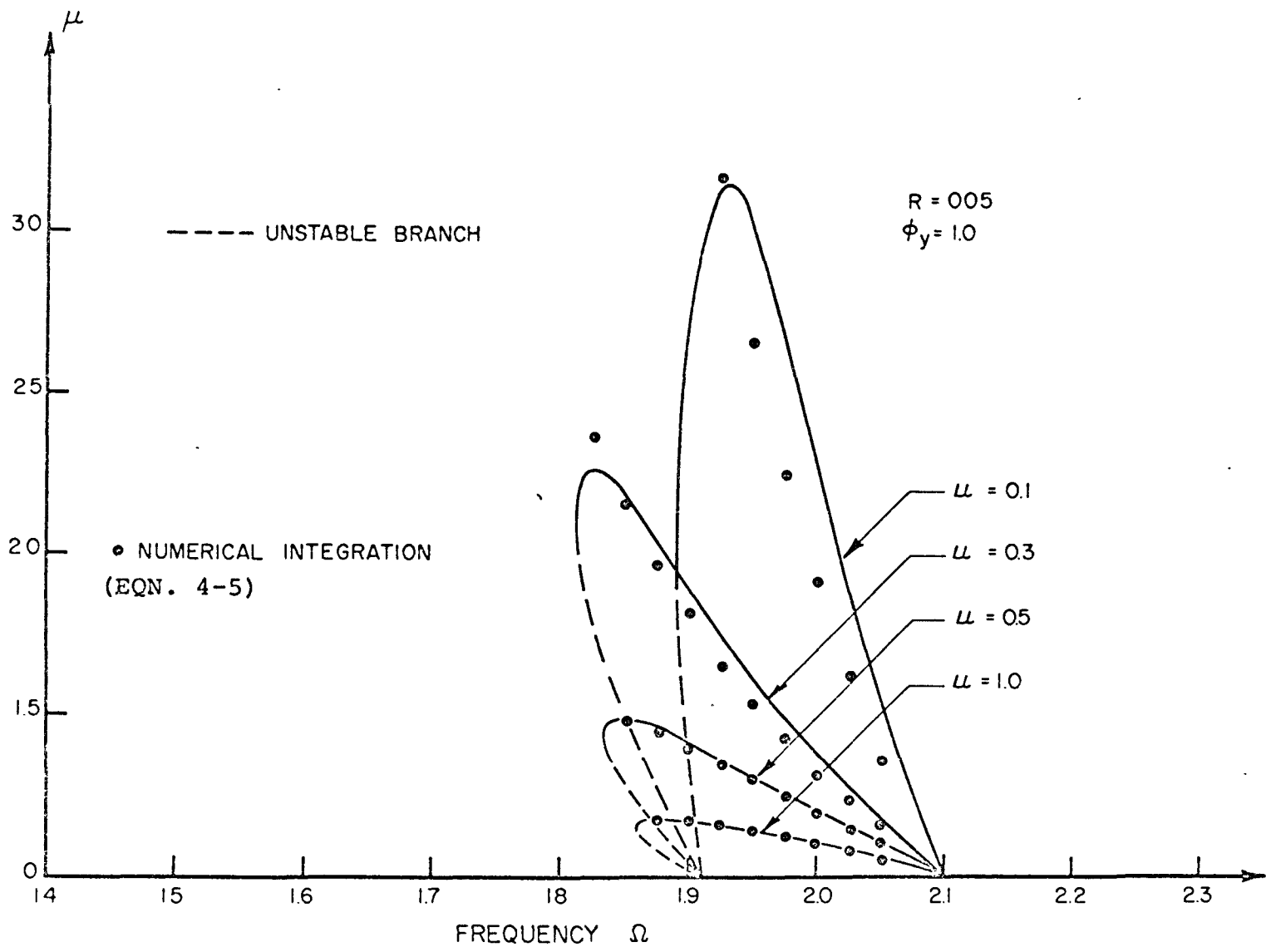


FIG. 4-7 RESPONSE CURVES (SECOND APPROXIMATION ($\sin \phi = \phi - \frac{\phi^3}{6}$))

decreasing frequency as compared to similar curves for the bilinear hysteretic system. The overhanging portions of the stable branch of the response curves outside the parametric resonant frequency range can only be reached when the initial disturbance is large. The effect of initial conditions will be discussed later in the section on transient response.

Response curves for the second approximation obtained from equation 4-24 for two values of ϕ_y corresponding to $\phi_y = 0.2$ radian and $\phi_y = 1$ radian respectively are shown in Figure 4-6 and 4-7. While figures 4-6 and 4-5 are similar, the response curves in figure 4-7 differ considerably from those in figures 4-5 and 4-6. Results obtained from numerically integrating the exact equation 4-5 are also shown on figure 4-7. It can be seen that while the response curve expression for the first approximation may be an adequate representation of the exact equation for small yield rotation ϕ_y , results based on higher order approximations have to be used when the yield rotation ϕ_y is large.

(c) The Ramberg-Osgood Hysteretic Model

For the smoothly curved Ramberg-Osgood hysteretic functions explicit analytical expressions for the value of $C(\mu)$ and $S(\mu)$ in terms of the displacement variable μ are difficult to obtain. These functions can be evaluated numerically direct from their integral definitions given by equations 4-15 and 4-16. The functions $C(\mu)$ and $S(\mu)$ are dependent on the scaling parameters α and n . In Fig. 4-8 the steady state curves are plotted for the value $\alpha = 0.1$ and the three values of n , $n = 3, 9$ and 21 . It is seen that for $n = 3$ there is a large overhang extending to the low frequency side a distance of approximately 40% of the instability zone. This compares closely with the response curve of the double-bilinear model for the case $u = 0.5$. As n increases, the response of the system decreases. For $n = 21$ the response compares closely with the response of

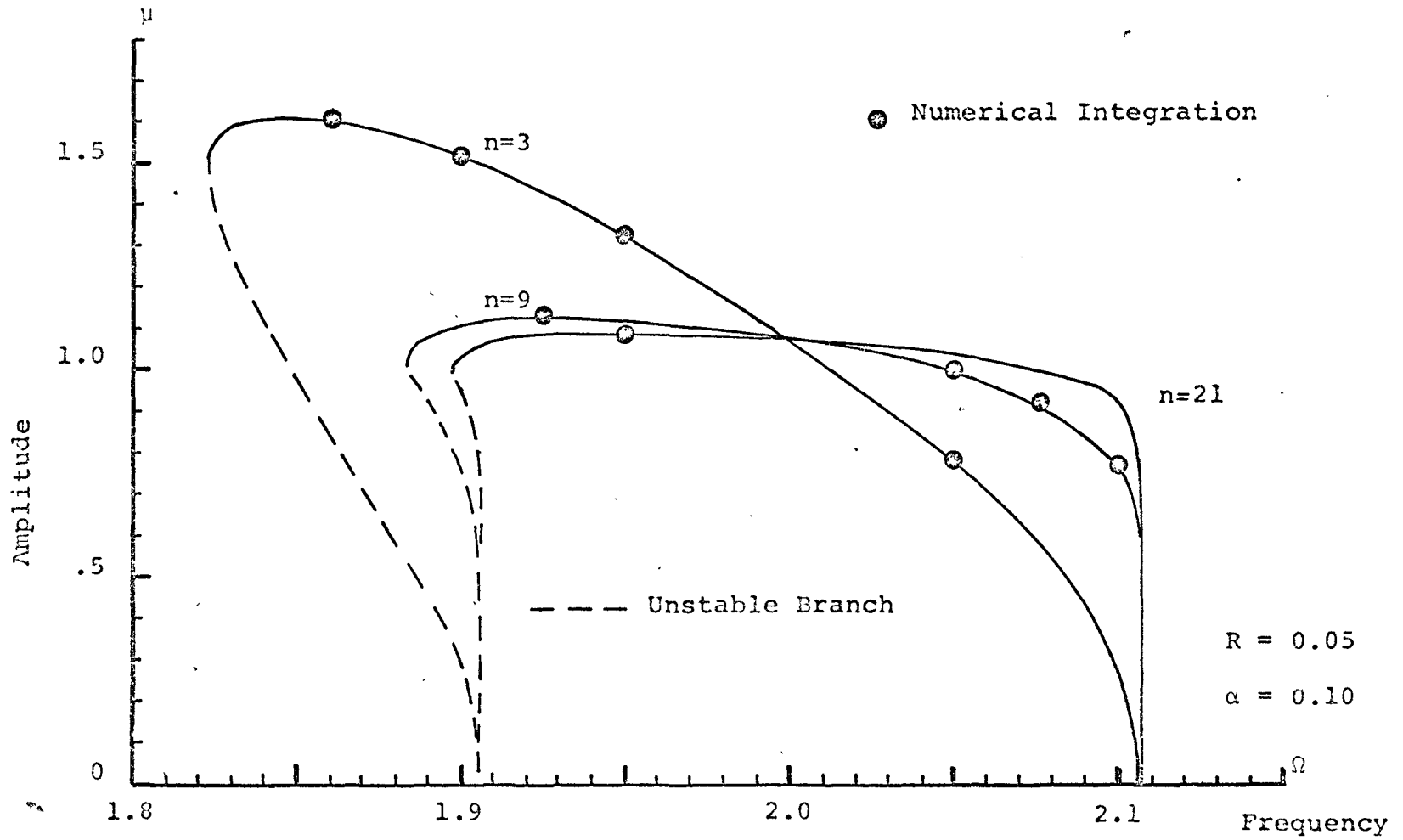


FIG. 4-8 RAMBERG-OSGOOD STEADY STATE CURVE ($\sin \phi = \phi$)

the bilinear system for $u = 1.0$. The stability of the steady-state curves was checked by direct numerical integration and the unstable portions are shown as dashed lines.

4.6 Stability of Steady-State Solution

To investigate the stability of the steady-state response curves, the variational equations based on the steady-state solutions of the first approximation will be studied. Let

$$Q = Q_0 + \xi \quad 4-27a$$

$$\theta = \theta_0 + \eta \quad 4-27b$$

where ξ and η are small quantities representing the deviation from the steady-state solution. Substituting equations 4-27a,b into equations 4-13 and 4-14, neglecting higher order terms in ξ and η , and also making use of relationship 4-19a,b there is obtained

$$\Omega \dot{\xi} = [S'(Q_0) - \frac{S(Q_0)}{Q_0}] \xi + [\frac{1}{2} \Omega^2 Q_0 - 2C(Q_0)] \eta \quad 4-28a$$

$$\Omega Q_0 \dot{\eta} = [C'(Q_0) - \frac{C(Q_0)}{Q_0}] \xi + 2 S(Q_0) \eta \quad 4-28b$$

$$S'(Q_0) \equiv \left. \frac{\partial S(Q)}{\partial Q} \right|_{Q = Q_0} \quad 4-29a$$

$$C'(Q_0) \equiv \left. \frac{\partial C(Q)}{\partial Q} \right|_{Q = Q_0} \quad 4-29b$$

Seeking a solution of the form

$$\begin{bmatrix} \xi \\ \eta \end{bmatrix} = \begin{bmatrix} \bar{\xi} \\ \bar{\eta} \end{bmatrix} e^{\lambda \tau} \quad 4-30$$

equations 4-28a,b can be written in matrix form as

$$\begin{bmatrix} S'(Q_0) - \frac{S(Q_0)}{Q_0} - \lambda \Omega & \frac{1}{2} \Omega^2 Q_0 - 2C(Q_0) \\ C'(Q_0) - \frac{C(Q_0)}{Q_0} & 2S(Q_0) - \lambda \Omega Q_0 \end{bmatrix} \begin{bmatrix} \bar{\xi} \\ \bar{\eta} \end{bmatrix} = 0 \quad 4-31$$

For a given pair of values Q_0 and Ω , the values of λ are to be determined by equating the determinant of the matrix in equation 4-31 to zero. If all values of λ determined have negative real parts then any perturbation from the steady-state motion tends to die out; hence the steady-state solution is stable. On the other hand, if one λ has a positive real part, the perturbations will grow and the steady-state is unstable.

Equation 4-31 determines the stability of the steady state response curves of the first approximation. It is now necessary to substitute the appropriate values of $C(Q_0)$, $C'(Q_0)$, and $S(Q_0)$, $S'(Q_0)$ corresponding to the hysteretic model which is being analyzed. Here only the stability condition for the bilinear hysteretic model will be evaluated explicitly. The procedure is identical for the double-bilinear model. For the Ramberg-Osgood model, analytical expression for the functions $C(Q_0)$, $C'(Q_0)$, $S(Q_0)$, $S'(Q_0)$ are not readily available and the stability of the response curves were checked by numerical integration. The unstable branches are shown in dashed lines in all response plots.

Setting the determinant of 4-31 to zero results in a quadratic equation in $\Omega\lambda$, namely

$$(\Omega\lambda)^2 + a_1(\Omega\lambda) + a_2 = 0 \quad 4-32$$

The coefficients $a_{1,2}$ can be evaluated by using the values of $C(Q_0)$, $S(Q_0)$ from equations 4-25a and 4-25b and the values of $S'(Q_0)$ and $C'(Q_0)$, where

$$S'(Q_0) = -\frac{u}{\pi} (1 - \cos \theta^*)^2 \quad 4-33a$$

$$C'(Q_0) = \frac{1}{\pi} [u\theta^* + (1 - u)\pi + \frac{u}{2} \sin 2\theta^* - 2u \sin \theta^*] \quad 4-33b$$

The coefficients of equation 4-32 are

$$a_1 = \frac{3u}{\pi} \sin^2 \theta^* + \frac{4u}{\pi Q_0} > 0 \quad 4-34a$$

$$a_2 = + \frac{1}{2} \left[-C'(Q_0) + \frac{C(Q_0)}{Q_0} \right] \Omega^2 + 2 \frac{C(Q_0)}{Q_0} \left[C'(Q_0) - \frac{C(Q_0)}{Q_0} \right] \\ + 2 \frac{S(Q_0)}{Q_0} \left[S'(Q_0) - \frac{S(Q_0)}{Q_0} \right] \quad 4-34b$$

Solving 4-32,

$$2\Omega\lambda = -a_1 \pm [a_1^2 - 4a_2]^{1/2} \quad 4-35$$

The characteristic roots λ will have positive real parts only when $a_2 < 0$. Consequently, the question of stability depends on the sign of a_2 . It can be shown that the equation of vertical tangency $\partial\Omega^2/\partial Q = 0$ is given by

$$a_2 = 0 \quad 4-36$$

Hence, the line of vertical tangency serves as a boundary separating the stable and unstable branch of the response curve. For a given value of Q_0 , a_2 can be treated as a function of Ω in equation 4-34. From 4-25a and 4-29b it is seen that the coefficient of the frequency term in 4-34 is positive, i.e.

$$\frac{1}{2} [-C'(Q_0) + \frac{C(Q_0)}{Q_0}] = \frac{2u}{\pi Q_0} \sin \theta^* \geq 0 \quad 4-37$$

since $\theta^* < \pi$. Let the value of the frequency corresponding to Q_0 on the line of vertical tangency be Ωv . Then an increase of frequency from Ωv will render a_2 positive, while a decrease of frequency from Ωv will make a_2 negative. Thus the branch of the response curve to the right of the vertical tangency is stable while the branch of the response curve to the left of the vertical tangency is unstable in the response amplitude-frequency plot.

4.7 "Exact" Analysis

To check the validity of the second approximation, the equation 4-5 is studied without making a simplification to the $\sin\phi$ function. Seeking a solution in the form of equation 4-8 and applying the method of averaging, the steady-state equations can be written as

$$S(Q_0) = -\frac{R\Omega^2}{\pi} [I_1(Q_0)\cos 2\theta_0 + I_2(Q_0)\sin 2\theta_0] \quad 4-38a$$

$$- \frac{1}{4} \Omega^2 Q_0 + C(Q_0)$$

$$= -\frac{R\Omega^2}{4} [I_3(Q_0)\cos 2\theta_0 + I_4(Q_0)\sin 2\theta_0] \quad 4-38b$$

where

$$I_{1,2}(Q_0) \equiv \int_0^{2\pi} \begin{bmatrix} \cos 2\psi \\ \sin 2\psi \end{bmatrix} \sin\psi \sin(Q_0 \cos\psi) d\psi \quad 4-39a$$

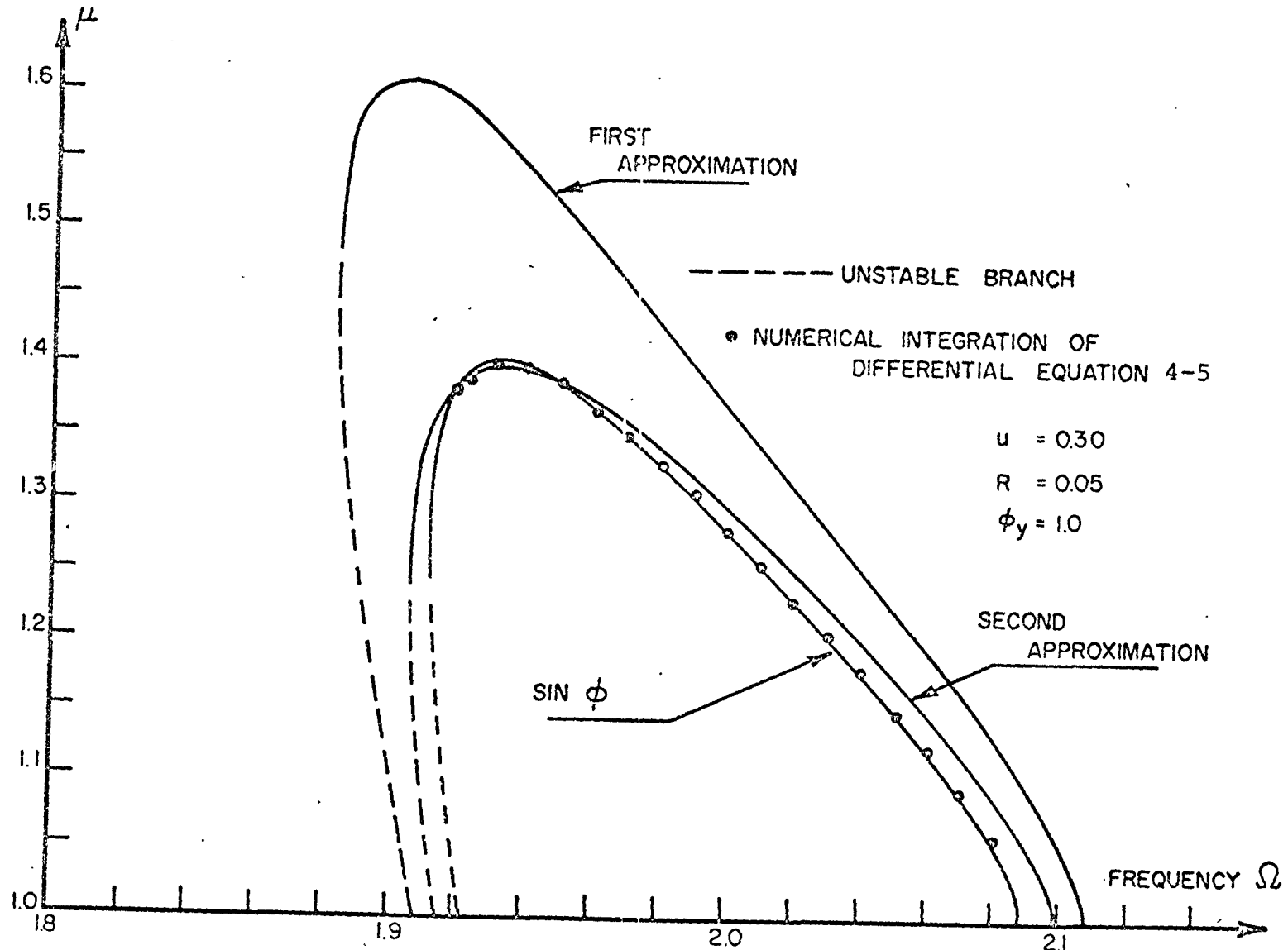
$$I_{3,4}(Q_0) \equiv \int_0^{2\pi} \begin{bmatrix} \cos 2\psi \\ \sin 2\psi \end{bmatrix} \cos\psi \sin(Q_0 \cos\psi) d\psi \quad 4-39b$$

The integrals defined in 4-39a,b are not conveniently expressible in terms of elementary functions, however, they can be evaluated numerically.

Numerical integration shows that I_1 and I_4 are zero for all applicable values of Q_0 . For each value of Q_0 , integrals I_2 and I_3 are evaluated and by eliminating the steady-state phase angle θ_0 the steady-state response curve can be plotted between Q_0 and Ω .

The steady-state curves were obtained for the bilinear hysteretic model and are shown in Fig. 4-9. This figure also compares the response of the first approximation, the second approximation and the numerical integration of the governing differential equation Eqn. 4-5. The steady-state response curve of equations 4-38a,b are almost the same as the response plot determined from the second approximation

FIG. 4-9 COMPARISON OF APPROXIMATE AND NUMERICAL STEADY-STATE RESPONSE CURVES
(FOR BILINEAR HYSTERETIC MODEL)



for yield rotation up to 1 rad. The numerically integrated points coincide with the "exact" analysis and the response curve given by the first approximation overestimates the response. It can be seen that the steady-state amplitude as predicted by the method of averaging agrees well with that obtained through direct numerical integration of the governing equation.

4.8 Transient Response

Unlike the forced-vibration problems, some nonzero initial conditions need to be specified to equation 4-5 or 4-7 in order to get a nontrivial response. Zero initial conditions will only lead to the trivial solution $\phi = 0$. The effect of initial conditions on the response of the system is studied by solving equation 4-5 and 4-7 numerically with a variety of initial conditions. Using a fourth order Runge-Kutta method for numerical integration the time response curves are obtained.

(a) Bilinear Hysteretic Model

Shown in Fig. 4-10 and 4-11 are two representative plots of the time history response curves by integrating the equation 4-7. Fig. 4-10 corresponds to the initial conditions $\phi(0) = 0.01$, $\dot{\phi}(0) = 0.01$ while Fig. 4-11 corresponds to the initial conditions of $\phi(0) = 0.01$, $\dot{\phi}(0) = -0.01$. It can be seen that both sets of initial conditions lead to the same magnitude of steady-state amplitude. The initial conditions only effect the time at which the steady-state condition is established. It is noted that the growth of the amplitude before it exceeds the yield level is an exponential growth just as predicted by the linear Mathieu equations. But, once the hysteretic damping mechanism takes effect, the amplitude quickly settles to the steady-state value. It should also be pointed out that the "overshoot" of the amplitude from the

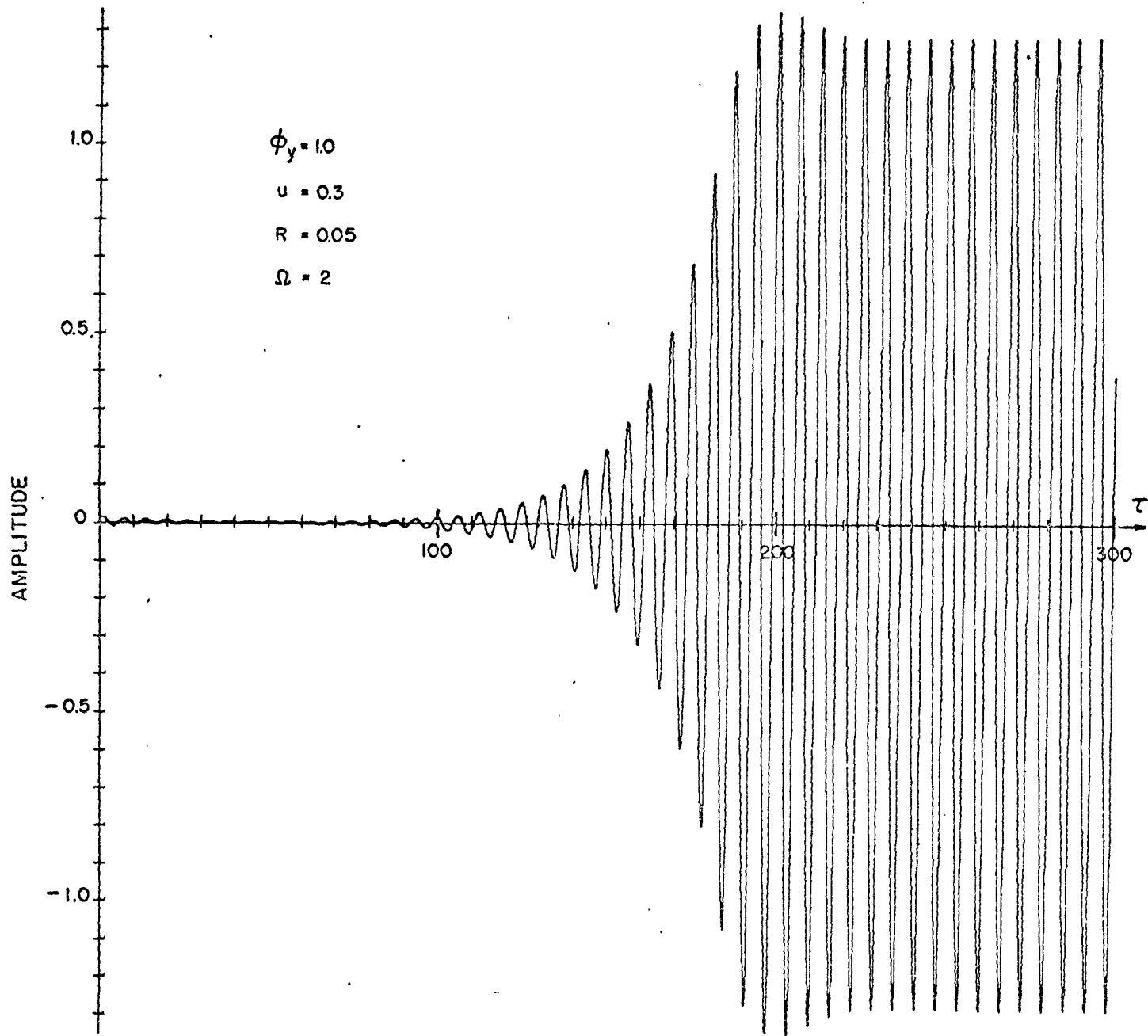


FIG. 4-10 EFFECT OF INITIAL CONDITIONS, $(\phi(0) = 0.01, \dot{\phi}(0) = 0.01)$

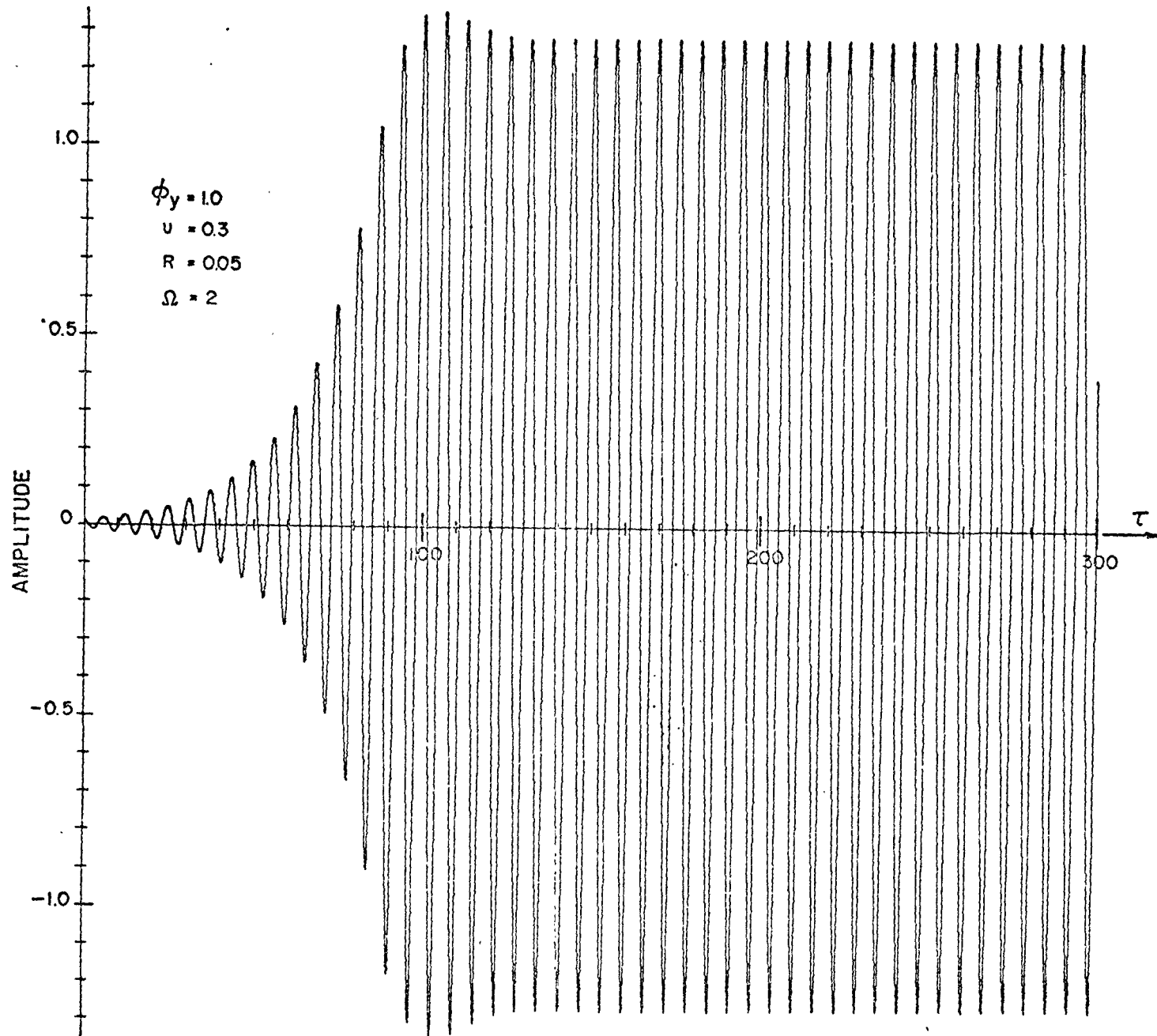


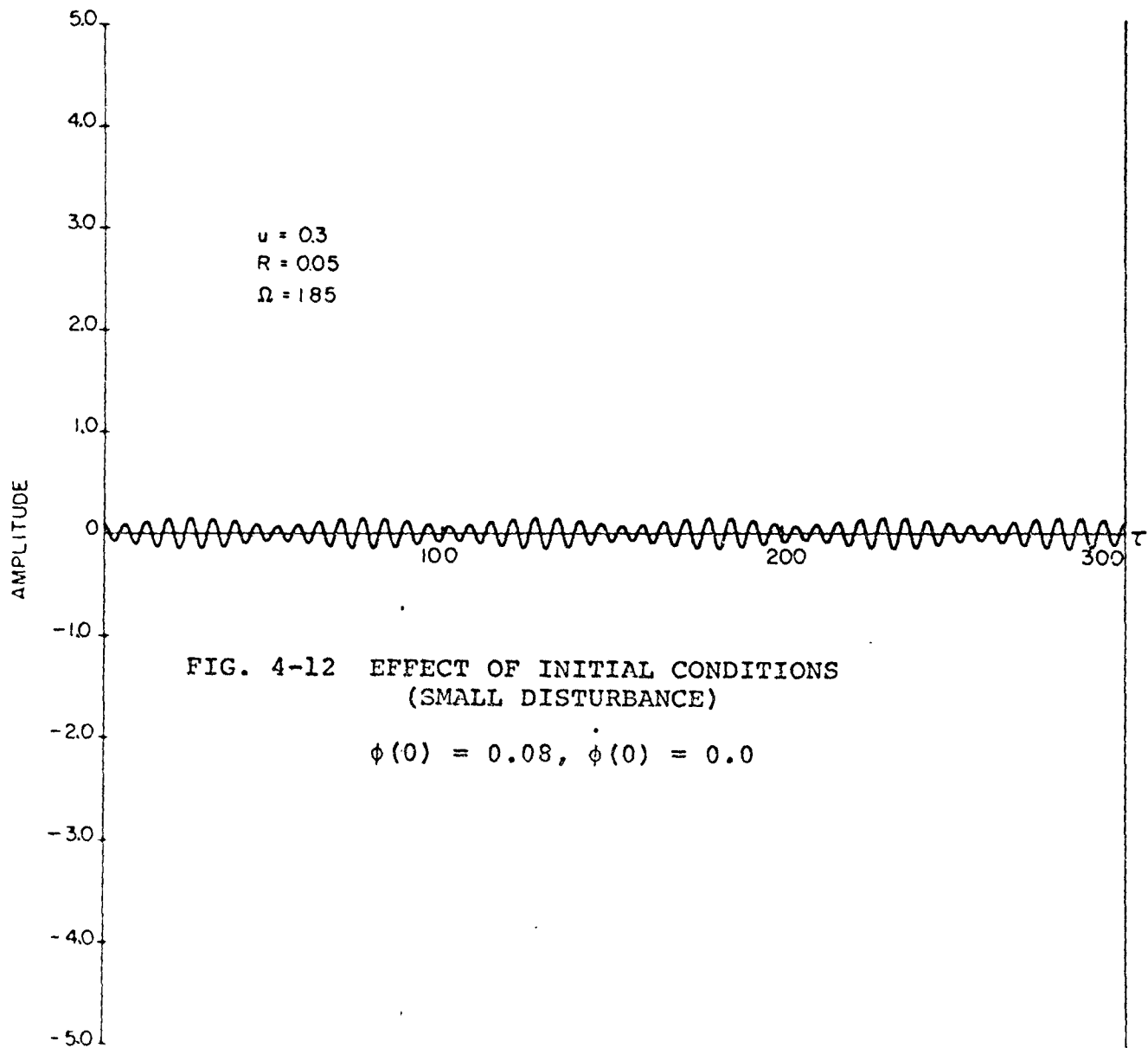
FIG. 4-11 EFFECT OF INITIAL CONDITIONS, ($\phi(0) = 0.01, \dot{\phi}(0) = -0.01$)

steady-state value is small. For this reason, the factor μ in the response plots can be treated as the ductility factor, a terminology commonly used in earthquake engineering to denote the ratio of maximum displacement to yield displacement. The amount of overshoot depends on the characteristic of the bilinear hysteretic parameter u . The overshoot is generally small for $u > 0.5$, but can amount to 20 percent of the steady-state amplitude when $u = 0.1$.

(b) Double Bilinear Hysteretic Model

In contrast to the bilinear hysteretic model, the steady-state response curves have a pronounced lean or "overhang" in the direction of decreasing frequency. In order to interpret the results properly, it is necessary to make a distinction between the magnitude of initial disturbances on the system from its equilibrium position $\phi = 0$. When the initial disturbance is small so that the maximum excursion of the system caused by the initial disturbance is less than the yield rotation ϕ_y , the system is initially non-hysteretic. In fact the system given by the equation 4-7 of the first approximation is then initially a linear system. The parametric stability of the system is given by the Strutt-Ince stability chart. Unless the exciting frequency is within the parametric resonance range, the system will not be parametrically excited into oscillating motion. Within the parametric resonance range, different small initial disturbances only affect the time at which the system attains steady-state vibration. The steady state amplitude is not affected by the initial conditions and can be predicted accurately by the response curve calculations.

If the initial disturbance is of such a magnitude that it causes the system to exceed the yield rotation during its first cycle of oscillation, then the system may be parametrically excited into large amplitude oscillations even



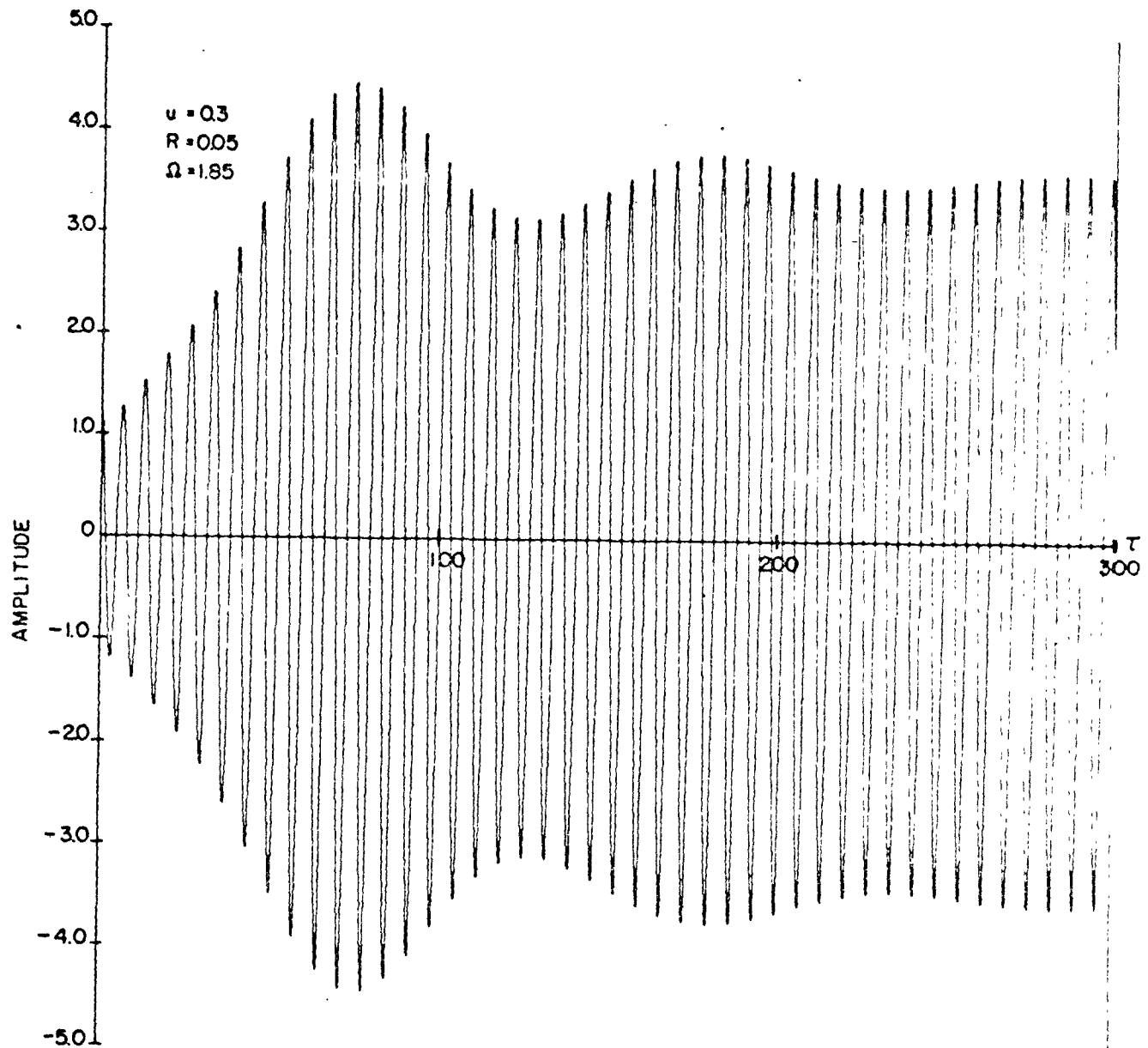


FIG. 4-13 EFFECT OF INITIAL CONDITIONS (LARGE DISTURBANCE)
($\phi(0) = 1.2, \dot{\phi}(0) = 0.0$)

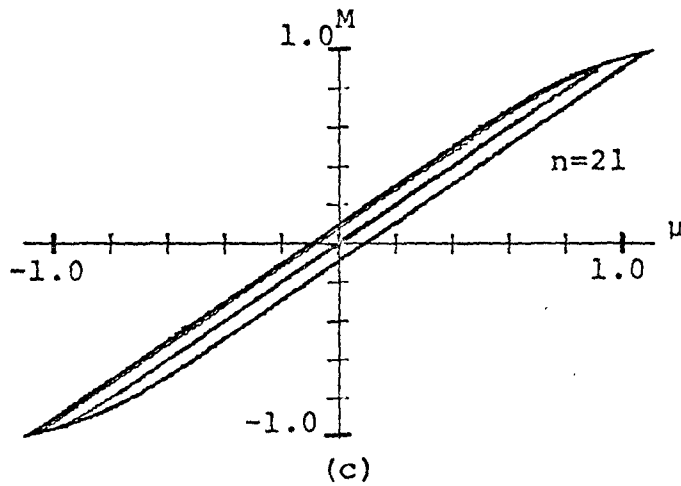
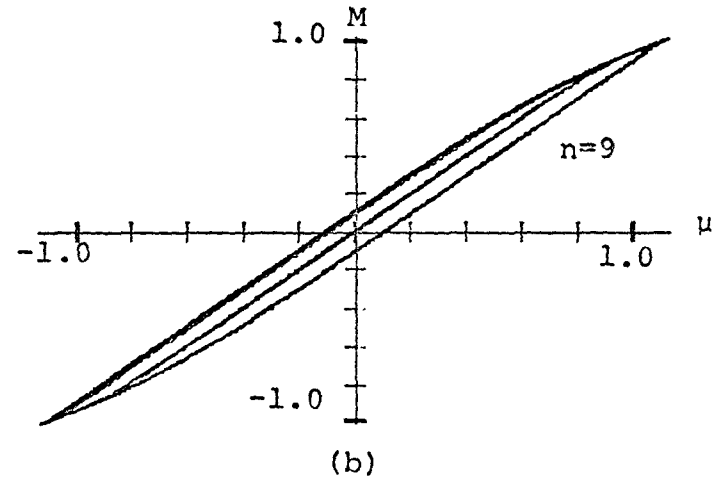
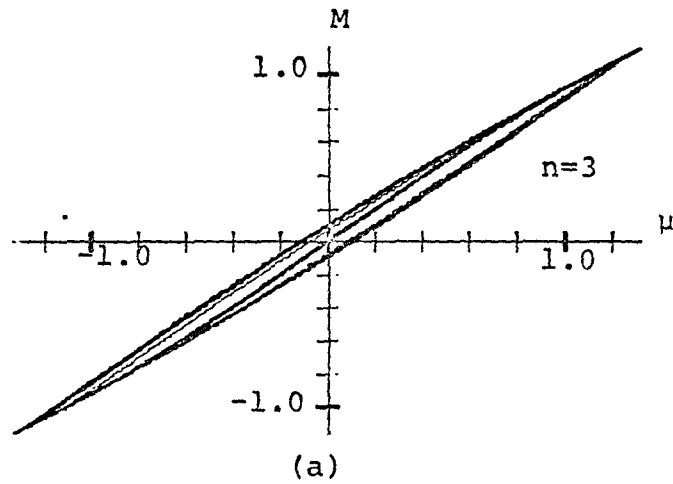


FIG. 4-14 TRACE OF RAMBERG-OSGOOD
HYSTERETIC CURVES (EQN. 4-7)

($R = 0.05$, $\Omega = 2.0$, $\alpha = 0.1$)

when the exciting frequency is outside the parametric resonant frequency range. The effect of initial disturbances is illustrated in Figures 4-12 and 4-13. Shown in Fig. 4-12 and 4-13 are the results of numerically integrating equation 4-7 under two different initial conditions. The parametric frequency $\Omega = 1.85$, is outside the parametric resonant range. Figure 4-12 shows that when the initial disturbance is small, the system is not excited. Figure 4-13 shows the response of the same system under the same condition of excitation. However, the values of initial conditions used are such that the system enters into the double bilinear hysteretic loop from the start. It can be seen that the system is parametrically excited. The steady-state amplitude of the resulting oscillation agrees with the values predicted from Fig. 4-5.

Instead of plotting the transient response* of the amplitude vs time relationship for the Ramberg-Osgood model the hysteretic moment-rotation curves are drawn to show the actual hysteretic loops as they are traced out from a small initial disturbance to a steady-state value. Fig. 4-14 compares the three hysteretic loops for $\alpha = .1$, $n = 3, 9$ and 21 at the frequency $\Omega = 2.0$. It can be seen, that following an initial small disturbance the relationship M/μ is at first approximately linear. As the amplitude increases the nonlinear effect becomes more pronounced until at steady-state identical branches of the ascending and descending curves of the hysteretic loop are continuously retraced.

4.9 Bounded Response Within the Linear Instability Zone

To obtain bounded response within the linear instability zone, both asymptotes of the steady-state response curves given by equation 4-21a should be outside the linear instability zones. The width of the instability zone for $\mu = 0$ is obtained from Equation 4-21a by setting $C(\mu)/\mu = 1$

*Note: Following the rules specified by Jennings [27]

and $S(\mu)/\mu = 0$, namely

$$\Omega^2 = \frac{4(1 \pm 2R)}{(1-2R)(1+2R)} \quad 4-40a$$

$$\Omega_1 = \frac{2}{\sqrt{1+2R}} \quad 4-40b$$

$$\Omega_2 = \frac{2}{\sqrt{1-2R}} \quad 4-40c$$

For the base excitation parameter $R = 0.05$,
 $\omega_1 = 1.91$ and $\omega_2 = 2.11$.

While it is true that when the steady-state response becomes large the steady equations 4-21a based on the first approximation may not be a good approximation to the exact equation 4-5, nevertheless, it is instructive to establish the conditions under which bounded responses are obtained. For the piecewise linear system

$$\lim_{\mu \rightarrow \infty} \Omega^2 = \frac{4(1-u)}{1 \pm 2R} \quad 4-41$$

The two asymptotes in the response plot are given by

$$\bar{\Omega}_1 = 2 \sqrt{\frac{(1-u)}{1+2R}} \quad 4-42a$$

$$\bar{\Omega}_2 = 2 \sqrt{\frac{(1-u)}{1-2R}} \quad 4-42b$$

In order to yield bounded response, both $\bar{\Omega}_1$, and $\bar{\Omega}_2$ of equations 4-42 should be outside the range of parametric resonance, i.e.

$$\bar{\Omega}_2 \leq \frac{2}{\sqrt{1+2R}} \quad 4-43$$

and the condition for bounded response is

$$(1-u) \leq \frac{(1-2R)}{(1+2R)} \quad \begin{array}{l} \text{(Piecewise Linear)} \\ (R < 0.5) \end{array} \quad 4-44$$

For the case of elasto-plastic deformation, $u=1$ and equation 4-44 is always satisfied. Hence bounded response is always possible during parametric resonance for a system with bilinear or double bilinear hysteresis with $u = 1$. For the Ramberg-Osgood function

$$\lim_{\mu \rightarrow \infty} \Omega^2 = 0 \quad \begin{array}{l} \text{(Ramberg-Osgood function)} \\ \end{array} \quad 4-45$$

and hence bounded response is always possible.

4.10 Characteristics of the Functions $C(\mu)/\mu$, $S(\mu)/\mu$

The steady state equations depend on the functions $C(\mu)/\mu$ and $S(\mu)/\mu$. These functions are derived as integral

expressions of the restoring moment $M(\phi, \dot{\phi})$ averaged over one cycle of oscillation where the integral $S(\mu)$ represents the energy dissipation property of the function $M(\phi)$ and the integral $C(\mu)$ represents the measure of frequency detuning. In this section, a study is made on the functions $C(\mu)/\mu$ and $S(\mu)/\mu$ for the three hysteretic models. Also it is intended to illustrate the difference between the hysteretic models and three common analytical representations of the restoring force characteristics.

(a) Analytical Representation of the Restoring Force Characteristics

Consider three cases where $M(\phi, \dot{\phi})$ is represented by a combination of linear and nonlinear terms of the co-ordinate ϕ and it's time-derivative $\dot{\phi}$.

$$(i) \quad M_1 = \phi + e\dot{\phi} - a\phi^3 \quad 4-46$$

$$(ii) \quad M_2 = \phi + e\dot{\phi}^3 \quad 4-47a$$

$$(iii) \quad M_3 = \phi + e\phi^2(\dot{\phi}) \quad 4-47b$$

In Equation 4-46 the restoring force M has in addition to its linear component ϕ a linear viscous damping term $e\dot{\phi}$ and a softening cubic nonlinear function $-a\phi^3$. It is assumed the coefficients e and a are small compared to unity.

Equation 47a is the case where M is linear in the displacement co-ordinate but a cubic viscous damping term $e\dot{\phi}^3$ is added. Equation 4-47b is similar to Equation 4-46 except that the nonlinear damping term $e\phi^2(\dot{\phi})$ consists of a mixed expression of amplitude and velocity. Such an expression is often

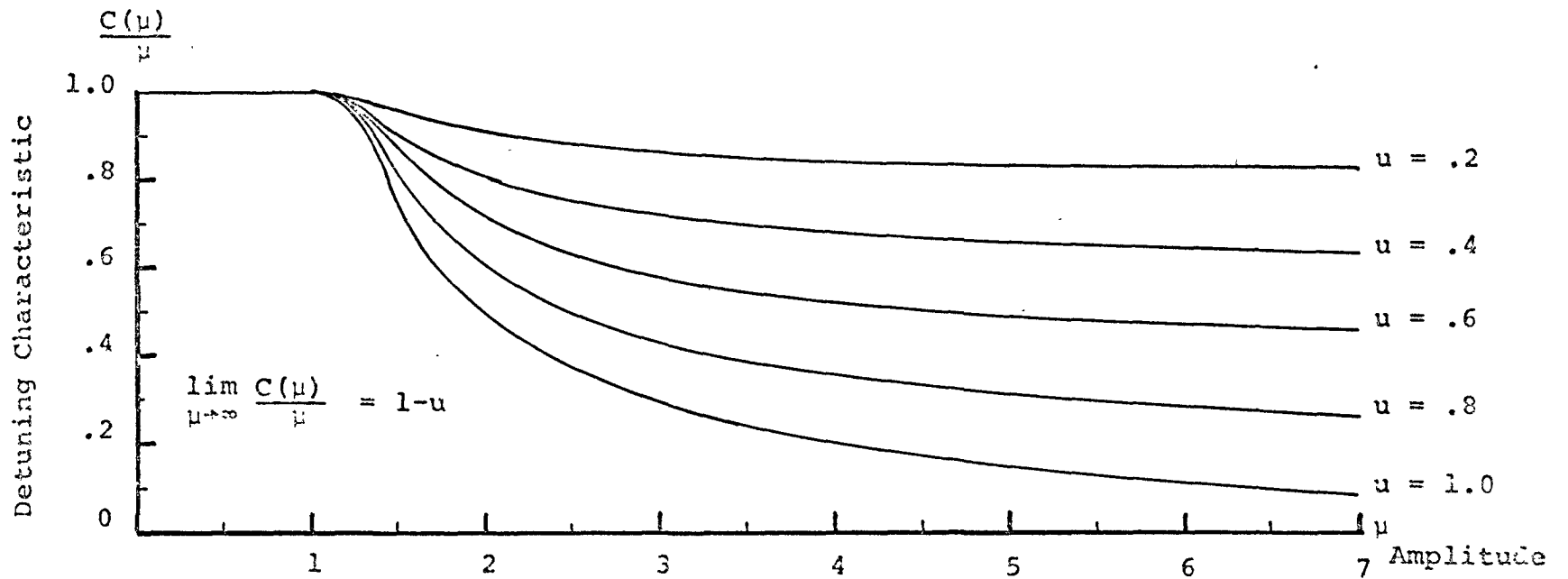


FIG. 4-15 DETUNING CHARACTERISTICS - BILINEAR MODEL

$$\frac{C(u)}{u} = 1 - \frac{u}{\pi} (\pi - \theta^* - \sin(\theta^*) \cos(\theta^*))$$

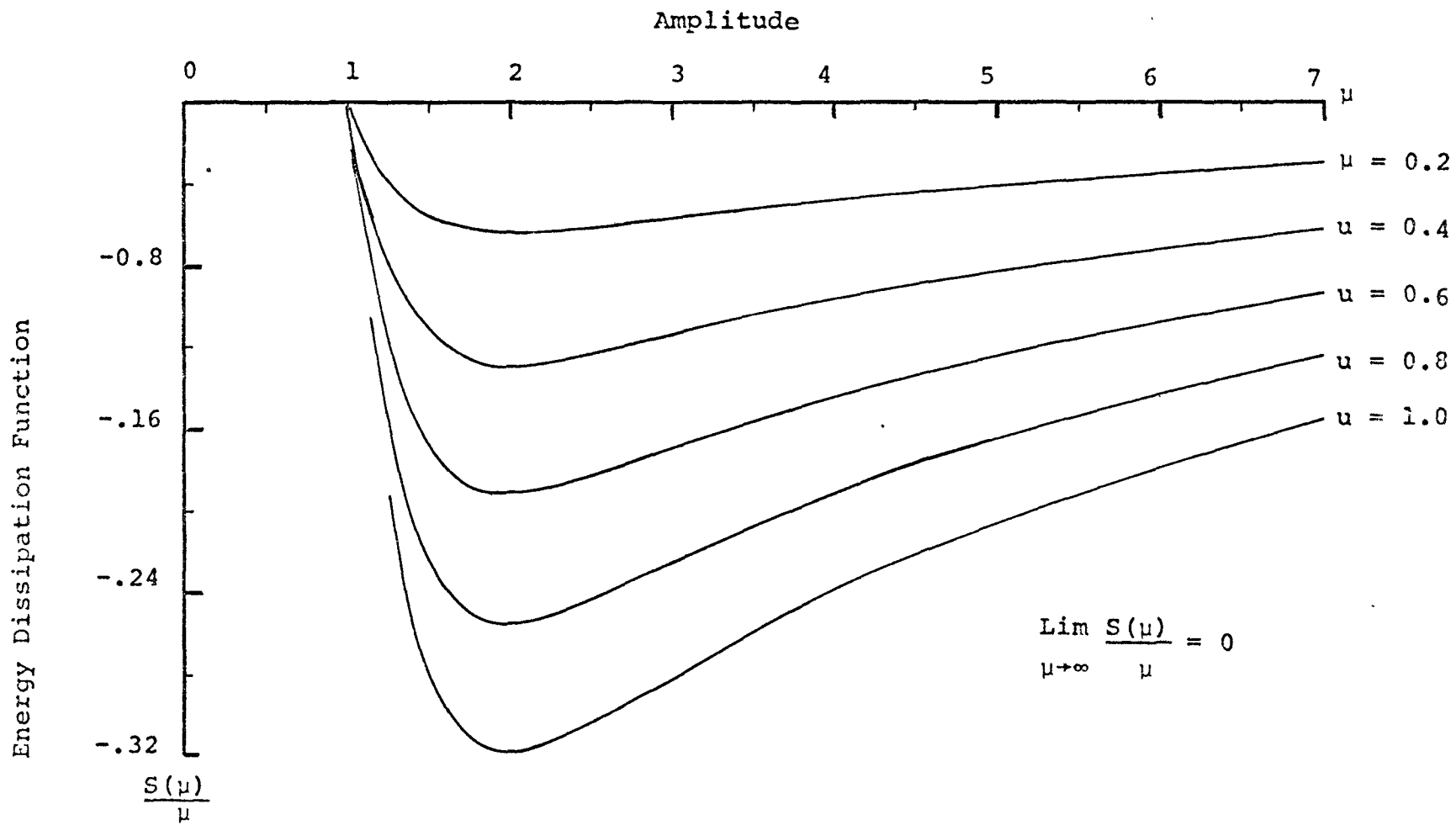


FIG. 4-16 DAMPING CHARACTERISTIC BILINEAR HYSTERETIC MODEL

$$\frac{S(\mu)}{\mu} = -\frac{4}{\pi} \frac{u}{\mu} \left(1 - \frac{1}{u}\right)$$

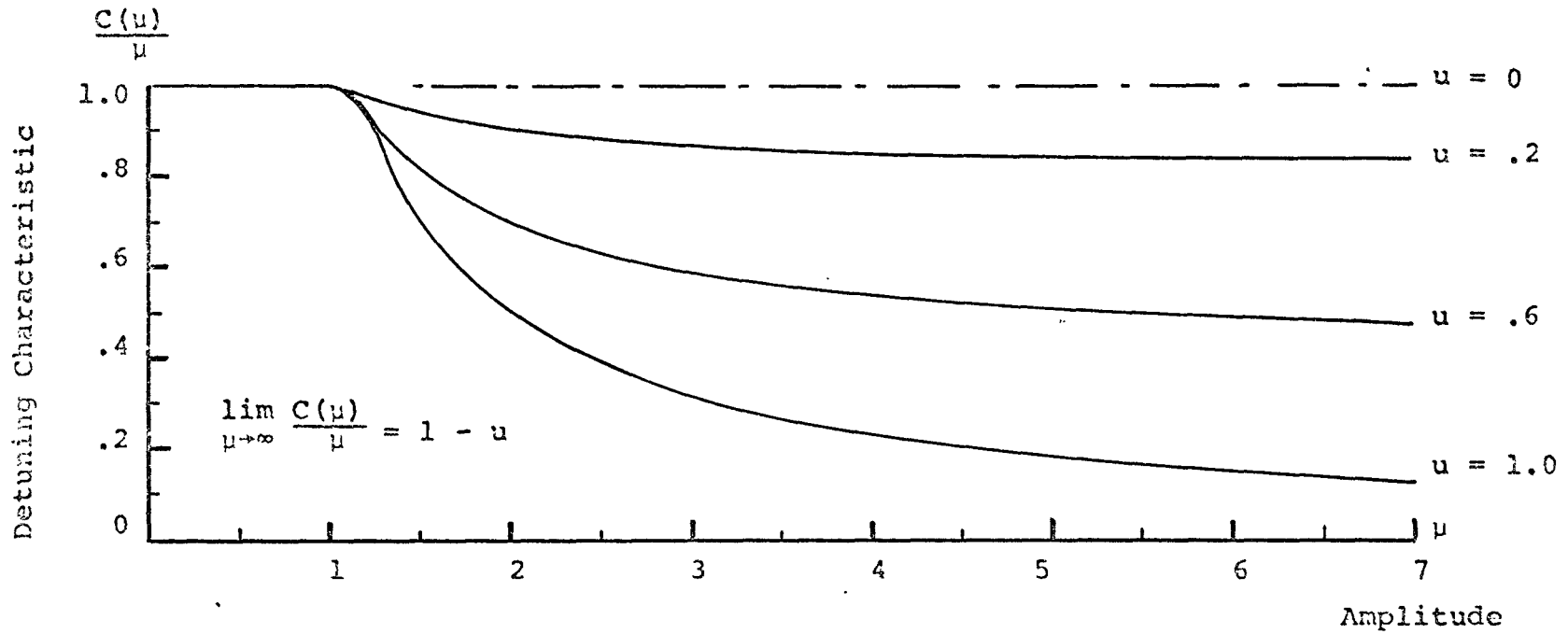


FIG. 4-17 DETUNING CHARACTERISTIC DOUBLE BILINEAR MODEL

$$\frac{C(u)}{\mu} = 1/\pi [u(\theta^*_1 + \theta^*_2 - 0.5 \sin(2\theta^*_1) - 0.5 \sin(2\theta^*_2) - \pi/2) + (1-u)\pi]$$

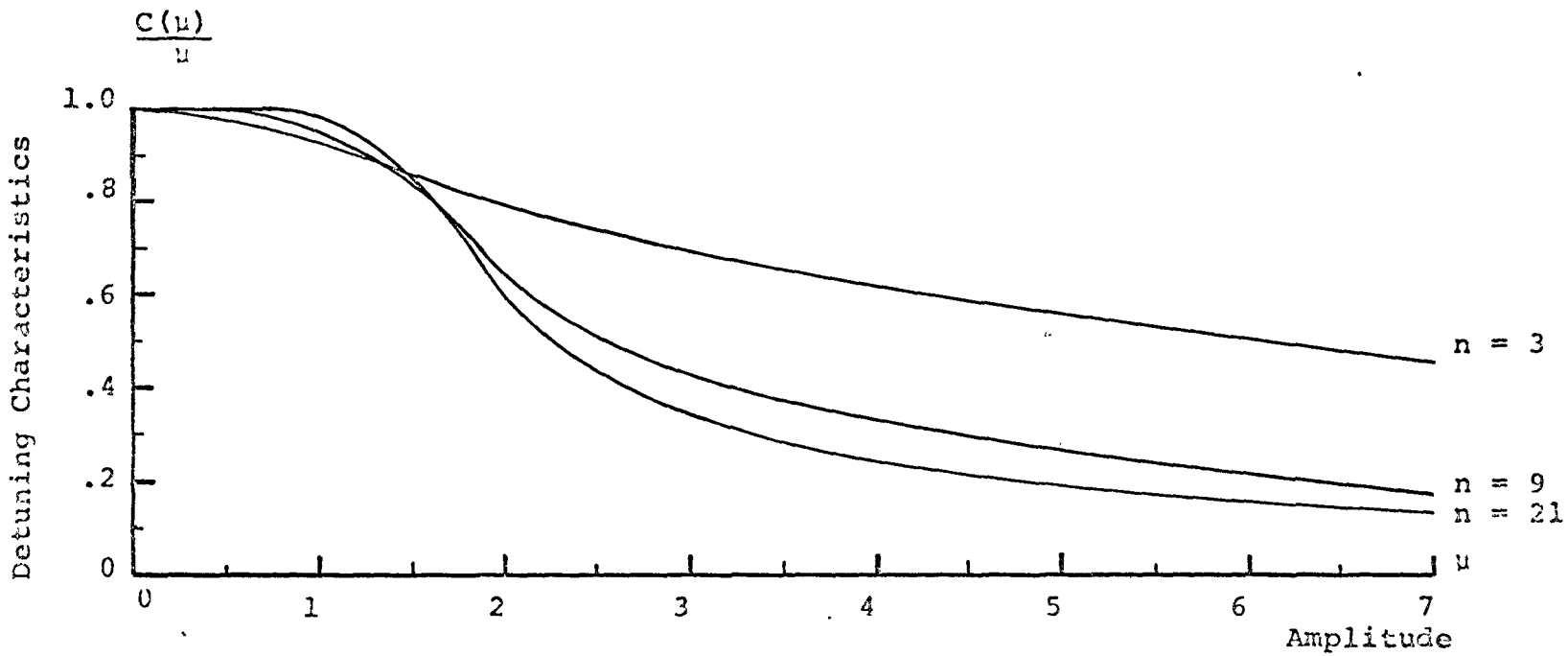


FIG. 4-18a DETUNING CHARACTERISTIC RAMBERG-OSGOOD HYSTERETIC MODEL ($\alpha = 0.1$)

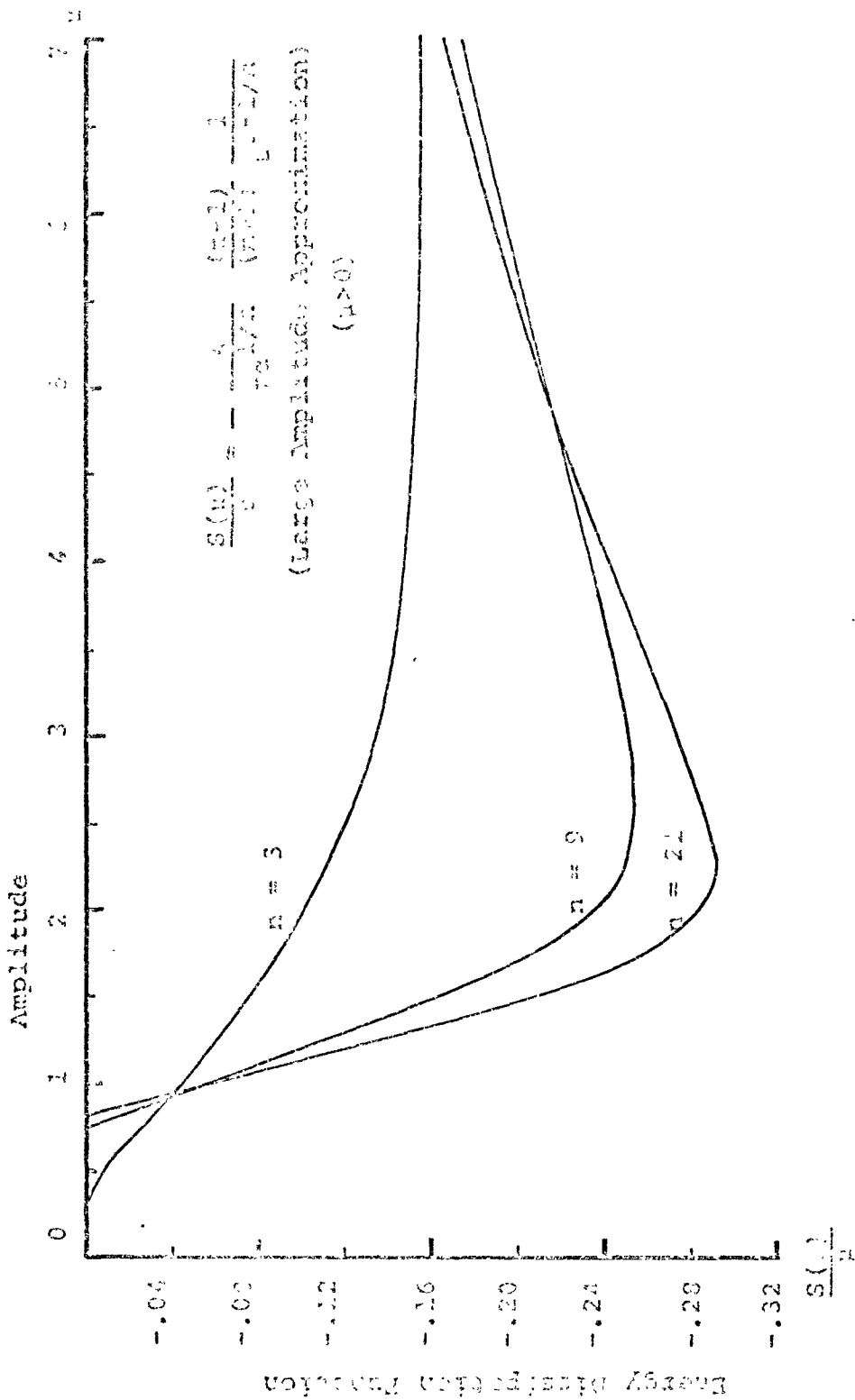


FIG. 4-10b DAMPING CHARACTERISTIC LAMBERG-OSGOOD MODEL ($\alpha = 0.1$)

used as an analytical form of hysteretic damping [Bolotin]. [4]

The values of $C(\mu)/\mu$ and $S(\mu)/\mu$ of the expressions 4-46, 47a, b are found to be

$$(i) \quad \frac{S(\mu)_1}{\mu} = -\frac{e}{2} \Omega \quad 4-48a$$

$$\frac{C(\mu)_1}{\mu} = 1 - \frac{3}{4} a \phi_y^2 \mu^2 \quad 4-48b$$

$$(ii) \quad \frac{S(\mu)_2}{\mu} = -\frac{3}{32} e \Omega^3 \phi_y^2 \mu^2 \quad 4-49a$$

$$\frac{C(\mu)_2}{\mu} = 1 \quad 4-49b$$

$$(iii) \quad \frac{S(\mu)_3}{\mu} = -\frac{1}{4} e \Omega \phi_y^2 \mu^2 \quad 4-50a$$

$$\frac{C(\mu)_3}{\mu} = 1 \quad 4-50b$$

In the steady-state equations 4-21a, viscous linear damping would be represented by the constant of equation 4-48a, nonlinear cubic viscous damping by the quadratic expression of equation 4-49a and nonlinear, analytic hysteretic damping by the quadratic expression of equation 4-50a. The frequency detuning parameter is a constant for the two nonlinear damping terms and is a quadratic expression in terms of μ for the cubic restoring moment. From the steady-state equation 4-21a a constant expression for $C(\mu)/\mu$ means that the "backbone" equation of the steady state

response curve defined by

$$\Omega^2 = 4 \frac{C(\mu)}{\mu} \frac{1}{(1-4R^2)} \quad 4-51$$

is a constant.

(b) Hysteretic Representation of the Restoring Force Characteristics

For the two piecewise linear models explicit expressions for $C(\mu)/\mu$, $S(\mu)/\mu$ can be obtained from equations 4-25 and 4-26. For the Ramberg-Osgood model the functions can be evaluated numerically from the integral definition of equations 4-15 and 4-16. As the nature of these functions is not readily apparent from their defining equations they are plotted against amplitude μ in Fig. 4-15.

Fig. 4-15 is a plot of the function $C(\mu)/\mu$ for the bilinear hysteretic model for the values of u ranging from 0.2 to 1.0. It is seen that the value of $C(\mu)/\mu$ decreases monotonically to the limit of $1-u$. The energy dissipation function $S(\mu)/\mu$ is plotted in Fig. 4-16. Here $S(\mu)/\mu$ reaches a minimum for $\mu = 2$ and then increases to zero as μ increases.

The function $C(\mu)/\mu$ for the double bilinear model is plotted in Fig. 4-17. The curves are similar to the bilinear model except that within the range $1 \leq \mu \leq 2$ the values $C(\mu)/\mu$ for a common value of u is slightly less for the double bilinear model and in the range $\mu > 2$ slightly more. The limit $C(\mu)/\mu$ as μ goes to infinity is the same as the bilinear model, namely, the limiting value is $1-u$. The function $S(\mu)/\mu$ is identical to the bilinear model of Fig. 4-16 with the ordinate divided by two, since the dissipation power for the double bilinear hysteretic model is half that of the

bilinear hysteretic model.

The functions $C(\mu)/\mu$ and $S(\mu)/\mu$ for the Ramberg-Osgood model are shown in Fig. 4-18a and Fig. 4-18b respectively. The parameter $\alpha = 0.1$ and three values of n are 3, 9, and 21. In contrast to the piecewise linear models where the functions are only defined for $\mu \geq 1$ for the Ramberg Osgood model the functions are continuous for $\mu \geq 0$. The asymptotic value of $S(\mu)/\mu$ as $\mu \rightarrow \infty$ is zero. An explicit limit expression is not readily obtainable for the function $C(\mu)/\mu$ but by numerical integration for large values of μ it was observed that the asymptotic value tends to zero.

(c) Comparison of Analytic and Hysteretic Restoring Functions

The equation 4-21a for the steady-state response curves is written in terms of the functions $C(\mu)/\mu$ and $S(\mu)/\mu$. For any system with given restoring moment characteristics, it is only necessary to substitute their respective values for the type of restoring moment under consideration. The analysis would be considerably simplified if the hysteretic nature of the restoring moment could be replaced by some combination of analytic functions of the angle of rotation and its time-derivatives. Such an approach would be valid if the functions $C(\mu)/\mu$ and $S(\mu)/\mu$ of the analytic expression are similar in a quantitative and qualitative manner to those of the hysteretic functions they are meant to replace.

Fig. 4-19 compares the function $C(\mu)/\mu$ for the cubic softening spring, the bilinear model ($u = 0.4$) and the Ramberg-Osgood model ($\alpha = .1, n = 9$). Fig. 4-20 compares the function $S(\mu)/\mu$ for linear viscous damping $\dot{\phi}$, analytic hysteretic damping $\phi^2(\dot{\phi})$, the Ramberg-Osgood Model ($\alpha = .1, n = 9$) and the bilinear hysteretic model ($u = .4$). By comparing these figures it is seen that the nonlinear analytical expressions could duplicate the effect of the hysteretic action for μ less than two. For μ greater than two the curvature and

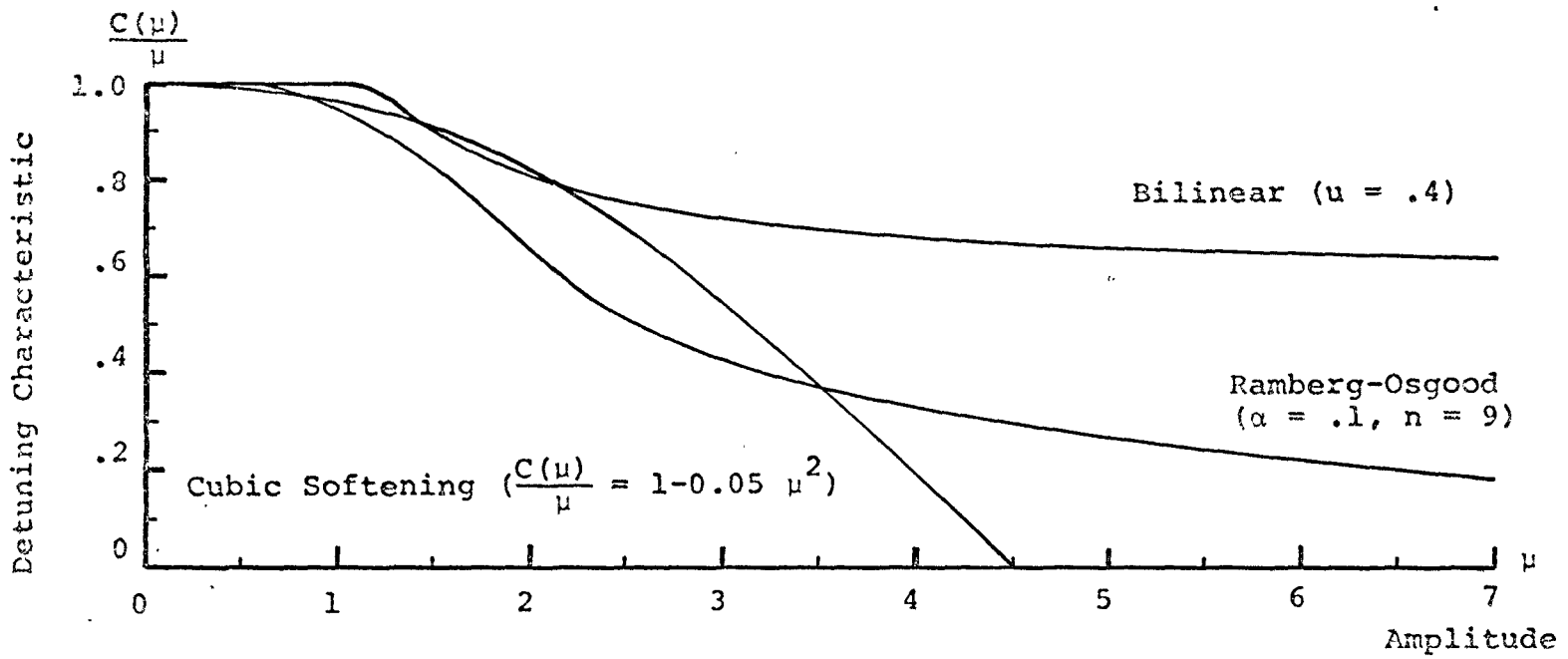


FIG. 4-19 COMPARISON OF ANALYTIC AND HYSTERETIC RESTORING FUNCTIONS ($\frac{C(\mu)}{\mu}$)

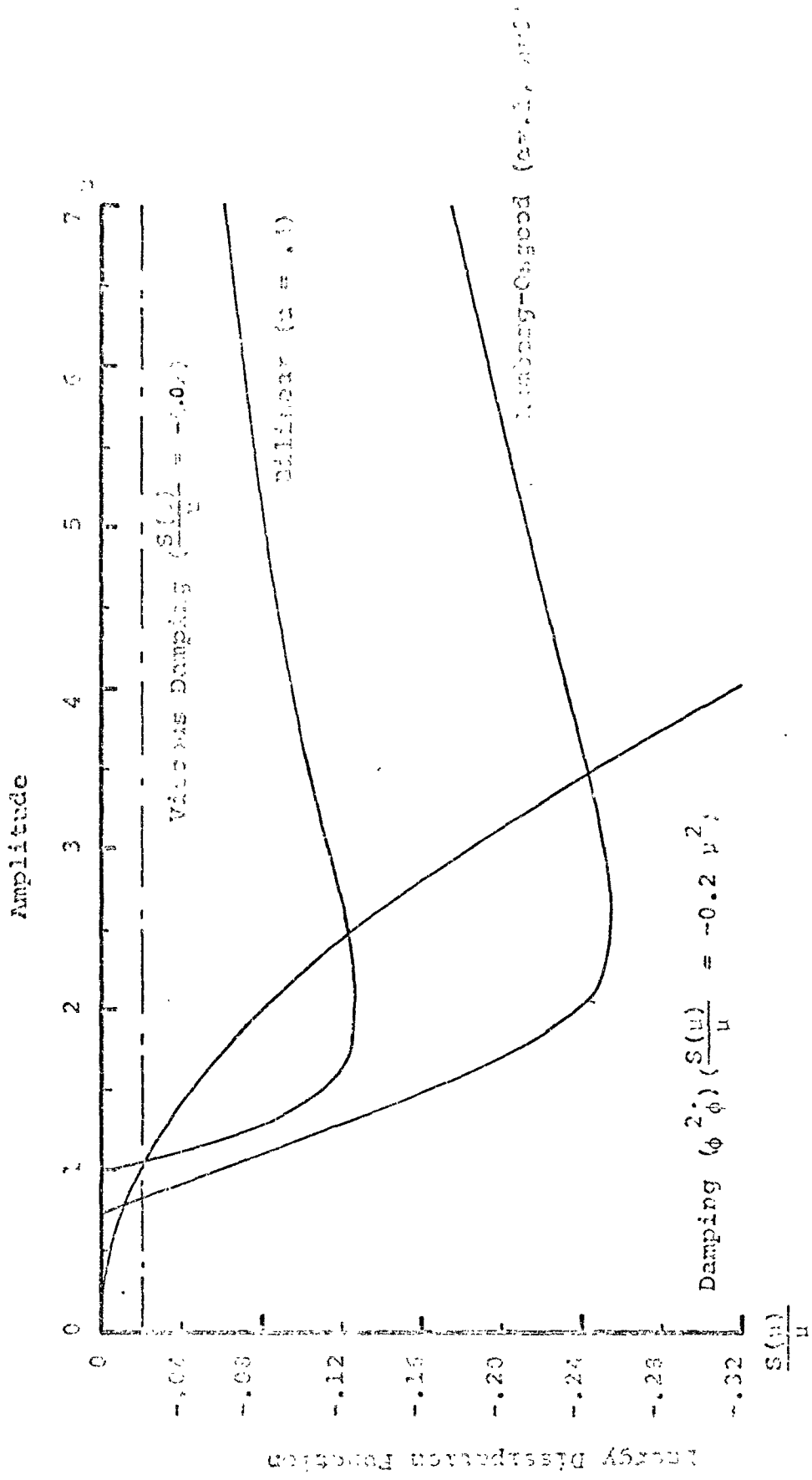


FIG. 4-20 COMPARISON OF ANALYTIC AND HYSTERETIC RESTORING FUNCTIONS ($\frac{S(u)}{u}$)

slope of the hysteretic functions change causing a qualitative difference which the nonlinear analytic functions can not duplicate.

How this difference manifests itself in the response curves can be seen by examining the steady-state equation 4-21a. The width of the response curve is governed by the expression under the square root sign and is

$$\Psi \equiv 4R^2 \left[\left(\frac{C(\mu)}{\mu} \right)^2 + \left(\frac{S(\mu)}{\mu} \right)^2 \right] - \left(\frac{S(\mu)}{\mu} \right)^2 \quad 4-52$$

Bounded response occurs when $\Psi \leq 0$. By comparing first the expressions for cubic restoring forces and analytic hysteretic damping, it is seen that bounded response always results provided that $R < 0.5$. For hysteretic damping the function Ψ is more complicated. Shown in Fig. 4-21 is a plot of Ψ for the bilinear hysteretic model for $R = 0.05$, $u = .2, .4, .6$ and $.8$.

The function Ψ and the corresponding amplitude-frequency steady-state curves are shown in Fig. 4-22 and Fig. 4-23 for the value $u = .2$ and $u = .4$ respectively. For $u = 0.2$, which represents a small hysteretic effect, Ψ is positive and the response curves do not close. The function Ψ approaches asymptotically the value

$$\Psi = 4R^2(1-u)^2 \quad 4-53$$

as $\mu \rightarrow \infty$.

Fig. 4-23 shows the response curves for $u = 0.4$. Here, the amplitude frequency plot can be divided into three zones. In zone A, bounded steady-state response is possible, in zone B no steady-state motion is possible and in zone C unbounded response is possible. The presence of zone C is a

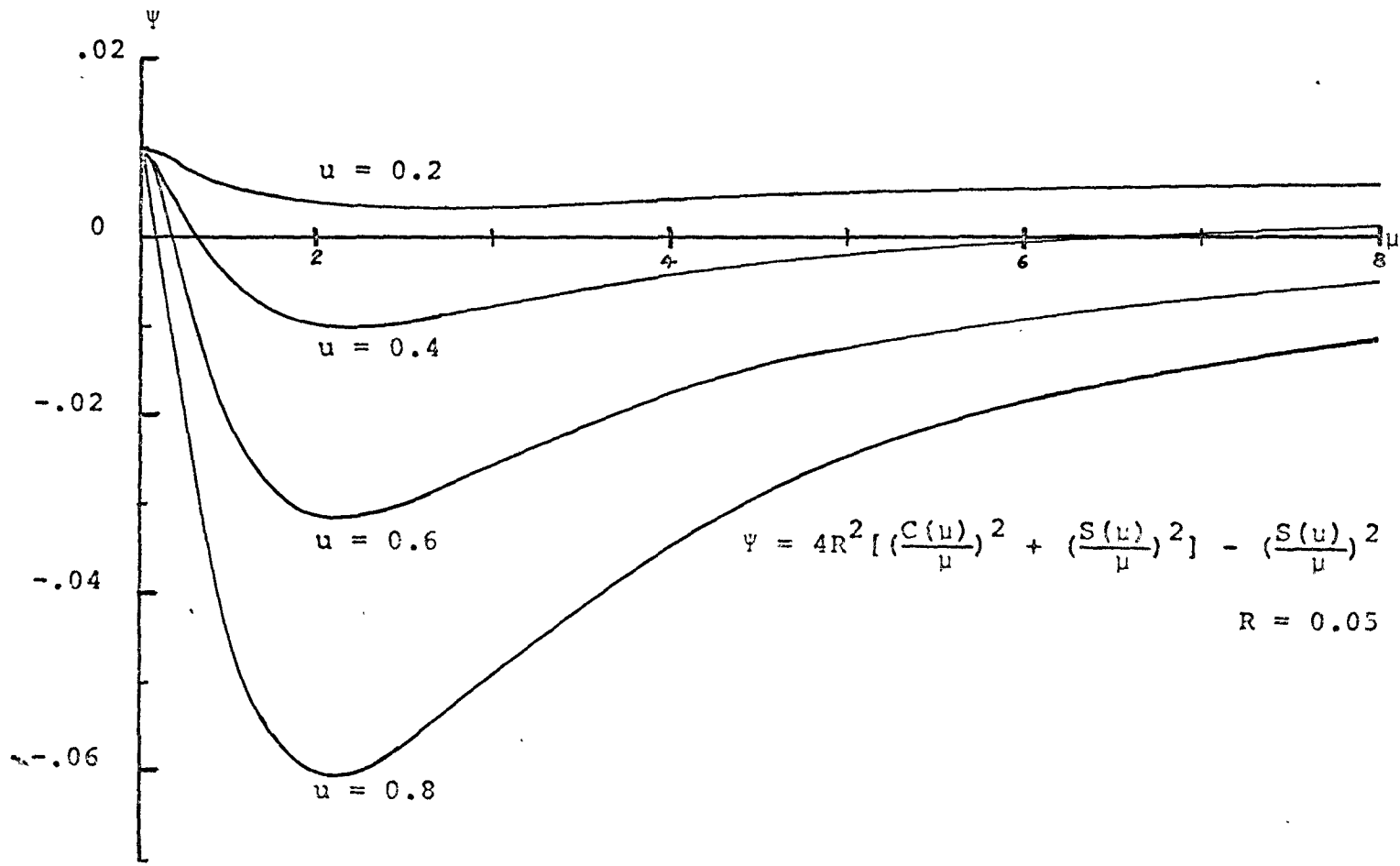


FIG. 4-21 PLOT OF THE FUNCTION ψ OF THE BILINEAR HYSTERETIC MODEL

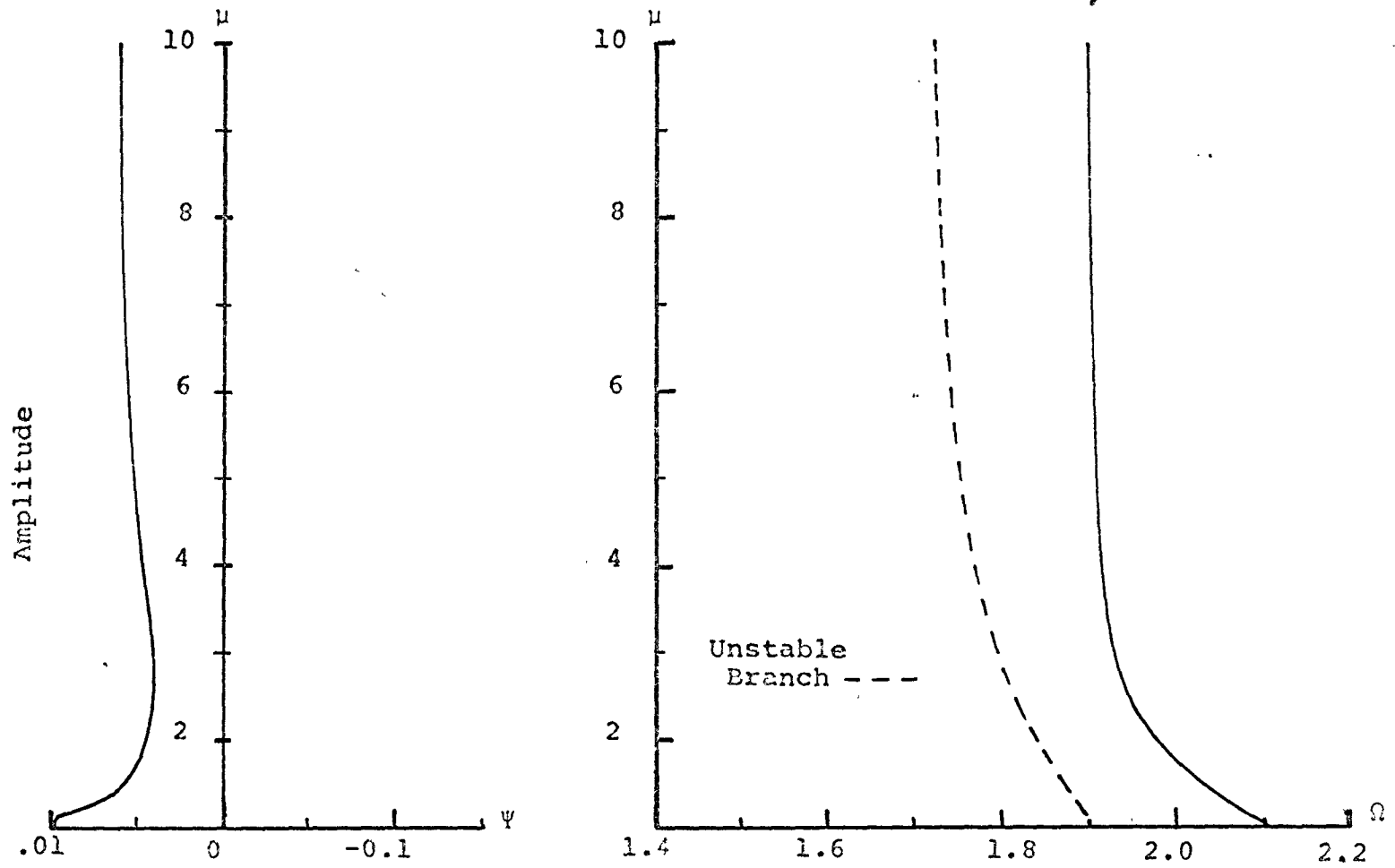


FIG. 4-22 STEADY-STATE RESPONSE CURVES AT LARGE AMPLITUDE LEVELS
 (Bilinear Hysteretic Model, $\mu = 0.2$)

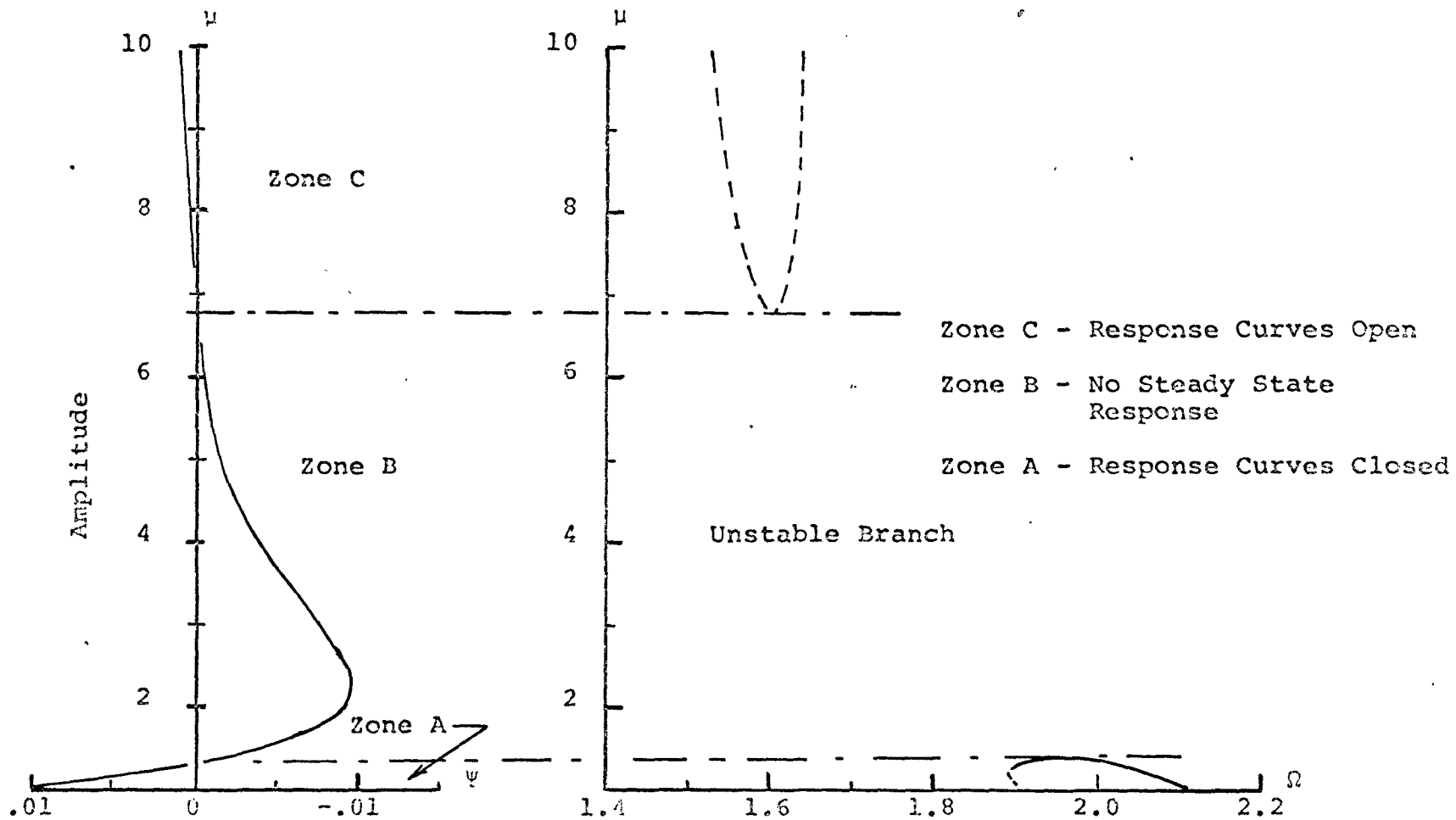


FIG. 4-23 STEADY-STATE RESPONSE CURVES AT LARGE AMPLITUDE LEVELS
(Bilinear Hysteretic Model, $u = 0.4$)

unique feature of the piecewise linear hysteretic systems. Zone C can only be reached by a large shock excitation. The response curves in zone C can be shown to be unstable branches; once the system has been shock excited into zone C infinite response is possible. As an amplitude $\mu > 6$ is uncommon in engineering materials the importance of zone C is questionable. It does however illustrate an additional qualitative difference between the analytic and hysteretic restoring functions.

4.11 Observations and Discussion

The following observations are based on the study of a single degree of freedom system under sinusoidal parametric excitation. Three types of hysteretic loops were considered: the bilinear, the double-bilinear and the Ramberg-Osgood hysteretic curve.

1. Unlike linear viscous damping, a linear system with hysteretic damping representation in the form of a hysteretic loop generally leads to bounded response during parametric resonance. Exceptional cases are systems with very narrow piece-wise linear hysteretic loops.
2. The damping mechanism of hysteretic elements is two-fold and is caused by (a) energy dissipation, (b) frequency detuning. The area of the hysteretic loop is a measure of the energy dissipation within the structure. This energy dissipation will attenuate high amplitude oscillations caused by impulse loading, such as shock excitation and prevent the build-up of large amplitude oscillations caused by a resonant state. The frequency of the responding system is amplitude dependent; this mechanism of frequency change in the responding structure causes a detuning of the driving frequency with the frequency of the system which in turn limits the

amplitude at which resonance can occur. It is these two properties that reinforce each other to prevent high-amplitude oscillations and cause bounded response.

3. At steady-state, the frequency of the responding oscillation is entrained to exactly one half the frequency of the external excitation. This synchronized response is possible because the influence of the external force depends on the motion of the system.

4. The accuracy of using the first and second approximation for the $\sin \phi$ function in the equation depends on the magnitude of $\bar{\phi}_{\max}$. If $\sin \bar{\phi} = \bar{\phi}$ is a good approximation, then the response curve based on the first approximation will provide accurate results. In the same spirit, if $\sin \bar{\phi} = \bar{\phi} - \bar{\phi}^3/6$ is a good approximation, the response curves based on the second order approximation analysis is useful. The advantage of using the first or second approximation of $\sin \phi$ instead of using the function $\sin \phi$ itself is that the response curves are expressible in terms of elementary functions so that the result can be obtained more easily. It should be noted that the first order approximation results overestimate the true response and may be treated as an upper bound.

5. The steady-state response curves lean towards the lower frequencies and thus exhibit a softening effect. Three cases of steady-state amplitude exist over a certain range of frequencies. Portions of the response curves are unstable branches and the "jump" phenomenon is possible within this range of frequencies. For small hysteretic effect the Ramberg-Osgood and double bilinear models have a very pronounced lean with a resulting large overhang. The overhang portion of the steady-state curves can be reached through

large initial disturbances. This means both the double-bilinear and the Ramberg-Osgood hysteretic systems can be parametrically excited into large amplitude oscillations outside the linear instability region.

6. For the Ramberg-Osgood hysteretic function there is no well defined yield point particularly if n is small. For this system the equations of motion must be considered hysteretic nonlinear for any finite initial disturbance. The double-bilinear model can not be excited into resonance outside the linear instability zone unless the initial conditions are such that the angle of rotation ϕ exceeds the yield point ϕ_y or $\mu > 1$. The Ramberg-Osgood Model, however, can be excited into resonance outside the linear instability zone for $\mu < 1$. This property should suggest caution when substituting piecewise linear hysteretic models for curved ones.

7. The double bilinear hysteretic system is less effective in limiting the growth of oscillations during parametric resonance than a similar system with bilinear or curved hysteretic characteristics.

8. The initial conditions do not affect the steady-state amplitude but only affect the time at which this steady-state takes place. The overshoot of the response amplitude over the steady-state value depends on the parameter u in the piecewise linear models and the parameter n in the curved model. For hysteretic loops approximating the elastic, perfectly plastic behaviour, or elastic with slight linearly hardening behaviour of materials, the overshoot is small and the steady-state amplitude can be taken as the maximum response of the system.

9. It appears to be impossible to duplicate the hysteretic

effect of structural systems by any combination of the common, non-linear analytic elements such as cubic damping $(\dot{x})^3$, "hysteretic" damping $x^2(\dot{x})$ and anti-symmetric restoring forces x^{2n-1} ($n > 1$).

10. Hysteretic damping does not affect the width of the parametric instability zone, whereas viscous damping can narrow the width of the instability zone, or completely eliminate the instability for a given parametric excitation. Therefore a threshold effect is not possible in hysteretic damped systems.

CHAPTER V

PARAMETRIC RESONANCE OF A TWO DEGREE OF FREEDOM BILINEAR HYSTERETIC SYSTEM

5.1 Introduction

The purpose of this chapter is to extend the analysis of the previous chapter to two degrees of freedom. Two degree of freedom systems under parametric resonance can have a one mode or two mode response depending on the system and the value of the external excitation frequency. A parametric type I resonance may occur when the frequency of the external excitation is approximately twice one of the natural frequencies and a parametric type II combination resonance may occur when the frequency is approximately equal to the sum or difference of two natural frequencies. The type I resonance causes a monofrequency response in one of the natural frequencies of the system, while the type II resonance causes a response in both natural frequencies.

A monofrequency response causes the hysteretic loops to trace out a steady-state pattern. In this case a general treatment of the two degree of freedom system with hysteretic constitutive relationships is possible. Previous analysis for forced resonance^[24, II] and self excited systems^[28] have made use of this fact. For the combination resonance the hysteretic loops do not, necessarily, trace out a steady state pattern. In this case the analysis must be restricted to special systems where a steady state pattern can be obtained.

It is the purpose of this chapter to analyse the response of a two degree of freedom system to parametric excitation. It consists of two parts: firstly, the monofrequency response of a general two degree of freedom system, secondly,

the two mode response of a particular two degree of freedom system. The bilinear hysteretic representation will be used for both parts.

5.2 Statement of the Problem

The equations of motion of a two degree of freedom system subjected to parametric excitation with bilinear hysteretic restoring elements considered in this chapter can be written as:

$$\begin{bmatrix} 1 & 0 \\ 0 & 1 \end{bmatrix} \begin{Bmatrix} \ddot{\phi}_1 \\ \ddot{\phi}_2 \end{Bmatrix} + \begin{bmatrix} b_{11} & b_{12} \\ b_{21} & b_{22} \end{bmatrix} \begin{Bmatrix} F_1 \\ F_2 \end{Bmatrix} + \epsilon \cos(\Omega t) \begin{bmatrix} c_{11} & c_{12} \\ c_{21} & c_{22} \end{bmatrix} \begin{Bmatrix} \phi_1 \\ \phi_2 \end{Bmatrix} = 0$$

5-1

The functions $F_j(\phi_j, u_j, t)$ represent the hysteretic, nonlinear force-displacement relationships. The functions are such that as $u_j \rightarrow 0$, $F_j(\phi_j, u_j, t) \rightarrow \phi_j$. The relationship between F_j and ϕ_j is shown in the Appendix, Fig. A-1.

The natural frequencies of the system are obtained by linearising the F_j terms i.e. by setting $u_j = 0$, and solving the eigenvalue problem

$$|[b_{ij}] - \omega^2[I]| = 0 \quad 5-2$$

Let $x_{1,2}$ be the normal co-ordinates corresponding to the diagonalized system

$$[a_{ij}]^{-1} [b_{ij}] [a_{ij}] = D_{\text{diag}}(\omega_j^2) \quad 5-3$$

Then

$$\phi_j = a_{j1}x_1 + a_{j2}x_2 \quad 5-4$$

where a_{ij} is the i^{th} component of the j^{th} normalized eigenvector.

Returning to equation 5-1 and considering the non-linear functions F_j as elements of the vector f ,

$$\text{i.e. } \{f\} \equiv \text{col}[F_1(a_{11}x_1 + a_{12}x_2), F_2(a_{21}x_1 + a_{22}x_2)]$$

the system is converted to normal co-ordinates by the transformation:

$$\begin{aligned} [a_{ij}]^{-1}[I][a_{ij}]\{\ddot{x}\} + [a_{ij}]^{-1}[b_{ij}]\{f\} \\ + \epsilon \cos(\Omega t) [a_{ij}]^{-1}[c_{ij}][a_{ij}]\{x\} = 0 \quad 5-5 \end{aligned}$$

with the result that the hysteretic elements are now a function of the two normal co-ordinates. In Chapter II and Chapter III the F_j were analytic functions of their arguments and the method of averaging could be applied directly. If the arguments of F_j are almost periodic the hysteretic elements will not trace out a steady-state hysteresis pattern with respect to their arguments. In this case the averaging process is not clearly defined.

5.3 Monofrequency Response

(a) The Equations of Motion

In terms of the normal co-ordinates x_1 and x_2 the equations of motion are:

$$\begin{aligned} \ddot{x}_1 + B_{11}F_1(a_{11}x_1 + a_{12}x_2) + B_{12}F_2(a_{21}x_1 + a_{22}x_2) \\ + \cos(\Omega t) [C_{11}x_1 + C_{12}x_2] = 0 \quad 5-6a \end{aligned}$$

$$\ddot{x}_2 + B_{21}F_1(a_{11}x_1 + a_{12}x_2) + B_{22}F_2(a_{21}x_1 + a_{22}x_2) + \cos(\Omega t)[C_{21}x_1 + C_{22}x_2] = 0 \quad 5-6b$$

$$\text{where } [B_{ij}] = [a_{ij}]^{-1} [b_{ij}] \quad 5-7a$$

$$[C_{ij}] = [a_{ij}]^{-1} [c_{ij}] [a_{ij}] \quad 5-7b$$

For the linearized system, $u_1 = u_2 = 0$,

$$F_1(a_{11}x_1 + a_{12}x_2) = a_{11}x_1 + a_{12}x_2 \quad 5-8a$$

$$F_2(a_{21}x_1 + a_{22}x_2) = a_{21}x_1 + a_{22}x_2 \quad 5-8b$$

$$\text{and } B_{11}F_1 + B_{12}F_2 = \omega_1^2 x_1 \quad 5-8c$$

$$B_{21}F_1 + B_{22}F_2 = \omega_2^2 x_2 \quad 5-8d$$

Substituting the results of Equation 5-8 into Equation 5-6 it is seen that for the linearized system the coupling between the restoring forces has been removed. For $\Omega \approx 2\omega_1$ a predominantly monofrequency response in the first mode will exist and the normal co-ordinates x_2 is not expected to be excited. Assuming that x_2 is not excited, the analysis can be concentrated on Equation 5-6a alone by setting $x_2 = 0$. It is reasonable to assume that for a system with

hysteretic elements the value of x_2 will also be small and can be set equal to zero.

The approximate analysis is now based on the equation

$$\ddot{x}_1 + B_{11}F_1(a_{11}x_1) + B_{12}F_2(a_{21}x_1) + C_{11} \cos(\Omega t)x_1 = 0 \quad 5-9$$

The correctness of the approximation ($x_2 = 0$) will be verified later by the direct numerical integration of the system 5-6a and 5-6b.

Substituting

$$\tau = \omega_1 t \quad 5-10a$$

$$\bar{B}_{11} = B_{11}/\omega_1^2 \quad 5-10b$$

$$\bar{B}_{12} = B_{12}/\omega_1^2 \quad 5-10c$$

$$\bar{C}_{11} = C_{11}/\omega_1^2 \quad \eta = \Omega/\omega_1 \quad 5-10d,e$$

the equation 5-9 can be written in nondimensional parameters as

$$x_1'' + \bar{B}_{11}F_1 + \bar{B}_{12}F_2 + \bar{C}_{11} \cos(\eta\tau) x_1 = 0 \quad 5-11$$

The approximation solution of equation 5-11 now follows along the procedure outlined in Chapter IV.

$$\text{Let } x_1 = Q_1(\tau) \cos\left(\frac{\eta}{2}\tau + \theta_1\right) \quad 5-12a$$

$$\equiv Q_1 \cos \psi_1 \quad 5-12b$$

$$x'_1 = - Q_1 \left(\frac{\eta}{2}\right) \sin \psi_1 \quad 5-13$$

Equation 5-11 can now be transformed to a system of first order differential equations:

$$\begin{bmatrix} \cos \psi_1 & - Q_1 \sin \psi_1 \\ - \frac{\eta}{2} \sin \psi_1 & - Q_1 \frac{\eta}{2} \cos \psi_1 \end{bmatrix} \begin{bmatrix} Q'_1 \\ \theta'_1 \end{bmatrix} = \begin{bmatrix} 0 \\ -g \end{bmatrix} \quad 5-14$$

$$g = - Q_1 \left(\frac{\eta}{2}\right)^2 \cos \psi_1 + \bar{B}_{11} F_1(a_{11} x_1) + \bar{B}_{12} F_2(a_{21} x_1) \quad 5-15$$

Further simplification of 5-14 leads to

$$Q'_1 = - Q_1 \left(\frac{\eta}{2}\right) \cos \psi_1 \sin \psi_1 + \frac{2}{\eta} \bar{B}_{11} F_1(a_{11} x_1) \sin \psi_1 \quad 5-16$$

$$+ \frac{2}{\eta} \bar{B}_{12} F_2(a_{21} x_1) \sin \psi_1 + \frac{2}{\eta} \bar{C}_{11} \cos(\eta \tau) Q_1 \cos \psi_1 \sin \psi_1$$

$$\theta'_1 = - \frac{\eta}{2} \cos^2 \psi_1 + \left\{ \frac{2}{\eta} \frac{\bar{B}_{11}}{Q_1} F_1(a_{11} x_1) + \frac{2}{\eta} \frac{\bar{B}_{12}}{Q_1} F_2(a_{21} x_1) \right\} \cos \psi_1$$

$$+ \frac{2}{\eta} \bar{C}_{11} \cos(\eta \tau) \cos \psi_1 \sin^2 \psi_1 \quad 5-17$$

The averaged equations are:

$$nQ'_1 = \bar{B}_{11} s_1(Q_1) + \bar{B}_{12} s_2(Q_2) + \frac{\bar{C}_{11}}{2} Q_1 \sin 2\theta_1 \quad 5-18$$

$$nQ_1 \theta'_1 = -\frac{n^2}{4} + \bar{B}_{11} c_1(Q_1) + \bar{B}_{12} c_2(Q_2) + \frac{\bar{C}_{11}}{2} \cos 2\theta_1 \quad 5-19$$

where the symbols $S_1(Q_1)$, $S_2(Q_2)$, $C_1(Q_1)$ and $C_2(Q_2)$ represent the integrals

$$S_1(Q_1) = \frac{1}{\pi} \int_0^{2\pi} F_1(a_{11}Q_1 \cos \psi_1) \sin \psi_1 d\psi_1 \quad 5-20a$$

$$S_2(Q_2) = \frac{1}{\pi} \int_0^{2\pi} F_2(a_{21}Q_1 \cos \psi_1) \sin \psi_1 d\psi_1 \quad 5-20b$$

$$C_1(Q_1) = \frac{1}{\pi} \int_0^{2\pi} F_1(a_{11}Q_1 \cos \psi_1) \cos \psi_1 d\psi_1 \quad 5-20c$$

$$C_2(Q_2) = \frac{1}{\pi} \int_0^{2\pi} F_2(a_{21}Q_1 \cos \psi_1) \cos \psi_1 d\psi_1 \quad 5-20d$$

The steady state solution can be obtained by setting $Q'_1 = \theta'_1 = 0$ in Equation 5-18,19 and solving the resulting algebraic equations in terms of the steady-state variables Q°_1 and θ°_1 . The transient response can be obtained by direct numerical integration of the system 5-18, 5-19.

In order to determine the functions $S_j(Q_j)$, $C_j(Q_j)$, ($j = 1,2$) it is necessary to specify the form of the hysteretic characteristics. An example of a system with bilinear hysteretic restoring forces will be given to illustrate the technique involved in obtaining the response of a two degree of freedom to parametric resonance.

Consider a two degree of freedom hysteretic system given in terms of the generalized co-ordinates by,

$$\begin{bmatrix} 1 & 0 \\ 0 & 1 \end{bmatrix} \begin{Bmatrix} \phi_1 \\ \phi_2 \end{Bmatrix} + \begin{bmatrix} 2 & -1 \\ -1 & 2 \end{bmatrix} \begin{Bmatrix} F_1 \\ F_2 \end{Bmatrix} + 0.1\Omega^2 \begin{bmatrix} .7 & .1 \\ .1 & .1 \end{bmatrix} \begin{Bmatrix} \phi_1 \\ \phi_2 \end{Bmatrix} \cos \Omega t = 0 \quad 5-21$$

The functions $F_1(\phi_1, u_1)$, $F_2(\phi_2, u_2)$ are bilinear hysteretic functions defined in the Appendix by Fig. A-1. Setting $u_1 = u_2 = 0$, the natural frequencies of the linear system are

$$\omega_1 = 1 \quad 5-22a$$

$$\omega_2 = \sqrt{3} \quad 5-22b$$

The modal matrix can be written as

$$a_{ij} = \frac{1}{\sqrt{2}} \begin{bmatrix} 1 & 1 \\ 1 & -1 \end{bmatrix} \quad 5-23$$

and it is seen that the modal matrix is orthonormal

$$a_{ij}^{-1} = a_{ij}^T \quad 5-24$$

In terms of the normal co-ordinates, the generalized co-ordinates are given by equation 5-4

$$\phi_1 = \frac{1}{\sqrt{2}} (x_1 + x_2) \quad 5-24a$$

$$\phi_2 = \frac{1}{\sqrt{2}} (x_1 - x_2) \quad 5-24b$$

Applying the transformation of Equation 5-5 and making use of the change of variables of Equation 5-10 the system of equations 5-21 in terms of normal co-ordinates is

$$\begin{aligned} \ddot{x}_1 + \frac{1}{\sqrt{2}} [F_1[\frac{1}{\sqrt{2}}(x_1 + x_2)] + F_2[\frac{1}{\sqrt{2}}(x_1 - x_2)]] \\ + \eta^2 \cos(\eta\tau) [.05 x_1 + .03 x_2] = 0 \end{aligned} \quad 5-25a$$

$$\begin{aligned} \ddot{x}_2 + \frac{3}{\sqrt{2}} [F_1[\frac{1}{\sqrt{2}}(x_1 + x_2)] - F_2[\frac{1}{\sqrt{2}}(x_1 - x_2)]] \\ + \eta^2 \cos(\eta\tau) [.03 x_1 + .03 x_2] = 0 \end{aligned} \quad 5-25b$$

Assuming only the first mode is excited, the system to be analysed is

$$\ddot{x}_1 + \frac{1}{\sqrt{2}} [F_1(x_1/\sqrt{2}) + F_2(x_1/\sqrt{2})] + .05 \eta^2 \cos(\eta\tau)x_1 = 0 \quad 5-26$$

(b) Steady-State Solution

The steady state solutions can be obtained from the system of equations 5-18,19, where $\bar{C}_{11} = .05\eta^2$ and $\bar{B}_{11} = \bar{B}_{12} = 1/\sqrt{2}$. The steady state equations are

$$\frac{1}{\sqrt{2}} [S_1(Q^\circ_1) + S_2(Q^\circ_1)] = - \frac{.05}{2} \eta^2 Q^\circ_1 \sin 2\theta^\circ_1 \quad 5-26a$$

$$\frac{\eta^2 Q_1^\circ}{4} - \frac{1}{\sqrt{2}} [c_1(Q_1^\circ) + c_2(Q_1^\circ)] = \frac{.05}{2} \eta^2 Q_1^\circ \cos 2\theta_2 \quad 5-26b$$

with

$$s(Q^\circ) = \frac{1}{\sqrt{2}} [s_1(Q_1^\circ/\sqrt{2}) + s_2(Q_1^\circ/\sqrt{2})] \quad 5-27a$$

$$c(Q^\circ) = \frac{1}{\sqrt{2}} [c_1(Q_1^\circ/\sqrt{2}) + c_2(Q_1^\circ/\sqrt{2})] \quad 5-27b$$

the equations 5-26 are of identical form to the steady state equations of Chapter IV.

$$\Omega^2 = \frac{4 \frac{C(Q^\circ)}{Q^\circ} \pm 4 \sqrt{4R^2 \left[\left(\frac{C(Q^\circ)}{Q^\circ} \right)^2 + \left(\frac{S(Q^\circ)}{Q^\circ} \right)^2 \right] - \left(\frac{S(Q^\circ)}{Q^\circ} \right)^2}}{(1 - 4R^2)} \quad 5-28$$

where $R = 0.05$.

In Fig. 5-1 the steady-state response is plotted in terms of the nondimensional amplitude $\mu_1 = Q_1^\circ/\phi_{y1}$ against the non-dimensional frequency η . The value of u_1 of the hysteretic loop F_1 is kept constant at $u_1 = 0.3$, but the value of u_2 of the hysteretic loop F_2 is varied from $u_2 = 0, .3, .5$ and 1.0 . The ratio of the yield points is taken as $\phi_{y2}/\phi_{y1} = 2.0$.

It is seen that three separate regions of the response curves exist. The first region correspond to the linearized equation where the amplitude $Q_1^\circ/\sqrt{2}$ is less than the lowest value of the two yield points of F_1 and F_2 . The second region is that region where one of the elements F_1 or F_2 has reached it's yield point, and the third region is where both F_1 and F_2

have exceeded their yield points.

Consider the case where only the first element F_1 displays a hysteretic property with $u_1 = .3$ and F_2 is a linear function. In this case unbounded response is possible. The range of η for which unbounded response is possible can be determined from Equation 5-28 by using the large amplitude approximations for $S(Q^\circ)/Q^\circ$ and $C(Q^\circ)/Q^\circ$, namely,

$$\frac{S(Q^\circ)}{Q^\circ} = 0 \quad 5-29a$$

$$\frac{C(Q^\circ)}{Q^\circ} = 1 - 0.5 u_1 \quad 5-29b$$

Therefore, unbounded response following a small initial disturbance is possible in the range of frequencies

$$\frac{2}{\sqrt{1+2R}} < \eta < \frac{2}{\sqrt{1-2R}} \sqrt{1 - 0.5 u_1} \quad 5-30a$$

For the numerical example, $R = 0.05$, $u_1 = 0.3$

$$1.908 < \eta < 1.94 \quad 5-30b$$

With only one yielding element large amplitude response is possible. In fact, as the analysis has shown, unbounded response is possible. By introducing the second yield element $u_2 \neq 0.0$ the resonant amplitude can be reduced considerably. A steady-state is now possible for a short excursion into the yield range of the element F_2 .

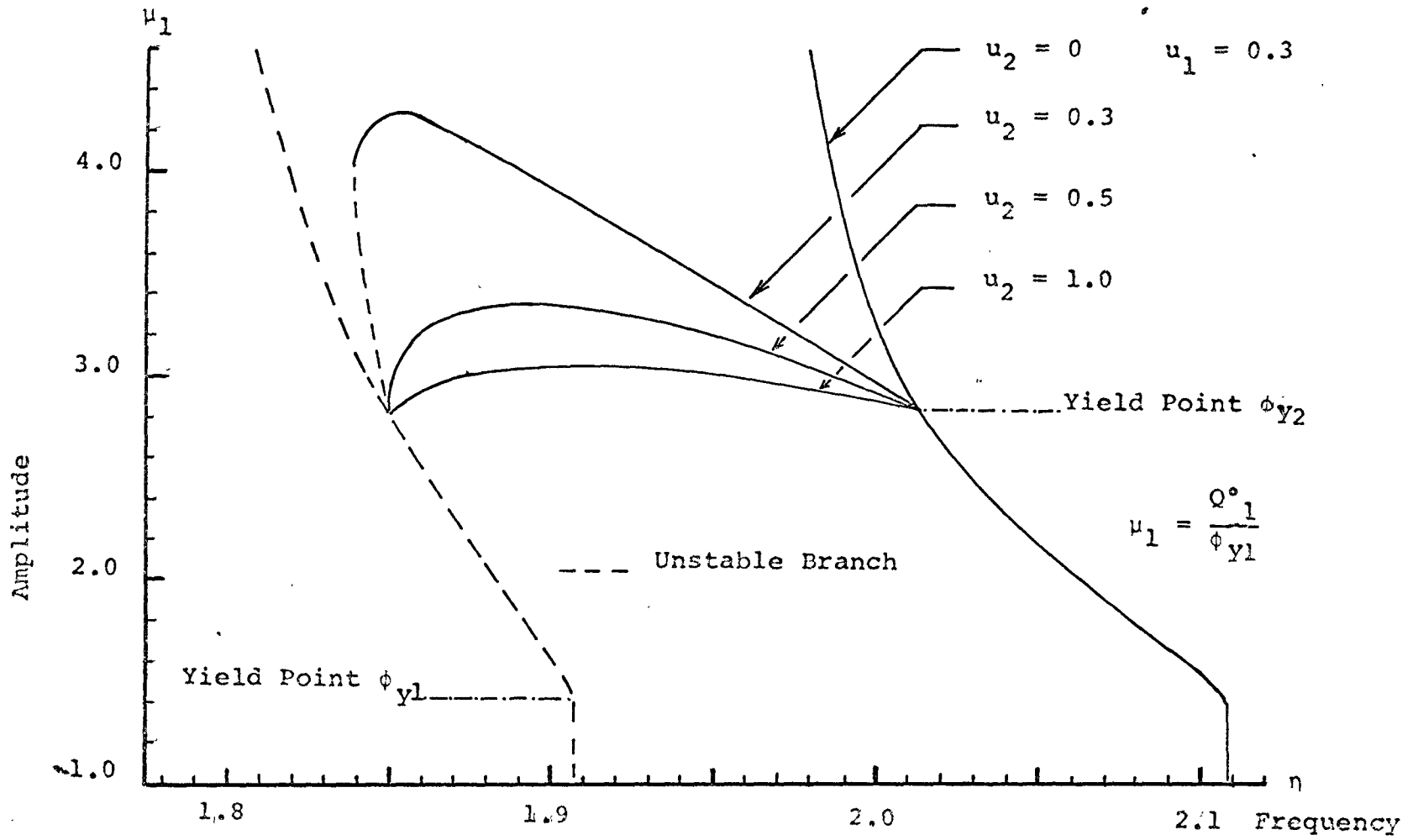


FIG. 5-1 STEADY-STATE RESPONSE - ONE MODE APPROXIMATION ($\phi_{y2}/\phi_{y1} = 2$)

(c) Transient Response

The key assumptions of the steady-state analysis carried out in the previous section were (a) that only one mode x_1 participates in the resonant oscillations and (b) that a monofrequency response occurs. It is now necessary to verify these assumptions. This is done by comparing the time history response of the averaged and exact equations of the two frequencies $\eta = 1.95$ and $\eta = 2.05$. The first frequency corresponds to the case where both elements F_1 and F_2 have entered the hysteretic range and the second frequency corresponds to the case where only element F_1 has entered the yield range.

The transient response of the averaged equation is obtained by integrating the system of equations 5-18,19. The transient response of the exact equations is obtained by integrating the system of equations 5-25a,b. The results of the averaged equations are shown in Fig. 5.2 and the results of the exact integration in Fig. 5-3 for the parameters $\eta = 1.95$, $u_1 = 0.3$, $u_2 = 0.5$. The yield point of the hysteretic element F_2 is taken to be twice the value of the yield point F_1 . To obtain a consistent measure of amplitude, the amplitude of the normal modes x_1 and x_2 are plotted in terms of the ratio's $\mu_1 = x_1/\phi_{y1}$, $\mu_2 = x_2/\phi_{y1}$.

Fig. 5-3 shows that a monofrequency response does indeed take place once the transient phase of oscillations has passed. The response of the exact integration can now be compared to the solution obtained by the method of averaging. For the exact integration $\mu_1 = 3.6$, $\mu_2 = 0.5$. This compares to $\mu_1 = 3.2$, $\mu_2 = 0$ of the approximate solution. Fig. 5-4 and Fig. 5-5 show similar time history comparison response at $\Omega = 2.05$. The steady-state amplitude of the approximate solution $\mu_1 = 2.16$ and compares to $\mu_1 = 2.10$ of the exact integration. The mode μ_2 does not appear to be excited and

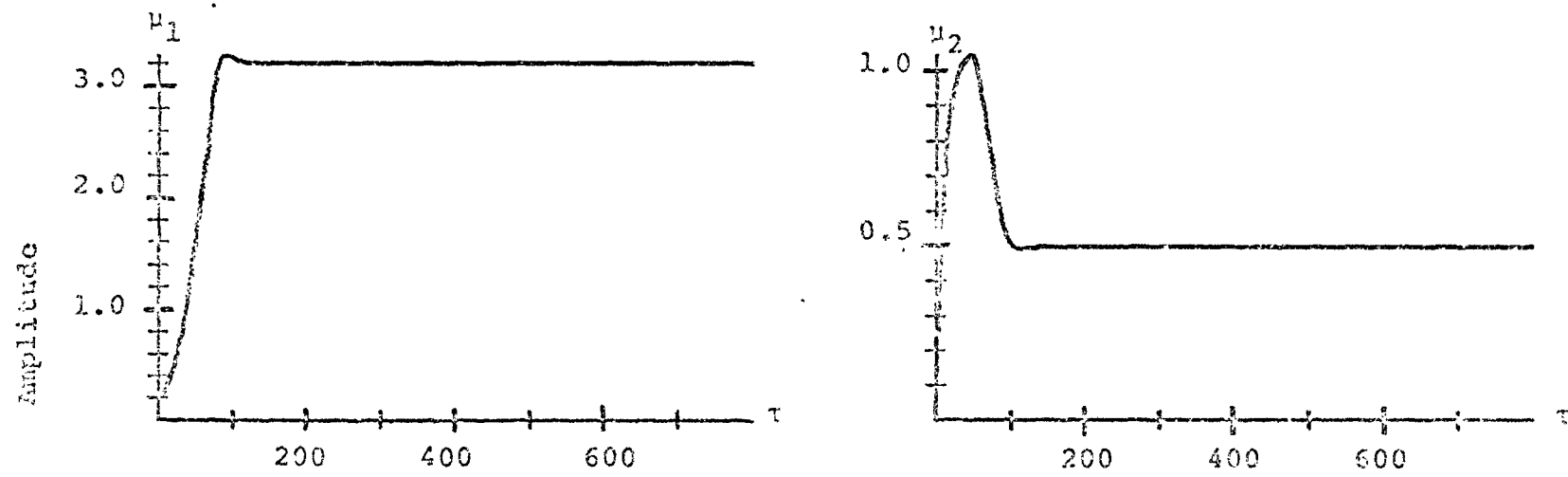


FIG. 5-2 TIME HISTORY RESPONSE OF AVERAGED EQUATIONS: $\eta = 1.95$

$$(\phi_{y2}/\phi_{y1} = 2, u_1 = 0.3, u_2 = 0.5)$$

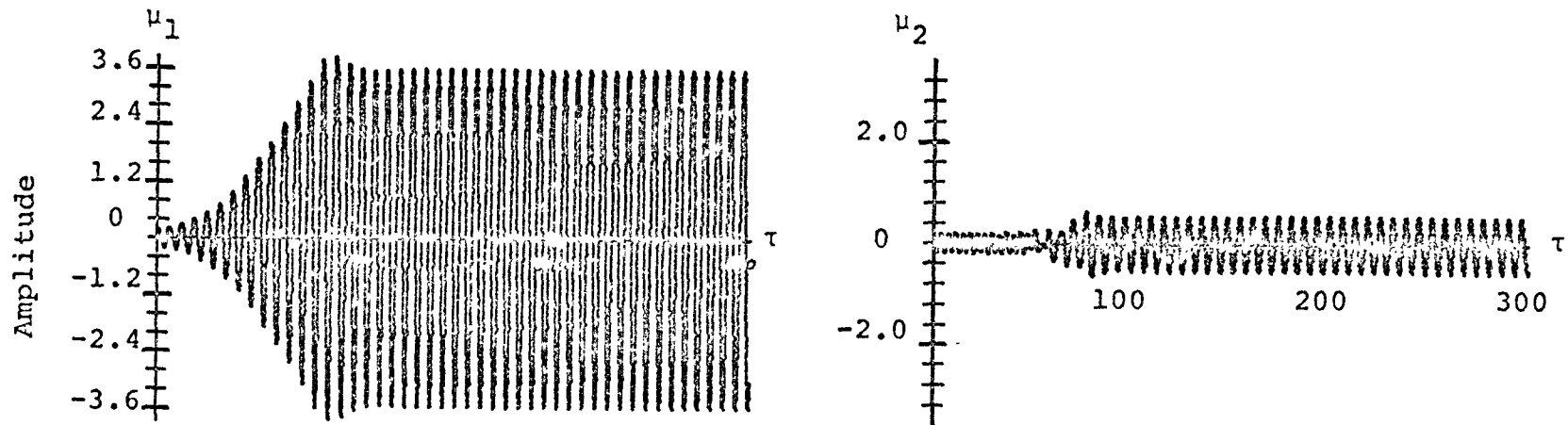


FIG. 5-3 TIME HISTORY RESPONSE EXACT NUMERICAL INTEGRATION
 ($\eta = 1.95, \phi_{y2}/\phi_{y1} = 2, u_1 = 0.3, u_2 = 0.5$)

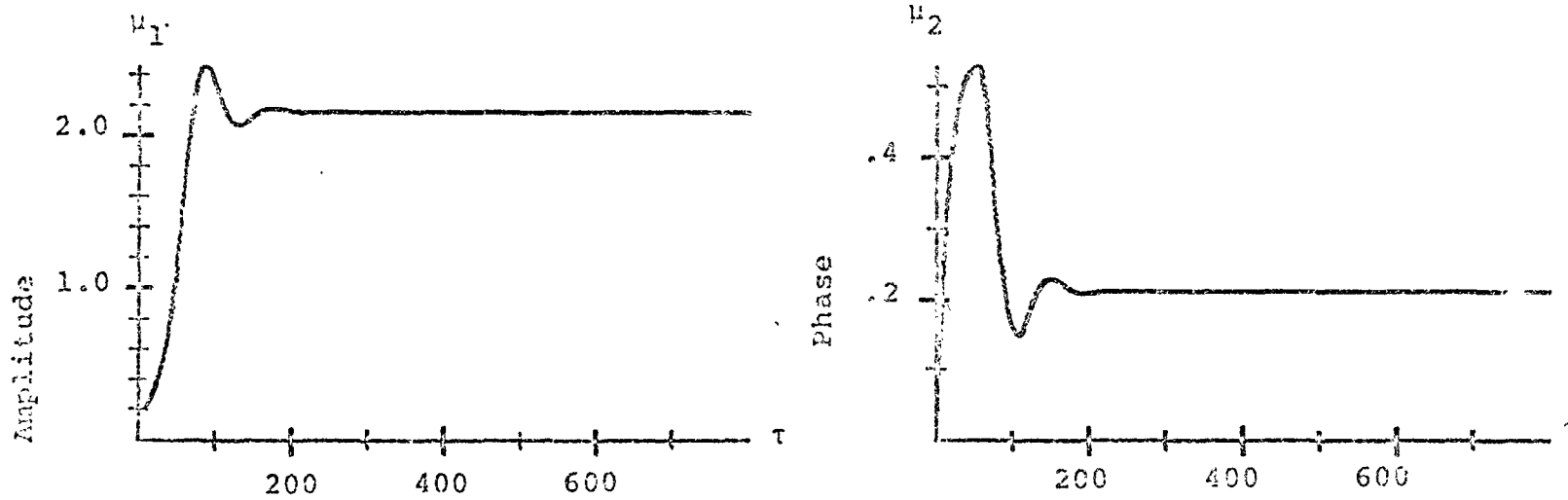


FIG. 5-4 TIME HISTORY RESPONSE OF AVERAGED EQUATIONS: $\Omega = 2.05$

$$(\phi_{y2}/\phi_{y1} = 2, u_1 = 0.3, u_2 = 0.5)$$

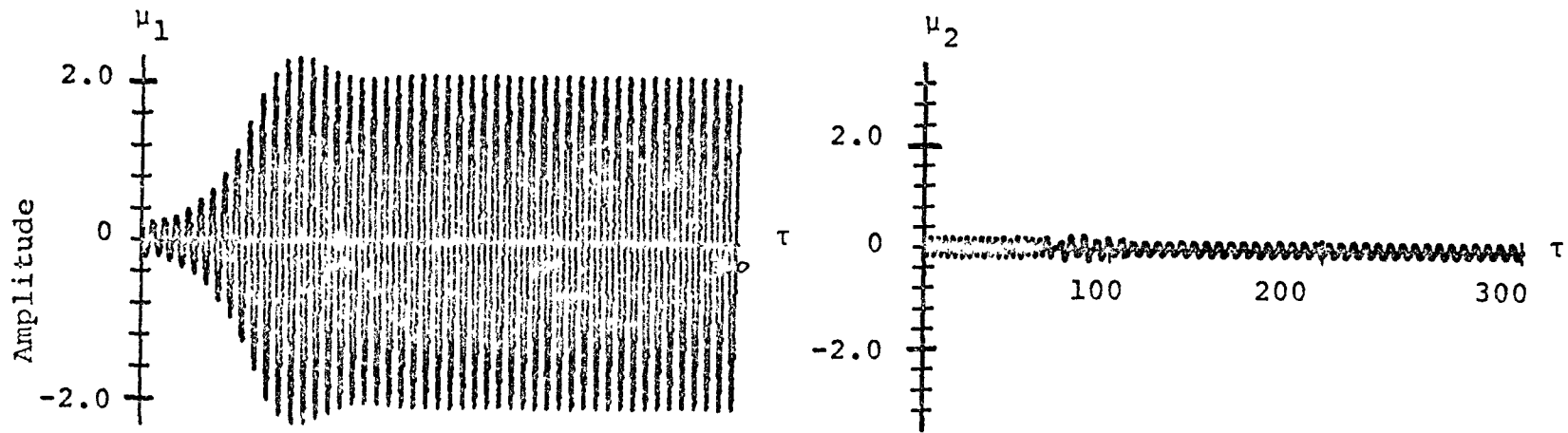


FIG. 5-5 TIME HISTORY RESPONSE EXACT NUMERICAL INTEGRATION

($\eta = 2.05$, $\phi_{y2}/\phi_{y1} = 2$, $u_1 = 0.3$, $u_2 = 0.5$)

only reflects a small background forced oscillation.

The results of this numerical example can be summarized as follows: (a) A one mode approximation allows a relatively simple determination of the parametric instability zone, steady-state and transient response. (b) The assumption of a monofrequency response is correct. (c) A one mode approximation can obtain the correct order of magnitude of the steady-state amplitudes.

5.4 Combination Resonance

(a) Equations of Motion

The system 5-1 subjected to combination resonance will respond with large amplitude oscillations in both normal modes. This causes the nonlinear hysteretic elements to be functions of almost periodic arguments and makes a general analysis of the two-degree of freedom system under combination resonance difficult. However a special system can be obtained from Equation 5-1 in which the arguments of the hysteretic elements are each a function of only one normal co-ordinate. Setting $b_{12} = b_{21} = c_{11} = c_{22} = 0$ and $b_{11} = \omega_1^2$, $b_{22} = \omega_2^2$, $c_{12} = -\epsilon b_1$, $c_{21} = -\epsilon b_2$ the equations of motion are:

$$x_1 + \omega_1^2 F_1(x_1) - \epsilon b_1 x_2 \cos(\Omega t) = 0 \quad 5-31a$$

$$x_2 + \omega_2^2 F_2(x_2) - \epsilon b_2 x_1 \cos(\Omega t) = 0 \quad 5-31b$$

Equation 5-31 corresponds to the problem of Chapter II with the exception that there is no nonlinear coupling. As was shown, the system 5-31 can be excited into combination resonance if $\Omega \approx \omega_1 + \omega_2$.

The bilinear hysteretic functions are specified by the

value of their yield points x_{y1} , x_{y2} and yielding parameters u_1 and u_2 . To study the effect of two different yield points, it is convenient to carry out the change of variables

$\mu_1 = x_1/x_{y1}$, $\mu_2 = x/x_{y2}$ in equations 5-31, i.e.

$$\mu_1 + \omega_1^2 \bar{F}_1(\mu_1) - \epsilon b_1 r \mu_2 \cos(\Omega t) = 0 \quad 5-32a$$

$$\mu_2 + \omega_2^2 \bar{F}_2(\mu_2) - \frac{\epsilon b_2}{r} \mu_1 \cos(\Omega t) = 0 \quad 5-32b$$

where

$$\bar{F}_1(\mu_1) = F_1(x_1)/x_{y1} \quad 5-33a$$

$$\bar{F}_2(\mu_2) = F_2(x_2)/x_{y2} \quad 5-33b$$

$$r = x_{y2}/x_{y1} \quad 5-33c$$

$$\text{Let} \quad \tau = \omega t \quad 5-34a$$

$$\Omega = \Omega^\circ (1-\lambda) \quad 5-34b$$

$$K_1 = \omega_1/\Omega^\circ \quad 5-34c$$

$$K_2 = \omega_2/\Omega^\circ \quad 5-34d$$

Substituting the change of variables of Equation 5-34

into Equation 5-32 there results,

$$\ddot{\mu}_1 + \kappa_1^2 [1+2\lambda] \bar{F}_1(\mu_1) - \frac{\epsilon b_1 r}{\omega^2} \mu_2 \cos \tau = 0 \quad 5-35a$$

$$\ddot{\mu}_2 + \kappa_2^2 [1+2\lambda] \bar{F}_2(\mu_2) - \frac{\epsilon b_2}{r\omega^2} \mu_1 \cos \tau = 0 \quad 5-35b$$

where primes denote differentiation with respect to the non-dimensional time τ and λ represents a small detuning of the external excitation frequency.

Seeking a response

$$\mu_j(\tau) = Q_j(\tau) \cos (K_j \tau + \theta_j(\tau)) \quad 5-36a$$

$$\equiv Q_j \cos \psi_j \quad (j = 1, 2)$$

$$\mu'_j(\tau) = -Q_j K_j \sin \psi_j \quad 5-36b$$

and substituting into 5-35, the system of second order differential equations is transformed into the system of first order equations.

$$\begin{bmatrix} \cos \psi_j & -Q_j \sin \psi_j \\ -K_j \sin \psi_j & -Q_j K_j \cos \psi_j \end{bmatrix} \begin{Bmatrix} Q'_j \\ \theta'_j \end{Bmatrix} = \begin{Bmatrix} 0 \\ -g_j \end{Bmatrix} \quad 5-37a$$

Where:

$$g_j = -Q_j K_j^2 \cos \psi_j + K_j^2 [1+2\lambda] \bar{F}_j - \frac{\epsilon b_j}{r \omega^2} Q_m \cos \psi_m \cos \tau \quad 5-37b$$

$$(j = 1, 2; m = 1, 2; j \neq m)$$

(b) The Averaged Equations

To obtain an approximate solution of the system 5-37 the method of averaging is applied. The averaged equations are:

$$Q'_1 = K_1 [1+2\lambda] \frac{S_1(Q_1)}{2} - \frac{B_1 r}{4K_1} Q_2 \sin(\theta_1 + \theta_2) \quad 5-38a$$

$$Q'_2 = K_2 [1+2\lambda] \frac{S_2(Q_2)}{2} - \frac{B_2}{4K_2} \frac{Q_1}{r} \sin(\theta_1 + \theta_2) \quad 5-38b$$

$$Q_1 \theta'_1 = -\frac{K_1 Q_1}{2} + K_1 [1+2\lambda] \frac{C_1(Q_1)}{2} - \frac{B_1 r}{4K_1} Q_2 \cos(\theta_1 + \theta_2) \quad 5-38c$$

$$Q_2 \theta'_2 = -\frac{K_2 Q_2}{2} + K_2 [1+2\lambda] \frac{C_2(Q_2)}{2} - \frac{B_2 Q_1}{4K_2 r} \cos(\theta_1 + \theta_2) \quad 5-38d$$

where:
$$S_j(Q_j) \equiv \frac{1}{\pi} \int_0^{2\pi} \bar{F}_j(Q_j \cos \psi_j) \sin \psi_j d\psi_j \quad 5-37a$$

$$C_j(Q_j) \equiv \frac{1}{\pi} \int_0^{2\pi} \bar{F}_j(Q_j \cos \psi_j) \cos \psi_j d\psi_j \quad 5-39b$$

and
$$B_j = \frac{\epsilon b_j}{(\Omega^0)^2} \quad (j = 1, 2) \quad 5-40a$$

For convenience in notation let

$$\bar{B}_1 = B_1 r \quad 5-40b$$

$$\bar{B}_2 = \frac{B_2}{r} \quad 5-40c$$

The instability region of the linearized system can be obtained from Equation 5-38. For the linear case:

$$\bar{F}_j(Q_j \cos \psi_j) = Q_j \cos \psi_j \quad 5-41a$$

$$S_j(Q_j) = 0 \quad 5-41b$$

$$C_j(Q_j) = Q_j \quad 5-41c$$

Substituting the relations 5-42 into 5-38 the linearized equations are:

$$Q'_1 = -\frac{\bar{B}_1}{4K_1} Q_2 \sin(\theta_1 + \theta_2) \quad 5-42a$$

$$Q'_2 = -\frac{\bar{B}_2}{4K_2} Q_1 \sin(\theta_1 + \theta_2) \quad 5-42b$$

$$Q_1 \theta'_1 = \lambda K_1 Q_1 - \frac{\bar{B}_1}{4K_1} Q_2 \cos(\theta_1 + \theta_2) \quad 5-42c$$

$$Q_2 \theta'_2 = \lambda K_2 Q_2 - \frac{\bar{B}_2}{4K_2} Q_1 \cos (\theta_1 + \theta_2) \quad 5-42d$$

To determine the instability zone, it is necessary to determine the conditions when the trivial solution $Q_1 = Q_2 = 0$ is unstable. This is obtained most conveniently with the change of variables.

$$y_j = Q_j \cos \theta_j \quad 5-43a$$

$$z_j = Q_j \sin \theta_j \quad 5-43b$$

and investigating the stability of the trivial solution $y_j = 0, z_j = 0, (j = 1, 2)$. Carrying out the substitution 5-43 the system of equations 5-42 is transformed to the following system in terms of the new variables.

$$\begin{Bmatrix} y'_j \\ z'_j \end{Bmatrix} = \begin{bmatrix} \cos \theta_j & -\sin \theta_j \\ \sin \theta_j & \cos \theta_j \end{bmatrix} \begin{Bmatrix} Q'_j \\ Q_j \theta'_j \end{Bmatrix} \quad (j = 1, 2) \quad 5-44$$

Carrying out the substitution indicated in Equation 5-44 and seeking a solution in the form

$$y_j = Y_j e^{\rho \tau} \quad 5-45a$$

$$z_j = Z_j e^{\rho \tau} \quad 5-45b$$

the question of the stability of the variables y_j and z_j is determined by the eigenvalue problem

$$|[M] - \rho[I]| = 0 \quad 5-46a$$

where

$$M \equiv \begin{bmatrix} 0 & 0 & -\lambda K_1 & -\frac{\bar{B}_1}{4K_1} \\ 0 & 0 & -\frac{\bar{B}_2}{4K_2} & -\lambda K_2 \\ \lambda K_1 & -\frac{\bar{B}_1}{4K_1} & 0 & 0 \\ -\frac{\bar{B}_2}{4K_2} & \lambda K_2 & 0 & 0 \end{bmatrix} \quad 5-46b$$

The system 5-45 is unstable if $R(\rho) > 0$. It can be shown by expanding Equation 5-46a that $R(\rho) > 0$, and consequently the trivial solution $Q_1 = Q_2 = 0$ is unstable if

$$|\lambda| < \frac{1}{2} \sqrt{\frac{B_1}{K_1} \frac{B_2}{K_2}} \quad 5-47$$

It should be noted that Equation 5-47 is independent of the yield point ratio, r .

(c) Steady-State Response Curves

To obtain the steady-state response curves, Equation

5-38 can be rewritten as:

$$Q'_1 = K_1 [1+2\lambda] \frac{S_1(Q_1)}{2} - \frac{\bar{B}_1}{4K_1} Q_2 \sin \phi \quad 5-48a$$

$$Q'_2 = K_2 [1+2\lambda] \frac{S_2(Q_2)}{2} - \frac{\bar{B}_2}{4K_2} Q_1 \sin \phi \quad 5-48b$$

$$\begin{aligned} \phi' = \frac{[1+2\lambda]}{2} [K_1 \frac{C_1(Q_1)}{Q_1} + K_2 \frac{C_2(Q_2)}{Q_2}] - \frac{1}{2} [K_1 + K_2] \\ - \frac{1}{4} [\frac{\bar{B}_1}{K_1} \frac{Q_2}{Q_1} + \frac{\bar{B}_2}{K_2} \frac{Q_1}{Q_2}] \cos \phi \end{aligned} \quad 5-48c$$

where $\phi = \theta_1 + \theta_2$

Setting $Q'_1 = Q'_2 = \phi' = 0$ in Equation 5-48 the steady-state equations in terms of the variable Q°_1 , Q°_2 and ϕ° are

$$0 = K_1 [1+2\lambda] \frac{S_1(Q^{\circ}_1)}{2} - \frac{\bar{B}_1}{4K_1} Q^{\circ}_2 \sin \phi^{\circ} \quad 5-49a$$

$$0 = K_2 [1+2\lambda] \frac{S_2(Q^{\circ}_2)}{2} - \frac{\bar{B}_2}{4K_2} Q^{\circ}_1 \sin \phi^{\circ} \quad 5-49b$$

$$\begin{aligned} 0 = \frac{[1+2\lambda]}{2} [K_1 \frac{C_1(Q^{\circ}_1)}{Q^{\circ}_1} + K_2 \frac{C_2(Q^{\circ}_2)}{Q^{\circ}_2}] - \frac{1}{2} [K_1 + K_2] \\ - \frac{1}{4} [\frac{\bar{B}_1 Q^{\circ}_2}{K_1 Q^{\circ}_1} + \frac{\bar{B}_2 Q^{\circ}_1}{K_2 Q^{\circ}_2}] \cos \phi^{\circ} \end{aligned} \quad 5-49c$$

The relationship between Q°_1 , Q°_2 can be obtained from the first two equations 5-49a,b to give

$$Q^{\circ}_2 = Q^{\circ}_1 \left(\frac{\bar{B}_2}{\bar{B}_1} \frac{K_1^2}{K_2} \right) \left(\frac{S_1(Q^{\circ}_1)}{S_2(Q^{\circ}_2)} \right) \quad 5-50$$

Now, from 5-49a

$$\sin \phi^{\circ} = \frac{2K_1^2}{B_1} [1+2\lambda] \frac{S_1(Q^{\circ}_1)}{Q^{\circ}_2} \quad 5-51a$$

and substituting

$$\cos \phi^{\circ} = \pm (1 - \sin^2 \phi^{\circ})^{1/2} \quad 5-51b$$

into 5-49c

$$0 = \frac{[1+2\lambda]}{2} \left[K_1 \frac{C_1(Q^{\circ}_1)}{Q^{\circ}_1} + K_2 \frac{C_2(Q^{\circ}_2)}{Q^{\circ}_2} \right] - \frac{1}{2} \quad 5-52$$

$$\pm \left[\frac{\bar{B}_1}{K_1} \frac{Q^{\circ}_2}{Q^{\circ}_1} + \frac{\bar{B}^{\circ}_2}{K_2} \frac{Q^{\circ}_1}{Q^{\circ}_2} \right] \sqrt{1 - \left[\frac{2K_1}{\bar{B}_1} [1+2\lambda] \frac{S_1(Q^{\circ}_1)}{Q^{\circ}_2} \right]^2}$$

a relationship between amplitude and frequency is obtained. Solving for the explicit amplitude frequency relationship and remembering that

$$\lambda = 1 - \frac{\Omega}{\Omega^{\circ}} \quad 5-53$$

there is obtained

$$(1-\lambda) = 1.5 - \frac{1}{4} \frac{\alpha}{[\alpha^2 + \beta^2 \zeta^2]} \pm \frac{1}{2} \frac{\beta\alpha}{[\alpha^2 + \beta^2 \zeta^2]} \sqrt{1 + \frac{1}{4} \frac{\zeta^2}{\alpha^2} [4\beta^2 - 1]}$$

5-54

where $\alpha = \frac{K_1}{2} \frac{C_1(Q_1^\circ)}{Q_1^\circ} + \frac{K_2}{2} \frac{C_2(Q_2^\circ)}{Q_2^\circ}$ 5-55a

$$\beta = \frac{1}{4} \left[\frac{\bar{B}_1}{K_1} \frac{Q_2^\circ}{Q_1^\circ} + \frac{\bar{B}_2}{K_2} \frac{Q_1^\circ}{Q_2^\circ} \right]$$

5-55b

$$\zeta = \frac{2K_1 S_1(Q_1^\circ)}{\bar{B}_1 Q_2^\circ}$$

5-55c

Here β represents the strength of the parametric external excitation. The term ζ represents the effect of the hysteretic energy dissipation, and the term α the detuning effect due to the hysteretic nonlinearity.

An examination of equations 5-54 and 5-55 show that unbounded response is possible if

$$4\beta^2 > 1$$

5-56

Equation 5-54 is the steady-state equation applicable to any desired nonlinear restoring functions. It is only necessary to substitute the appropriate functions for $S_1(Q_1^\circ)$, $S_2(Q_2^\circ)$, $C_1(Q_1^\circ)$ and $C_2(Q_2^\circ)$. The steady-state response curves and the transient solutions will be given for the bilinear hysteretic model.

To evaluate the steady-state response curves it must be assumed that both amplitudes Q_1 and Q_2 are within the hysteretic range. This means that Q_1° and Q_2° must be equal to or greater than one, i.e.

$$Q^{\circ}_1 \geq 1; \quad Q^{\circ}_2 \geq 1$$

5-57a,b

Fig. 5-8 to 5-10 plot the steady-state response amplitude of μ_1 and μ_2 against frequency. The ratio of yield points $r = 2$ in Fig. 5-8, 5-9 and $r = 1$ in Fig. 5-10. The values of the coefficients used are $B_1 = B_2 = 0.05$, $K_1 = 0.366$, $K_2 = 0.634$. The bilinear hysteretic parameter $u_2 = 0.5$ and $u_1 = 0.3, 0.5, \text{ and } 1.0$.

Examining Fig. 5-8 it is seen that the boundaries of the linear parametric resonance zone and the steady-state curves do not coincide. In fact, they can be made to coincide for only one specific ratio of the yield points, r . For the equality relationship of Equation 5-57 a,b

$$S_j(Q^{\circ}_j) = 0 \quad 5-58a$$

$$C_j(Q^{\circ}_j) = 1 \quad 5-58b$$

and Equation 5-54 reduces to

$$\lambda = \pm \frac{1}{4} \left[\frac{B_1}{K_1} r + \frac{B_2}{K_2} \frac{1}{r} \right] \quad 5-59$$

For the specific yield point relationship

$$r = \sqrt{\frac{B_2}{B_1} \frac{K_1}{K_2}} \quad 5-60$$

the equation 5-59 coincides with equation 5-54 and the discontinuity is removed. For any other ratio x_{y2}/x_{y1} the width of

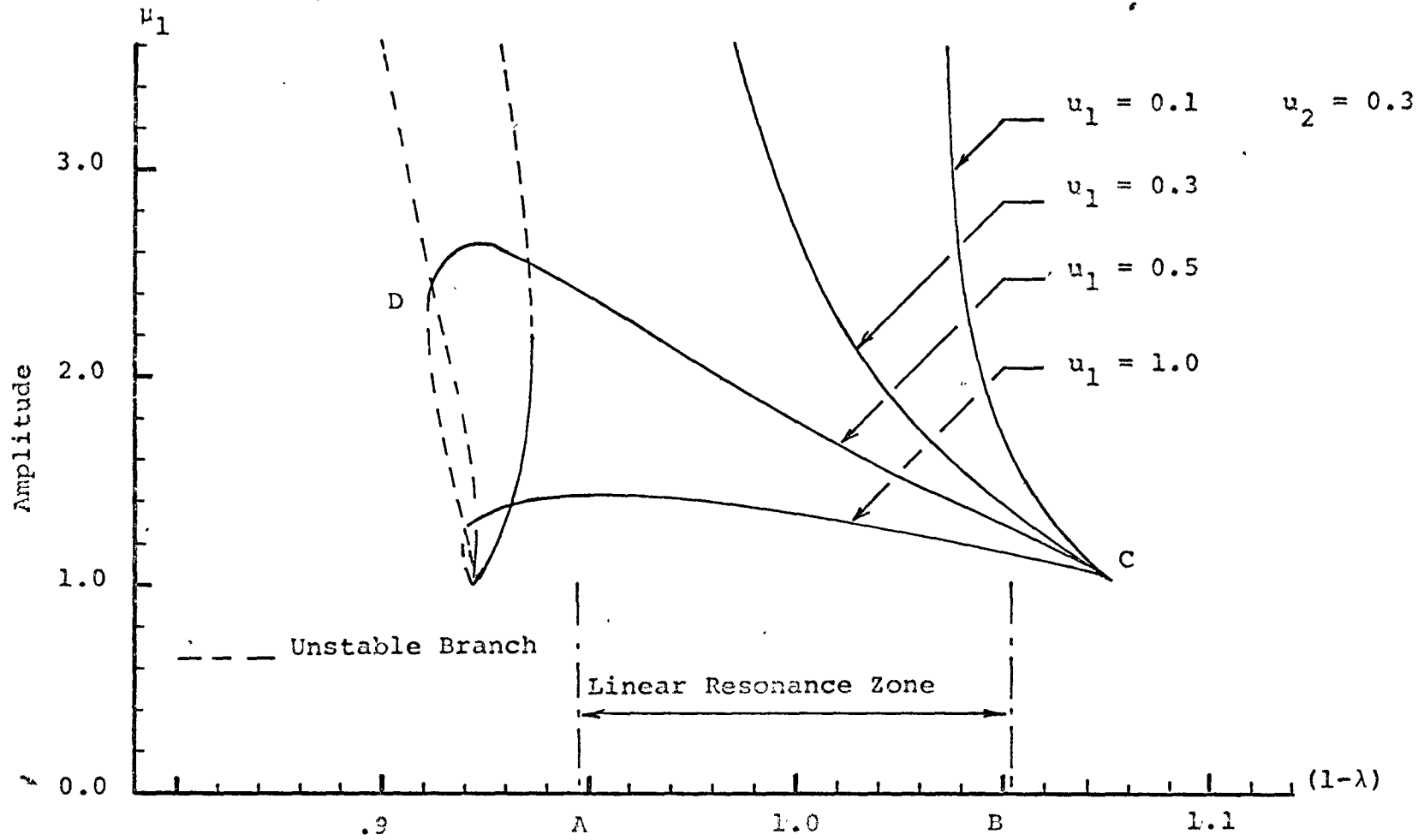


FIG. 5-8 DESTABILIZING EFFECT OF THE BILINEAR HYSTERETIC RESTORING FUNCTIONS
 ($\omega_1 = 1.0$, $\omega_2 = \sqrt{3}$, $B_1 = B_2 = 0.05$, $r = 2$)

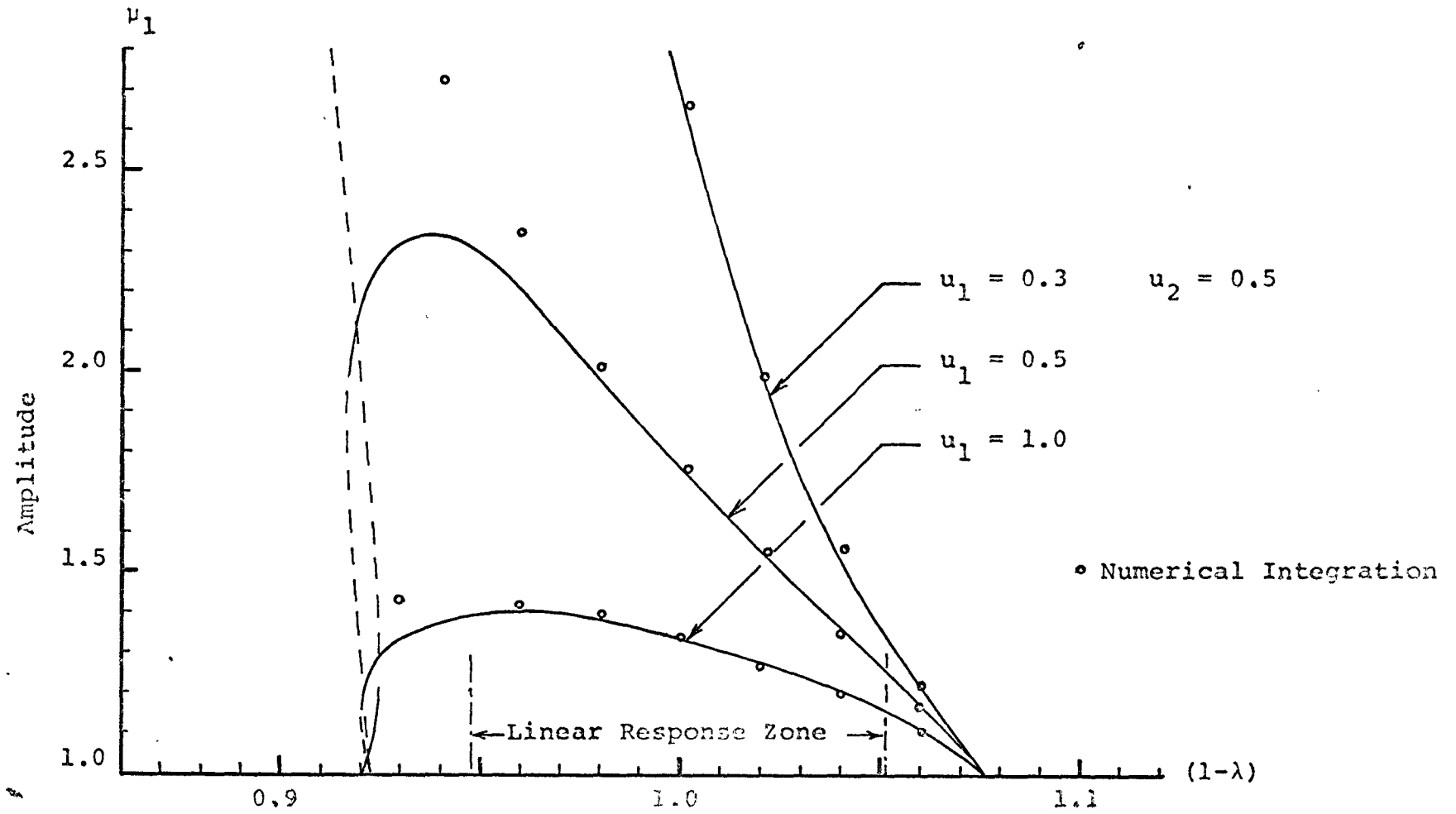


FIG. 5-9 STEADY-STATE RESPONSE CURVES (Ratio of Yield Points $r = 2$)

$(\omega_1 = 1.0, \omega_2 = \sqrt{3}, B_1 = 0.05, B_2 = 0.05)$

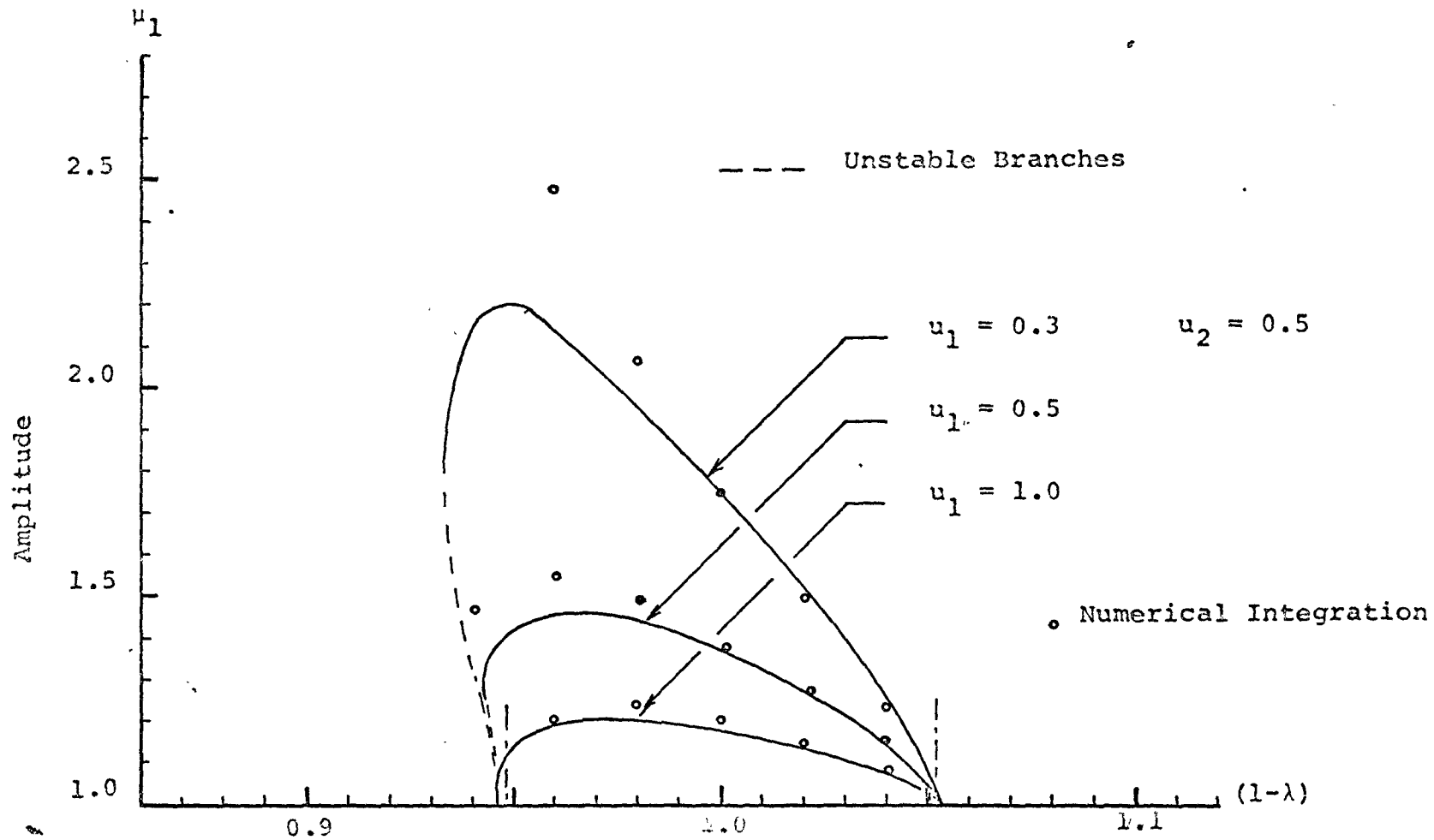


FIG. 5-10 STEADY-STATE RESPONSE CURVES (Ratio of Yield Points $r = 1$)

$$(\omega_1 = 1.0, \omega_2 = \sqrt{3}, B_1 = 0.05, B_2 = 0.05)$$

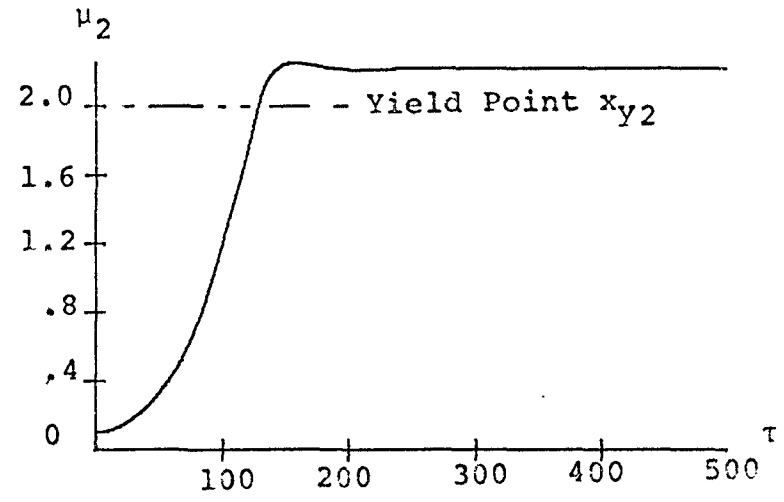
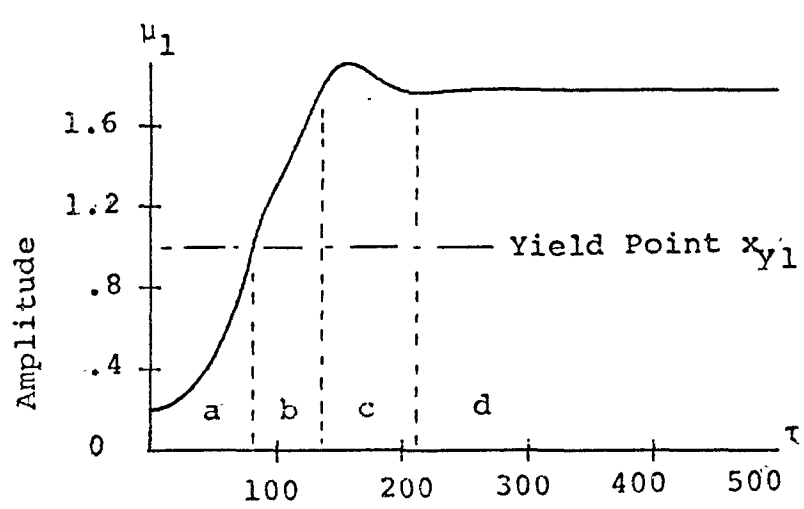


FIG. 5-11 TRANSIENT RESPONSE OF THE AVERAGED EQUATIONS

$$(u_1 = 0.5, u_2 = 0.3, (1-\lambda) = 1.0, r = 2, B_1 = B_2 = 0.05, \omega_1 = 1.0, \omega_2 = \sqrt{3})$$

the response curve given by Equation 5-59 increases in relation to Equation 5-47. For example, the stationary value of λ with respect to r is obtained from the equation

$$\frac{\partial \lambda}{\partial r} = 0 \quad 5-61a$$

or

$$r = \sqrt{\frac{B_2 K_1}{B_1 K_2}} \quad 5-61b$$

Since the second derivation $\partial^2 \lambda / \partial r^2 > 0$, λ and consequently the width of the response curves can only be equal to or greater than the width of the linear parametric instability zone.

Fig. 5-11 shows the time history response of the averaged equations 5-48. The transient response can be viewed as consisting of four stages: (a) the initial amplitude growth of the linear equations, (b) the co-ordinate x_1 enters the yield range, (c) the co-ordinate x_2 enters the non-yield range, and (d) steady state. These four phases are shown in Fig. 5-11.

(d) Passage Through Resonance

For the yield point ratio $r = 2$ Fig. 5-8 and Fig. 5-9 show that large amplitude response can occur outside the linear instability zone. The steady-state response curves lean towards the lower frequencies and a large "overhanging" region exists. For a fixed external frequency within the region of the overhang, a small disturbance will not excite the system into resonance. The disturbance must be large enough so that the system co-ordinates exceed their yield points, before a resonance condition can be reached. There is however another mechanism by which these large amplitude

regions can be reached. This occurs during a passage through resonance.

As the external frequency Ω is increased from some small value, only a small background vibration exists until the frequency reaches the lower boundary of the linear resonance zone (point A in Fig. 5-8). A resonant build-up of oscillations occurs at point A and the oscillations experience a sudden jump to their respective steady-state curves. As Ω is further increased the amplitude of oscillations follow the steady-state curve to point C. At point C the system is no longer in a resonant state, the phase angles are no longer synchronized to the external frequency and the steady-state pattern of the oscillations break down. The amplitudes fall below their respective yield points and the system is no longer hysteretic. As the frequency is further increased oscillations with amplitudes less than the yield points will continue indefinitely.

If the external frequency is decreased from a large value, only a small background oscillation exists until the higher boundary (point B) of the linear resonance zone is reached. At point B the oscillations jump to their respective steady-state curves. As Ω is further decreased the amplitudes follow the steady-state curves until the lower limit is reached at point D. At point D the system is no longer in a resonant state and the oscillations break down. Again, as the frequency is further decreased oscillations with amplitudes less than their respective yield points will continue indefinitely. It must be noted that for small hysteretic effect, the steady-state response curves do not close. (For example $u_1 = u_2 = 0.3$ in Fig. 5-8). In this case, very large response is to be expected as the frequency passes through resonance from a high value to a low value.

Fig. 5-12 and Fig. 5-13 show the time history response of a passage through resonance as the frequency is decreased

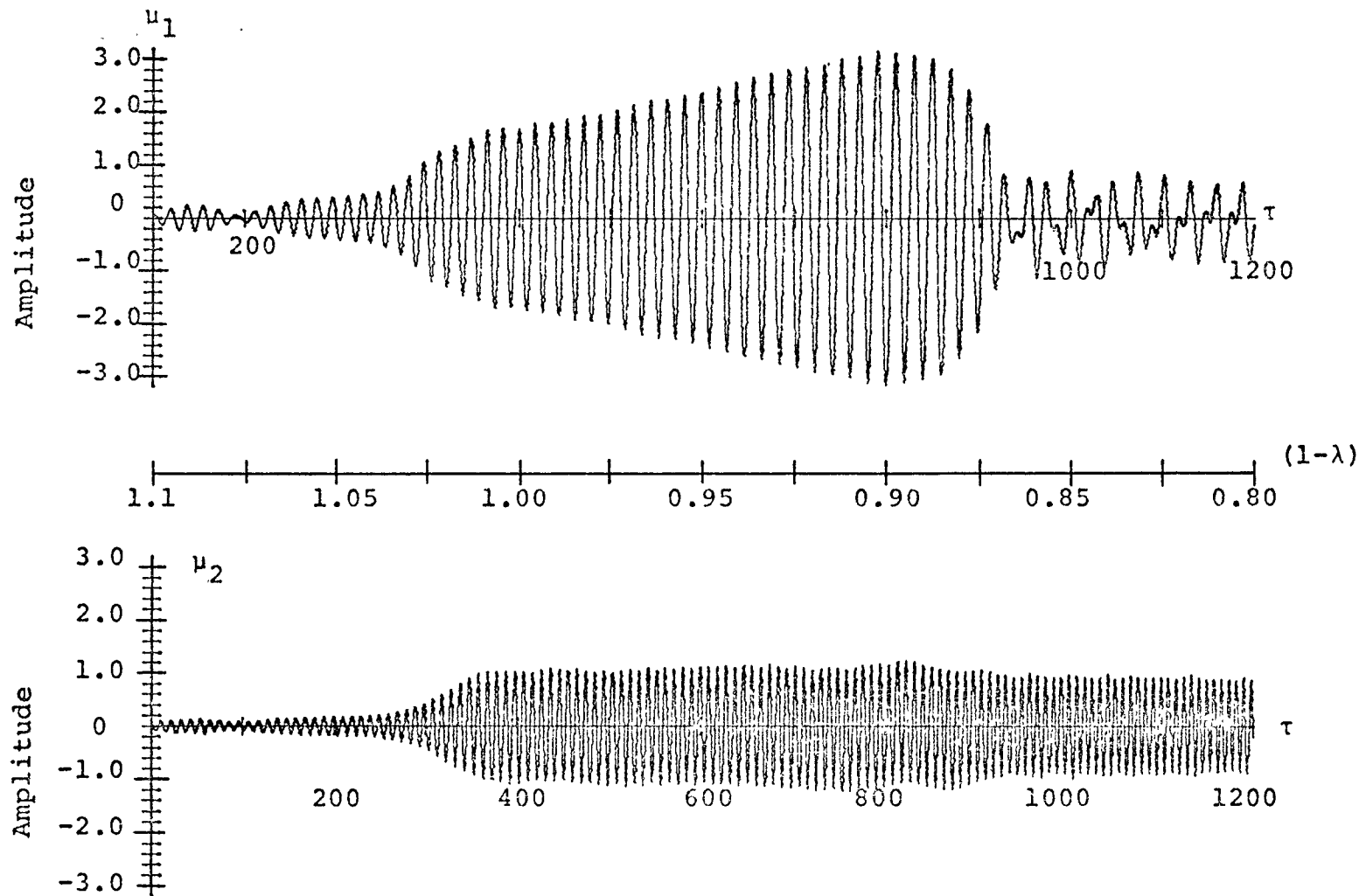


FIG. 5-12 PASSAGE THROUGH RESONANCE - BILINEAR HYSTERETIC FUNCTION

$$(\omega_1 = 1.0, \omega_2 = \sqrt{3}, B_1 = B_2 = 0.05, u_1 = 0.5, u_2 = 0.5, r = 2)$$

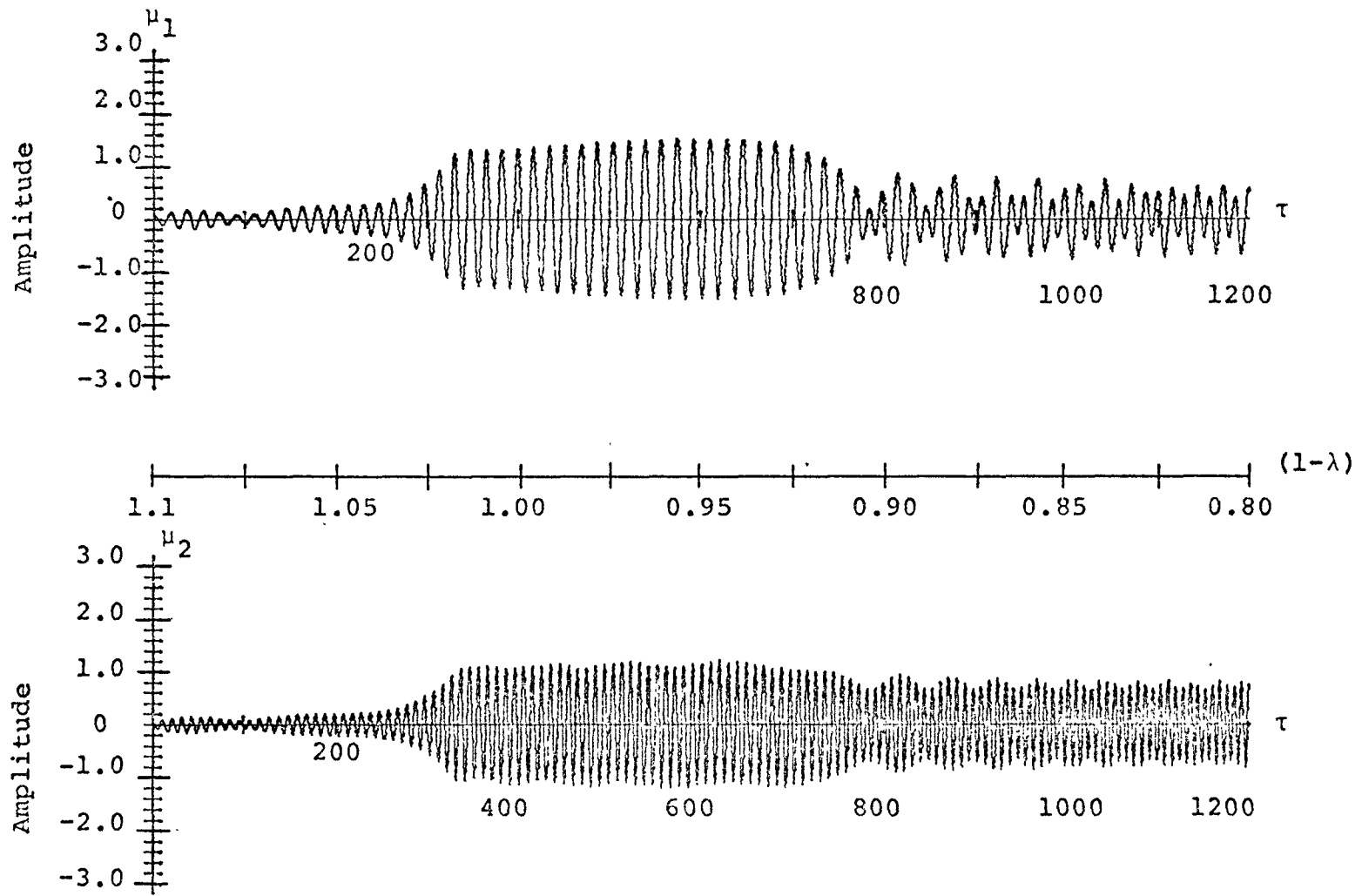


FIG. 5-13 PASSAGE THROUGH RESONANCE - BILINEAR HYSTERETIC FUNCTION
 $(\omega_1 = 1.0, \omega_2 = \sqrt{3}, B_1 = B_2 = 0.05, u_1 = 0.5, u_2 = 0.5, r = 1)$

from $(1-\lambda) = 1.1$ to $(1-\lambda) = 0.8$ over a time interval $\tau = 1200$. Fig. 5-12 corresponds to the steady-state response curve $u_1 = 0.5, u_2 = 0.5, r = 2$ of Fig. 5-9 and Fig. 5-13 corresponds to the steady-state response curve $u_1 = 0.5, u_2 = 0.5, r = 1$ of Fig. 5-10. Both the amplitude and time scales of Fig. 5-12 and Fig. 5-13 are identical. In comparing the response of these two curves it is noticed that the oscillations do follow closely the steady-state response curves. Fig. 5-12 was integrated with the ratio $r = 2$. This increase of the ratio r has a two-fold effect on the response. It causes both a larger amplitude of response and increases the duration that the system is in a resonant state. In terms of engineering design an increase of r causes both an increase in stress and an increased fatigue effect.

5.5 Observations and Discussions

1. A two degree of freedom ^{hysteretic} system parametrically excited can exhibit a monofrequency response if the value of the external frequency is approximately twice the value of one of the natural frequencies. In this case, an approximate solution of the general two-degree of freedom system is possible.
2. The approximate solution is obtained by assuming both a monofrequency response and a single mode response. A one mode approximation allows a relatively simple determination of the parametric instability zone, steady-state response and transient response. The second mode, although not parametrically excited at it's own natural frequency is nevertheless coupled to the motion of the first mode by both the nonlinear hysteretic elements and the linear parametric terms. These terms do cause a forced response of the second mode. As a result, the approximate method may not obtain the exact steady-state amplitude; it does, however obtain the correct magnitude of response.

3. Analytical solutions of a general two degree of freedom systems subjected to combination parametric resonance is a difficult task. The interaction of two modes each excited at it's own natural frequency renders unclear the averaging process of the hysteretic elements as they do not, in general, trace out a steady-state pattern. However, a special two degree of freedom system is analysed in which each hysteretic element is a function of only one normal co-ordinate. In this way a steady-state solution is possible and the effect of hysteretic damping can be investigated.

4. In order to reach a steady-state, both restoring elements must enter the hysteretic zone. This is in sharp contrast to the first example where steady-state is possible with only one hysteretic element. Here, even though one co-ordinate has passed its yield point, it is drawn further into the yielding zone until the hysteretic action of the second element causes a steady-state to occur.

5. A system with bilinear hysteretic damping can assume a dual-state depending upon the amplitude levels. At small amplitudes, where the oscillations are less than the yield points the equations of motion are linear and undamped. At large amplitude levels, the system is nonlinear, hysteretic. The steady-state curves of the hysteretic system depend on the actual value and the ratio's of the parametric coefficients B_j , the normalized natural frequencies K_j , the ratio of the yield points, and the hysteretic parameters u_j . The instability zone of the trivial solution of the undamped system depends on the product of the parametric coefficients and the distribution of the natural frequencies only. At the interface between these two systems the resonance zones do not coincide. In general, the width of the steady-state response curve is larger than the linear resonance zone.

6. The increased width of the steady-state zone is caused by the ratio of yield points. In this respect the ratio of yield points determines the maximum amplitude of response and the duration that a system is in a resonant state. The ratio r for minimum response can be calculated. In this way a design aid is available to minimize the response.

CHAPTER VI

COMBINATION RESONANCE OF A TWO DEGREE OF FREEDOM SYSTEM WITH THE "RAMBERG-OSGOOD" HYSTERETIC RESTORING FUNCTIONS

6.1 Introduction

In chapter V a two degree of freedom system subjected to combination resonance was investigated. The restoring functions were assumed to follow the piece-wise linear representation of the bilinear hysteretic model. It was observed that bilinear hysteretic damping does in general cause bounded response. However, it was also observed that hysteretic damping caused a wider parametric resonance zone. Damping in engineering structures is widely considered to provide a beneficial effect. It is often purposely introduced to restrict the amplitudes of motion during resonant oscillations. In this way, damping acts to stabilize the system. Of great concern is the fact that the addition of damping may cause a system to become more susceptible to resonant oscillation. In this way, damping causes a destabilizing effect.

A destabilizing effect of viscous damping in parametric combination resonance was first noted by Schmidt and Weidenhammer^[44]. Hagedorn^[15] extended the investigation to nonlinear viscous damping and found that this form of damping can also widen the resonance zone and cause a destabilizing effect. In stability analysis the use of viscous damping leads to similar findings. Ziegler^[58] has shown that linear viscous damping in a circulatory system may lower the critical flutter load compared to the critical load of the undamped system. At the time it was proposed by

Ziegler that internal damping of physical systems is usually connected with a hysteresis effect which is not represented if the damping forces are assumed to be velocity dependent. Jong^[28] by using the bilinear form of hysteretic damping concluded that this hysteretic model generally removed the destabilizing effect.

It is the purpose of this chapter to investigate whether hysteretic damping causes a dynamical system to become more susceptible to parametric combination resonance. The bilinear hysteretic model is not suitable to study the motion of hysteretic systems when the amplitudes of motion are less than the yield points. For this purpose the smoothly varying Ramberg-Osgood hysteretic model is used.

6.2 The Equations of Motion

The equations of motion of the two degree of freedom system considered in this chapter are:

$$\ddot{x}_1 + \omega_1^2 F_1(x_1, \alpha_1, n_1) - \epsilon b_1 x_2 \cos(\Omega t) = 0 \quad 6-1a$$

$$\ddot{x}_2 + \omega_2^2 F_2(x_2, \alpha_2, n_2) - \epsilon b_2 x_1 \cos(\Omega t) = 0 \quad 6-1b$$

Equation 6-1 corresponds to the problem treated in Chapter V. The system is subjected to combination parametric resonance, type II. The restoring functions $F_1(x_1, \alpha_1, n_1)$ and $F_2(x_2, \alpha_2, n_2)$ represent the Ramberg-Osgood hysteretic force-displacement relationships. The functions are such that for $\alpha_1 = \alpha_2 = 0$, $F_1(x_1) = x_1$ and $F_2(x_2) = x_2$. With the change of variables, $\mu_1 = x_1/x_{y1}$, $\mu_2 = x_2/x_{y2}$ the equations 6-1 can be written as:

$$\ddot{\mu}_1 + \omega_1^2 \bar{F}_1(\mu_1) - \epsilon b_1 r \mu_2 \cos(\Omega t) = 0 \quad 6-2a$$

$$\ddot{\mu}_2 + \omega_2^2 \bar{F}_2(\mu_2) - \frac{\epsilon b_2}{r} \mu_1 \cos(\Omega t) = 0 \quad 6-2b$$

where $\bar{F}_1(\mu_1) = F_1(x_1)/x_{y1}$ 6-3a

$$\bar{F}_2(\mu_2) = F_2(x_2)/x_{y2} \quad 6-3b$$

$$r = x_{y2}/x_{y1} \quad 6-3c$$

The relationship between the functions $\bar{F}_1(\mu_1)$, $\bar{F}_2(\mu_2)$ against their arguments μ_1 , μ_2 is shown in the Appendix in Fig. A-3. With the change of variables

$$\tau = \Omega t \quad 6-4a$$

$$\Omega = \Omega^\circ (1-\lambda) \quad 6-4b$$

$$K_1 = \omega_1/\Omega^\circ \quad 6-4c$$

$$K_2 = \omega_2/\Omega^\circ \quad 6-4d$$

the equations 6-2 can be rewritten to form the system

$$\ddot{\mu}_1 + K_1^2 (1+2\lambda) \bar{F}_1(\mu_1) - \frac{\epsilon b_1 r}{\Omega^{\circ 2}} \mu_2 \cos \tau = 0 \quad 6-5a$$

$$\mu_2'' + K_2^2 (1+2\lambda) \bar{F}_2(\mu_2) - \frac{\epsilon b_2}{r \Omega^2} \mu_1 \cos \tau = 0 \quad 6-5b$$

where primes denote differentiation with respect to the non-dimensional time τ and λ represents a small detuning of the external frequency.

6.3 Approximate Method of Solution

Seeking a response

$$\mu_j(\tau) = Q_j(\tau) \cos (K_j \tau + \theta_j(\tau)) \quad 6-6a$$

$$\equiv Q_j \cos \psi_j \quad 6-6b$$

and specifying that

$$\mu_j'(\tau) = -Q_j K_j \sin \psi_j \quad (j = 1, 2) \quad 6-7$$

the averaged equations can be obtained from the system 6.5. The averaged equations are

$$Q_1' = K_1 (1+2\lambda) \frac{S_1(Q_1)}{2} - \frac{B_1}{4K_1} r Q_2 \sin (\theta_1 + \theta_2) \quad 6-8a$$

$$Q_2' = K_2 (1+2\lambda) \frac{S_2(Q_2)}{2} - \frac{B_2}{4K_2} \frac{Q_1}{r} \sin (\theta_1 + \theta_2) \quad 6-8b$$

$$Q_1 \theta_1' = -\frac{K_1 Q_1}{2} + K_1 (1+2\lambda) \frac{C_1(Q_1)}{2} - \frac{B_1 r}{4K_1} Q_2 \cos (\theta_1 + \theta_2) \quad 6-8c$$

$$Q_2 \theta'_2 = - \frac{K_2 Q_2}{2} + K_2 (1+2\lambda) \frac{C_2(Q_2)}{2} - \frac{B_2}{4K_2} \frac{Q_1}{r} \cos(\theta_1 + \theta_2) \quad 6-8d$$

$$\text{where } S_j(Q_j) \equiv \frac{1}{\pi} \int_0^{2\pi} \bar{F}_j(Q_j \cos \psi_j) \sin \psi_j \, d\psi_j \quad 6-9a$$

$$C_j(Q_j) \equiv \frac{1}{\pi} \int_0^{2\pi} \bar{F}_j(Q_j \cos \psi_j) \cos \psi_j \, d\psi_j \quad 6-9b$$

$$\text{and } B_j = \frac{\epsilon b_j}{(\Omega^\circ)^2} \quad (j = 1, 2) \quad 6-10$$

6.4 Steady State Response

The steady-state response in terms of the amplitude Q°_1 and Q°_2 and the frequency $(1-\lambda)$ can be obtained from the averaged equations 6-8 by setting $Q_j = Q^\circ_j$, $Q'_j = 0$, $\theta_j = \theta^\circ_j$ and $\theta'_j = 0$, ($j = 1, 2$). By substitution and elimination a relationship between the steady-state amplitudes can be obtained, i.e.

$$Q^\circ_2 = \frac{Q^\circ_1}{r^2} \frac{B_2}{B_1} \frac{K_1^2}{K_2^2} \frac{S_1(Q^\circ_1)}{S_2(Q^\circ_2)} \quad 6-11$$

$$(1-\lambda) = 1.5 - \frac{1}{4} \frac{\alpha}{[\alpha^2 + \beta^2 \zeta^2]} \pm \frac{1}{2} \frac{\beta \alpha}{[\alpha^2 + \beta^2 \zeta^2]} \sqrt{1 + \frac{1}{4} \frac{\zeta^2}{\alpha^2} [4\beta^2 - 1]} \quad 6-12$$

$$\text{where } \alpha = \frac{K_1}{2} \frac{C_1(Q^\circ_1)}{Q^\circ_1} + \frac{K_2}{2} \frac{C_2(Q^\circ_2)}{Q^\circ_2} \quad 6-13$$

$$\beta = \frac{1}{4} \left[\frac{B_1 r Q_2^\circ}{K_1 Q_1^\circ} + \frac{B_2 Q_1^\circ}{r K_2 Q_2^\circ} \right] \quad 6-14$$

$$\zeta = \frac{2K_1 S_1(Q_1^\circ)}{B_1 r Q_2^\circ} \quad 6-15$$

Equation 6-11 and 6-12 are the steady-state equations applicable to any desired nonlinear restoring functions. In Chapter V the steady-state response curves were obtained for the bilinear hysteretic function. Here the steady-state curves will be calculated for the Ramberg-Osgood hysteretic function.

The Ramberg-Osgood hysteretic function is specified by the two parameters α and n . The equation for the backbone curve for the restoring functions \bar{F}_j is:

$$\mu_j = \bar{F}_j + \alpha_j \bar{F}_j^{n_j} \quad 6-16$$

For the evaluation of the steady-state and later for the transient response only the parameter n_j will be varied. It will further be assumed that $r=1$ and $\alpha_1=\alpha_2$.

The functions $S_1(\mu_1)$, $S_2(\mu_2)$, $C_1(\mu_1)$ and $C_2(\mu_2)$ of the Ramberg-Osgood hysteretic model in general can not be evaluated explicitly in terms of the amplitude levels and a numerical analysis is necessary. For small amplitude levels $\mu_j \ll 1$ the approximations

$$C_j(\mu_j) \approx \mu_j \quad 6-17a$$

$$S_j(\mu_j) \approx - \frac{4\alpha}{\pi} \frac{(n_j-1)}{(n_j+1)} \mu_j^{n_j} \quad 6-17b$$

can be made.

Then the ratio of amplitudes as given by equation 6-11 is

$$\frac{\mu_2}{\mu_1} = (\mu_1)^{\frac{n_1+1}{n_2+1} - 1} \left(\frac{B_2}{B_1} \frac{K_1^2}{K_2^2} \frac{(n_1-1)}{(n_1+1)} \frac{(n_2+1)}{(n_2-1)} \right)^{\frac{1}{n_2+1}} \quad 6-18$$

$$\text{For } n_2 > n_1 \quad \lim_{\mu_1 \rightarrow 0} \frac{\mu_2}{\mu_1} = \infty \quad 6-19a$$

$$\text{For } n_1 > n_2 \quad \lim_{\mu_1 \rightarrow 0} \frac{\mu_2}{\mu_1} = 0 \quad 6-19b$$

$$\text{For } n_1 = n_2 = n \quad \lim_{\mu_1 \rightarrow 0} \frac{\mu_2}{\mu_1} = \left(\frac{B_2}{B_1} \frac{K_1^2}{K_2^2} \right)^{\frac{1}{n+1}} \quad 6-19c$$

The steady-state response curves for $\alpha = 0.1$, $n_2 = 9$, and different values of n_1 are plotted in Fig. 6-1 to Fig. 6-3. The three curves are all plotted for the value of the coefficients $B_1 = B_2 = 0.05$, $\omega_1 = 1.0$, $\omega_2 = \sqrt{3}$, $K_1 = .366$, $K_2 = 0.634$, and $r=1$.

The largest response is given by $n_1 = 3$ and the least response by $n_1 = 15$. For $n_1 = 9$ the maximum response within the resonance zone is approximately $\mu_1 = 1.3$. As n_1 is increased further there appears to be only a slight decrease in the maximum response and for $n_1 = 15$, $\mu_1 = 1.23$. The steady-state response curves were checked by exact numerical inte-

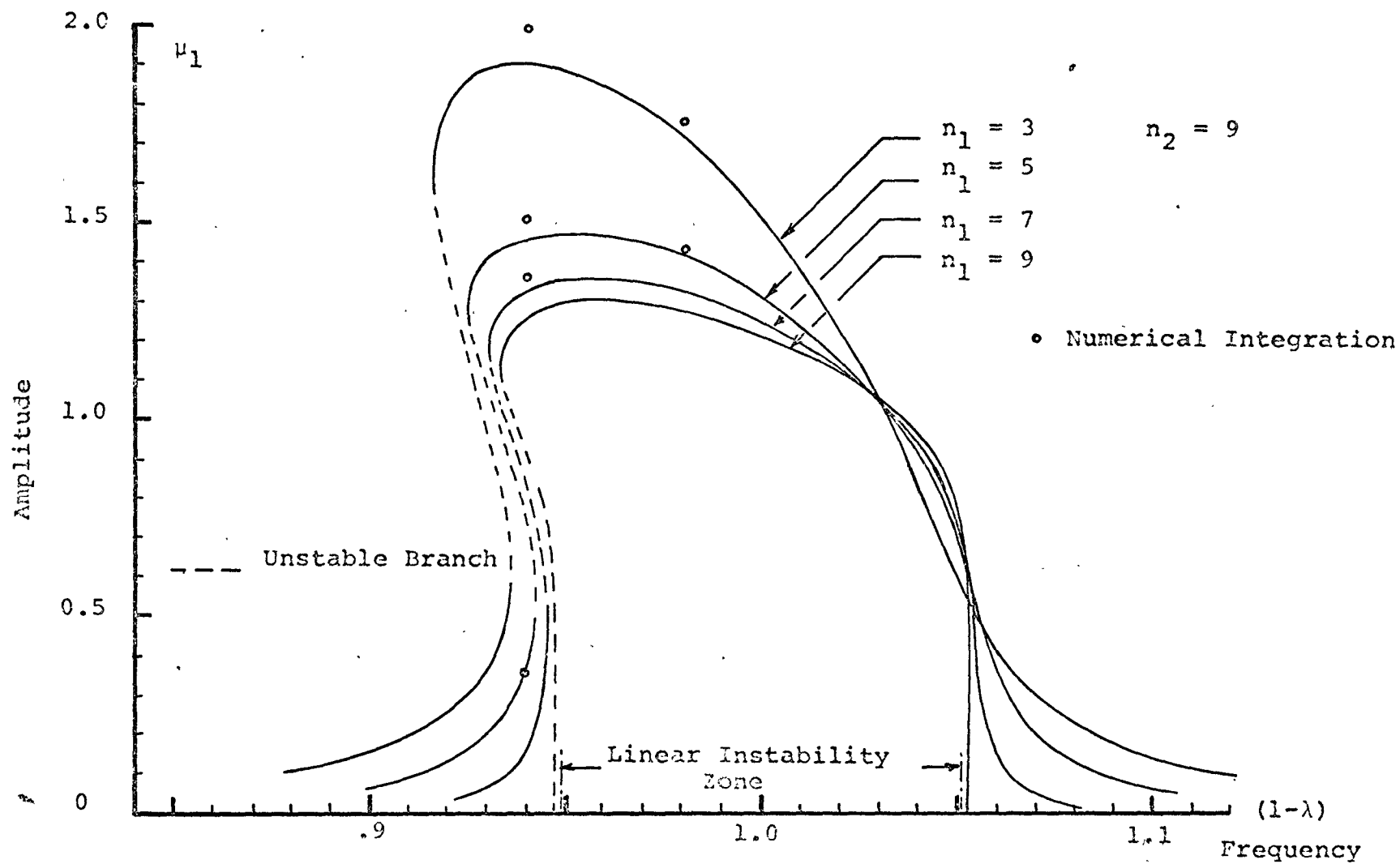


FIG. 6-1 STEADY STATE CURVES OF THE RAMBERG-OSGOOD HYSTERETIC FUNCTION

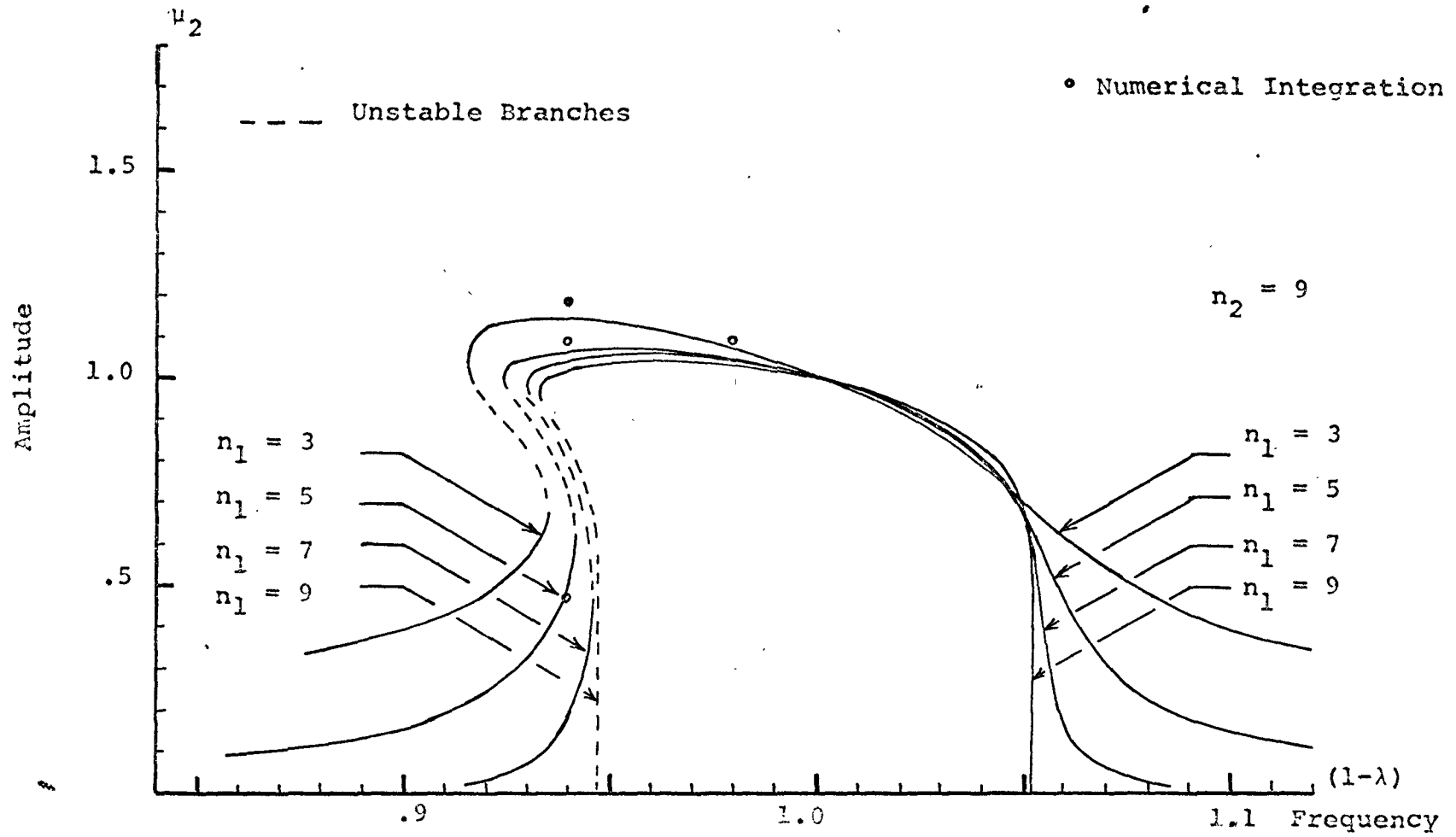


FIG. 6-2 STEADY-STATE CURVES OF THE PAMBERG-OSGOOD HYSTERETIC FUNCTION

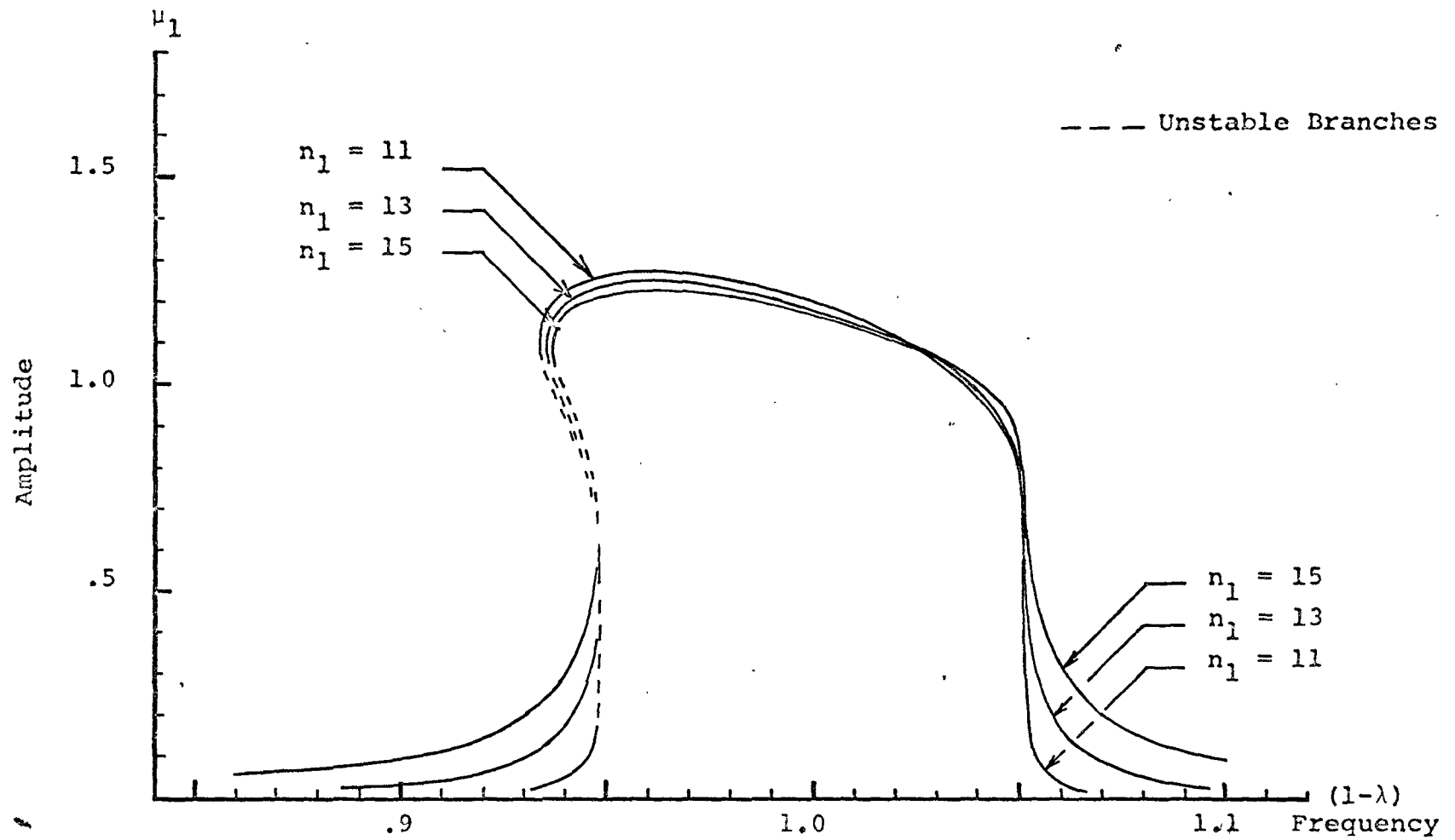


FIG. 6-3 STEADY-STATE RESPONSE OF THE RAMBERG-OSGOOD HYSTERETIC FUNCTION

gration and close agreement was obtained.

The steady-state curves have a pronounced softening effect and lean to the low frequency side. The stability of the steady-state curves were checked numerically and the unstable portions are shown as dashed lines. At small amplitude levels, the steady-state curves diverge for all values n_1 not equal to n_2 ; only when $n_1 = n_2$ can the steady-state curves be extrapolated to the zero amplitude axis. This raises the question of the stability of the trivial solution $\mu_1 = \mu_2 = 0$. For the undamped system the instability region is $|\lambda| < .0519$. Within this region $R(p)$ of the associated eigenvalue problem is positive and an instability occurs. Outside the instability zone $R(p) = 0$ and the question of instability is undecided from a linear analysis. This question was discussed by Hagedorn^[15] in his investigation of cubic viscous damping. Using Liapunov's second method he concluded, that the trivial solution was also unstable in the region outside the linear instability zone. In terms of practical stability, it can be seen that irrespective of the initial values large amplitude can only be maintained in the frequency region $.916 < (1-\lambda) < 1.0526$. This amounts to an increase of 30% over the linear instability zone. Within this enlarged region the question of stability must be answered in terms of degree of instability. In the linear instability zone any initial disturbance no matter how small will be followed by an exponential rise in amplitudes. Outside this zone, very small initial disturbances will cause, in practical terms almost no hysteretic damping effect. However, for large initial disturbances and low values of n_1 the hysteretic damping effect will become evident and cause the destabilizing effect which in turn will cause the amplitudes to increase.

6.5 Transient Response

To illustrate the actual behaviour of the system to

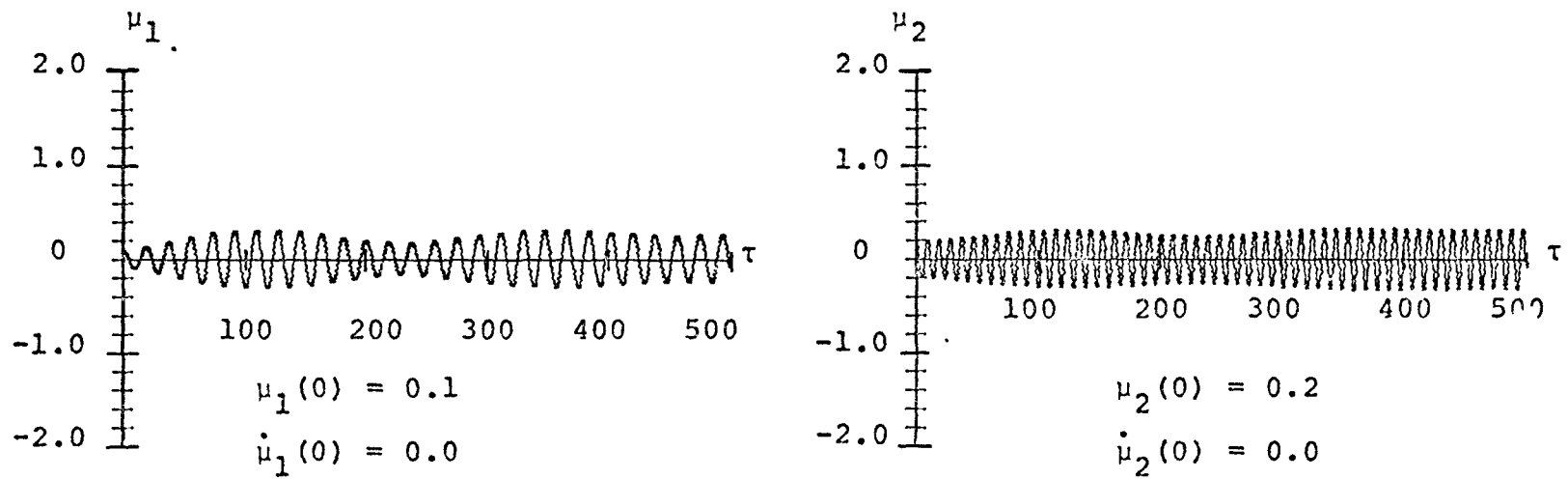


FIG. 6-4 EFFECT OF SMALL INITIAL CONDITIONS OUTSIDE THE LINEAR RESONANCE ZONE
 ($(1-\lambda) = 0.94$)

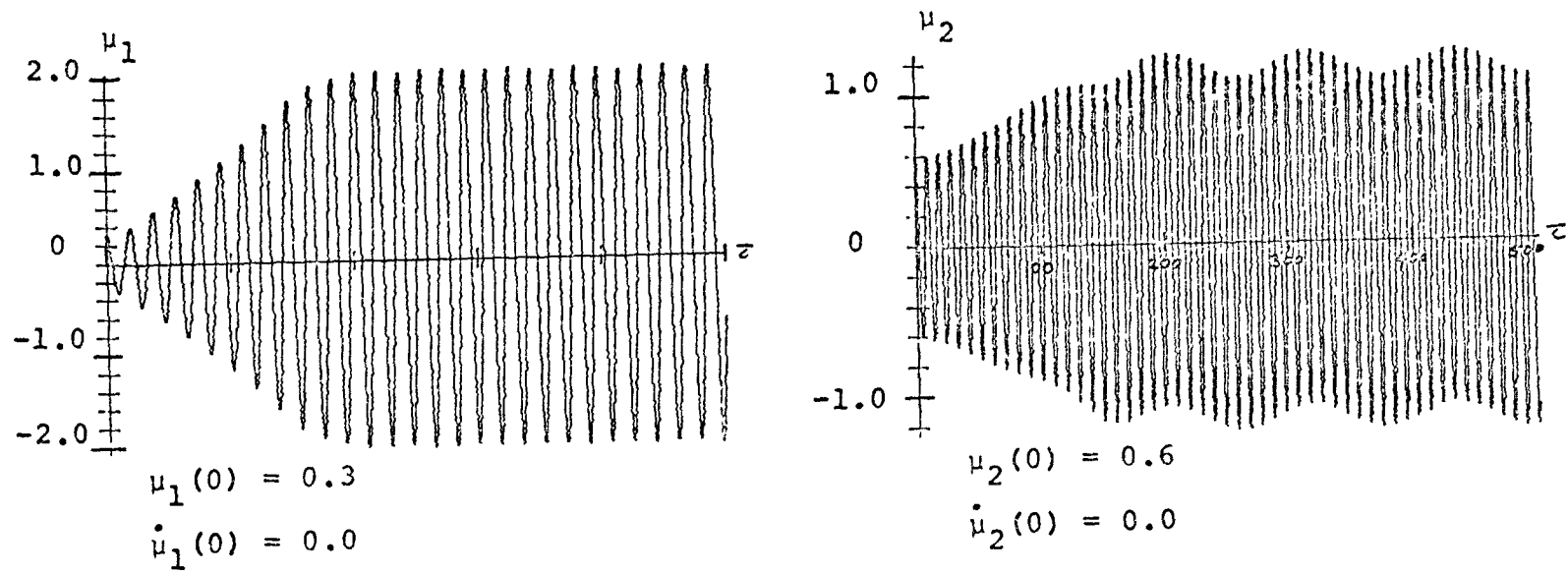


FIG. 6-5 EFFECT OF LARGE INITIAL CONDITIONS OUTSIDE THE LINEAR RESONANCE ZONE
 $((1-\lambda) = 0.94)$

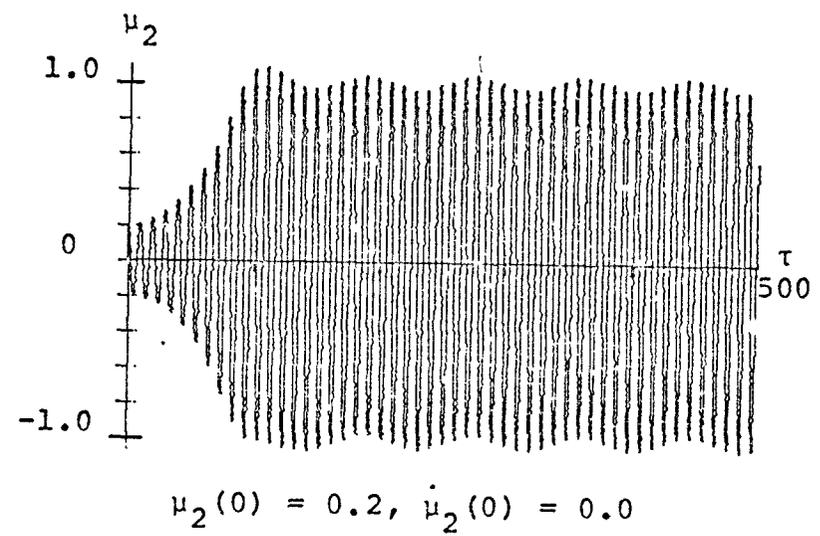
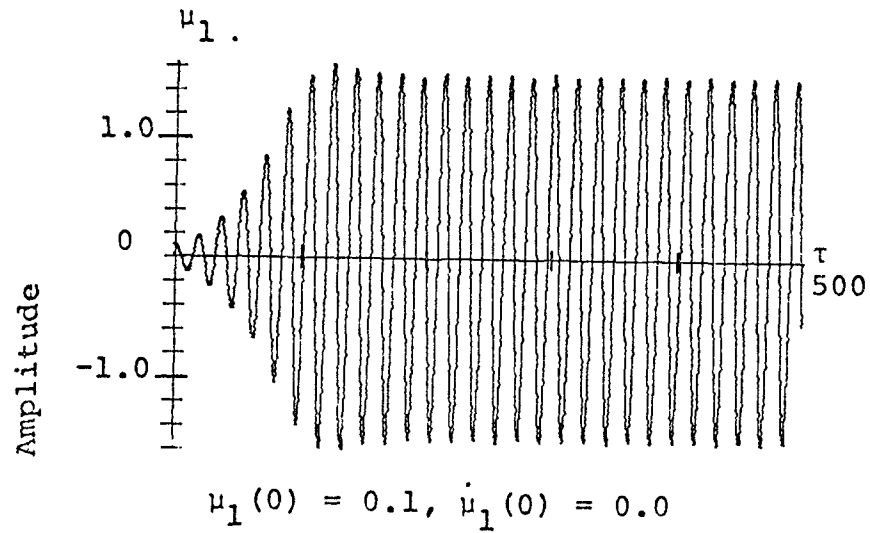


FIG. 6-6 RESPONSE WITHIN THE LINEAR RESONANCE ZONE $[(1-\lambda) = 1.00]$

hysteretic damping the Equations 6-2 are integrated numerically.* Fig. 6-4 shows the response of the system for small initial conditions at the frequency $(1-\lambda) = 0.94$. This frequency is outside the linear instability zone but within the region where large steady-state response can occur. It is seen that the amplitudes of motion do not undergo a significant increase within the integration time $\tau < 500$. Fig. 6-5 shows the effect of large initial conditions at the same frequency. Here, the destabilizing effect of the hysteretic damping is evident. The amplitudes grow rapidly and reach a steady-state motion at $\tau = 200$. Within the linear instability zone small initial conditions cause an immediate growth of amplitudes. Fig. 6-6 shows the response of the system at the frequency $(1-\lambda) = 1.0$.

The large amplitude regions which are outside the linear instability zone can be reached without specifying large initial disturbances. This happens during a passage through resonance where the resonance zone is traversed from a high frequency to a lower frequency. Fig. 6-7 shows the response for a passage through resonance with the parameters of the Ramberg-Osgood function $n_1 = 3, n_2 = 9$. Fig. 6-8 shows a similar response for $n_1 = 9, n_2 = 9$. The initial phase of motion up to $\tau = 200$ is the same for both sets of response curves. A resonant build-up is seen to occur at $(1-\lambda) = 1.05$. As the external frequency is further decreased the resonant amplitudes follow closely the values given by the steady-state curves. The resonant state ends at $\tau = 550$ for the case $n_1 = n_2 = 9$ and at $\tau = 600$ for the case $n_1 = 3, n_2 = 9$. A further decrease in frequency causes only a small decrease in amplitudes.

Comparing the time history response of the system to the steady-state response the following observations are made. For small initial disturbances resonant oscillations do not take place unless the external frequency is within the boundaries of the linear instability zone. The large amplitude

*Note: Transient response follows the rules by Jennings [27]

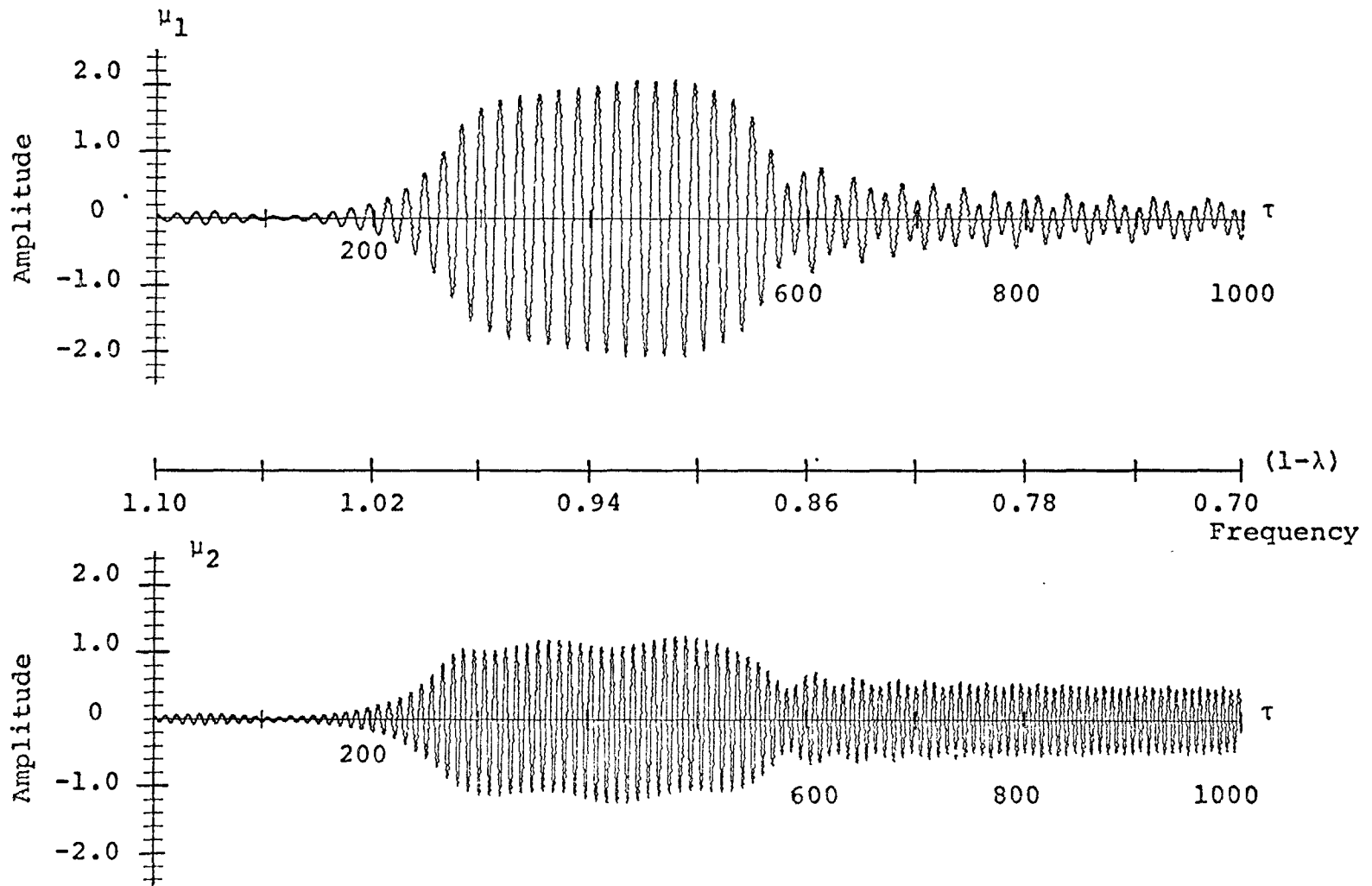


FIG. 6-7 PASSAGE THROUGH RESONANCE - RAMBERG-OSGOOD FUNCTION
 $(n_1 = 3, n_2 = 9, \alpha = 0.1)$

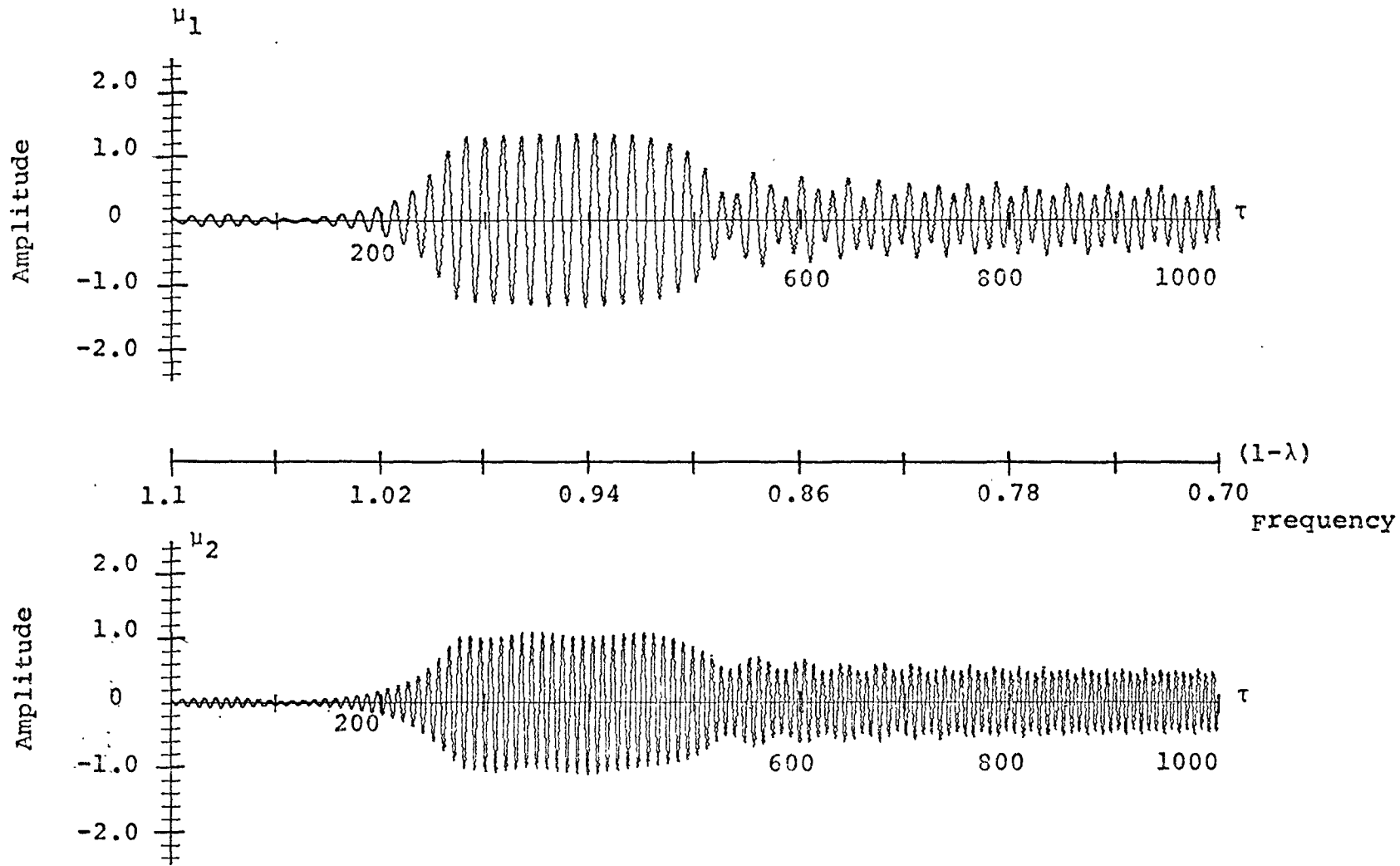


FIG. 6-8 PASSAGE THROUGH RESONANCE - RAMBERG-OSGOOD FUNCTION

$$(n_1 = 9, n_2 = 9, \alpha = 0.1)$$

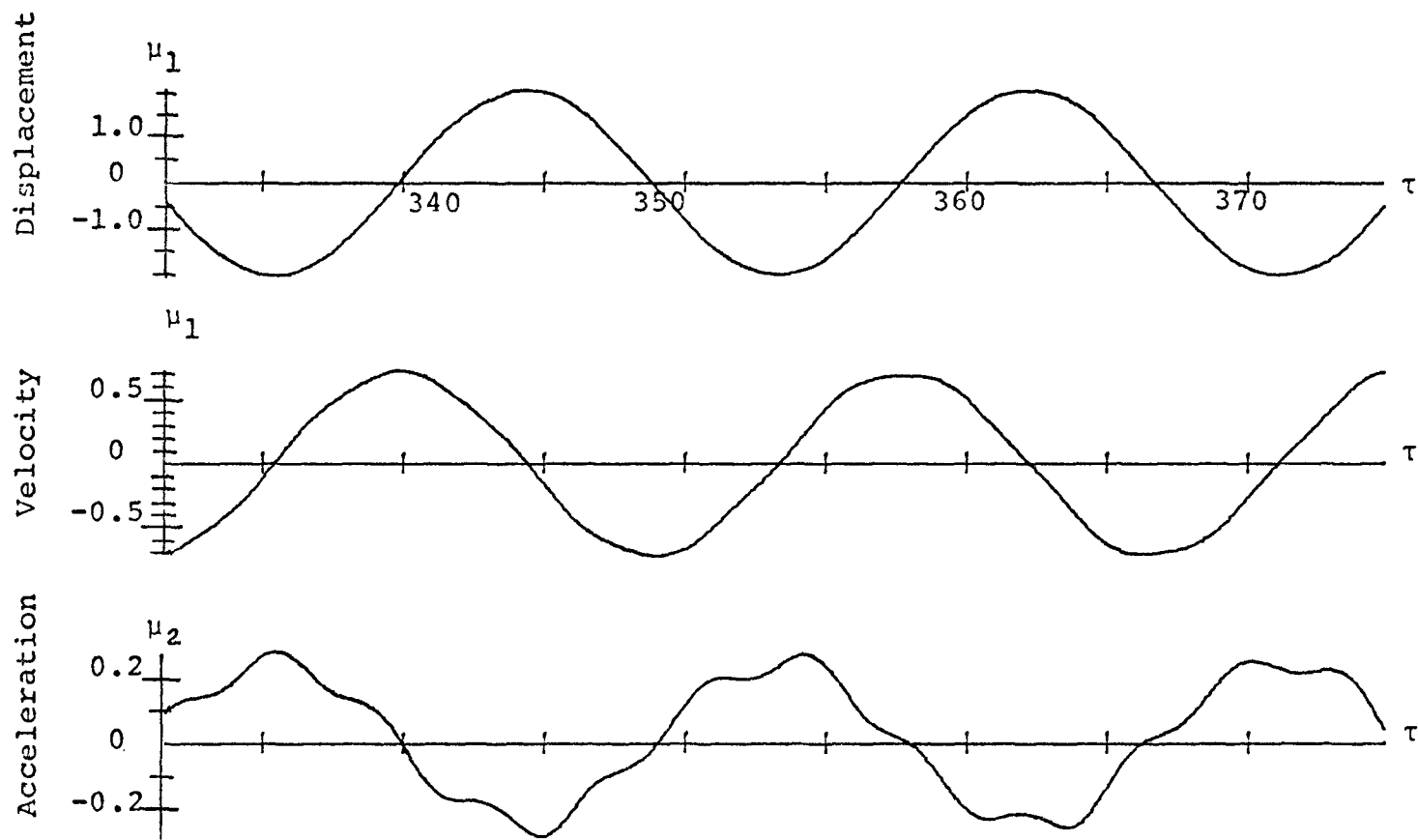


FIG. 6-9 ANALYSIS OF WAVE FORM OF FIRST MODE - $(1-\lambda) = 0.94$

$$(n_1 = 3, n_2 = 9, \alpha = 0.1)$$

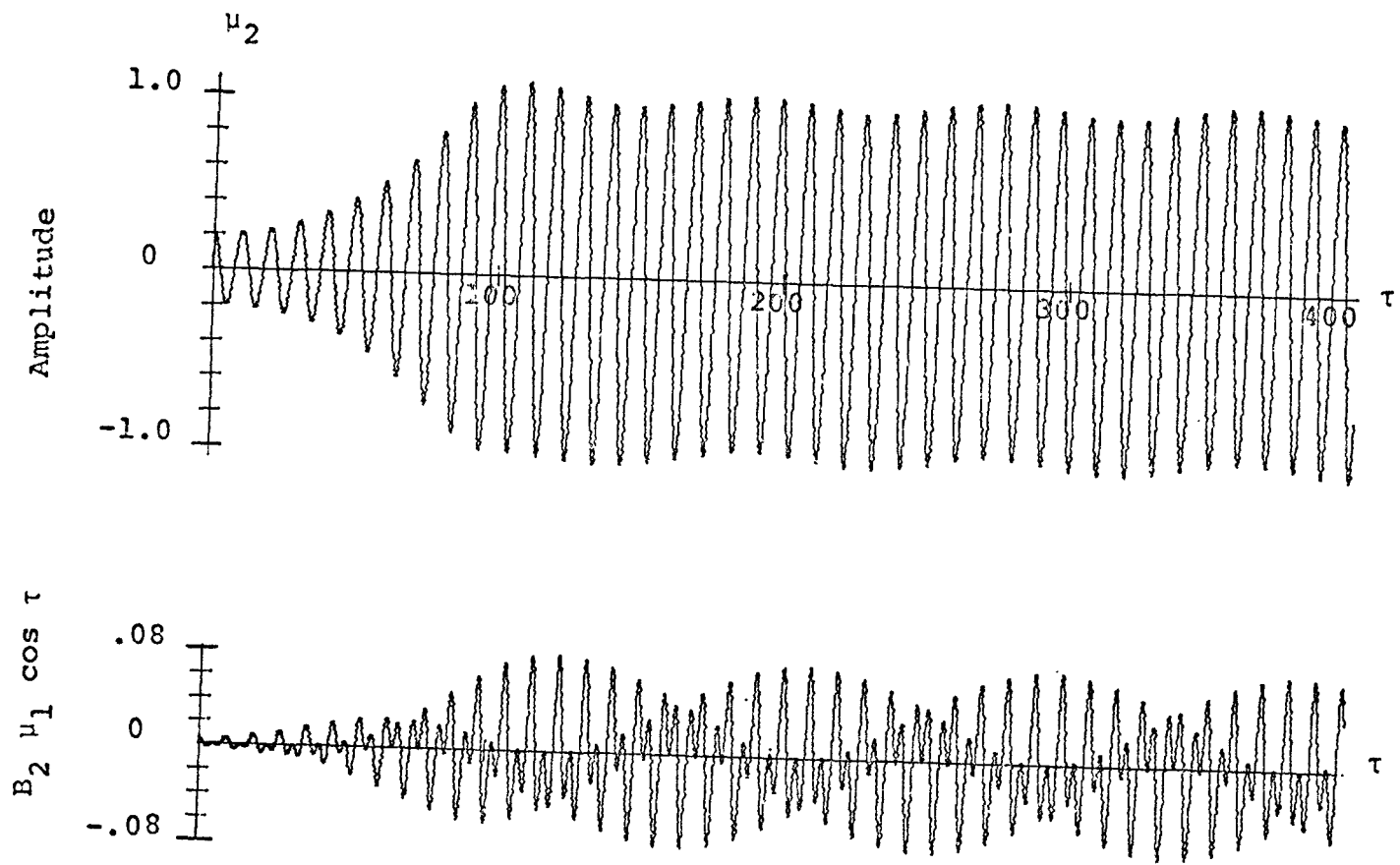


FIG. 6-10 RESPONSE OF SECOND MODE AND PARAMETRIC DRIVING FORCE
 $((1-\lambda) = 1.0, n_1 = 3, n_2 = 9, \alpha = 0.1)$

regions outside the linear instability zone can be reached either by large initial disturbances or by a passage through resonance. The widening of the resonance zone at small amplitude levels for $n_1 \neq n_2$ appears to have no practical significance.

6.6 Presence of Higher Order Harmonics

The response curves of μ_2 in Fig. 6-5 to 6-8 show a slow frequency modulation of the order of 10% superimposed on the motion $\mu_2 = Q_2 \cos \psi_2$. As the averaged equations predict a steady-state it is of interest to see how this slow frequency component is generated. Fig. 6-9 plots the displacement, velocity and acceleration response for the first mode μ_1 . The acceleration record indicates the presence of a third order harmonic in the wave form.

Expanding the parametric term of the second mode and including a third order harmonic in μ_1 , i.e.

$$\mu_1 = Q_1 \cos (K_1 \tau + \theta_1) + a \cos (3K_1 \tau + b) \quad 6-20$$

the lowest frequency obtained is $(3K_1 - 1)$. For $K_1 = .366$ this frequency has a period in the order of 6.5 times the natural period of the second mode. The actual time history response of the parametric driving term $B_2 \mu_1 \cos \tau$ is plotted in Fig. 6-10. Here the slow frequency component is seen to have a period approximately 9 times the period of the second mode. To obtain the effect of the higher order harmonics the method of averaging must be extended to higher order approximations.

6.7 Observations and Discussion

Based on the present analysis of a two degree of freedom system with hysteretic damping modelled by the Ramberg-Osgood functions, the following observations are

drawn.

1. For all practical purposes, a system with hysteretic damping has the same parametric instability zone as a system without damping. In other words, a small disturbance can only cause a rapid rise of amplitudes if the frequency of the external excitation is within the linear instability zone. Therefore, the addition of hysteretic damping can not cause a system to become more susceptible to parametric combination resonance.

2. Once, a parametric resonance does take place, then the hysteretic properties of the system influence the responses. The steady-state curves of the hysteretic system depend on the ratio of the yield points r and the parameters α and n . By varying the parameter n it was observed that large amplitude oscillations are possible over a region that is 30% larger than the undamped instability zone. This enlarged resonance region at large amplitude levels is particularly important when a passage through resonance occurs.

3. At small amplitude levels, the steady-state curves in general diverge and do not exhibit the usual bifurcation points which are associated with parametric resonance problems. The divergence of the response curves is caused by a difference in the hysteretic properties of the two restoring elements.

CHAPTER VII

CONCLUSIONS AND RECOMMENDATIONS FOR FURTHER RESEARCH

7.1 Conclusions

In the present investigation the resonant response of nonlinear dynamical systems of one and two degree of freedom subjected to external monofrequency, parametric excitation was examined. The resonance phenomena was divided into external resonance and internal resonance and two interaction problems were studied: first, the interaction of an external parametric resonance and an internal resonance caused by the nonlinear coupling terms, second the interaction of two external parametric resonances. The nonlinearities were grouped into those that were analytic functions of the co-ordinates and their time-derivatives and those that were hysteretic, time-history dependent functions of the co-ordinates. The problems studied are typical of those that occur in the theory of dynamic stability. Whereas an extensive literature exists on the forced resonance of nonlinear mechanical systems, few contributions exist within the context of dynamic stability. In particular, no research has been reported either on the interaction of resonance zones or the response of hysteretic systems. The approximate method of analysis employed was the method of averaging.

Based on the present analysis, the following conclusions were obtained.

1. A nonlinear coupling between modes can cause an interaction effect between an external parametric resonance and an internal resonance. The parametric resonance zone can be divided into

two regions; (a) that region in which a small disturbance will grow rapidly and after the initial transient motion is passed will reach a steady-state, (b) that region in which a small disturbance will again cause a resonant build-up of amplitudes but the envelope at maximum response instead of reaching a steady-state will continue to oscillate about some mean value. The former condition is typical of systems without internal resonance and the latter condition may occur in systems with internal resonance. This qualitative difference in the response is the main difference that is caused by an internal resonance. Taking as an example a thin-walled beam subjected to pulsating end moments it was found that an internal resonance occurred as the two natural frequencies of bending and torsion coincided. As the two frequencies approached each other a strong modulated response occurred which consisted of a slow frequency wave form superimposed on the envelope of maximum response. This non-steady state motion was called a quasi-steady motion to distinguish it from a true steady-state condition. The modulated motion appeared to be periodic but was too complex for an analytical analysis.

2. An approximate solution of a system that can manifest an internal resonance condition involves a two-fold analysis of varying difficulties. The first analysis neglects the internal resonance effect and obtains the steady-state response of the system except in the neighbourhood of those frequencies that will cause an internal resonance condition. The second analysis includes the internal resonance effect, but is only valid in the region of internal resonance. There exists a transition zone as the frequencies approach an internal resonance condition where the first method of analysis must be changed to the second. Because of the techniques of the approximate method of analysis the second method does not degenerate into the first method as the frequencies diverge

from the internal resonance condition. Accurate values of the response in this transition zone can only be obtained by direct numerical analysis; however, within their respective regions of validity both approximate methods of analysis do provide accurate response.

3. In two degree of freedom systems subjected to follower forces, two external parametric zones can coincide and reinforce each other when the natural frequencies of the loaded system are near the ratio 3 : 1. This ratio may occur in structural systems due to the action of the external loading notwithstanding the fact that the frequencies of the unloaded system may be well separated from that specific ratio. When the two parametric resonance zones coincide an explicit algebraic solution of the steady-state response is not possible; instead, the steady-state curves must be obtained by numerical trial and error methods. Again as was shown in the example of internal resonance a steady-state condition may not be possible over a portion of the parametric resonance zone. The response that occurs in lieu of the steady-state is a modulated response. A transfer of energy between the modes caused by the parametric coupling terms appears to be the reason for these modulations. These modulated motions were found to be quite pronounced and exceeded by 50% the maximum amplitude of the steady-state curves that neglected the interaction effect.

4. The instability zone of the parametric combination resonance is a function of the ratio of the damping coefficients. For the non-conservative system studied, the ratio of the damping coefficients of the first and second modes was (1/38). This caused the system to be extremely susceptible to parametric combination resonance. However, although the zone of instability was wide it was found that the transient

solution had a very slow rate of rise near the boundaries of the instability zone. This introduced the concept of degree of instability in parametric resonant systems and it was concluded that a dynamic instability had to be measured not only in the width of the resonance zone, but also in the character of the transient motion.

5. Simple analytical expressions of the energy dissipation mechanism of real physical system are not suitable for the study of parametric resonance. Linear viscous damping, does not cause bounded response and nonlinear forms of viscous damping predict an unacceptable destabilizing effect in the case of combination resonance. In addition, these forms of analytic damping do not correspond to the actual force-deformation characteristics measured experimentally. By using hysteretic damping in the form of the bilinear, double-bilinear and Ramberg-Osgood functions, bounded response was obtained during parametric resonance. The damping mechanism of these hysteretic elements is two-fold and is caused by energy absorption and frequency detuning. The area of the hysteretic loop is a measure of the energy dissipation within the structure. Because the frequency of the responding system is amplitude dependent, this causes a detuning of the excitation frequency which in turn limits the resonant amplitude. It is these two properties that reinforce each other to cause bounded response. The steady-state response curves of hysteretic systems lean towards the lower frequencies and thus exhibit a softening effect. Portions of the response curves have unstable branches and the "jump" phenomenon is possible. For small hystéretic effect it was found that the Ramberg-Osgood and double bilinear models have a pronounced lean with a resulting large overhang. This overhang portion of the steady-state curves can be reached through large initial disturbances with the result that these systems can be parametrically

excited into large amplitude oscillations outside the linear instability zones. For the one degree of freedom system, it was found that hysteretic damping does not affect the width of the parametric instability zone. In contrast, viscous damping can narrow the width of the instability zone and if it surpasses a critical value it can completely eliminate the instability for a given parametric excitation.

6. Hysteretic damping of two degree of freedom system subjected to parametric resonance can cause extreme analytical difficulties. However, by treating two restricted problems of the general two degree of freedom system a number of conclusions can be drawn. First, the two degree of freedom systems may be parametrically excited into a mono-frequency response where both co-ordinates respond at one-half the frequency of the external excitation and the frequency of response is close to the frequency of the first or second mode. For the case of mono-frequency response an approximate solution of the general two degree of freedom system is possible. By using the assumption that only one mode was excited into parametric resonance the two degree of freedom problem was reduced to one degree and the steady-state solutions were easily obtained. Numerical integration showed that the one mode approximation allowed a relatively simple determination of the instability zone, the steady-state response curves and the transient solutions.

7. The second problem that was treated involved the combination parametric resonance of a specialized hysteretic system where each hysteretic element was a function of only one normal co-ordinate. With this system, a steady state solution was possible and the destabilizing effect of hysteretic damping was investigated. The destabilizing affect caused by the addition of damping to systems subjected to combination

resonance is also evident in hysteretic structures. However, the destabilizing effect does not manifest itself until the system undergoes large amplitude oscillations. For all practical purposes, a system with hysteretic damping has the same parametric instability zone as a system without damping. Once parametric resonance does take place, then the hysteretic properties can influence the response. It was found that the ratio of yield points was the important parameter that determined the effective width of the hysteretic resonance zone. This ratio determined the maximum amplitude of response and the duration that a system is in a resonant state, during a transition through resonance.

7.2 Suggestions For Future Research

The theoretical investigations of the simultaneous occurrence of two resonance conditions has shown that the resulting motion is sufficiently different from the case when only one resonance is considered to justify an experimental investigation. The investigation of the thin-walled beam was restricted to a two mode approximation. The inclusion of additional modes will increase the accuracy of the analysis and may indicate some new qualitative changes in the response. Other elastic bodies such as plates and shells where the natural frequencies of various modes of motion may coincide should be investigated.

The study of systems subjected to non-conservative time-dependent loading should be expanded from its present application in aero-space engineering to other engineering systems where such loadings are feasible. One such application could be in the area of wind or hydraulic loading of structures. As the non-conservative loading is increased it reaches a critical value where self-excited oscillations are possible. A worthwhile investigation would be the interaction of a self-excited and parametric resonance.

Investigations of hysteretic systems are becoming increasingly more important. Here the emphasis on research should concentrate on multiple degrees of freedom. In particular, the effect of nonlinear coupling, internal resonance and combination resonance should receive further attention. The effect of degrading material properties should also be investigated.

Extension of the method of averaging to higher order approximations is feasible. A worthwhile mathematical investigation would be to evaluate the significance of the higher order resonant zones.

REFERENCES

1. Beal, T.R., "Dynamic Stability of a Flexible Missile Under Constant and Pulsating Thrust", AIAA Journal, Vol. 3, No. 3, March 1965, pp. 486-494.
2. Benz, G., "Schwingungen Nichtlinearer Gedämpfter Systeme mit Pulsierenden Speicher-Kennwerten, Thesis, Karlsruhe, 1962.
3. Bogoliubov and Mitropolsky, "Asymptotic Methods in the Theory of Nonlinear Oscillations", Hindustan Publishing Corpn., India, 1961.
4. Bolotin, V.V., "The Dynamic Stability of Elastic Systems", Holden Day Inc., 1964.
5. Bolotin, V.V., "Non-conservative Problems of the Theory of Elastic Stability", Pergamon Press, 1963,
6. Carpenter, L.D., Lu, L.W., "Repeated and Reversed Load Tests on Full-Scale Steel Frames", 4th World Conf. on Earthquake Engineering, B-2, pp. 125-136.
7. Caughey, T.K., "Sinusoidal Excitation of a System with Bilinear Hysteresis", J. of Appl. Mech., Vol. 27, ASME, 1960, pp. 640-643.
8. Cesari, L. "Asymptotic Behaviour and Stability Problems in Ordinary Differential Equations", Academic Press, New York.
9. Cullimore, M.S.G., "The Shortening Effect - A Nonlinear Feature of Pure Torsion", Research Engineering Supplement, London 1949, pp. 153-163.
10. Den Hartog, J.P., "Vibration - A Review of Interesting Cases", Proceedings, 3rd Canadian Congress of Applied Mechanics, Calgary, 1971, pp. 17-27.

11. Dokainish, M.A., Sahay, B., "Steady-State Response of a Two-Degree-of-Freedom Double Bilinear Hysteretic System", ASME Paper, 69-V/BR-27, (1969).
12. Evan-Iwanowski, R.M., "On the Parametric Response of Structures", Applied Mechanics Reviews, Vol. 18, No. 9, Sept. 1965, pp. 699-702.
13. Evan-Iwanowski, R.M., "Nonstationary Vibrations of Mechanical Systems", Applied Mechanics Review, 1970, pp. 213-219.
14. Ghobarah, A.A., "Nonlinear Behaviour of Open Thin-Walled Elastic Beams", Thesis, McMaster University, 1970.
15. Hagedorn, P., "Kombinationen resonanz Und Instabilitätsbereiche Zweiter Art bei Parametererregten Schwingungen mit Nichlinearer Dämpfung", Ing. Arch., Vol. 38, 1969, pp. 80-96.
16. Hagedorn, P., "Zur Realisierbarkeit Pulsierender Folgelasten ", ZAMM, 51, 1971, T188-T190.
17. Hanson, R.D., "Comparison of Static and Dynamic Hysteresis Curves", J. of Eng. Mech., ASCE, Oct. 1966, pp. 87-113.
18. Herrmann, G., Jong, I.C., "On the Destabilizing Effect of Damping in Nonconservative Elastic Systems", J. of App. Mech., Vol. 32, 1965, pp. 592-597.
19. Hsu, C.S., "On the Parametric Excitation of a Dynamic System Having Multiple Degrees of Freedom", J. of App. Mech., Vol. 30, ASME, 1963, pp. 367-372.
20. Hsu, C.S., "Further Results on Parametric Excitation of a Dynamic System", J. of App. Mech., June 1965, pp. 373-377.
21. Hutton, R.E., "An Investigation of Resonant, Non-Linear, Non-Planar Free Surface Oscillations of a Fluid NASA TN D-1870 (1963).
22. Iwan, W.D., "The Steady-State Response of the Double-Bilinear Hysteretic Model", J. of Appl. Mech., 32, 1965, pp. 921-925.

23. Iwan, W.D., "The Dynamic Response of the One-Degree-of-Freedom Bilinear Hysteretic System" Proc. of the Third World Conf. on Earthquake Engineering, 1965.
24. Iwan, W.D., "The Steady-State Response of a Two-Degree of Freedom Bilinear Hysteretic System", J. of Appl. Mech., ASME, Vol. 32, 1965, pp. 151-156.
25. Iwan, W.D., "On the Nature of Ultraharmonic Oscillations in Yielding Systems", Int. J. Non-Linear Mechanics, Vol. 5, pp. 247-258, 1970.
26. Jacobsen, L.S., "Damping in Composite Structures", 2nd World Conf. on Earthquake Engineering, Tokyo, 1960, pp. 1029-1044.
27. Jennings, P.C., "Response of Simple Yielding Structures to Earthquake Excitation", Earthquake Engineering Research Laboratory, California Inst. of Tech., June 1963.
28. Jong, I.C., "On Stability of a Circulatory System with Bilinear Hysteresis Damping", J. of Appl. Mech., Vol. 36, ASME, 1969, pp. 76-82.
29. Lazan, B.J., "Damping of Materials and Members in Structural Mechanics", Pergamon Press, 1968.
30. Malkin, I.G., "Some Problems in the Theory of Nonlinear Oscillations", U.S. Dept. of Commerce, AEC-TR-3766, (Translated from the Russian, Moscow, 1956), p. 320.
31. Mettler, E., "Allgemeine Theorie Der Stabilität Erzwungener Schwingungen Elastischer Körper", Ing. Arch., Vol. 17, 1949, pp. 418-449.
32. Mettler, E., "Nichtlineare Schwingungen Und Kinetische Instabilität by Saiten Und Stäben", Ing. Arch., Vol. 23, 1955, pp. 354-364.
33. Mettler, E., "Stability and Vibrations Problems of Mechanical Systems Under Harmonic Excitation", 1965, pp. 169-188, Perg. P.
34. Mettler, E., "Combination Resonances in Mechanical Systems Under Harmonic Excitation", 4th Conf. of Nonlinear Oscillations, Prague, 1967, pp. 51-70.

35. Miles, J.W., "Stability of Forced Oscillations of a Spherical Pendulum", *Quart. Appl. Math.*, Vol. 20, 1962, pp. 21-32.
36. Minorsky, N., "Nonlinear Oscillations", Van Nostrand, New Jersey, 1962.
37. Mitropolsky, Iu. A., "Averaging Method in Non-Linear Mechanics", *Int. J. Non-Linear Mechanics*, Vol. 2, 1967, pp. 69-96.
38. Piszczek, K., "Parametric Combination Resonance (of the Second Kind) in Non-Linear Systems", *Rozprawy Inzynierskie*, (In Polish), Vol. 2, 1960, pp. 211-229.
39. Popov, E.P., Pinkney, R.B., "Behaviour of Steel Building Connections Subjected to Inelastic Strain Reversals", *American Iron and Steel Institute, Bulletin No. 13*, Nov. 1968.
40. Rea, D., et al, "Damping Capacity of a Model Steel Structure", *4th World Conf. of Earthquake Engineering*, B-2, pp. 63-73.
41. Reckling K., "Die Stabilität Erzwungener Schwingungen von Stäben Und Trägern Nach Rechnung Und Versuch", *Schiffstechnik*, Vol. 3, (1955/56), pp. 135-140.
42. Rocard, Y. "Dynamic Instability", Crosby Lockwood & Son, Ltd., London, 1957.
43. Rosenblueth, E., discussion to "Equivalent Viscous Friction for Hysteretic Systems with Earthquake-like Excitations", by D.E. Hudson, *Proc. of the 3rd World Conf. on Earthquake Engineering*, Vol. II, 1965.
44. Schmidt, G., Weidenhammer, F., "Instabilitäten Gedämpfter Rheolinerer Schwingungen", *Math. Nachrichten*, Vol. 23, 1961, pp. 301-318.
45. Sethna, P.R., "Coupling in Certain Classes of Weakly Nonlinear Vibrating Systems", *Nonlinear Differential Equations and Nonlinear Mechanics*, Ed. LaSalle and Lefschetz, pp. 58-70.

46. Sethna, P.R., "Vibrations of Dynamical Systems with Quadratic Nonlinearities", J. of Appl. Mech., ASME, 1965, pp. 576-582.
47. Shiga, T., Ogawa, J., "The Experimental Study of the Dynamic Behaviour of Reinforced Concrete Frames, 4th World Conference on Earthquake Engineering, Chile, 1969, B-2, pp. 165-176.
48. Skalak, R., and Yarymovych, M.L., "Subharmonic Oscillations of a Pendulum", J. of Appl. Mech., Vol. 27, March, 1960, pp. 159-164.
49. Struble, R.A. and Heinbockel, J.H., "Resonant Oscillations of a Beam-Pendulum System", Trans. ASME, Vol. 30, Series E, No. 2, June, 1963, pp. 181-188.
50. Szemplinska-Stupnicka, W., "On the Phenomenon of the Combination Type Resonance in Non-Linear Two Degree-of-Freedom Systems", Int. J. Non-Linear Mech., Vol. 4, 1969, pp. 335-359.
51. Tanabashi, R., "Nonlinear Vibration Problems in the Field of Earthquake Engineering", 2nd Conference on Nonlinear Oscillations, Prague, 1962.
52. Tanabashi, R., "Nonlinear Transient Vibration of Structures", 2nd World Conference on Earthquake Engineering, Tokyo, 1960, pp. 1223-1238.
53. Tondl, A., "On the Internal Resonance of a Nonlinear System with Two Degrees of Freedom", Nonlinear Vibration Problems, Vol. 5, 1963, pp. 207-222.
54. Tondl, A., "On the Combination Resonance of a Non-Linear System with Two Degrees of Freedom", Rev. Mec. Appl., Vol. 8, 4., 1963.
55. Tso, W.K., Asmis, K.G., "Parametric Excitation of a Pendulum with Bilinear Hysteresis", J. of Appl. Mech., ASME, Dec. 1970, pp. 1061-1068.

56. Yamada, M., "Low Cycle Fatigue Fracture Limits of Various Kinds of Structural Members Subjected to Alternately Repeated Plastic Bending Under Axial Compression as an Evaluation Basis or Design Criteria for Aseismic Capacity", 4th World Conference on Earthquake Engineering, B-2, pp. 137-151.
57. Yamamoto, T., Hayashi, S., "On the Response Curves and the Stability of Summed and Differential Harmonic Oscillations", Bull. of JSME, Vol. 6, No. 23, 1963, pp. 420-429.
58. Ziegler, H., "Principles of Structural Stability", Blaisdell, 1968.

APPENDIX

Evaluation of the Hysteretic Functions C(Q), S(Q)

The integrals C(Q), S(Q) for the bilinear, double bilinear and Ramberg-Osgood hysteretic relationships were first evaluated by Caughey^[7], Iwan^[22] and Jennings^[27] respectively. For completeness the results will be derived here in detail.

(a) Bilinear Hysteretic Model

The bilinear hysteretic function is shown in the Fig. A-1. Along the branch BC the restoring force M is

$$M_1 = Q \cos \psi - uQ + u\phi_y \quad \text{A-1}$$

Along the branch CD the restoring force M₂ is

$$M_2 = Q \cos \psi - Qu \cos \psi - u\phi_y \quad \text{A-2}$$

The integration is performed over each line segment with the first integration period defined by the angle

$$0 \leq \psi \leq \theta^* \quad \text{A-3}$$

where

$$\cos \theta^* = \frac{Q - 2\phi_y}{Q} \quad \text{A-4}$$

The functions C(Q) and S(Q) are symmetric with respect to one half period of integration

$$S(Q) = \frac{1}{\pi} \int_0^{2\pi} M \sin \psi \, d\psi$$

$$\begin{aligned}
&= \frac{2}{\pi} \left[\int_0^{\theta^*} M_1 \sin \psi \, d\psi + \int_{\theta^*}^{\pi} M_2 \sin \psi \, d\psi \right] \\
&= \frac{2}{\pi} \left[\int_0^{\theta^*} [Q \cos \psi - uQ + u\phi_y] \sin \psi \, d\psi \right. \\
&\quad \left. + \int_{\theta^*}^{\pi} [Q \cos \psi - Qu \cos \psi - u\phi_y] \sin \psi \, d\psi \right] \quad \text{A-5}
\end{aligned}$$

$$\begin{aligned}
S(Q) &= -\frac{uQ}{\pi} \sin^2 \theta^* \\
&= -\frac{4u}{\pi} \phi_y \left[1 - \frac{\phi_y}{Q} \right] \quad Q \geq \phi_y \quad \text{A-6}
\end{aligned}$$

$$S(Q) = 0 \quad Q < \phi_y \quad \text{A-7}$$

$$\begin{aligned}
C(Q) &= \frac{1}{\pi} \int_0^{2\pi} M \cos \psi \, d\psi \\
&= \frac{2}{\pi} \left[\int_0^{\theta^*} M_1 \cos \psi \, d\psi + \int_{\theta^*}^{\pi} M_2 \sin \psi \, d\psi \right] \quad \text{A-8} \\
&= \frac{2}{\pi} \left[\int_0^{\theta^*} [Q \cos \psi - uQ - u\phi_y] \sin \psi \, d\psi \right. \\
&\quad \left. + \int_{\theta^*}^{\pi} [Q \cos \psi - Qu \cos \psi - u\phi_y] \sin \psi \, d\psi \right]
\end{aligned}$$

$$C(Q) = Q \left[1 - u + \frac{u\theta^*}{\pi} - \frac{u}{\pi} \sin \theta^* \cos \theta^* \right] \quad Q \geq \phi_y \quad \text{A-9}$$

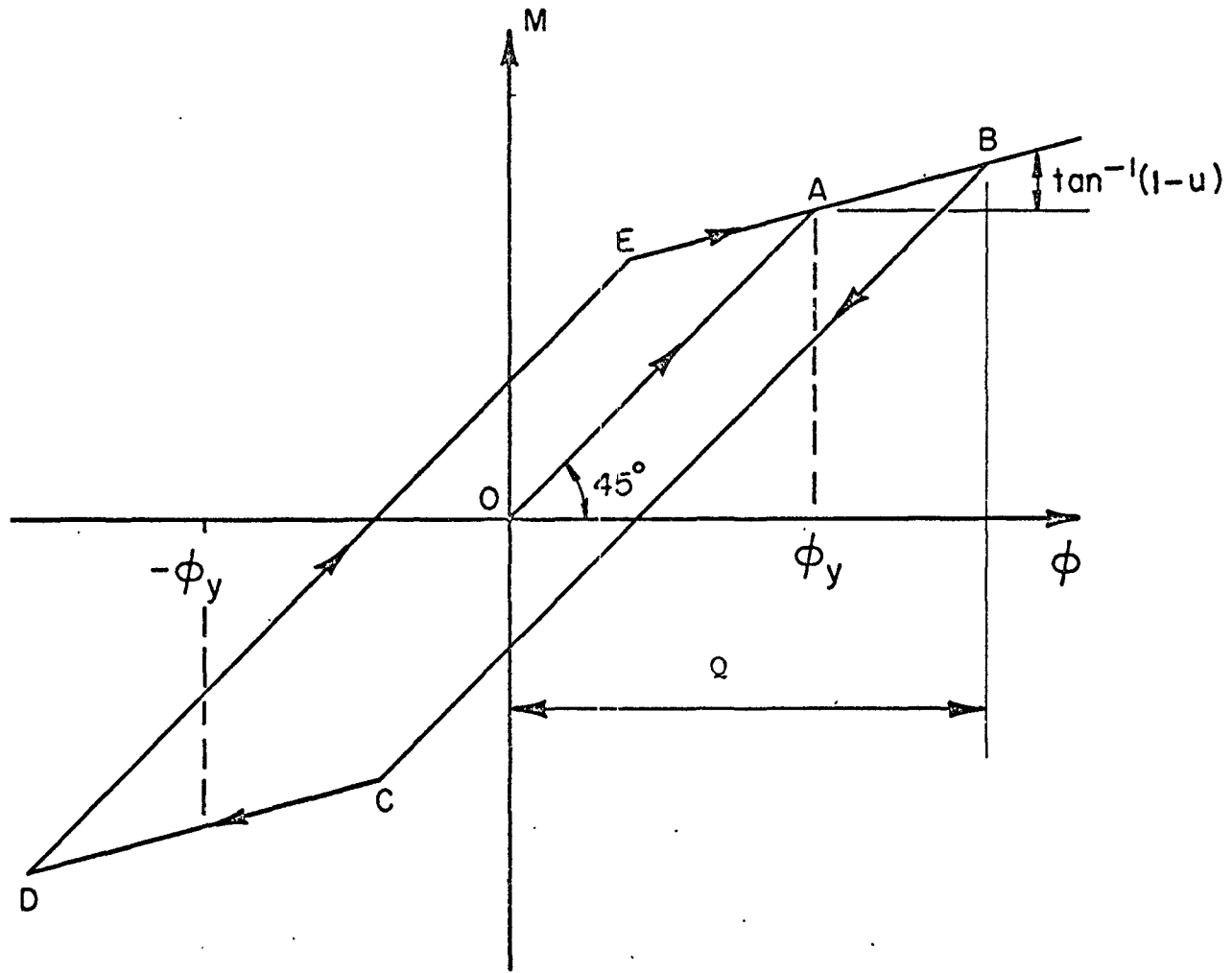


FIG. A-1 BILINEAR HYSTERETIC FUNCTION

$$C(Q) = Q \quad Q < \phi_y \quad A-10$$

(b) Double Bilinear Hysteretic Function

The double bilinear hysteretic function is shown in Fig. A-2. The restoring force M is defined on the four linear branches as follows:

$$\begin{aligned} M &= Q \cos \psi - u(Q - \phi_y); & (Q - \phi_y) < Q \cos \psi < Q \\ &= (1 - u) Q \cos \psi; & 0 < Q \cos \psi < (Q - \phi_y) \\ &= Q \cos \psi; & -\phi_y < Q \cos \psi < 0 \\ &= (1 - u) Q \cos \psi - u\phi_y; & -Q < Q \cos \psi < -\phi_y \end{aligned} \quad A-11$$

$$\text{Let } \theta_1 = \cos^{-1} \left(\frac{Q - \phi_y}{Q} \right) \quad A-12a$$

$$\theta_2 = \cos^{-1} \left(-\frac{\phi_y}{Q} \right) \quad A-12b$$

Then S(Q) may be evaluated as follows

$$\begin{aligned} S(Q) &= \frac{2}{\pi} \left\{ \int_0^{\theta_1} [Q \cos \psi - u(Q - \phi_y)] \sin \psi \, d\psi \right. \\ &\quad + \int_{\theta_1}^{\pi/2} (1-u) Q \cos \psi \sin \psi \, d\psi + \int_{\pi/2}^{\theta_2} Q \cos \psi \sin \psi \, d\psi \\ &\quad \left. + \int_{\theta_2}^{\pi} [(1-u) Q \cos \psi - u\phi_y] \sin \psi \, d\psi \right\} \quad A-13 \end{aligned}$$

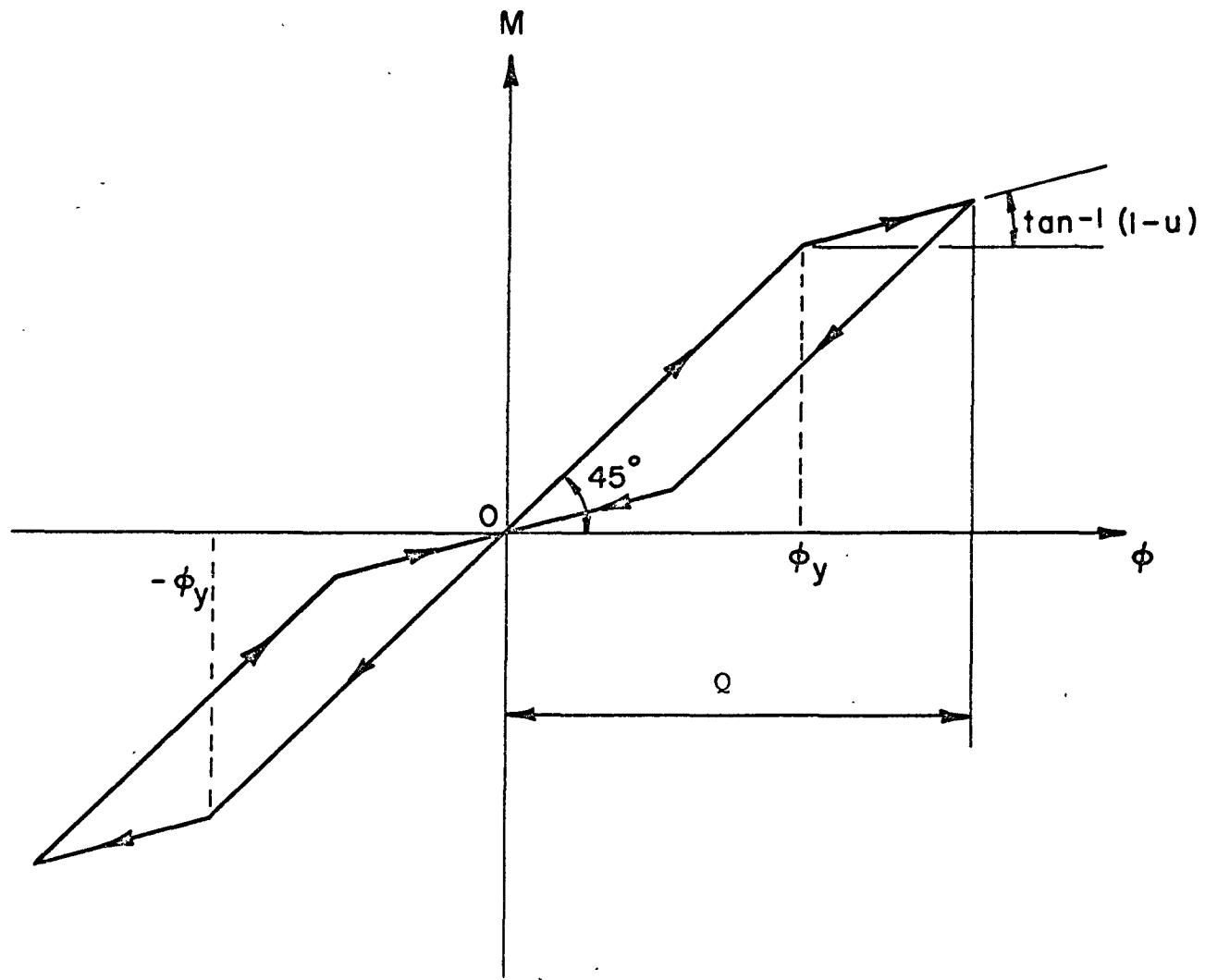


FIG. A-2 DOUBLE-BILINEAR HYSTERETIC FUNCTION

Upon integration

$$\begin{aligned}
 S(Q) = & \frac{2}{\pi} \left\{ \frac{Q \sin^2 \theta_1}{2} - u(Q - \phi_y) (-\cos \theta_1 + 1) \right. \\
 & + (1-u) \frac{Q}{2} (1 - \sin^2 \theta_1) + \frac{Q}{2} (\sin^2 \theta_2 - 1) \\
 & \left. - (1-u) \frac{Q}{2} \sin^2 \theta_2 + u \phi_y (1 + \cos \theta_2) \right\} \quad A-14
 \end{aligned}$$

Substituting θ_1 and θ_2 and simplifying

$$S(Q) = - \frac{2}{\pi} u \phi_y \left(\frac{Q - \phi_y}{Q} \right) \quad Q \geq \phi_y \quad A-15$$

In a similar manner

$$\begin{aligned}
 C(Q) = & \frac{Q}{\pi} \left\{ u(\theta_1 + \theta_2 - \frac{\sin_2 \theta_1}{2} - \frac{\sin_2 \theta_2}{2} - \frac{\pi}{2}) + (1-u)\pi \right\} \quad A-16 \\
 & Q \geq \phi_y
 \end{aligned}$$

(c) The Ramberg-Osgood Hysteretic Function

The Ramberg-Osgood Hysteretic function is shown in Fig. A-3. The function is specified conveniently in the non-dimensional amplitude ratio $\mu = \phi/\phi_y$. Explicit expressions of $S(\mu_0)$ and $C(\mu_0)$ in terms of the amplitude μ_0 are not readily available. The integrals can be conveniently evaluated directly from the defining integrals

$$S(\mu_0) = \frac{2}{\pi} \int_0^{\pi} M(\mu_0 \cos \psi) \sin \psi \, d\psi \quad \text{A-17a}$$

$$C(\mu_0) = \frac{2}{\pi} \int_0^{\pi} M(\mu_0 \cos \psi) \sin \psi \, d\psi \quad \text{A-17b}$$

by the use of Simpson's Rule.

A mixed analytical expression in terms of M_0 and μ_0 is readily calculated for the integral $S(\mu_0)$.

With the change of variable

$$\mu = \mu_0 \cos \psi \quad \text{A-18a}$$

$$d\mu = -\mu_0 \sin \psi \, d\psi \quad \text{A-18b}$$

the integral A-17a can be rewritten as

$$S(\mu_0) = -\frac{2}{\mu_0 \pi} \int_{+\mu_0}^{-\mu_0} M(\mu) \, d\mu \quad \text{A-19a}$$

$$= -\frac{2}{\mu_0 \pi} \int_{+M_0}^{-M_0} M \frac{d\mu}{dM} \, dM \quad \text{A-19b}$$

From Fig. A-3

$$\left(\frac{\mu - \mu_0}{2}\right) = \left(\frac{M - M_0}{2}\right) + \alpha \left(\frac{M - M_0}{2}\right)^n \quad \text{A-20a}$$

Consequently

$$\frac{d\mu}{dM} = 1 + \alpha n \left(\frac{M - M_0}{2}\right)^{n-1} \quad \text{A-20b}$$

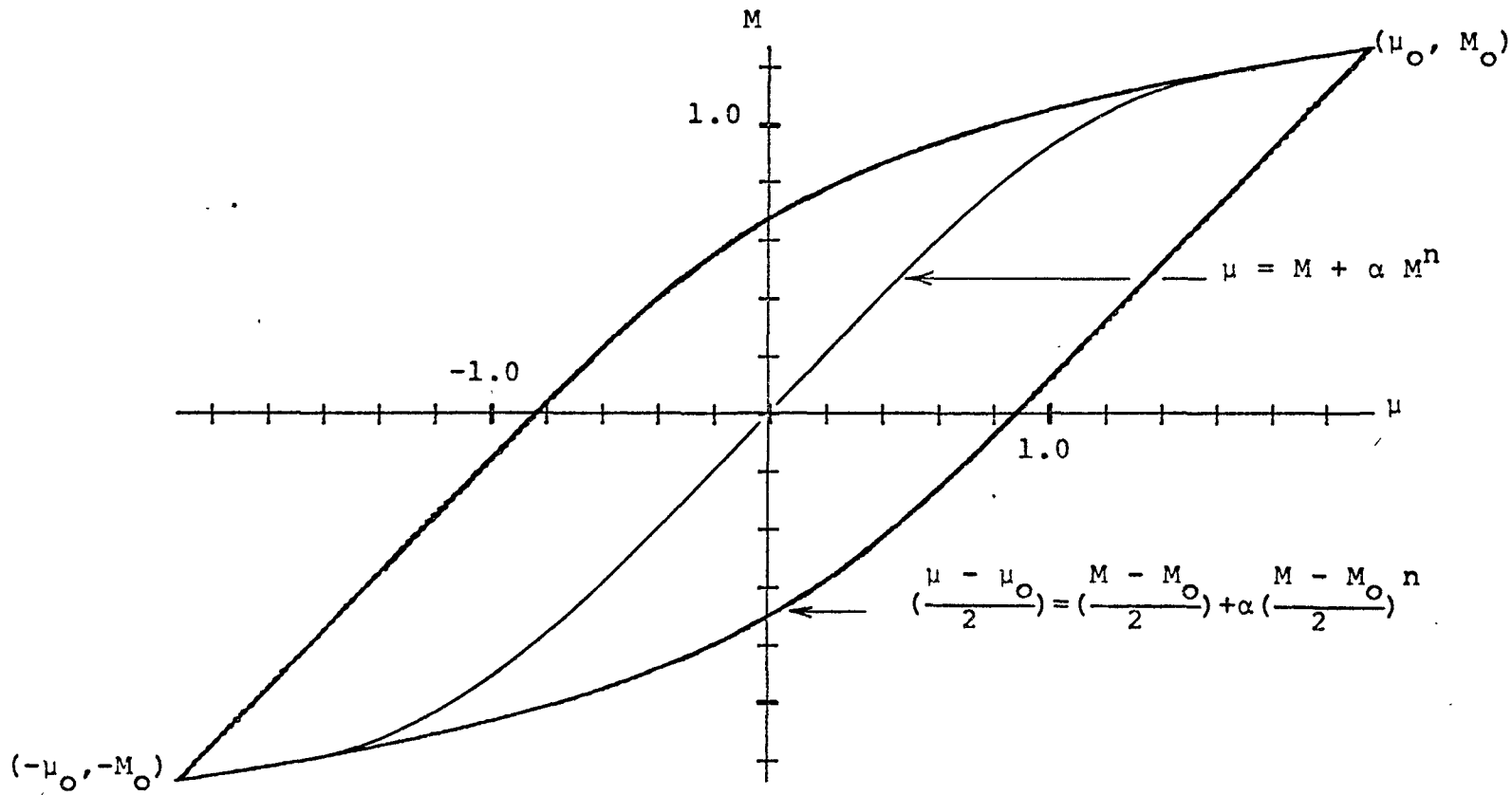


FIG. A-3 RAMBERG-OSGOOD HYSTERETIC FUNCTION

Now

$$\begin{aligned}
 S(\mu_0) &= - \mu_0 \frac{2}{\pi} \int_{M_0}^{-M_0} \left\{ M + \alpha n M \left(\frac{M - M_0}{2} \right)^{n-1} \right\} dM \\
 &= - \mu_0 \frac{2}{\pi} \left[0 + \alpha n \int_{M_0}^{-M_0} M \left(\frac{M - M_0}{2} \right)^{n-1} dM \right]
 \end{aligned}
 \tag{A-21}$$

Let $\xi = M - M_0$ A-22

Then

$$\begin{aligned}
 S(\mu_0) &= - \mu_0 \frac{2}{\pi} \alpha n \int_0^{-2M_0} (\xi + M_0) \left(\frac{\xi}{2} \right)^{n-1} d\xi \\
 &= - \frac{4\alpha}{\pi\mu_0} \frac{(n-1)}{(n+1)} M_0^{n+1}
 \end{aligned}
 \tag{A-23}$$

$S(\mu_0)$ is now given as a mixed expression in terms of M_0 and μ_0 . These variables are related by the expression

$$\mu_0 = M_0 + \alpha M_0^n \tag{A-24}$$

For large displacements

$$\mu_0 \approx \alpha M_0^n \quad \mu_0 \gg 1 \tag{A-25a}$$

$$M_0 = \left(\frac{\mu_0}{\alpha} \right)^{1/n} \tag{A-25b}$$

For small displacements

$$\mu_0 \approx M_0 \quad \mu_0 \ll 1 \tag{A-26a}$$

and

$$S(\mu_0) \approx -\frac{4\alpha}{\pi} \frac{(n-1)}{(n+1)} \mu_0^n \quad \text{A-26b}$$

Area of hysteresis loop

The area of the hysteretic loop can be evaluated from the integral

$$\text{Area} = \int M d\mu = \int_0^{2\pi} M \frac{d\mu}{d\psi} d\psi \quad \text{A-27}$$

$$\text{Now } \mu = \mu_0 \cos \psi \quad \text{A-28a}$$

$$\frac{d\mu}{d\psi} = -\mu_0 \sin \psi \quad \text{A-28b}$$

$$\text{Area} = -\mu_0 \int_0^{2\pi} M \sin \psi d\psi \quad \text{A-29a}$$

$$\text{Area} = -\mu_0 \pi [S(\mu_0)] \quad \text{A-29b}$$

Consequently the integral $S(\mu_0)$ is a measure of the area contained within the hysteretic loop.